論文 / 著書情報
Article / Book Information

題目(和文)	
Title(English)	Experimental Studies on Stability of Piled Raft Fonudation for Oil Storage Tanks against Dynamic Loadings
著者(和文)	SAHRAEIANSeyed Mohammad Sadegh
Author(English)	Seyed Mohammad Sadegh Sahraeian
出典(和文)	学位:博士(学術), 学位授与機関:東京工業大学, 報告番号:甲第10679号, 授与年月日:2017年9月20日, 学位の種別:課程博士, 審査員:竹村 次朗,北詰 昌樹,髙橋 章浩,岩波 光保,田村 修次
Citation(English)	Degree:Doctor (Academic), Conferring organization: Tokyo Institute of Technology, Report number:甲第10679号, Conferred date:2017/9/20, Degree Type:Course doctor, Examiner:,,,,
学位種別(和文)	博士論文
Type(English)	Doctoral Thesis

Experimental Studies on Stability of Piled Raft Foundation for Oil Storage Tanks against Dynamic Loadings

Seyed Mohammad Sadegh Sahraeian

DISSERTATION

submitted in partial fulfillment of the requirements for the degree of

DOCTOR OF PHILOSOPHY

at

TOKYO INSTITUTE OF TECHNOLOGY

2017

ACKNOWLEDGMENTS

I would like to declare my sincere gratitude to my supervisor, Associate Professor Jiro Takemura for his kind support and guidance during my PhD period. His knowledge and encouragement have provided the essential support throughout my research period in Japan. He continuously provided me lots of innovative ideas and valuable advices. His role in this thesis was highly significant and I could not finish it without his help and effort.

I am really appreciated to Professor Masaki Kitazume and Professor Akihiro Takahashi due to their valuable comments during my lab seminars and their important suggestions on my doctoral thesis. Also, I am thankful to the other committee members, Professor Mitsuyasu Iwanami and Associate Professor Shuji Tamura for their kind suggestions and helpful comments.

I would like to extend my special thanks to my lab technician, Mr. Sakae Seki for his efforts and guidance during my experiments. Surely, the experiments would not be successfully completed without his helps. My sincere gratitude goes to the Ministry of Education, Culture, Sports, Science and Technology (MEXT) of Japan for granting me a Monbukagakusho scholarship during my research and PhD period in Japan.

Lastly, but not the least, I would like to thank my dear family, my parents, Mr. S. Abdolhosein Sahraeian and Mrs. Zohreh Deihimi for not only providing me the support, love and encouragement but also teaching me to believe in myself and my brother, Meisam and sister, Tahereh for their help, support and love.

ABSTRACT

Some level of settlement is allowed in the design of oil tank if the uneven settlement can be controlled in an allowable value. Considering the critical condition of Piled Raft Foundation (PRF), that is, secure contact of raft base to the ground surface, and the expected function of piles to impose additional resistance against the local settlement, the piled raft foundation is considered as one of the rational foundation systems for the oil storage tanks. However, this foundation system has a complex interaction with soil under horizontal seismic loading, especially if the tank rests on a liquefiable soil, which may cause an extreme change of the soil stiffness under the tank.

On the other hand, pile installation method might affect the pile bearing capacity and the liquefaction resistance of the sand as well. In this study, a series of centrifuge model tests was performed to investigate the mechanical behavior of oil tank supported by the piled raft foundation on the liquefiable saturated sand and non-liquefiable dry sand. In the tests, two types of foundations were modeled for oil tank; one slab foundation and another one piled raft foundation. In the case of piled raft foundation two different methods of pile installation (Driven and non-Driven) were modelled and the result was compared. Also the Driven piled raft foundation was modelled with two different numbers of piles to consider the effect of piles number on the foundation performance. Using the observed results, such as accelerations of the tank and ground, dynamic and permanent displacement of the foundation, excess pore water pressures of the ground and sloshing behavior of liquid in the tank, the advantage and limitation of piled raft foundation for the application to the oil storage tanks on non-liquefiable and liquefiable sandy soil are discussed.

Regarding the tests results, the performance of piled raft foundation of oil tank on the dry sand was positive. The foundation system could efficiently reduce the tank rocking motion, settlement and uneven settlement due to the contribution of the piles. Although the piles load proportion was significant in this condition, both piles and raft contributed against the loads and rotational moment in the dynamic loading.

On the other hand, the behavior of piled raft foundation of oil tank on saturated sand was more complicated. The raft base contact pressure changed considerably during the dynamic

loading. As a common trend in the piled raft foundation cases, the raft load proportion increased by the reduction of piles resistance due to liquefaction and decreased gradually by the recovery of piles resistance during the EPWP dissipation period. The pile driving process (Driven piles) could increase the density and lateral stress of sand between piles, so the reduction of pile resistance could be slowed by the pile driving but effect was diminished after a large shake. Also the driven PRFs comparing to non-driven PRFs were more effective in reducing the tank rocking motion. The piled raft foundation was effective in reducing the tank settlement compared to the slab foundation but relatively large raft load proportion which can develop enough and uniform raft base contact, is a necessity for preventing a large settlement and uneven settlement of the foundation. Generally, the better performance of piled raft foundation comparing to slab foundation cannot be guaranteed in case of complete liquefaction in the entire ground and piles length.

Another concern in the behavior of oil tank is liquid sloshing inside the tank. The sloshing of liquid was relative to the tank acceleration and it was more critical in dry sand cases while the tank acceleration was larger in such a condition. But the PRF could reduce the sloshing waves of tank liquid in the condition that tank resting on the dry sand while it was not so impressive in case of saturated sand.

Also considering this research results and prior investigations, some practical hints for the application and design of piled raft foundation for oil storage tanks are indicated. The practical points are presented for the conditions that oil tanks are located on non-liquefiable or liquefiable sandy soil separately.

Table of Contents

Chapter 3. Development of centrifuge modeling of oil tank with slab and piled raft foundation

Chapter 1 – Introduction

1.1. Background

Generally, two types of foundations (shallow and deep foundation) have been utilized in real projects in order to transfer oil storage tank load to the soil surface. In case of shallow foundations earth foundation (Figure 1.1(a)) and slab foundation (Figure 1.1(b)) are suitable foundation types for oil tanks if bearing capacity of the foundation and superstructure settlement is below an allowable value. But in some cases, shallow foundation is not adequate to support the structural loads and deep foundation is necessary. Pile foundation (Figure 1.1(c)) as a type of deep foundation is required in the conditions that total settlement or uneven settlement is more than allowable values despite of sufficient bearing capacity of the raft.

In this kind of situations, piles are utilized beneath the raft in order to control not only the total settlement but also uneven settlement of superstructure. In the common design methods of pile foundation, the piles number and dimensions e.g. pile length and diameter are estimated while the bearing capacity of the raft and piles cap are ignored even though the raft has contact with the ground surface. There are two reasons for the application of this conservative design procedure. The first reason is the complex interaction between pile, raft and ground which makes the estimation of load proportion between piles and raft so difficult. Another reason is, complying safety concerns in the design of foundation by ignoring the raft bearing capacity. On the other hand, because the subsurface ground can settle during and after construction, unreliable contact condition between raft base and ground surface may occur. Therefore, the bearing capacity of the foundation can be overestimated if the bearing capacity of the raft is taken into account during the foundation design.

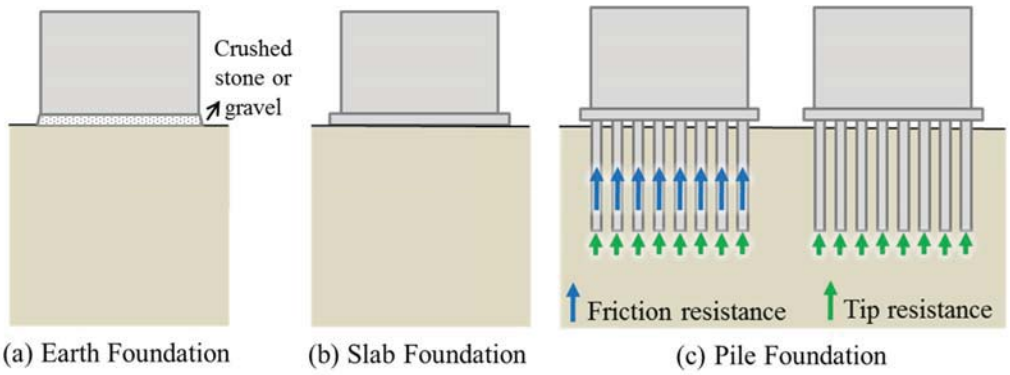

Figure 1.1. Different foundation types for oil tanks.

Piled raft foundations (PRFs) have received considerable attention in the recent years, especially since Burland et al. (1977) introduced the settlement reducer concept of PRF. The raft in this foundation system has adequate bearing capacity; therefore, the main objective of introducing the pile elements is to control or minimize the settlement, especially uneven settlement, rather than to carry the major portion of the vertical loads. Although the settlement in this foundation system can be reduced comparing to slab foundation but it is more than regular pile foundation. This larger settlement can secure the raft base contact with subsoil which is necessary in the concept of piled raft foundation.

One of the most important concerns in the seismic design of piled raft foundation is the secure contact of the raft to the subsoil. Without the contact, the contribution of raft cannot be assured against the horizontal load. To achieve the secure contact, the foundation settlement should be greater than the ground settlement. In the design of oil tank foundation, the main concern regarding the settlements is the uneven settlement, not the maximum settlement. For example, an allowable uneven settlement is 1/300 of tank diameter (FDMA, 1974), which implying that some level of tank foundation settlement is permitted if the uneven settlement is controlled below the allowable value. Therefore, the piled raft foundation is considered one of the rational foundation systems for the oil storage tanks.

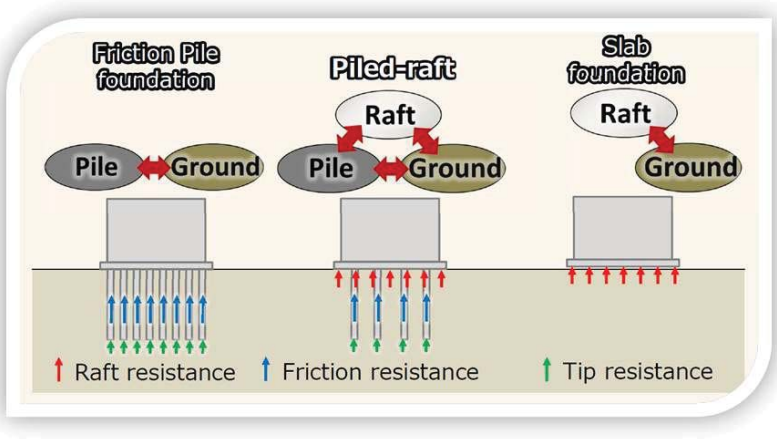

Figure 1.2. Foundation types and their bearing capacity mechanism.

On the other hand, while piles can either be driven into the ground (driven piles) or be installed in a predrilled hole (bored or non-driven piles) bearing capacity of foundation system depends on the pile installation procedure since it changes not only the structural behavior of the piles but also the stiffness and strength of the soil.

1.2. Objectives

In spite of some studies about piled raft foundations and also related case studies, optimal and rational design methods of piled raft foundation have not been extended to the civil engineering infrastructures. This is partly due to the complex soil-structure interaction between raft, ground and piles (Figure 1.2) especially during an earthquake. In particular, if the piled raft resting on a liquefiable ground, the soil-foundation interaction becomes more complex. Because of this complexity and possible large settlement, the practical implementation of piled raft foundation is further hindered.

The difference between behavior of piled raft foundations with driven and non-driven piles is another concern. Despite previous studies, the difference between the behavior of PRF with

driven and non-driven piles during dynamic loading has not been well investigated. On the other hand, although there are some studies about PRF design in the literature, the effect of piles number on the piled raft foundation of oil tanks on liquefiable sand has not been considered.

Physical modeling can be an appropriate way for investigating the behavior of oil tanks with piled raft foundation while it can consider different factors under clear boundary and initial conditions. In this way the superstructure behavior on the liquefiable and non-liquefiable ground and the PRF with driven and non-driven piles might be studied precisely. Therefore, in this research, dynamic centrifuge model tests were performed to investigate the mechanical behavior of oil tank supported by piled raft foundation on the liquefiable saturated sand and non-liquefiable dry sand. Also, a special setting was developed to model a driven PRF for the oil tank in-flight condition. In order to compare the behavior of oil tank supported by PRFs with driven and non-driven piles on the liquefiable saturated sand, some additional tests were performed. Moreover, for the driven piles PRF, the effect of piles number on the performance of PRF was also investigated.

1.3. Thesis Structure

This thesis consists of these chapters:

1. The literature review is explained in chapter 2. The previous studies about oil storage tank foundations are indicated. Also, the former researches about piled raft foundations such as numerical modeling, field studies, PRFs under various loading conditions, physical modeling of PRFs and PRFs with different pile installation method (driven and non-driven) are illustrated in the chapter.

2. Development of centrifuge modeling of oil tank with slab and piled raft foundation is

discussed in Chapter 3. Principles of centrifuge modeling, the modelled foundation and superstructure and instrumentations used in the tests are explained in this chapter. Furthermore, calibration techniques and tests procedures are included in the chapter.

3. The behavior of ground and tank on the dry (non-liquefiable) sand and saturated (liquefiable) sand are presented in Chapter 4. It includes ground response and tank response (tank accelerations, settlement and rotation). Also, piles and raft resistances during dynamic loading are considered in this Chapter. Furthermore ground excess pore water pressures in cases of saturated sand are discussed in detail in this chapter. Also, some introduction about soil liquefaction is included and liquid behavior inside the tank (sloshing) is explained for all cases.

4. Chapter 5 focuses on the practical application of the study. Pile and piled raft foundation differences are discussed in this chapter. Furthermore, special considerations for the rational design of piled raft foundations are described in this chapter. Also some practical points for the application of piled raft foundation for oil storage tanks on non-liquefiable and liquefiable sand are presented by employing the results of this study.

5. Chapter 6 illustrates the conclusions of the study along with some suggestions for the future researches.

Chapter 2 – Literature Review

2.1. Introduction

The Majority of existing oil storage tanks in Japan were constructed before early 1970's when the soil liquefaction was first considered in the design of tank foundation. Since the 1964 Niigata earthquake, the 1978 Miyagiken-oki earthquake (Ishihara et al., 1980) and the 1995 Hyogoken-Nambu (Kobe) Earthquake, it has become an urgent matter for geotechnical engineers to assess the seismic stability of existing oil storage tanks and implement proper countermeasures against soil liquefaction.

Since the concept of settlement reducer was introduced by Burland et al. (1977), piled raft foundation (PRF) has received remarkable attention, especially in reducing the construction expenses due to reducing the required piles number. The raft in this foundation system has adequate bearing capacity; therefore, the main objective of introducing the pile elements is to control or minimize the settlement, especially uneven settlement, rather than to carry the major portion of the vertical loads. Therefore, a major question on this type of foundation is how to design the piles optimally to control the settlement.

On the other hand, as mentioned before, a fundamental concern in this foundation system is secure contact between raft and subsoil. Because some level of settlement is acceptable in oil tank foundation while uneven settlement is less than an allowable value, this foundation can be considered as a rational foundation system in this kind of superstructures.

Furthermore, pile installation effect is another basic issue which affects the behavior of foundation and oil tank accordingly. Also, piles number is another effective parameter in piled

raft foundations behavior which should be contemplated seriously.

Considerable investigations have been conducted on the piled raft foundation especially foundation of regular buildings. Also some studies considered oil storage tank foundations. In addition, pile installation methods were concept of some researches previously. In this chapter, as the literature review, the prior investigations on the oil storage tank foundation will be discussed firstly. Afterwards, the previous studies on the piled raft foundation will be indicated and the literature review of pile installation techniques will be considered finally.

2.2. Oil Storage Tank Foundation

Some researchers have studied about oil tank foundations and have utilized different foundation systems in order to transfer storage tanks load into the ground. For example, performances of pile foundation of storage tanks were investigated in some case studies (Cubrinovski et al., 2001; Fellenius et al., 2013).

A case study of oil tank on pile foundations which was attacked by Kobe earthquake (1995) were carried out by Cubrinovski et al., (2001). They investigated the effects of ground improvement and liquefaction and piles response due to lateral spreading of liquefied soils is discussed. They conducted two series of analyses separately in order to examine the effects of cyclic liquefaction and subsequent lateral spreading. Based on their results, in both loading phases, the large lateral ground displacement was the main reason of piles response and a sand compaction ground improvement effectively reduced the deformation of the subsoil and enhanced the performance of the piles (Figure 2.1 and 2.2).

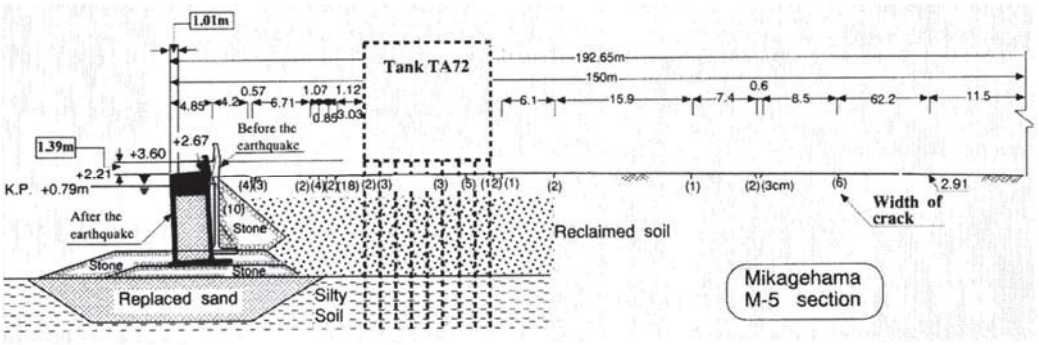

Figure 2.1. Detailed profile of the quay wall movement and ground deformation in the tank location. (Cubrinovski et al., 2001)

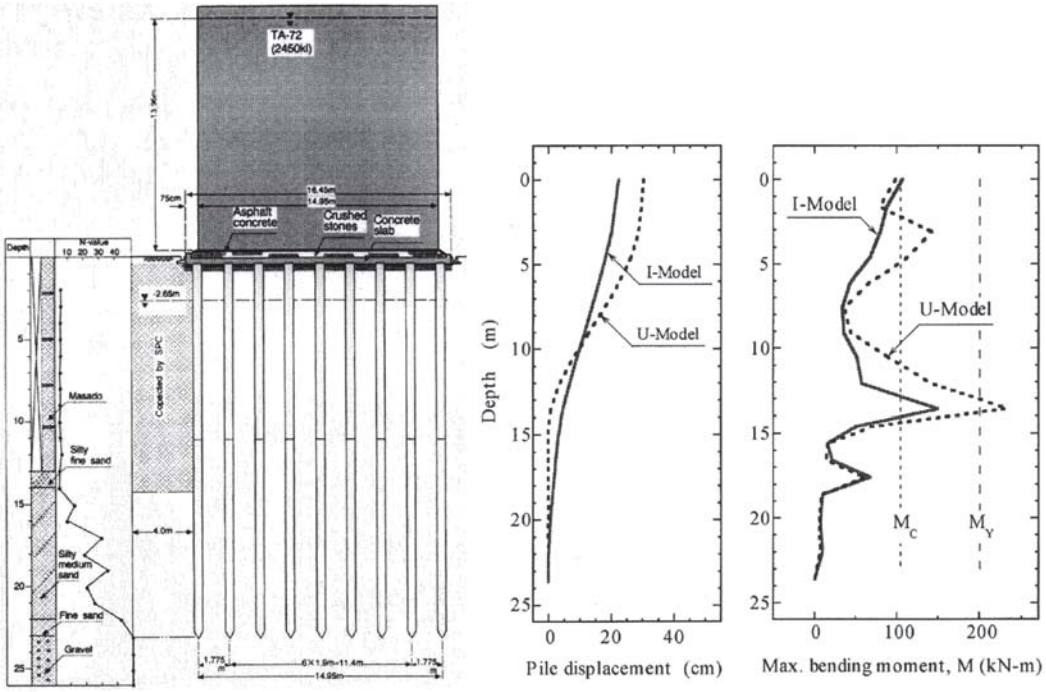

(a) Cross sectional view of tank. (b) Computed response of piles in FEM.

Figure 2.2. (Cubrinovski et al., 2001).

Also, Fellenius et al. (2013) reanalyzed settlement of five case studies and the findings are used to address the analysis of a typical large piled foundation for a LNG tank at a site with a thick soil profile consisting of clay, sand and gravel. The differential settlement and effect of

drag and down drag load were discussed. Furthermore, the limitations of drag load as an effect of the pile spacing and the weight of the soil in-between the interior piles are discussed. Sento et al. (2004) reported case studies about oil tanks on liquefiable sandy soil and compaction method as the countermeasure. They used sand compaction pile method and compared seven liquefaction analysis codes mostly used for practical design in Japan. They studied effect of input wave amplitude and configuration of compacted soil cross section. The results show that despite some differences among codes in vertical displacement quantitatively, reasonable tendencies on input wave amplitude and the effectiveness of countermeasure were confirmed qualitatively. The results might be beneficial to determine the countermeasure configuration in cross section for tanks foundation.

Also a few researchers have considered piled raft foundations for the oil tanks. A case study of oil storage tank with piled raft foundation was done by Liew et al. (2002). They present the design concept to support 2500ton oil storage tanks on a very soft alluvial clayey soil of about 40m thick. The floating piles were designed to support the tanks seating on a 20m diameter circular raft. Using different instrumentation it has been shown that the floating piles can be a cost effective design to support heavy structures on very soft compressive deposits with satisfactory performance. Chaudhary (2007) utilized FEM to study the behavior of piled raft foundation for a huge storage tank. He investigates the application of a group of 1072 piles for controlling settlement of an important structure founded on weak rock. 2D axi-symmetrical and 3D FEM are employed to model the raft underlying rock and pile layout. Effectiveness of piled raft foundation in reducing settlement is assessed by comparing the results with the case of raft foundation alone. He concludes that the piles are so effective in reducing settlement for rafts founded on weak rock (Figure 2.3).

As few researches on PRF of oil tanks on the liquefiable sand, Imamura et al. (2010) and Takemura et al. (2014) investigated about the dynamic response of oil tank supported by PRF using centrifuge modelling. Imamura et al. (2010) compared mechanical behavior of piled raft and slab foundation on liquefiable sand. Based on their results, due to higher excess pore water pressure generated by shaking under the piled raft foundation, the piles bearing load decreased caused increase of raft load proportion (RLP). Despite larger settlement of piled raft due to increase of raft load, the uneven settlement was smaller for the piled raft than the slab foundation (Figure 2.4).

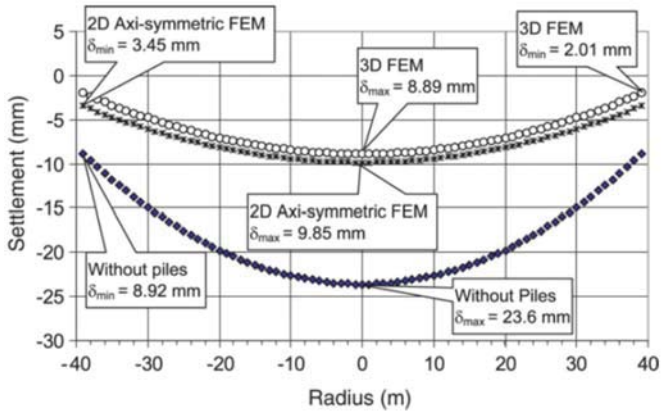

Figure 2.3. Comparison of raft settlement in radial direction (Chaudhary, 2007).

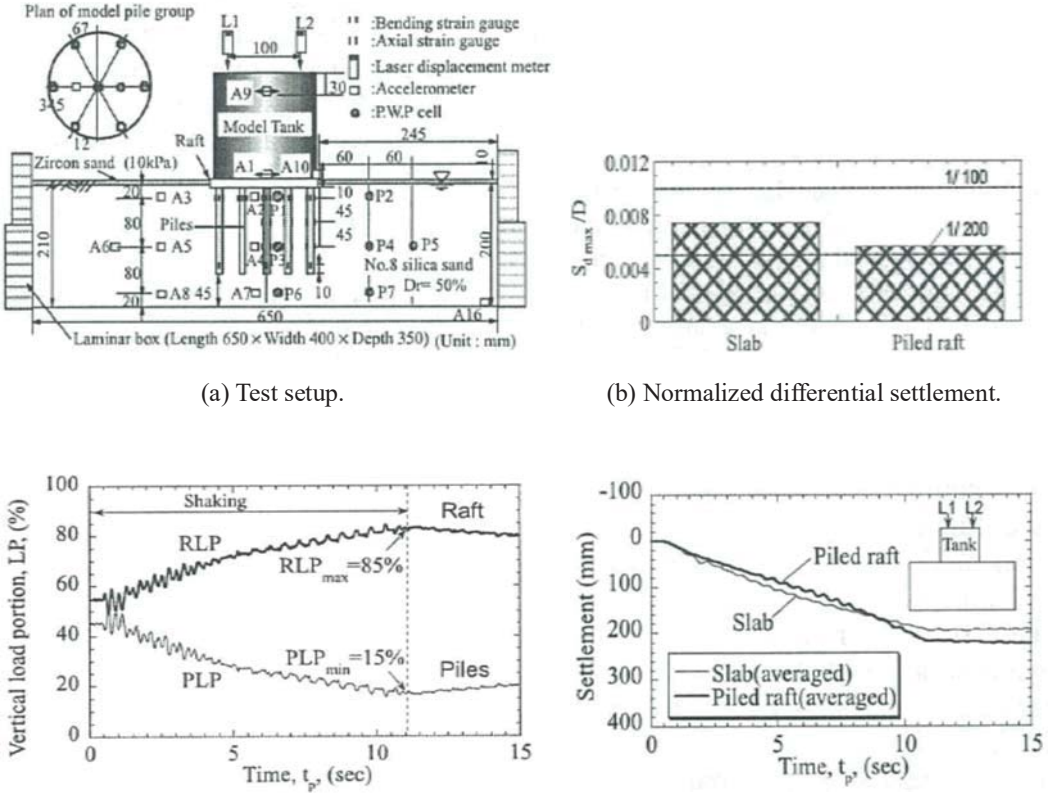

(a) Test setup. (b) Normalized differential settlement.

(c) Variation of vertical load portion during shaking. (d) Tank settlement during shaking.

Figure 2.4. (Imamura et al., 2010).

Also Takemura et al. (2014) performed a series of centrifuge model tests to investigate mechanical behavior of oil tank supported by piled raft foundation on liquefiable and dry sand. They modelled two types (slab and piled raft) of foundations. They concluded that PRF is so effective in reducing uneven settlement of tank in dry sand. In saturated sand their result shows effectiveness of piled raft foundation in reducing rocking motion of tank but not in decreasing the settlement when the water table is on the sand surface. By decreasing the water table height the performance of piled raft was improved significantly (Figure 2.5). From these researches dynamic and permanent behavior of foundations were well observed. However, the observations were only made in the shaking direction, not in the different directions.

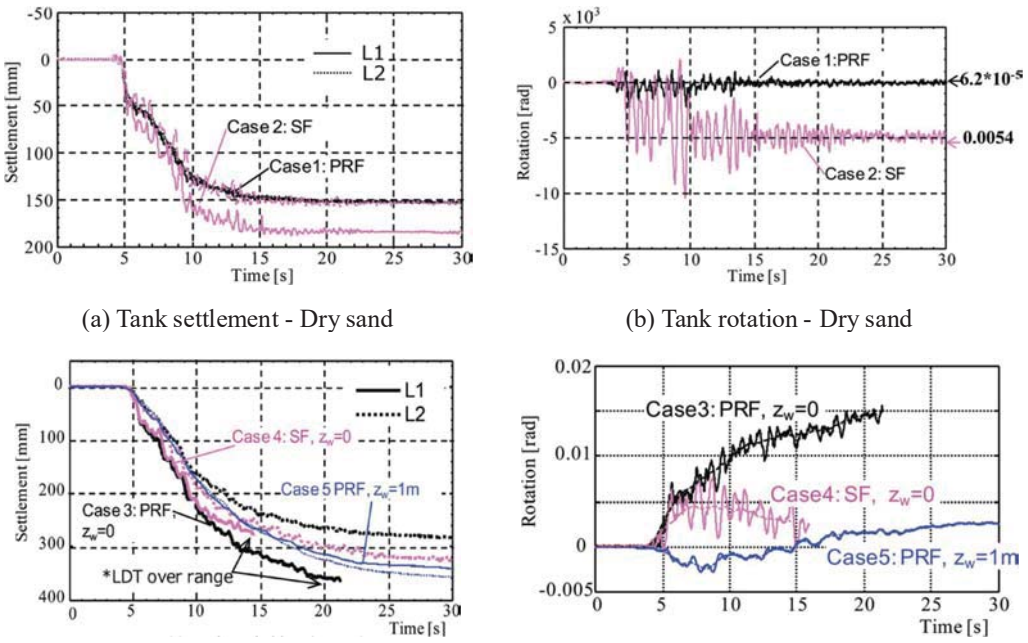

(a) Tank settlement - Dry sand

(b) Tank rotation - Dry sand

(c) Tank settlement - Saturated sand

(d) Tank rotation - Saturated sand

Figure 2.5. Tank settlement and rotation on dry and saturated sand (Takemura et al., 2014).

2.3. Piled Raft Foundation

Some investigations have been conducted on the behavior of piled raft foundation under various loading conditions and by different study methods which is presented in this section. Some of these studies applied this foundation system for real structures but almost all of these efforts were focused on the regular structures or normal high-rise buildings. On the other words, up to now, slender structures were the major purpose of these studies while the main objective of this research is oil storage tank which is a flat or wide structure. The main difference between these two types is the loading mechanism. In the oil tanks the ratio of structure weight to overturning moment is larger than high-rise buildings which deeply affect the distribution of the loads between foundation elements. Another gap in the previous studies of PRF is the foundation performance on the liquefiable ground due to difficulties in the modeling of the foundation system and measurement of raft and piles load proportions. Furthermore, piles installation procedure is another concern and will be discussed later.

2.3.1. Analytical Study

A major design question in piled raft foundations is how to design the piles optimally to control the settlement. For this purpose, some analytical researches have been conducted in order to present design methodology of this foundation system. Poulos (2001) discussed the philosophy of using piles as settlement reducers and the conditions under which such an approach may be successful. He proposed a three-step design procedure. The first stage is a preliminary step in which the effects of the number of piles on load capacity and settlement are assessed via an approximate analysis. The second step is a more comprehensive check to evaluate where piles are essential and to obtain some hint of the piling necessities. The third is a detailed design phase in which a more refined analysis is employed to confirm the optimum number and location of the piles. Furthermore, some applications of PRFs are explained and computed and measured behavior of foundations are compared.

Horikoshi et al. (1998) presented a framework for a new design concept via the results of a parametric study, in which piles are installed only beneath the central area of a relatively flexible raft to minimize the differential settlement. They used the hybrid approach which was developed by Clancy. The results indicated that PRF may be designed for insignificant uneven settlements by introducing a group of pile in the central part (16-25%) of the raft. In this case, the stiffness of pile group should be similar to that of the raft alone nearly. The total pile capacity should be about 40-70% of the total applied load, depending on the pile group area ratio and the Poisson's ratio of the soil. They checked the validity of the procedure through their centrifuge model tests results.

Poulos et al. (2011) considered design of piled raft foundations for tall buildings. Their research sets out some principles of design for piled raft foundations, including design for the

geotechnical ultimate limit state, the structural ultimate limit state and the serviceability limit state. The advantages of using a piled raft was described with consideration of a small pile group subjected to lateral loading and the design of a tall building in South Korea. They focused on the improvement of foundation behavior because of the raft contact with, and embedded within, the soil. Their results indicate that for tall buildings which are supported by PRF with a large number of piles, a conventional pile group analysis may be satisfactory, while it may be conservative, for assessing the vertical and lateral behavior of the foundation and the pile load and bending moment distributions between the piles.

Also, design issues on piled raft foundation system were discussed with particular reference to buildings on soft ground by Tan et al. Their design method is divided into two types, i.e. low-rise buildings and medium-rise buildings. The piled raft system for low-rise buildings is generally based on the concept of settlement reducing piles to control local deformation where piles of short length are strategically located beneath concentrated loads. For medium rise buildings, piles of varying length with the longest piles in the middle and progressively shorter piles towards the edge are adopted to control uneven settlement within allowable limits. They validated the proposed design approach using various case histories designed by them and extensive monitoring results on the completed structures. Cooke (1986) tried to combine information on some of the aspects of design. He considered un-piled rafts, free-standing piles and piled rafts of various sizes. The research recommends that the settlements of structures on PRFs are possible to be similar with the settlements of structures on un-piled rafts of similar sizes at the same safety factors. In this study, the empirical methods are presented for evaluating the contribution of the raft and for eastimating the numbers of piles essential for settlement reduction. The need for piles to be as long as possible in relation to the width of the foundation is illustrated.

Some researchers utilized Finite element modelling (FEM) to study the effect of raft and pile dimension on the behavior of this foundation system. Alnuiam et al. (2013) established a 3D finite element model to analyze the response of piled raft foundation system installed in cohesion-less soil with linearly increasing stiffness with depth. The model was calibrated/verified using geotechnical centrifuge test data. The calibrated model was then employed to investigate the effect of raft dimensions and piles diameter and spacing on the load sharing between piles and raft. Based on their results, the load share carried by piles is higher for a rigid raft due to the minimal interaction between the raft and subsoil compared to the perfectly flexible raft. The piles load proportion increases as the pile diameter increases. However, the rate of increase is higher for small size piles and diminishes as the pile diameter increases. Ziaie-Moayed et al. (2010) investigated the behavior of piled raft foundations with different pile diameters under vertical loading. They modelled the raft, piles and supporting soil by 3D FEM. Based on their results, using piled raft with different pile diameters in all types of soils, with unequal applied loads, has better operation than piled raft system with similar piles. But its behavior is not the same in all soils. Results show that the piled raft foundation with different pile diameters may be a good solution to reduce total and uneven settlements if the bottom layer is a dense soil. Otherwise, using piled raft with different piles diameter is not a good way to control maximum and uneven settlement. In this condition, piled raft with different length piles may be a reasonable substitute to control the total and uneven settlements. The bearing-settlement behavior of combined pile-raft foundations on medium dense sand was investigated by Baziar et al. (2009). They utilized 1g physical model test on a circular rigid raft underpinned with four model piles along with Numerical simulation using FLAC-3D, to show compatibility of the numerical analysis with the test. The obtained results showed very good accuracy of the numerical method used in this study as long as the applied load does not exceed

the working load, while the performance of numerical model was relatively good for the loads beyond working load. Singh et al. (2008) presents the result of a FEM for piled rafts in cohesive soils. The research recommends that a thicker raft is not beneficial necessarily in reducing settlement. Based on their result, the center pile carries the maximum load, followed by the edge pile and then the corner pile, which carries the minimum load. The piles reach their ultimate capacity earlier than the raft, and are thus effective in reducing overall settlement. They declared restricting the number of piles to make them reach their ultimate capacity earlier than the raft is more beneficial. Eslami et al. (2012) modelled connected and non-connected pile-raft systems employing 2D and 3D FEM on three case studies; a 12-storey residential building in Iran, a 39-storey twin towers in Indonesia, and the Messeturm tower, 256m high, in Frankfurt, Germany. They investigated about the effect of different parameters, e.g. piles spacing, embedment length, piling configuration and raft thickness in order to optimize the design. The role of each parameter is also investigated. The results of study and the comparison to some field measurements show that by concentrating the piles in the central part of the raft the optimum design with the minimum total length of piles is obtained. This can be considered as a criterion for project cost efficiency. On the other hand, non-connected PRFs can remarkably decrease the settlements and raft internal bending moments via enhancing the subsoil stiffness. Finally, the comparison indicates that simple and faster 2D analysis has almost similar results to the time consuming and complicated 3D analysis. In addition to these studies, Prakoso et al. (2001) presented a broad-based parametric study on the behavior of vertically loaded piled raft foundations using elastic and elastic-plastic finite element models. They investigated the effects of geometry of elements and pile group compression capacity on the uneven settlements, raft bending moments and pile load ratio. The results showed that, the most important parameters of system geometry are the pile group to raft width ratio and pile depth. A width ratio of one is the

most effective to minimize the average displacement while a width ratio of 0.5 is the most effective to minimize the differential displacement. The width ratio and pile depth should be determined together by an iteration process in order to minimize both displacements. A pile to raft area ratio, which is a combination of pile spacing and pile diameter, of about 5-6% is adequate to minimize the displacements. Smaller pile to raft area ratio causes less raft bending moments and more efficient pile group load transfer mechanism. The raft thickness should be best determined based on the structural design. They combined the results in order to present a more integrated displacement-based design approach for piled raft foundations.

Lee et al. (2016) presented a computer program that utilizes a hybrid analysis procedure for design of piled raft foundations. The interactions between pile-soil, raft-soil, pile-soil-pile and raft-soil-pile are considered in their method. Also, influence of nonlinear behavior of piles and the interactions between piled raft components and soil are studied by comparing with 3D FEM program analysis results. The results indicate that if a stress larger than yielding stress is applied on the piles, the linear analysis methods show significant error. So it is necessary to estimate the non-linear behavior of piles after yielding for the economic design of piled raft foundations.

Chaithra et al. (2015) presented the results of an evaluation of seismic performance of a fifteen stores building with piled raft foundation. They used linear time history analysis by FEM and different parameters like displacements, base shear and settlements are compared and effect of piled raft foundation is studied. Their results show that the soil structure interaction effects are almost same for raft and piled raft foundations when the structure is located on hard and dense soil. But in case of soft soil the interaction effect is larger and the building with raft foundation vibrates more than piled raft foundation. Regarding the results the base shear and displacements increases with soil flexibility. The base shear is related to the soil condition. They

declared that displacement in the soft soil may be decreased by providing piled raft foundation and the same happened for the raft settlement in the existence of piles beneath the raft.

Some case studies of piled raft foundation of high-rise buildings are presented by Shukla et al. (2011, 2013, 2015). They utilized FEM method using SAP2000 in order to conduct 3D time history analysis of non-linear soil-foundation-structure models under dynamic loading. They also, studied the effect of various parameters such as size and thickness of raft, piles diameter and length, configuration of piles and stiffness of raft and piles which affect the performance of piled raft foundation. Type of sub-soil was also considered in the analysis. Based on their results they declared that in order to decrease the uneven settlement of foundation piles should be located strategically by trial and error. They also indicated the effectiveness of FEM method and recommended to use shell elements for modeling the raft, beam elements for the piles and soil beneath the raft and around the piles can be modelled by spring elements. Also they showed that PRF can have better performance on dense sand.

2.3.2. Field Study

Piled raft foundations have been used for building design and some case studies of buildings have been reported. Field measurements were employed in these cases to estimate several parameters such as settlement, uneven settlement, load sharing between piles and the raft and effective pile spacing.

Five recent case histories of piled raft foundations in Japan are presented by Yamashita et al. (2011) and Yamashita (2012). The buildings are with different heights and were completed recently. The piled rafts were designed based on a simple analytical method developed by the authors. In order to validate the foundation design method, field measurements were performed

on the foundation settlements and the load sharing between the rafts and the piles by monitoring the five structures from beginning of their construction to some month after the end of their construction. The measured settlements were 19 to 24 mm, and the ratios of the load carried by the piles to the effective load of each structure in the tributary area, α_P', were estimated to be 0.61 to 0.93 at the end of the observation period. The predicted maximum settlements and angular rotations of the rafts in the design were generally consistent with the measured values, and the ratios of the load carried by the piles to the total load assumed in the design were also consistent with those estimated from the measurements. Based on their current and previous results, it has been found that the value of α_P' generally decreases as the pile spacing ratio is increased. This value seems to decrease gradually with a pile spacing ratio larger than about six, whereas the value decrease significantly as the pile spacing ratio is increased from about four to six (Figure 2.6). Their results suggest that piled rafts work more effectively at a pile spacing ratio of larger than about six, where at least 30% of the effective load of the structure can be carried by the rafts.

Also Yamashita et al. (2014) offers a case study of a low-rise building, located in Ibaraki, Japan. The structure is supported by a piled raft in medium to dense sand underlain by over consolidated silty soil. To confirm the validity of the foundation design, field measurements were performed on the foundation settlement and the load sharing between the piles and the raft from the beginning of the construction to 80 months after the end of construction. During the monitoring period, 44 months after the end of the construction, the 2011 off the Pacific coast of Tohoku earthquake struck the site of the building. The peak horizontal ground acceleration of 3.24 m/s^2 was observed in the neighborhood of the building. Although the foundation settlement in raft center increased by 4 mm due to earthquake (Figure 2.7), the load sharing of piles and raft does not have significant change during the shaking.

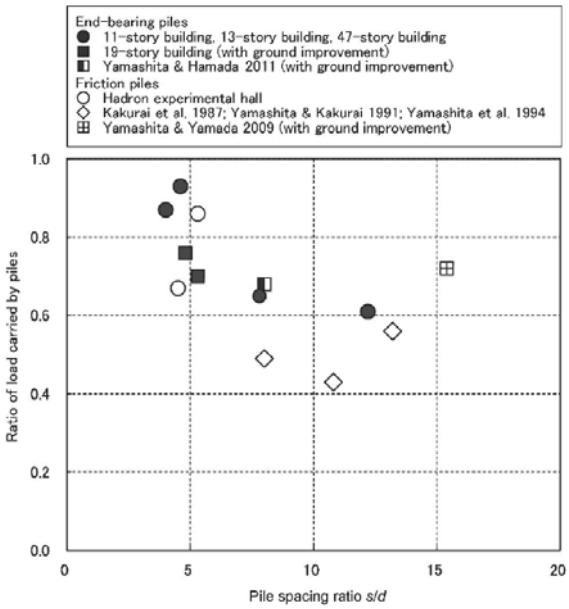

Figure 2.6. Ratio of load carried by piles to effective load vs pile spacing ratio (Yamashita et al., 2011).

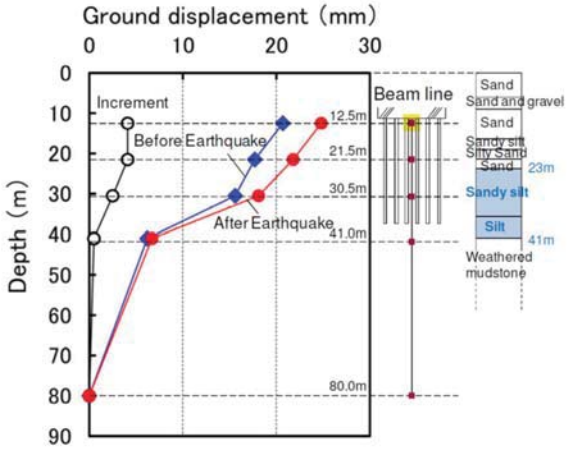

Figure 2.7. Profile of vertical ground displacements (Yamashita et al., 2014).

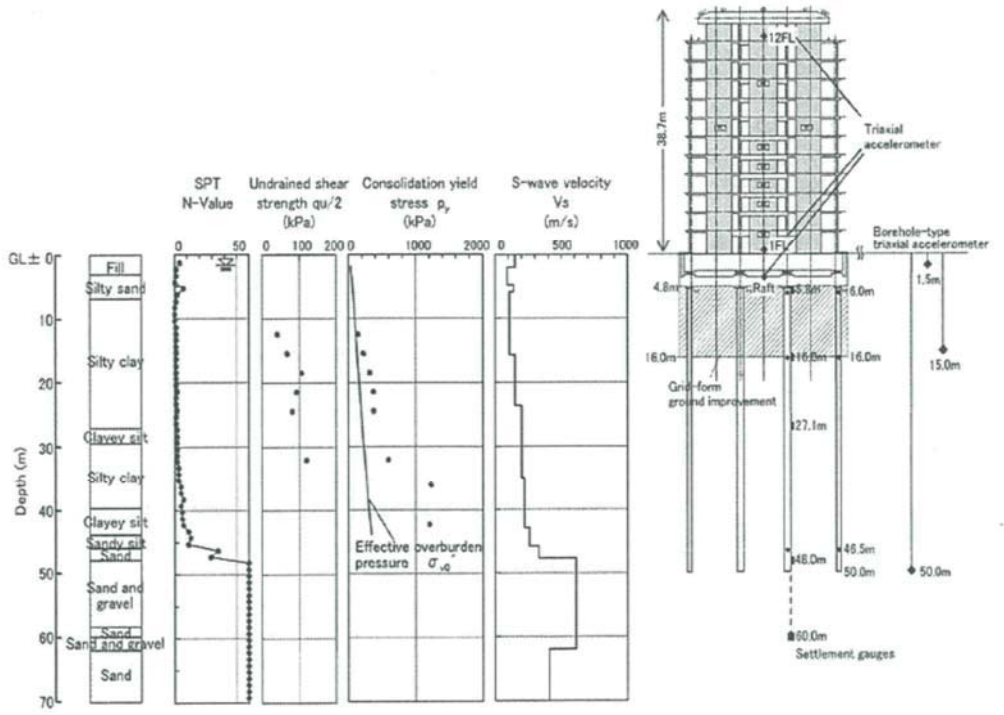

Figure 2.8. Schematic view of building and foundation with soil profile (Yamashita et al., 2012).

Using monitoring of the soil–foundation–structure system, the static and seismic behavior of a piled raft foundation, supporting a 12-story base-isolated building in Tokyo (Figure 2.8), is investigated by Yamashita et al. (2012). A PRF with grid-form deep cement mixing walls was utilized to deal with the liquefiable sand in addition to enhance the bearing capacity of the raft foundation while the structure was constructed on loose silty sand which was underlain by soft cohesive soil. Field measurements were carried out on the ground settlements, the pile loads, the contact pressure and the pore-water pressure beneath the raft from the beginning of the construction to 43 months after the end of the construction in order to confirm the reliability of the foundation design. 30 months after the end of the construction, the 2011 off the Pacific coast of Tohoku Earthquake struck the building site. During the earthquake, the seismic response of the ground and the foundation–structure system was successfully recorded, and a peak

horizontal ground acceleration of 1.75 m/s^2 was observed at the site of the building. A little change in the foundation settlement and the load sharing between the raft and the piles before and after the earthquake was found based on static and dynamic measurement results (Figure 2.9). The horizontal accelerations of the superstructure were reduced to approximately 30% of those of the ground near the ground surface by the input losses due to the kinematic soil–foundation interaction in addition to the base isolation system. Consequently, the piled raft with grid-form deep cement mixing walls was found to be quite stable in the soft ground during and after the earthquake.

Hirakawa et al. (2016) presented a case history of the tallest building in Japan that is 300m height above ground level and located in Osaka. The structure foundation is a piled raft that includes a raft at 30.5m below ground level and cast-in-place concrete piles embedded in dense gravel layer. They performed a field monitoring on the settlement and the load sharing of the piled raft. The observation results indicate the acceptable performance of the foundation. Furthermore, it is observed that measured settlements and estimated load sharing between the piles and raft are compatible with the design values.

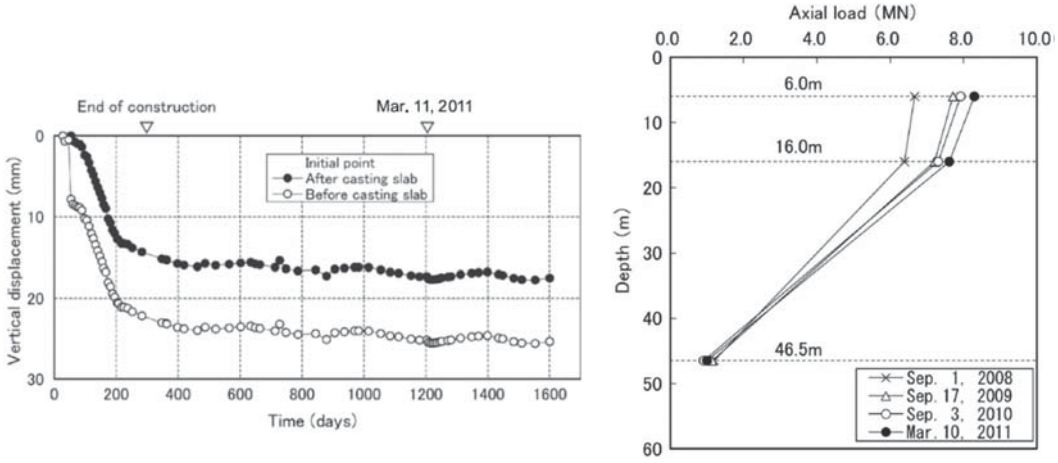

(a) Foundation settlements. (b) Measured axial load distribution on a pile.

Figure 2.9. (Yamashita et al., 2012).

Also, Poulos et al. (2008) reported a case history of using piled raft foundation for the tallest high-rise building in the world (the Burj Dubai) located in Dubai, Emirates. The foundation system, a piled raft rests on deep deposits of carbonate soils and rocks. The detailed design process and geotechnical experiments utilized for the foundation design is explained by the authors. Using the instrumentations, the settlements of the tower measured during the construction is compared with the predicted values. The results show that the settlements observed during construction are consistent but smaller than predicted values and the general performance of the piled raft system is better than the expectations.

2.3.3. Study of Piled Raft Foundation under Various Loading Conditions

2.3.3.1. Static Loading

In order to investigate about complicated behavior of piled raft foundation system, some researches have been done about the application of this foundation under various loading conditions. Static lateral and vertical loading tests were conducted by some researchers to evaluate the application of piled raft foundation and discuss on the optimized parameters, e.g. raft size, number of piles, piles spacing and its behavior.

2.3.3.1.1. Horizontal Loading

The results obtained from lateral load tests on model pile groups and model piled raft foundations in Toyoura sand in 1g condition is presented by Pastsakorn et al. (2002). Raft size, piles number, piles spacing and pile rake angle were changed during the model tests. The piled raft foundation showed about two times higher lateral resistance than that of the pile group

foundation, for model foundations with the same configuration. The lateral resistance of the foundation in pile groups, increased almost linearly with the increasing number of piles. In piled rafts, the lateral resistance did not necessarily decrease with a decreasing number of piles, while the lateral resistance of the raft base compensated for the reduction of the number of piles. Also, they used batter piles in order to check their behavior. Use of them greatly improved the performance of not only pile groups but also pile raft foundation during lateral loading.

Static cyclic lateral loading tests on piled raft foundations at large scale conducted by Hamada et al. (2012) in order to study the influence of various vertical load and pile spacing ratio during earthquake. Pile groups and piled rafts were modeled with a concrete footing supported by 16 piles in 1g field. According to the results, majority of the lateral force was supported by raft friction while large contact earth pressure beneath the raft was measured, and the piles encountered pulling such as an anchor during large deformation. Using a simplified method based on Mindlin's solution considering a non-linearity of soil deposit and theoretical equations derived with some approximation and assumptions, simulation analysis on the tests were conducted. The calculated results showed good agreement with model tests results.

Furthermore, 1g experimental and analytical studies were performed by Matsumoto et al. (2004a, 2010) for static lateral loading conditions to investigate the effects of pile head connection conditions between the raft and piles. They modeled a series of static horizontal load tests on model piled rafts at 1g gravitational field by using dry Toyoura sand (Matsumoto et al., 2004a). Triaxial consolidated drained shear tests of the sand were performed to examine the effects of confined stress on soil modulus and confirmed the similitude for the present 1g models. The acting force height and the rigidity of the pile head connection were considered during the tests. Also, the results of the simplified three dimensional deformation analyses of the

model tests are presented in this paper. The results show reasonable agreement with the experimental results in the initial elastic region. It is indicated from the model tests and the analyses that horizontal displacement and inclination of the raft and bending moments of piles for a given horizontal load are increased as the height of horizontal loading point or moment load is increased. Furthermore, horizontal displacement and inclination of the raft and bending moments of piles are reduced in the piled raft with hinged pile head connection compared to the piled raft with rigid pile head connection when subjected to moment load.

2.3.3.1.2. Vertical Loading

Also, Matsumoto et al. (2010) conducted a series of experimental and analytical studies on the behaviors of model pile groups and model piled rafts in dry sand subjected to static vertical loading and static cyclic horizontal loading in order to study the influence of various pile head connection conditions between the raft and the piles on the behaviors of the foundations models and to examine the applicability of an simplified analytical method to simulate the load tests. The behaviors of the model foundations were investigated in the load tests, with particular focus on cyclic horizontal loading, and behavior such as horizontal stiffness and the rotation of the foundation, the load proportions between the raft and the piles, and the bending moments and shear forces generated in the piles. Furthermore, in order to simulate the tests a simplified three dimensional deformation analysis method was utilized. Regarding their results, the vertical settlement stiffness of the piled raft is larger than that of the pile group and the raft alone for smaller loads, and decrease to that of the raft alone as the vertical load increases. The pile head connection condition has little influence on the behavior of the pile groups and the pile rafts subjected to vertical load alone. Mobilized shaft resistance along the upper part of the pile in

piled rafts is much smaller than that in the pile group due to interaction between the raft and the piles through the ground. The horizontal stiffness of the piled rafts is larger than that of a pile group with the same configuration as the piled raft, because the raft acts effectively as a horizontal displacement reducer. Piled raft reduced the bending moment of piles comparing to pile groups. In the case of the piled rafts, rotation of the raft decreases as the pile head connection rigidity becomes lower, although the horizontal stiffness also becomes lower. Finally, the horizontal loads carried by the piles in the piled rafts are not influenced by the pile head connection rigidity, whereas the horizontal load proportion carried by the raft becomes lower as the pile head connection becomes less rigid (Figures 2.10).

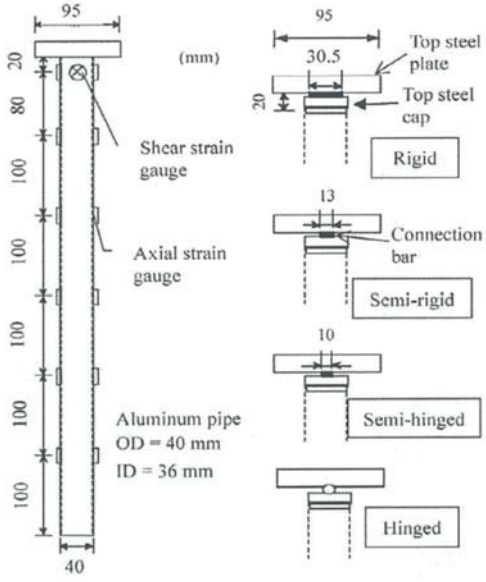

Figure 2.10 (a). Model piles with different pile head connection condition (Matsumoto et al., 2010).

Test name	Type of foundation	Pile head connection condition
Case 1: Raft	Raft alone	—
Case 2: PG-R	Pile Group	Rigid
Case 3: PG-H	Pile Group	Hinged
Case 4: PR-R	Piled Raft	Rigid
Case 5: PR-SR	Piled Raft	Semi-rigid
Case 6: PR-SH	Piled Raft	Semi-hinged
Case 7: PR-H	Piled Raft	Hinged

PG: Pile Group, PR: Piled Raft
R: Rigid connection, SR: Semi-rigid connection
H: Hinged connection, SH: Semi-hinged connection

Figure 2.10 (b). Test cases and pile head connection conditions (Matsumoto et al., 2010).

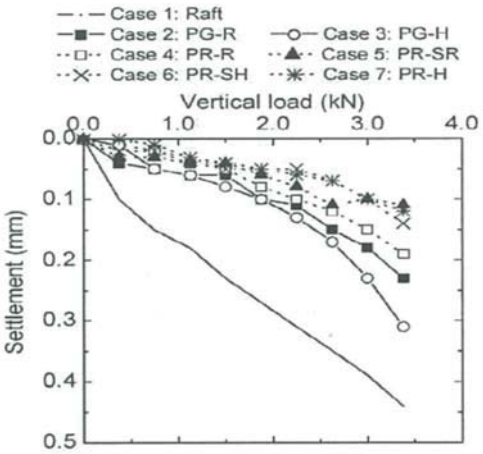

Figure 2.10 (c). Vertical load-settlement relationship (Matsumoto et al., 2010).

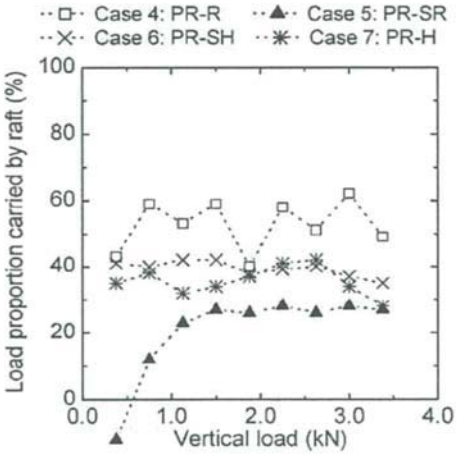

Figure 2.10 (d). Vertical load vs load proportion relationship (Matsumoto et al., 2010).

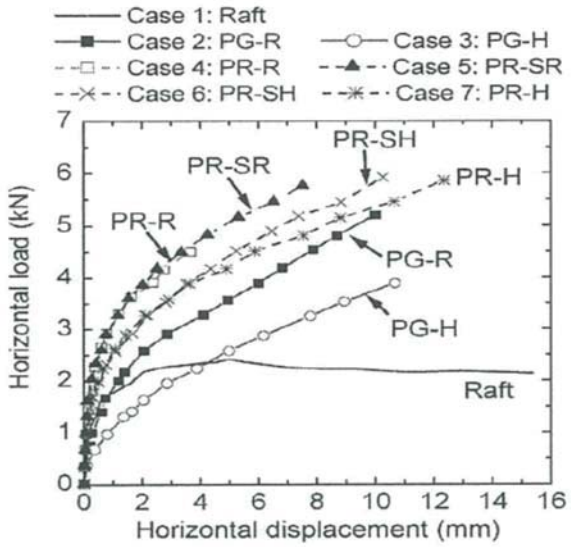

Figure 2.10 (e). Horizontal load vs horizontal displacement at maximum load in each cycle (Matsumoto et al., 2010).

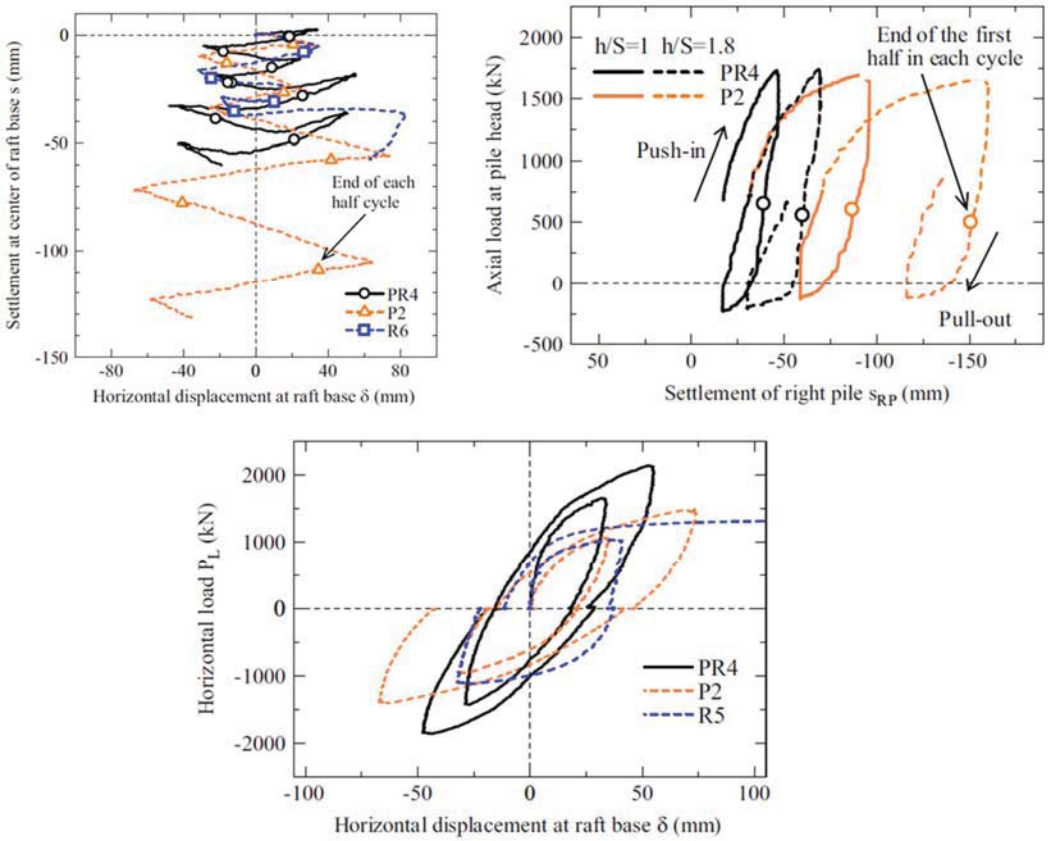

Figure 2.11. Comparison of behavior of piled raft (PR), pile (P) and raft (R) foundations (Sawada et al., 2014).

2.3.4. Study of Piled Raft Foundation Using Physical Model Tests

To study the mechanical behavior of piled raft foundation, physical model tests have also been conducted by some researchers not only under static loadings but also dynamic loadings.

2.3.4.1. Static Loading

2.3.4.1.1. Horizontal Loading

Sawada et al. (2014) conducted a series of static horizontal loading tests on raft, pile group

and piled raft foundation on sand using a geotechnical centrifuge. They investigated the influences of relatively large moment load and rotation on the performance of laterally loaded piled raft foundation. The results show that the vertical displacement due to horizontal loads is different between piled raft and pile group foundation, and it has important effects on the performance of laterally loaded piled raft foundation. The horizontal resistance of piles in the piled raft foundation is higher than those observed in the pile group foundation due to raft base contact pressure. Also, they showed that the vertical displacement of the foundation due to the horizontal loads affects the vertical resistances of piles, which results in the different mobilization of moment resistances between the piled raft and pile group foundations. They also declared the following points. The piled raft foundation can effectively reduce the settlement caused by the alternate loads while this horizontal and moment loads cause a large amount of settlement for the pile group foundation (Figure 2.11).

Also, using geotechnical centrifuge a series of horizontally and vertically static loading tests were conducted on piled raft models and their components (single piles and raft alone) on sand by Horikoshi et al. (2003). Load-displacement relationship and the load sharing between the piles and the raft in the piled raft system were focused more. Also, effects of the rigidity at pile head connection on the piled raft behavior were considered. Main findings from their research are: 1-Due to the difference in the confining stress condition around the piles, the stiffness and the resistance of the single pile in piled raft foundations are different from those observed in the isolated single piles of the same size. 2-Piles significantly increase horizontal ultimate resistance of piled raft foundation. 3-The initial horizontal stiffness of a piled raft is not always higher than that of a raft because the piles reduce the contact pressure between raft and soil, and the stiffness of the upper soil. 4-The piles with rigid pile head connection received higher horizontal load and caused higher initial horizontal stiffness compared with that in the

piled raft with hinged pile head connection. 5- The proportion of vertical load carried by the piles in a piled raft remains largely unchanged during horizontal loading while this proportion carried by the piles increased as the horizontal displacement increases (Figures 2.12).

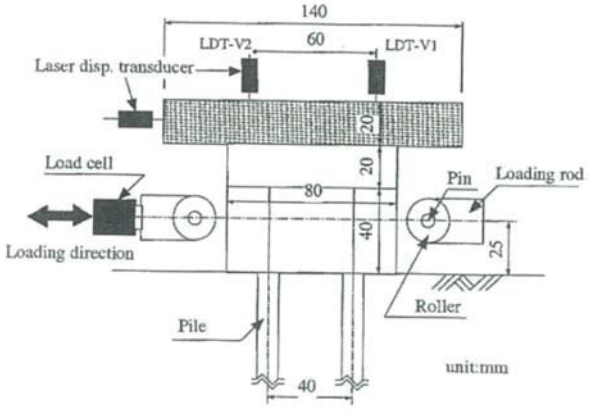

Figure 2.12 (a). Illustration of horizontal loading system (Horikoshi et al., 2003).

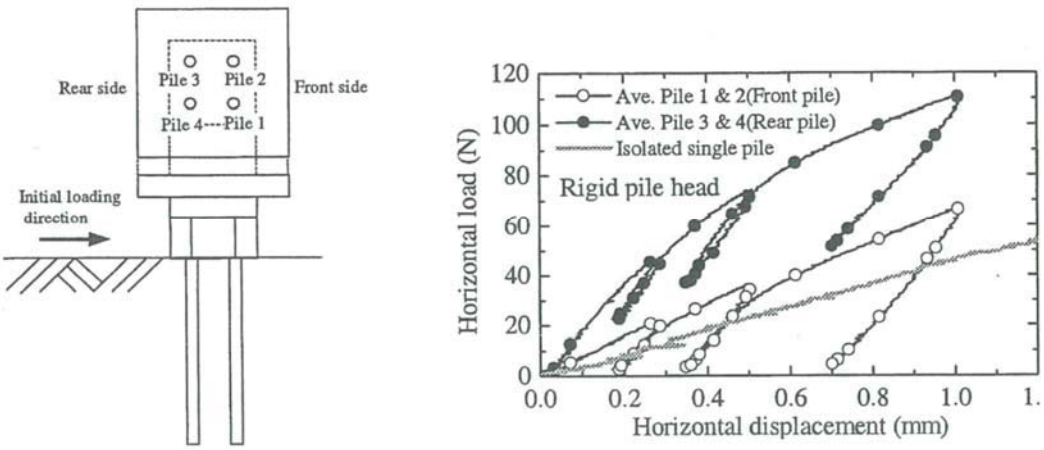

Figure 2.12 (b). Horizontal load-displacement relationships of piles in rigid pile head model, together with that of single pile (Horikoshi et al., 2003).

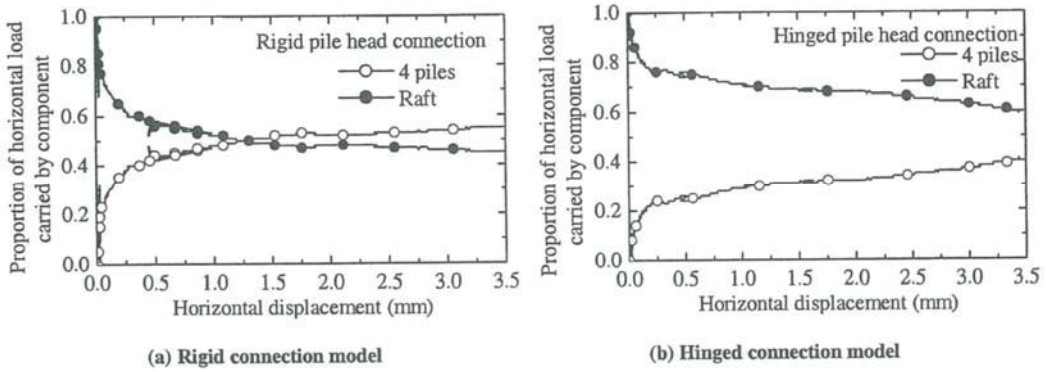

(a) Rigid connection model (b) Hinged connection model

Figure 2.12 (c). Proportion of horizontal load carried by each component (Horikoshi et al., 2003).

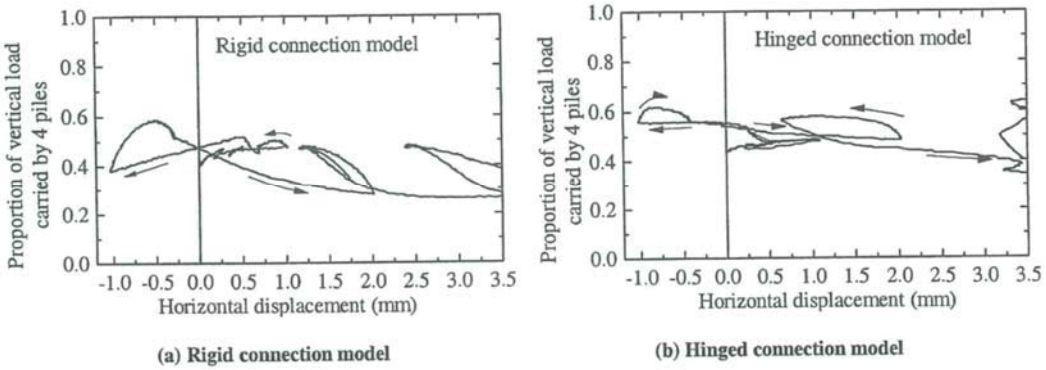

(a) Rigid connection model (b) Hinged connection model

Figure 2.12 (d). Proportion of vertical load carried by piles (Horikoshi et al., 2003).

2.3.4.1.2. Vertical Loading

Thaher et al. (1991) investigated about some aspects of the behavior of vertically loaded piled raft foundations on saturated over-consolidated clay using centrifuge model technique at the Bochum Geotechnical Centrifuge. They discussed the influence of pile number, length and diameter on the contact pressure and pile load distribution under working conditions. The load sharing between the raft and piles also is considered. They presented some points for design practice. Furthermore, the tests results are compared with prototype observation results. They modeled a case study of a tower piled raft foundation and the results are introduced. Based on

their results in a symmetrically and regularly arranged pile group underneath a rigid foundation raft, the contact pressure peak values and the pile load distribution is similar to the contact pressure distribution for the raft without piles. Also, as a result of consolidation, the total pile load increases up to 10% of the total structure load, which is related to decreasing of the total raft load. The total pile load depends strictly on the pile diameter and spacing. The effect of pile number is more important than that of the pile length. Regarding their results, a key parameter for piled raft foundation design is the ratio of pile spacing to pile diameter.

Horikoshi et al. (1994, 1996) investigated about the settlement behavior of a piled raft foundation with particular attention on uneven settlement by means of a series of centrifuge model tests. They compared results of a partially piled flexible raft foundation with those from an un-piled raft foundation. In the piled raft model, capped piles are installed beneath the raft. They also reported independent load tests on single uncapped and capped piles which allow a full comparison of the performance of each element of the foundation. The results show that a small pile cap on the shaft may have a significant effect on the total bearing capacity. The shaft capacity of the capped pile is also larger than that of the uncapped pile probably due to the different failure mechanism. Also, while the raft may carry the major portion of the applied load, a small number of piles situated near the center of the raft are an effective means of minimizing uneven settlement of the foundation.

Also they expanded their research to examine the role of a small centered pile group in reducing the settlement of the raft Horikoshi et al. (1996). They paid attention to the uneven settlement of the raft and the load transferred to the pile group during unload-reload cycles. They compared the results with those of a fully piled raft designed by a conventional method that contribution of raft or pile cap was ignored. Despite the small magnitude of settlements

observed in the models, the test results showed a high level of consistency. The results showed that, in spite of low loads being transferred to the pile group, a small pile group could effectively reduce the uneven settlement of the raft (Figures 2.13).

Long et al. (2010) are reviewed some experiments results conducted formerly by the authors which indicates the settlement reducing role of the piles. They also discussed on the application of FEM in design of piled raft foundations for high-rise buildings. Their results display a better understanding about the load-transfer mechanism of piled raft in sand along with its load-settlement behavior.

2.3.4.2. Dynamic Loading

Also dynamic physical modeling was conducted in order to study about the behavior of piled raft foundations against dynamic loading.

Horikoshi et al. (2002) used centrifuge modeling to study the behavior of piled raft foundation against horizontal loads. The tests consisted of horizontal and vertical loading tests of piled raft foundation and its components. Also shaking table tests of the same model were conducted. Based on their results, these points were indicated: 1) horizontal resistance of piled raft was higher than raft alone, despite of smaller raft resistance in case of piled raft. 2) initially raft bored more horizontal load than piles but after larger horizontal displacements piles contributed more, 3) proportion of vertical load carried by piles changed less in comparison to horizontal load, 4) in piled raft, horizontal stiffness of a pile was higher than horizontal resistance of a single pile loading test.

Using a geotechnical centrifuge, a series of dynamic loading tests were accomplished on

piled raft foundation on sand by Horikoshi et al. (2003). They compared the tests result with those of previous studies. They studied the effect of rigidity at pile head connection on the dynamic behavior. Also the results of the dynamic loading test of a free-standing pile group with same piles number was considered to study the load sharing in the raft. Their main findings are: 1) The horizontal load sharing between the components depend on the horizontal displacement of the piled raft. 2) The piled raft with hinged pile head connection had smaller horizontal stiffness in comparison to the piled raft with the rigid pile head connection. 3) During dynamic loading, the proportion of the vertical load bored by the piles remained unchanged when the horizontal displacement increased while the horizontal load sharing increased. 4) Because of the contribution of soil beneath the raft in case of piled raft foundation, the inclination of the piled raft during dynamic load was smaller than that of the pile group.

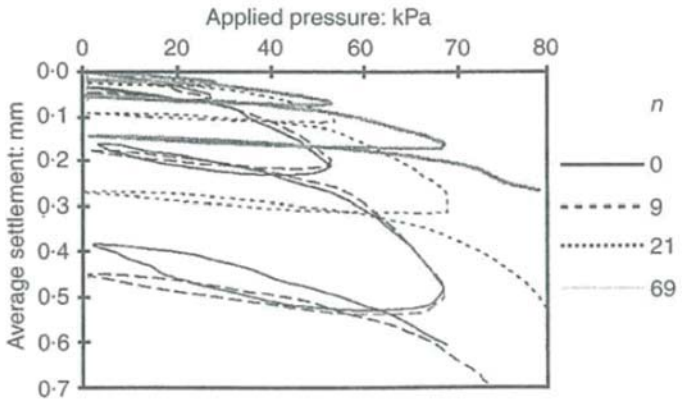

Figure 2.13 (a). Average settlement of tank during loading test (n=piles number) (Horikoshi et al., 1996).

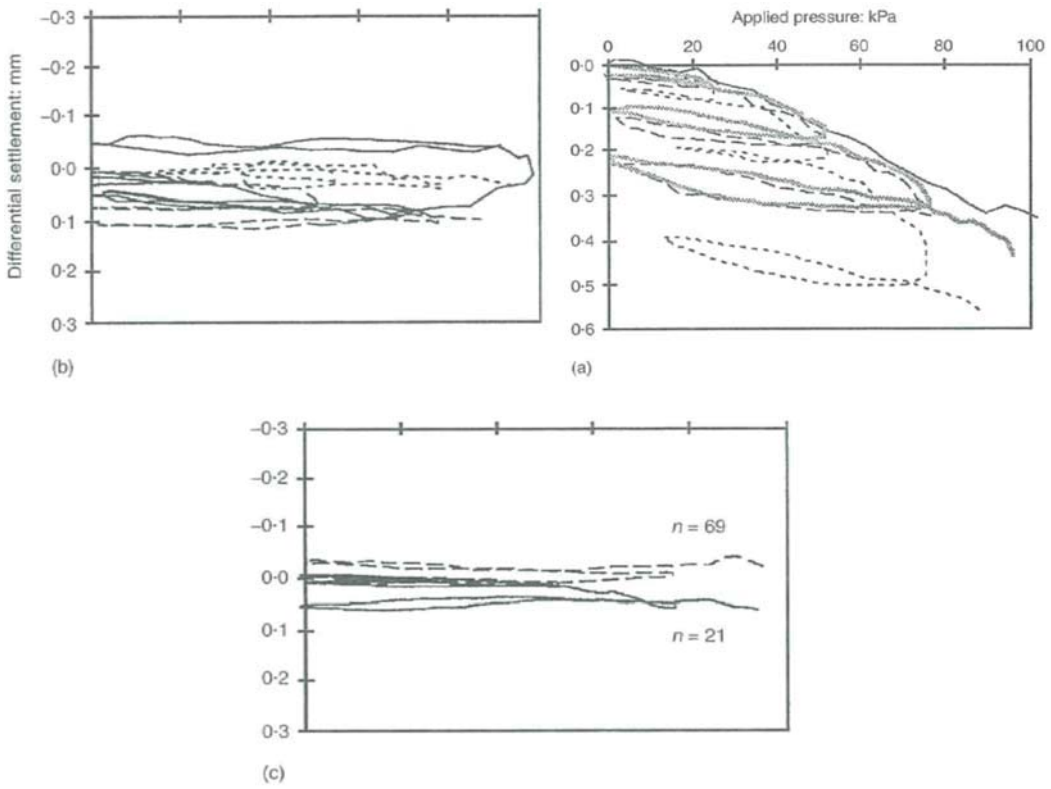

Figure 2.13 (b). Differential settlement of raft during loading test: (a) un-piled raft, (b) piled raft (n=9), (c) piled raft (n=21) (Horikoshi et al., 1996).

Also, Nakai et al. (2004) investigated about the dynamic characteristics of a structure supported by a piled raft foundation. They conducted a centrifuge model test and its simulation analysis and discussed on the results. Furthermore, a parameter study was accomplished using finite element analysis. Two types of foundations were modeled in the centrifuge tests, firstly, a structure supported by a piled raft foundation and secondly by a piled foundation. The foundation types and types of connection between the raft and the piles were discussed in the parameter study. The results showed that, existence of piles installed in the ground below the raft showed considerable effect on the superstructure response. However, the influence of the pile head connection condition on the superstructure response is small, but it affects the load bearing characteristics of piles even when piles are not connected to the raft foundation. Also,

the results indicate that dynamic response of the structure is reduced by developing contact between the raft and the subsoil.

In addition to these studies, a series of 1g shaking table tests were conducted on model piled rafts in dry Toyoura sand by Matsumoto et al. (2004b). They considered two parameters, frequency of input motion and superstructure center of gravity height while the superstructure mass was constant. The results of piled raft with rigid connection were compared with the previous results obtained from static horizontal load tests on the same model by the authors. The results showed that 1) Superstructure resonant frequency decreased when its center of gravity increased; 2) The behavior of piled raft subjected to shaking was close to those in static horizontal loading tests; 3) Although the horizontal acceleration responses at the center of gravity were same, raft inclination, piles shear forces and bending moments increased with increase of superstructure center of gravity height.

Hamada (2016) conducted a series of dynamic and static lateral loading tests on pile groups and piled raft foundations using centrifuge modeling in order to observe the effect of ground deformation on the bending moment in the piles. The results indicate that most of the superstructure inertial force was transferred to the ground by the friction between the raft and subsoil in case of piled raft foundation. So the bending moment induced by the inertial force of the structure on the piles is so smaller in piled raft in comparison to group piles. On the other hand, the dynamic loading tests include the effect of ground deformation while the static loading tests do not include that effect. In this way, the bending moment induced by ground deformation could be calculated approximately by subtracting the recorded piles bending moment during the static loading tests from those of the dynamic tests. Using this procedure he observed that both pile groups and piled raft systems have almost same bending moment

induced by ground deformation. Consequently, he conclude that lateral ground deformation should be considered in the seismic design of both pile groups and piled raft foundations.

2.4. Different Pile Installation Methods

Bearing capacity of foundation system depends on the pile installation procedure since it changes not only the structural behavior of the piles but also the stiffness and strength of the soil. In driven (displacement) piles, a pile displaces a large volume of soil which may affect its bearing capacity. In order to investigate this issue, some researches have been conducted about pile installation effect on the load capacity of piles.

2.4.1. Non-Driven Pile Installation

Centrifuge tests were conducted by Marshall et al. (2014) in order to validate a new analysis method for studying behavior of single and pile groups in layered soils. The model tests were developed to model non-displacement piles while it was an assumption of the analytical method. The layered ground was modeled using fine-grained silica sand as stiff layer and kaolin clay as soft layer. The data from the experiments are compared with those of the analytical results. The comparison of experimental results and analytical predictions based on linear elastic soil behavior show general agreement in trends but magnitudes of pile group efficiencies are different. So the analytical method should include non-linear soil behavior to enhance the predictions.

Adejumo et al. (2013) presented the results of a general investigation on the influence of installation procedures on the allowable bearing capacity of modeled circular piles in layered sandy clay soil. The results show the influence of driving by hammers and drop weights along with boring techniques on load capacity of wooden piles which are modeled driven or bored in

layers of inter-bedded sandy clay soil. The research was done in order to investigate the effect of both driving and boring techniques on 20mm diameter and 200mm long modeled circular piles which are driven or bored through layered sandy clay soil in a multi-purpose testing device in the laboratory. The incremental axial compressive load was applied on the piles until failure. Also, modeled reinforced concrete instrumental test piles with diameters of 200mm, 250mm, and 300mm were driven and bored through layered soil at a construction site. The influence of installation method on the pile-soil interaction and behavior as well as bearing capacity of the piles were investigated. The results show that driven piles have smaller bearing capacity than bored piles in similar conditions. Furthermore, the total settlement of the bored piles is less than the driven piles (Figure 2.14), but the driven piles have smaller settlement at lower depth beneath the pile cap than the bored one. Finally, the driven piles had less bearing capacity (about 12-18%) than the bored piles but they are handled simply and efficiently especially in cohesive soils (Table 2.1).

2.4.2. Driven Pile Installation

Randolph et al. (1994) reviewed current understanding of the factors that determine driven piles axial capacity in sand. They proposed a new framework for design which consider the physical processes and is consistent with the existing database of load test results, furthermore is flexible to allow purification as new data become available. It allows for the influence of confining stress on the frictional and compressibility characteristics of sand, and hence on end-bearing capacity. Same as field observations, shaft friction is assumed to reduce with driving of the pile past a particular location, from an initial maximum value linked to the local end-bearing capacity. The design approach is compared with field data, and effects of direction of loading are discussed.

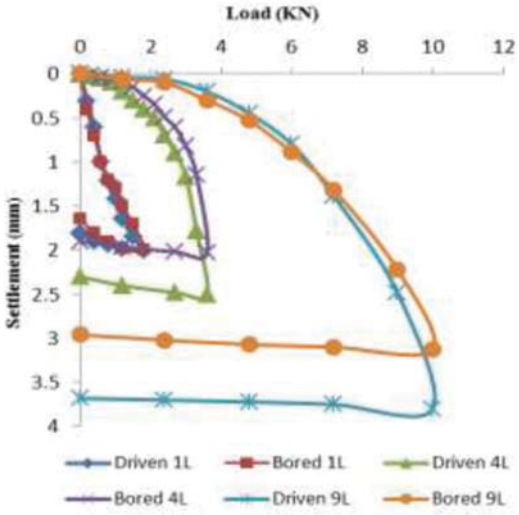

Figure 2.14. Load-Settlement curve (Adejumo et al., 2013).

Table 2.1. Summary of bearing capacity for the tested piles (Adejumo et al., 2013).

Pile Name	Static Load (kPa)	Factor of Safety	Ultimate Capacity (kPa)
DR-1	337.5	2.5	135
BO-1	375.0	2.5	150
DR-4	470.0	2.5	188
BO-4	500.0	2.5	200
DR-9	707.5	2.5	283
BO-9	752.5	2.5	301

DR – Driven Pile; BO – Bored Pile

The results of numerical analysis on the effects of a driven pile installation is presented by Randolph et al. (1979). The problem was simplified by some assumptions such as plane strain conditions and axial symmetry. They modelled pile installation as the undrained expansion of a cylindrical cavity. The excess pore pressures generated in this process was presumed to dissipate by means of outward radial flow of pore water. The consolidation of the soil was studied using an elasto-plastic soil model which allows the strength of the soil to change as the water content changes. So calculation of the new intrinsic soil strength at any stage during consolidation is possible. The long-term shaft capacity of a driven pile might be estimated from the final effective stress state and intrinsic strength of the soil adjacent to the pile. They conducted a parametric study on the effect of the past consolidation history of the soil on the stress changes due to pile installation. The results show that for any initial value of over-consolidation ratio, the final stress state adjacent to the pile is similar to that in a normally one-dimensionally consolidated soil except that the radial stress is the major principal stress. They presented a method which could extend the model of pile installation and subsequent consolidation to clays

that are sensitive. The method was used to predict changes in the strength and water content of soil near a driven pile which consist with two field tests data on driven piles. Also, it was indicated that the rate of increase of a driven pile bearing capacity might be estimated from the rate of increase in shear strength of the soil which is estimated by the analysis.

Jardine et al. (1988) proposed an approach for the prediction of axial load-displacement relationship for large pile foundations. The method is based on effective stress principles and considers the effects of pile installation and equilibration, the possible formation of an interface zone (with reduced frictional strength) near the pile shaft and non-linear soil constitutive behavior. They reviewed theoretical and experimental background of the topic and using finite element analysis the procedure applied in the piled foundations of a real case. They used a superposition method in order to estimate group behavior from predictions done for a single pile. The results show good compatibility with four independent foundations parameters recorded on site during platform installation.

Furthermore, Flynn et al. (2015) defines the installation, curing and maintained compression load testing of three temporary cased driven cast-in-situ (DCIS) test piles that are placed at a uniform sand site near Coventry, United Kingdom. Vibrating wire strain gauges were pasted on the piles in order to measure shear stress created on the pile shaft during compression loading. The results indicate that the peak average and local shear stresses tended to develop at larger shaft displacements than normal performed displacement piles during loading. In all piles, normalized local shear stresses and radial effective stress were reduced at failure with distance from the pile base, implying that radial stresses developed during driven installation of pile are not diminished. In addition, the normalized radial effective stresses at failure were similar to those of normal driven piles.

2.4.3. Study of Pile Installations Effect Using Physical Model Tests

Besides of the previous studies, some researchers utilized physical modeling in order to examine the effects of pile installation procedure on its behavior.

Bloomquist et al. (1991) developed a pile drive-load test device for in-flight installation of piles in sand and compared the pile load capacity of 1g statically pushed piles and in-flight driven piles (Figure 2.15). The driver uses a stepping motor and electromagnet that lifted and dropped a weight unto the pile. The results of in-flight driven and 1g statically pushed piles indicated a significant difference in capacity which show the importance of in-flight placement in sands (Figure 2.16). During the tests it was discovered that if a pile was driven into the soil using the stepping motor directly, similar load capacity in comparison to the weight drop technique were obtained. So the motor steps which operate at 5o Hz seems to simulate a diesel hammer. Based on these results the developed device was utilized to drive a series of 5 piles in any group configuration and driving sequence and in the next step, in-flight load test was applied on the group piles. The results of load test on both single and group model piles show group capacity efficiency of 80% and if the center pile drove last the higher capacity will be obtained (Figure 2.17).

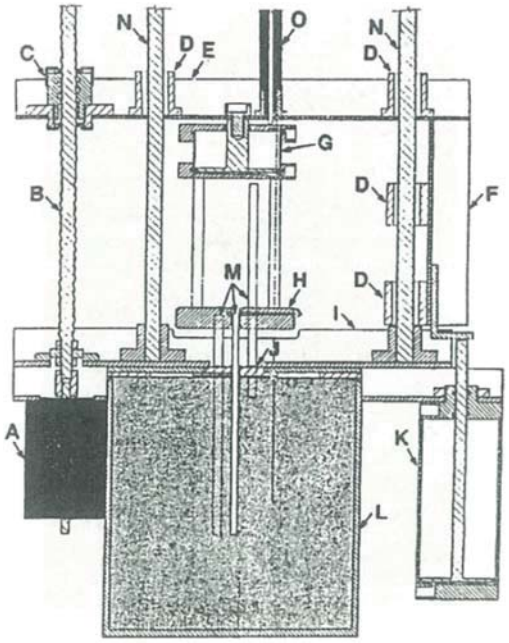

A. Stepping Motor
B. Ball Screw
C. Ball Nut
D. Pillow Block Bearing
E. Top Beam
F. Side Beam
G. Load Test Cylinder
H. PDS Plate
I. Base Beam
J. Pile Alignment Plate
K. Weight Relief Cylinder
L. Soil Container
M. Model Pile
N. Ball Bushing
O. DCDT

Figure 2.15. Developed pile driver (Bloomquist et al., 1991).

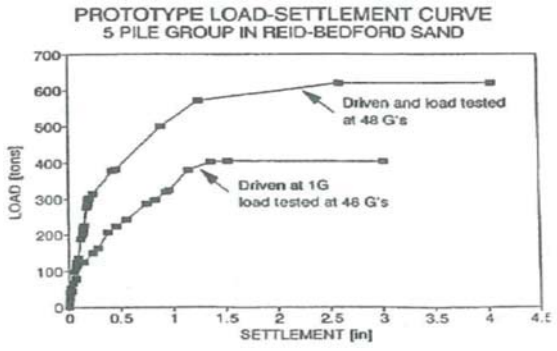

Figure 2.16. Influence of installation g-level (Bloomquist et al., 1991).

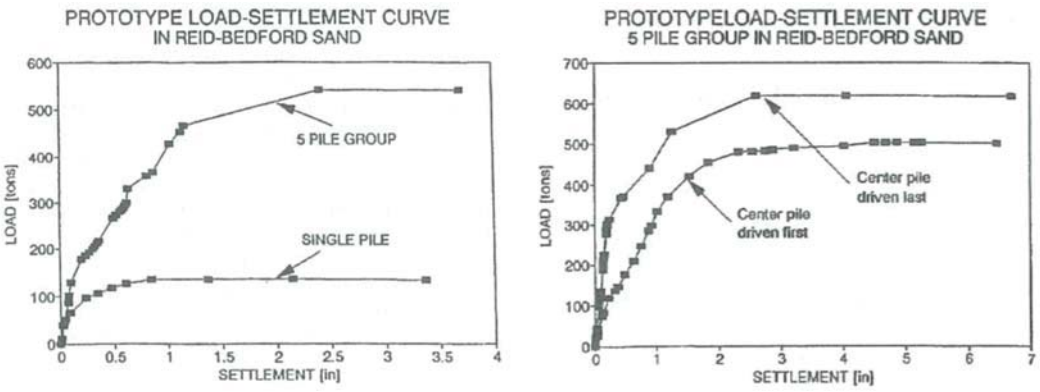

(a) Piles group capacity efficiency. (b) Effect of driving order on group capacity.

Figure 2.17. Typical centrifuge test results (Bloomquist et al., 1991).

Also, a new pile driver with loading set which can drive and load piles in a centrifuge was developed by Pan et al. (1999). The apparatus is light and can move in the X-Y plane easily on the model container. Using this apparatus, the piles can be pushed into the soil in centrifuge flight in the X-Y plane with different configurations at any position. In addition, the pile group can be driven into the soil one by one, and in-flight loading test of the pile group is possible without stopping the operation of the centrifuge (Figure 2.18).

A series of model pile tests was conducted by centrifuge modeling in order to investigate behavior of driven piles in homogeneous sand (Nicola et al., 1999). Using a miniature pile driving actuator open, sleeved and closed-ended piles were driven into silica sand with different densities. The piles were instrumented by strain gauges to record data during dynamic and static testing. The results of load tests show that the shaft friction increased almost linearly with depth at a low rate, but the rate increase near the pile tip. The closed-ended piles showed higher shaft friction comparing to open-ended piles. The average of shaft friction were greater than those of guidelines for design of offshore piles and the ratio of tensile to compressive shaft capacity was below one. The ratio of end-bearing and cone tip resistance decreased with depth for a given

base displacement. Based on the results, hyperbolic end-bearing curves are presented for design and compared with similar curves which are proposed by other researchers.

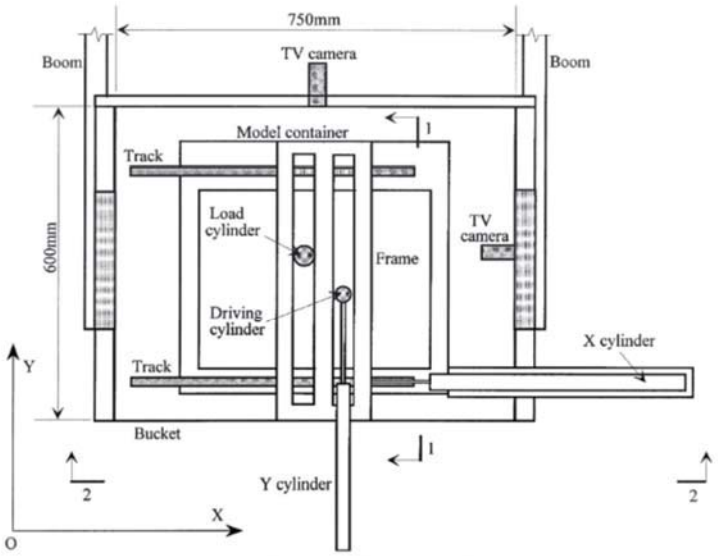

FIG. 3—*Plan view of the pile driver and loading equipment.*

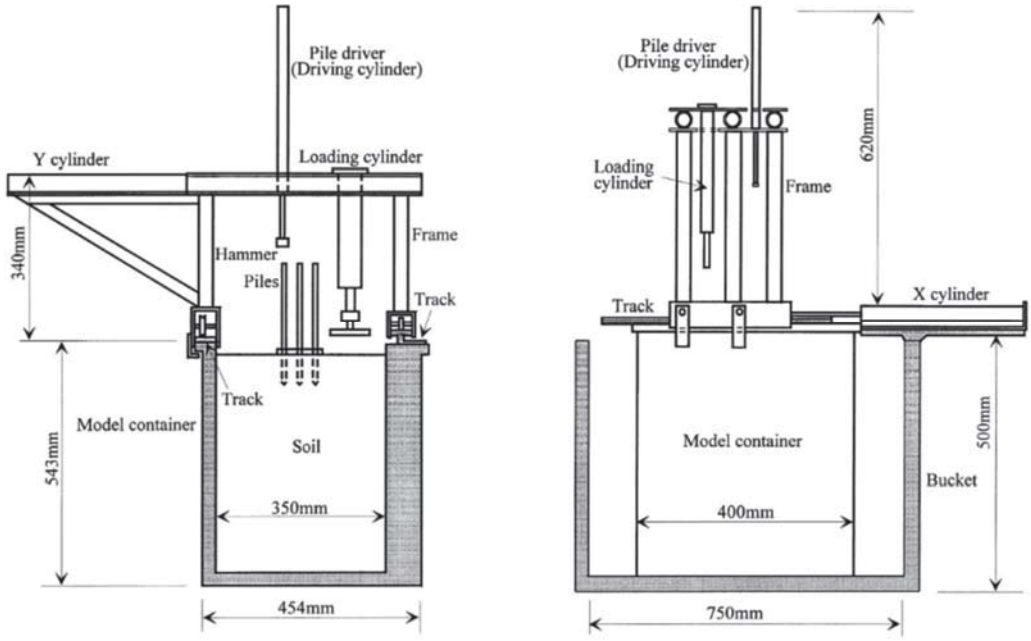

Figure 2.18. Pile driver and loading equipment (Pan et al., 1999).

Furthermore, Klotz et al. (2001) conducted a series of model pile tests in the centrifuge and installed driven piles into two sands with different geological origins and particle strengths. Also, triaxial tests were performed to establish critical state line of each types of sand and initial in situ state of each sample prior to pile installation was achieved. The results indicate that the initial state which is defined by the combination of density and stress level relative to the critical state line is a controlling parameter in estimation of pile capacity. Therefore, the design methods which are based on only relative density cannot be suitable widely. Also, it was declared that state should be defined as stress ratio not in terms of volume which is common.

In addition, a comparison between the seismic behavior of driven and non-driven PRF of oil tanks was presented by Sahraeian et al. (2015) using centrifuge modeling. In this research two types of foundations were considered, one was slab foundation and another one piled raft foundation. In the case of piled raft foundation two different methods of pile installation (Driven and non-Driven piles) were modelled and the result was compared. All the modelled piles were friction piles which were floating in the uniform sand. Using the observed results, such as excess pore water pressures of the ground, rotation and settlement of the tank, accelerations of the tank and the raft base pressures, dynamic and permanent displacement of the piled raft foundation were investigated and applicability of piled raft foundation for oil tanks on liquefiable ground was discussed.

The summary of previous studies on driven and non-driven piles is presented in Table 2.2.

Table 2.2. Previous studies on driven and non-driven piles.

Author	Pile type	Soil type	Study procedure
Adejumo et al. (2013)	Driven and non-Driven	Layered sandy clay	Field test
Randolph et al. (1979)	Driven	Clay	Numerical and field test
Randolph et al. (1994)	Driven	Sand	Analytical and field test
Jardine et al. (1988)	Driven	-	Analytical, FEM and case study
Flynn et al. (2015)	Driven cast-in-situ	Sand	Field test
Bloomquist et al. (1991)	Driven	Sand	Centrifuge
Pan et al. (1999)	Driven	-	Centrifuge
Klotz et al. (2001)	Driven	Sand	Centrifuge
Marshall et al. (2014)	non-Driven	Layered (sand & clay)	Centrifuge
Nicola et al. (1999)	Driven	Sand	Centrifuge
Sahraeian et al. (2015)	Driven and non-Driven	Sand	Centrifuge

2.5. Summary

According to aforementioned previous researches piled raft foundations have been investigated under different loading mechanisms for instance static and dynamic horizontal and vertical loadings or real seismic loadings. Also not only the analytical methods but also experimental and physical simulation was utilized to examine this foundation in different conditions. Furthermore some field studies were conducted to check the performance of this system in real projects and during real previous earthquakes.

On the other hand, this foundation has been topic of researches mostly on the dry sand with stable and enough bearing capacity. Also, it has been considered mainly for normal building

structures no other infrastructures like oil storage tanks and despite enormous studies on it, optimal and rational design methods of piled raft foundation have not been extended to the civil engineering infrastructures. This is partly due to the complex soil-structure interaction between raft-ground-piles during an earthquake and the difficulties for calculation of load sharing between raft and piles in this condition. In particular, if the piled raft resting on a liquefiable ground, the soil-foundation interaction becomes more complex. Because of this complexity and possible large settlement, the practical implementation of piled raft foundation is further hindered.

Another ambiguity on the performance of this foundation system is pile installation procedures which affect significantly bearing capacity of foundation system since it changes not only the structural behavior of the piles but also the stiffness and strength of the soil. Despite of some researches about piles installation method influence on the performance of the piles, this topic is almost ignored in case of piled raft foundation.

Therefore, in this thesis the main objective is to develop a system with proper instrumentation devices for centrifuge modeling of oil tank with slab, driven and non-driven piled raft foundation, in order to investigate the mechanical behavior of oil tank supported by piled raft on not only dry sand but also saturated and liquefiable sand.

Chapter 3 – Development of centrifuge modeling of oil tank with slab and piled raft foundation

3.1. Introduction

As previously explained dynamic centrifuge model tests were conducted in order to study the mechanical behavior of oil tank supported by piled raft foundation on the liquefiable saturated sand and non-liquefiable dry sand. Two types of foundations were modelled in the tests for oil storage tanks, namely, slab foundation (SF) and piled raft foundation (PRF). Also, a special setting was developed to model a driven piled raft foundation in-flight (50g) condition for oil tank. Moreover, in order to discuss about the effect of piles number on the performance of piled raft foundation of oil tanks, the driven piled raft foundation was modelled with two piles numbers.

In this chapter, firstly the principle of centrifuge modeling will be explained and the procedures of tests modeling and its details will be discussed secondly.

3.2. Principles of Centrifuge Modeling

Soil behavior and its nonlinear mechanical properties are significantly dependent on the effective confining stress and stress history. In order to simulate equal stresses in the model and prototype, the centrifuge increases gravitational acceleration of physical models. The identical stress scaling between geotechnical models and the real cases cause to obtain accurate data to study and enhance our understanding of basic mechanisms of complex geotechnical problems

such as liquefaction, soil-structure interaction and etc. In this way, centrifuge modeling is a powerful procedure in order to investigate about the geotechnical problems.

During the centrifuge rotation when the model is under designed gravity acceleration (ng), prototype dimension is n time of model dimension. In the other words, if the model is accelerated at n time of gravity, the length dimension of the model (L_m) will be equal to the prototype (L_p) where $L_p = n(L_m)$.

The model and prototype scale are shown in subscription of m and p respectively. In general, the model and prototype will have the relationships as the following.

$$L_p = n(L_m) \tag{3.1}$$

$$A_p = n^2(A_m) \tag{3.2}$$

$$V_p = n^3(V_m) \tag{3.3}$$

where L= length, A = area, V = volume

It should be mentioned that the vertical stress of the prototype and the model are equal while:

$$\sigma_p = \gamma_p z_p = (1/n)(\gamma_m)n(z_m) = \gamma_m z_m = \sigma_m \tag{3.4}$$

where σ = vertical stress, γ = soil unit weight, z = depth

Table 3.1 summarizes scaling law of various parameters in centrifuge modeling.

Table 3.1. Scaling relationships in centrifuge modeling.

Quantity	Unit	Ratio (Model/Prototype)
Gravity	g [m/s^2]	n
Density	ρ [kg/m^3]	1
Unit weight	γ [N/m^3]	n
Length	l [m]	1/n
Area	A [m^2]	1/n^2
Volume	V [m^3]	1/n^3
Stress	σ [N/m^2]	1
Strain	ε [-]	1
Force	F [N]	1/n^2
Moment load	M [Nm]	1/n^3
Young's modulus	E [N/m^2]	1
Bending rigidity	EI [Nm^2]	1/n^4
Axial rigidity	EA [N]	1/n^2
Time	t [sec]	1/n

3.3. Description of Centrifuge Apparatus and Model Details

3.3.1. Centrifuge Equipment (Tokyo Tech MARK III Centrifuge)

The geotechnical centrifuge utilized in this centrifuge modeling study is Mark III centrifuge which is installed at Tokyo Institute of Technology in 1995 (Figure 3.1). The centrifuge properties are described in detail by Takemura et al. (1999) but the main specifications are summarized in Table 3.2.

The centrifuge is a beam type which has a pair of parallel arms that hold two platforms. The model is mounted on the platform while the counterweight is placed on another platform to make a counter balance. The electrical slip-rings are installed above the rotational center, and the measurements can be done through them. Rotary joint is also installed at the center to supply the air and water during the centrifuge rotation.

Also a newly developed medium size shaking table with specifications mentioned in Table 3.2 was installed on the platform in order to exert dynamic loading on the model (Figure 3.2)

Table 3.2. Centrifuge specifications.

Effective radius	2.3m
Maximum centrifugal acceleration	150g
Maximum rotation speed	300rpm
Platform size	width 0.9m、breadth 0.9m、height 0.97m
Electrical slip-rings for operation	20 slip-rings
Electrical slip-rings for instrumentation	72 slip-rings
Available channels for measurement	64ch

Table 3.3. Shaking table specifications.

Type of actuator	Servo-hydraulic
Max. pay load	15kg under 50g
Table dimension	900mm×400mm
Max. acceleration	35g
Max. displacement	6mm
Max. velocity	70cm/sec
Frequency rang	DC~200Hz

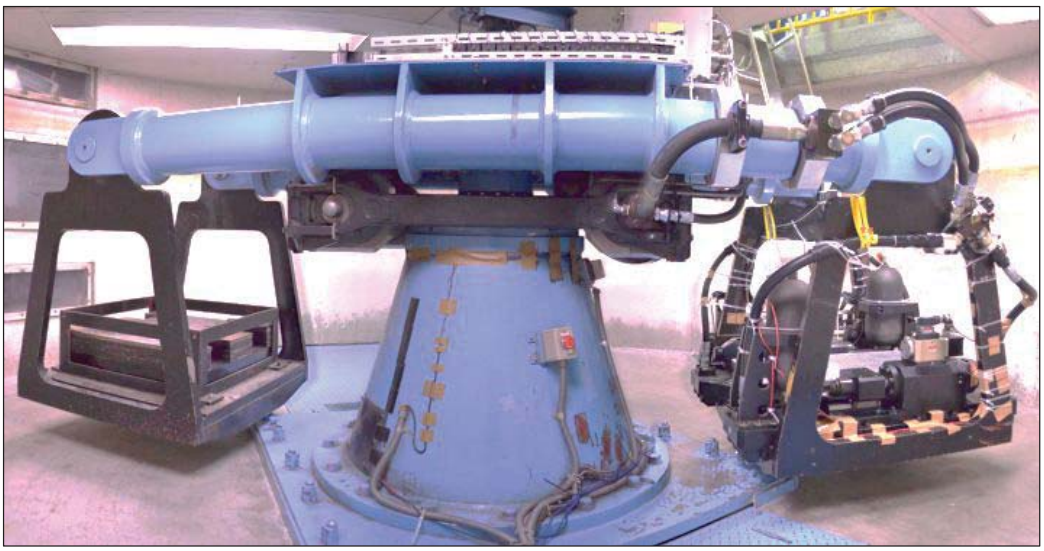

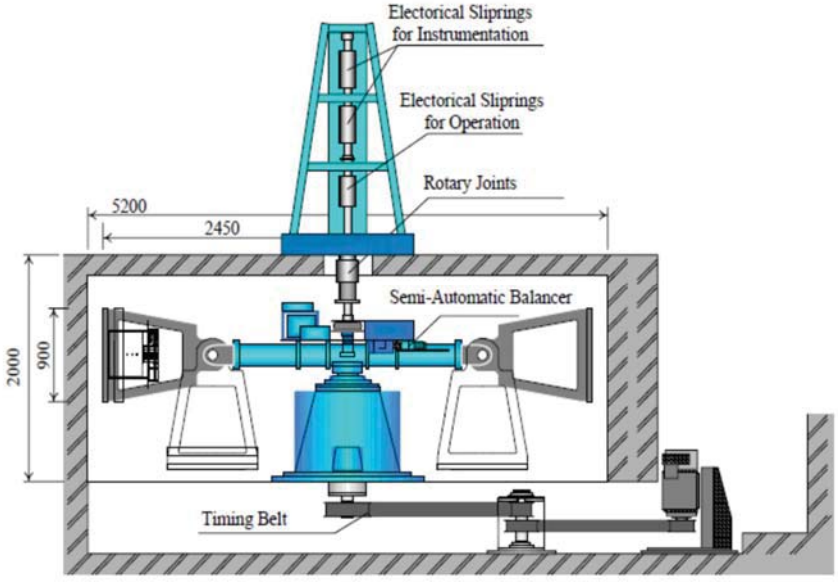

Figure 3.1. Tokyo Tech Mark III centrifuge.

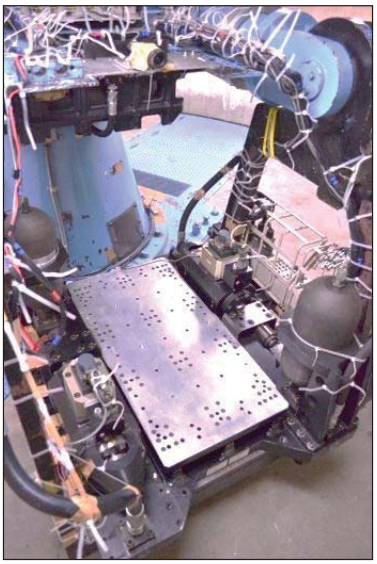

(a) Shaking table

(a) Shaking table with container

Figure 3.2. Shaking table of centrifuge.

3.3.2. Tank, Piles and Raft Models

3.3.2.1. Tank Model

In order to model oil storage tank, a tank model (Figure 3.3) that is made of an acrylic cylinder with 140mm outer diameter, 160mm height and 3mm thickness is utilized. It was glued to the slab/raft model made of an aluminum disk. Water was used as a liquid in the tank with a height of 140mm. The total weight of the water, tank and raft (2.9kg), created 81kPa of the average raft base pressure under 50g centrifugal acceleration. The detailed characteristics of tank in model and prototype scale are presented in Table 3.4.

Table 3.4. Tank model characteristics.

	Model	Prototype
material	acrylic cylinder	steel
outer diameter	140mm	7.0m
thickness	3mm	
height	160mm	8.0m
mass (liquid & raft)	2.9kg	363t
tank average pressure	81kPa	81kPa

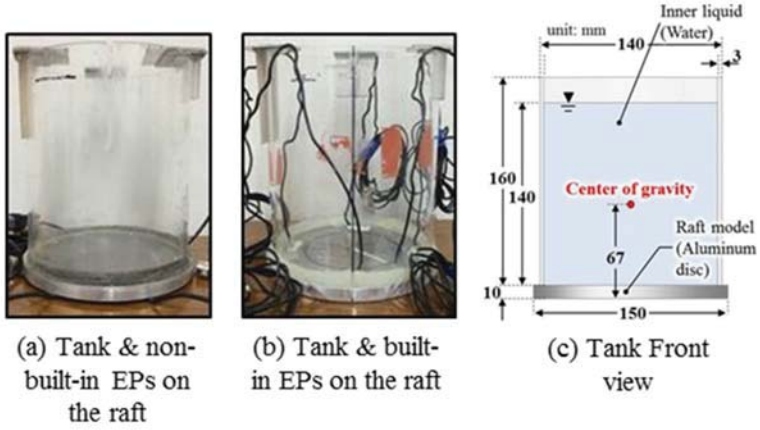

Figure 3.3. Tank model.

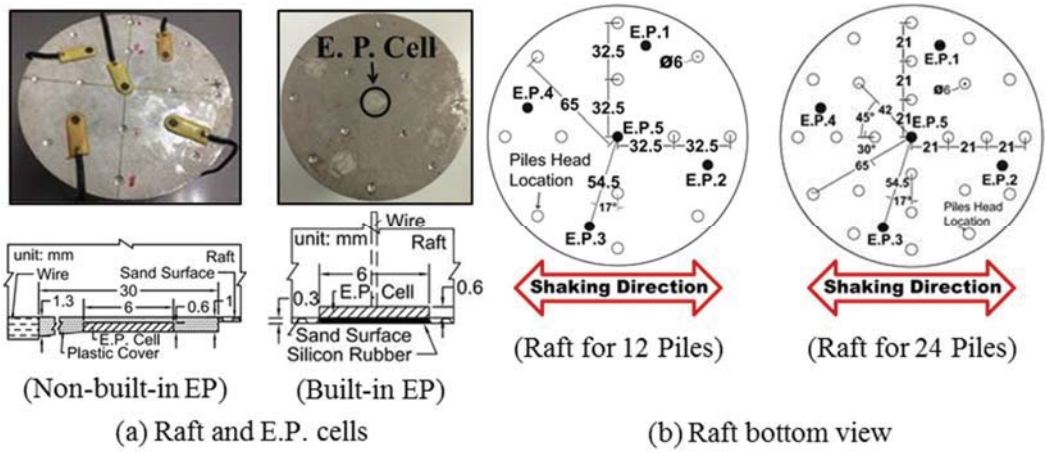

Figure 3.4. Raft model.

3.3.2.2. Raft Model

The raft model was made of aluminum disk with the diameter of 150mm and thickness of 10mm (Figure 3.3). The detailed characteristics of raft in model and prototype scale are presented in Table 3.5.

Table 3.5. Raft model characteristics.

	Model	Prototype
material	aluminum	RC
diameter	150mm	7.5m
thickness	10mm	0.5m
base surface	rough	rough

The raft model has 12 or 24 conical shape concave holes which are put on the pile heads (Figure 3.4 (b)). Furthermore, silica sand No.8, which was used for the model ground, was glued to the bottom surface of the model raft to create a rough surface condition.

In order to measure the raft contact pressure, five external (non-built-in) earth-pressure cells (E.P.s) were glued on the raft base in some tests which will be explained later. New raft models with 5 built-in earth-pressure cells covered by thin silicon rubber were employed in some other tests to improve the reliability of earth pressure measurements by eliminating the stress concentration on the attached E.P.s (Figure 3.4 (a)).

3.3.2.3. Piles Model

The piled raft foundations have 12 or 24 identical piles (the PRFs are with two different piles number which will be discussed later), made of an aluminum tube with outer diameter of 6mm, a thickness of 0.5mm, and length of 100mm as shown in Figure 3.5. The detailed

characteristics of piles in model and prototype scale are presented in Table 3.6. These piles were arranged symmetrically as shown in Figure 3.4(b). The piles heads were not rigidly fixed to the raft, but simply capped by the convex hole, which allows free rotation like pinned connection (Figure 3.6). In this way, the piles mostly were subjected to large axial and lateral forces and a small bending moment at the connection point to the raft. This condition is close to the actual situation of normal piled-foundation of oil tank as shown in Figure 3.5 (Ishimatsu et al., 2009). On the other hand, modeling of non-driven and driven piled raft foundation of oil tank with fixed piles to raft connection is almost impractical, so pin piles to raft connection is used to facilitate the modeling process. The rough piles shaft surface was also made by gluing silica sand No.8.

In order to measure the pile axial load and shaft friction, the piles that were used in a test (PRF on dry sand) were instrumented by axial strain gauges at the head and tip as shown in Figure 3.6(a). However, in other tests especially in PRFs on the saturated sand, to prevent the non-uniformity of the ground made by sand pouring due to the wires connected to the piles, non-instrumented piles were substituted Figure 3.6(b).

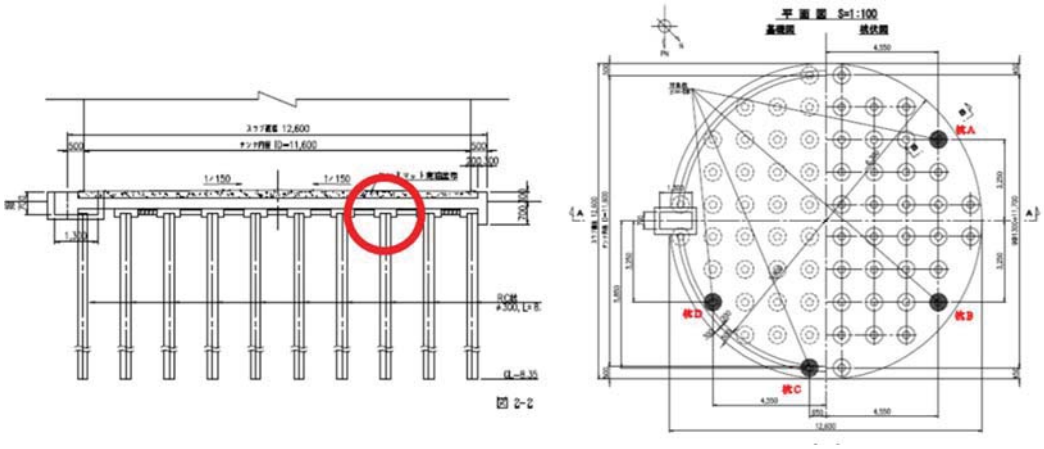

Figure 3.5. Pile connection in piled-foundation of oil tank (Ishimatsu et al., 2009).

Table 3.6. Pile model characteristics.

	Model	Prototype
material	aluminum	RC
outer diameter	6mm (0.5mm)	0.3m
thickness	0.5mm	25mm
axial rigidity: EA	596 kN	1.49 GN
bending rigidity: EI	0.0023 kNm^2	14.2 MNm^2
shaft surface	rough	rough

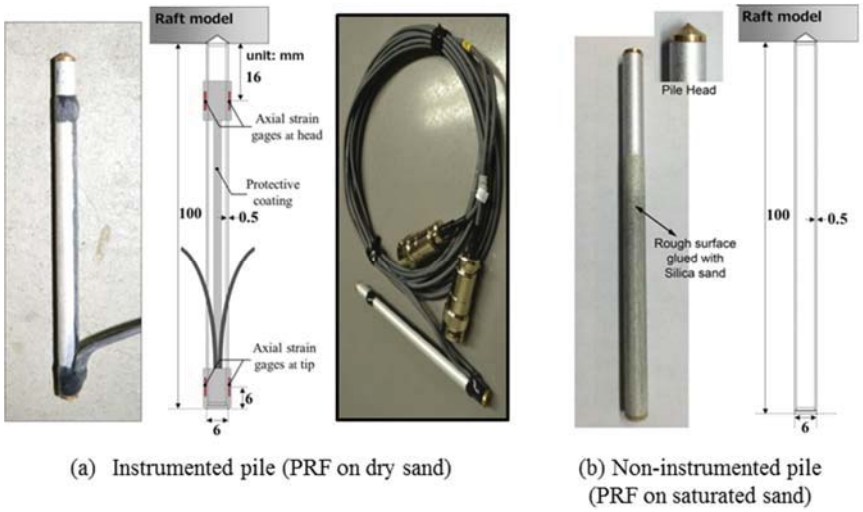

(a) Instrumented pile (PRF on dry sand)

(b) Non-instrumented pile (PRF on saturated sand)

Figure 3.6. Pile model.

3.3.3. Ground Model

Fine silica sand No.8 is used for ground modeling inside a laminar box in the tests while its physical properties have been well studied and known. Detailed properties of silica sands No. 3 and No. 8 are presented in Table 3.7.

Identical soil is generally utilized in the model and prototype in centrifuge modeling, in order to ensure the same stress-strain response in both model and prototype scale. In this way, the proportion of the particle size to structure size is larger for the model in comparison to the prototype, which may lead to scale effects. Because silica sand No.8 used in the present study is fine enough (Figure 3.7) the scale effect is negligible.

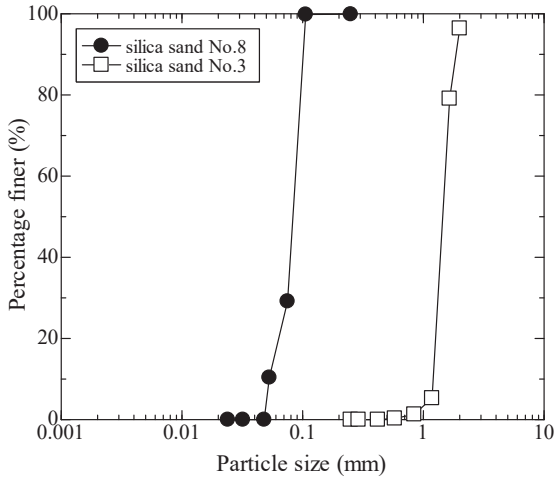

Figure 3.7. Grain size distribution curves of silica sand No.8 and No.3 (Yamada, 2012).

Table 1.7. Properties of silica sands.

		No.8	**No.3**
Specific gravity	Gs	2.65	2.56
Mean grain size	D_{50}(mm)	0.1	1.47
Effective grain size	D_{10}(mm)	0.041	1.21
Uniformity coefficient	Uc	2.93	1.26
Maximum void ratio	e_{max}	1.333	0.971
Minimum void ratio	e_{min}	0.703	0.702
Permeability coefficient (prototype for 50g)	k(m/s)	2.0×10^{-5} (1.0×10^{-3})	4.6×10^{-3} (2.3×10^{-1})

The coarse grain size silica sand No. 3 (Figure 3.8(a)) was utilized as the drainage layer at the model bottom to supply water evenly into the model ground during the saturation process. A filter sheet was put on the silica sand No.3, below the silica sand No.8 in order to prevent mixing of two types sand (Figure 3.8(a)). Using the air pluviation method, the sand layer with a target relative density of 65% (dry density (ρ_d) =1.4 gr/cm^3) was made, but in some cases, the final relative density had a few deviations from the target value. The piles were fixed in the

center of the modeling box by an aluminum guide in non-driven piled raft cases during pouring the sand (Figure 3.8(a), (b)). In the sand preparation, the accelerometers and pore water pressure transducers were placed at the prescribed locations as shown in Figure 3.8(c).

In order to make saturated sand in cases that tank was rested on liquefiable ground, after making the ground model; it was saturated in a vacuum tank by introducing de-aired water from the bottom of the container. Water was used as pour fluid of the sand. The prototype permeability of silica sand No.8 is about 1.0×10^{-3}m/s in 50g centrifugal acceleration. Although this value is relatively high, but it is low enough to accumulate excess pore water pressure and create liquefaction by the input motion applied in the tests.

The schematic diagram of the saturation process is presented in Figure 3.9. Also, the mentioned vacuum tank utilized for the saturation process is shown in Figure 3.10 (a). In order to conduct the saturation process, de-aired water was prepared one day before start of the saturation process firstly. The water was de-aired for about 24 hours by applying vacuum. Then the model ground container was slowly placed inside the vacuum tank (Figure 3.10 (b)). In the following, CO_2 gas was introduced from bottom of the model ground container in order to remove the air bubbles from the sand voids (Figure 3.10 (c)). Then, the open tank was placed above the model ground container inside the vacuum tank as shown in Figure 3.10 (b). The water carrying pipes were properly connected to the open tank and another side of the pipes was connected to the bottom of the model ground container. After connecting all the pipes, the vacuum tank was covered by its cover plate and fixed completely and all the valves were closed. Then the vacuum pump Figure 3.10 (d) was switched on and its valve was opened. The air inside the tank was sucked until the suction pressure reached 0.09 MPa. In the next step, the valves of water container located on top of the vacuum tank Figure 3.10 (e) was opened and

de-aired water was introduced slowly from the bottom of the model ground container under a vacuum of 0.09 MPa until the water level reached to the ground model level. The saturation process takes about 12 hours. Once the saturation process was completed, the vacuum was released slowly and vacuum tank upper plate was opened to remove model ground container from the vacuum tank.

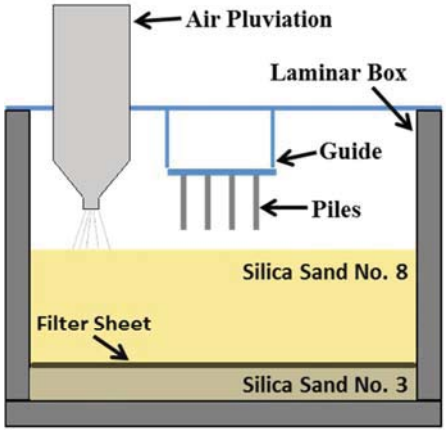

(a) Ground model details.

(b) Piles fixed at box center during sand pouring.

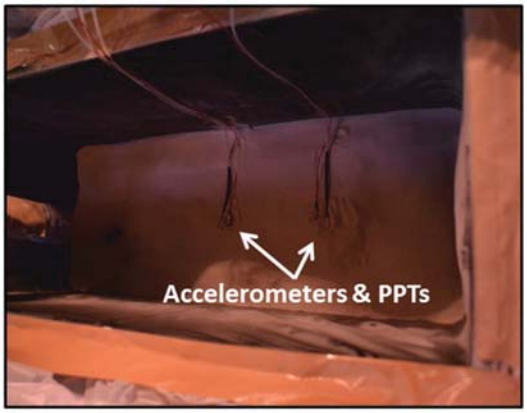

(c) Model ground sensors during sand pouring.

Figure 3.8. Ground modeling.

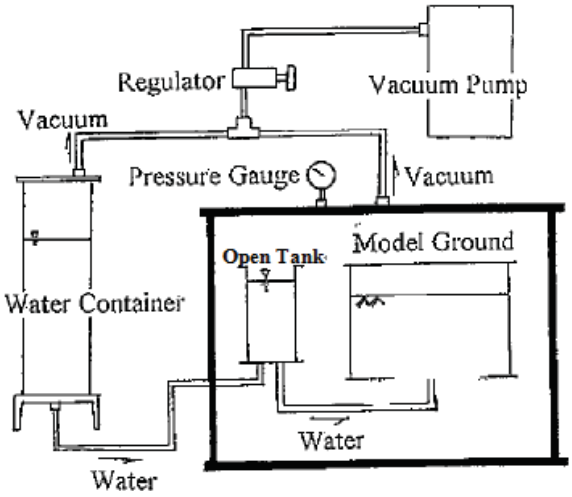

Figure 3.9. Saturation process diagram (Yamada, 2012).

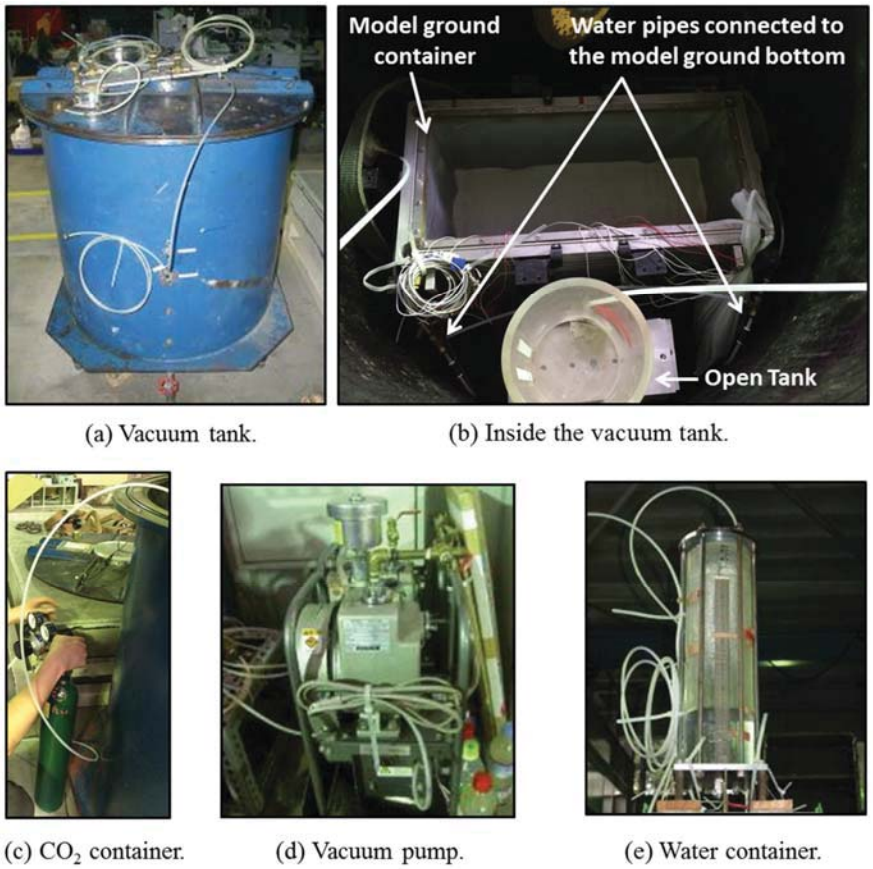

(a) Vacuum tank. (b) Inside the vacuum tank.

(c) CO_2 container. (d) Vacuum pump. (e) Water container.

Figure 3.10. Saturation devices.

3.3.4. Equipment and Instrumentations Used in the Tests

3.3.4.1. Laminar Box

The ground was modeled in a flexible laminar container with dimensions of 800×430×500 mm in length, width, and height, respectively and total weight of 95 kg. The laminar box top, front, and side views and its detailed dimensions are presented in Figure 3.11. The box includes 19 rectangular rings separated by linear roller bearings and this arrangement is to allow relative movement between rings with small friction. The lamina outer size is 680×330×22 mm in length, width, and height, respectively while its inner size is 600×250×22. This special configuration and rings permit the container to move with the soil while minimizes the side effects and not only establishes a flexible boundary but also ensures the uniform distribution of dynamic shear stresses within the model ground (Figure 3.12).

3.3.4.2. Laser Displacement Transducer

Four laser displacement transducers (LDTs) were installed at the top of tank in order to measure the horizontal and vertical displacement of tank (Figure 3.13). Three LDTs was used in vertical direction and one horizontally. Also, the tank rotation was estimated using three vertical LDTs. LDTs estimate the displacement by transmitting laser with wavelength of 780mm to the target, and measuring the phase difference between transmitted and reflected laser. In order to record the tank displacements by LDTs, target plates with a white tape glued on the plate surface were fixed on the tank in front of each LDT. The measurement range of LDTs is 40±10mm and the sensors are produced by Keyence Company.

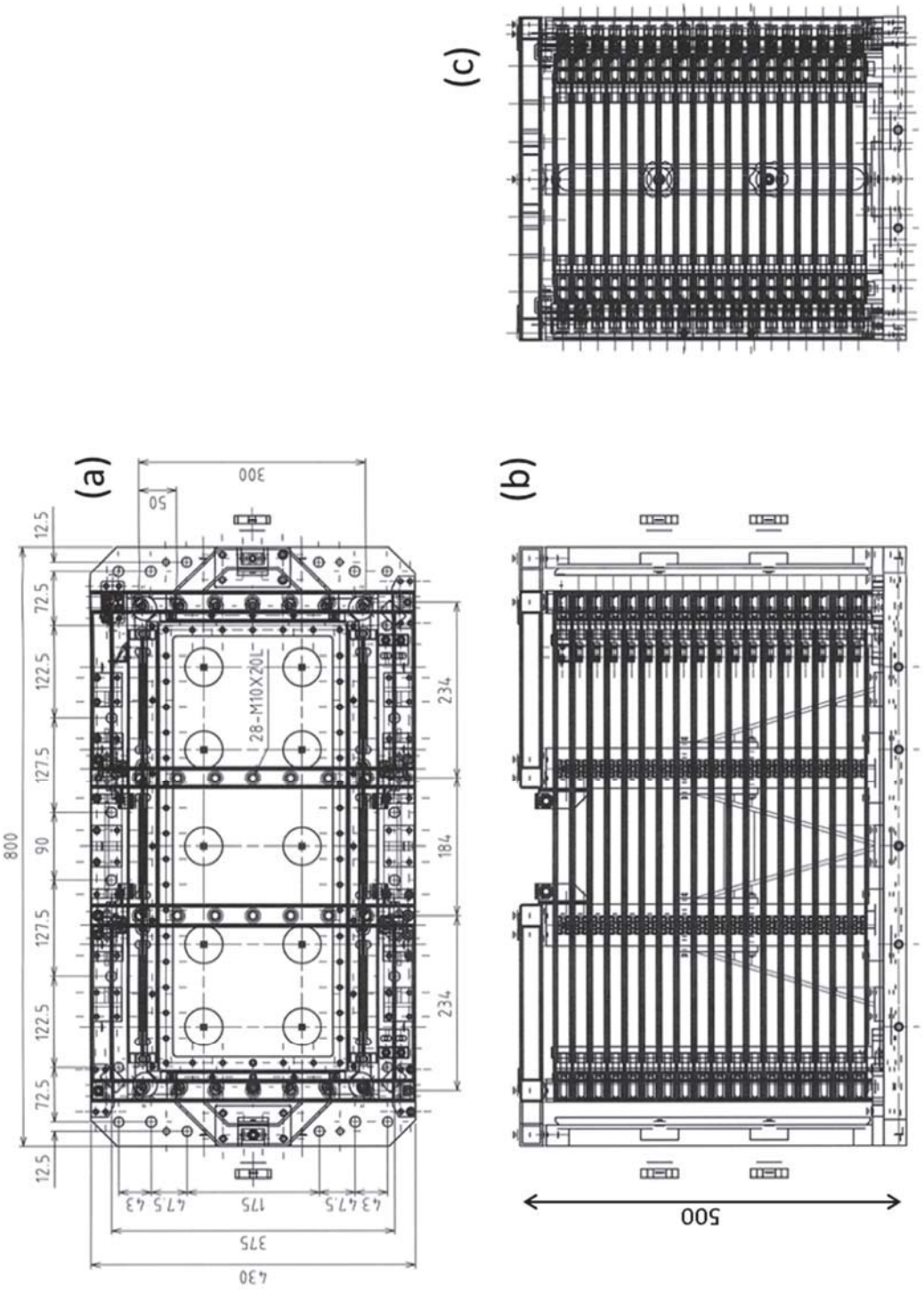

Figure 3.11. Laminar box details: (a) Top view, (b) Front view and (c) Side view.

Figure 3.12. Laminar box.

3.3.4.3. Accelerometer

In order to record acceleration of ground and tank during the dynamic loading, accelerometers were installed at the desired locations in the ground and on the tank during model preparation. The accelerometers are the piezoelectric type of Sekonic, 111BW with a dimension of 4 × 12 × 4 mm and a mass of 2g and 5000m/s^2 capacity (Figure 3.14 (a)).

3.3.4.4. Pore Pressure Transducer (PPT)

Pore pressure transducers (PPTs) were installed in the ground in the desired locations during model preparation to measure the pore water generated during dynamic loading. Also one PPT was attached inside the tank on the raft surface in order to record fluctuation of water pressure inside the tank during dynamic loading. The PPTs are SSK sensors with 6 mm diameter, 12 mm height and 1.5g mass and 200kPa capacity, fitted with a porous element to isolate the fluid pressure (Figure 3.14 (b)).

3.3.4.5. Potentiometer

Two potentiometers were utilized during pile installation in driven piled raft cases which will be discussed later. One was attached to the tank and another one to a jack to measure the vertical displacement of tank and jack during piles installation (Figure 3.15). The potentiometers capacity is 5cm and produced by Honeywell Company.

(a) The sensor (LDT). (b) Horizontal LDT installed in front of the tank.

Figure 3.13. Laser displacement transducer (LDT).

(a) Accelerometer (Acc). (b) Pore Pressure Transducer (PPT).

Figure 3.14. Accelerometer and Pore Pressure Transducer (PPT).

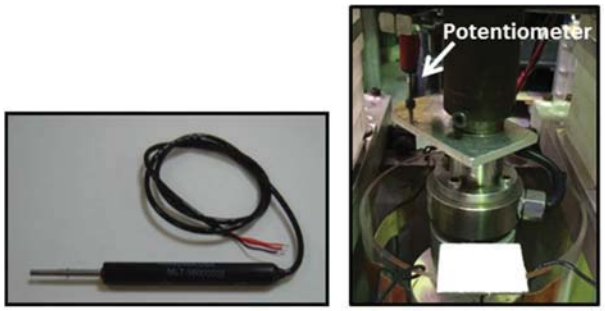

(a) The sensor.

(b) Potentiometer attached to the jack during pile installation.

Figure 3.15. Potentiometer.

3.3.4.6. Electrical Jack

An electrical jack was used in order to apply vertical load on the tank during preloading and piles installation in driven piled raft cases. The jack maximum load capacity is 1.5 ton and its weight is 11kg. Figure 3.16(a) and (b) shows the jack individually and when it was mounted on top of the model.

3.3.4.7. One-Directional Load Cell

A one-directional load cell, which could measure the vertical load, was attached to the electrical jack during jack loading. Due to large vertical load which must applied to the tank during the preloading and piles installation, one-directional load cells produced by Teac with large capacity of 20kN in 50g and 1kN in 1g conditions were utilized (Figure 3.16(c)).

3.3.4.8. Sand Hopper

The ground model was made by the air-pluviation method using a sand hopper as shown in Figure 3.17. The target relative density and ground depth were 65% and 220mm respectively.

3.3.4.9. Camera and LED Light

A digital camera was located inside the model container in front of the tank to record the behavior of tank during the experiment as shown in Figure 3.18. This camera could be connected to the control room during the centrifuge operation. Also, a row of LED lights was installed in the container in order to enhance the video quality.

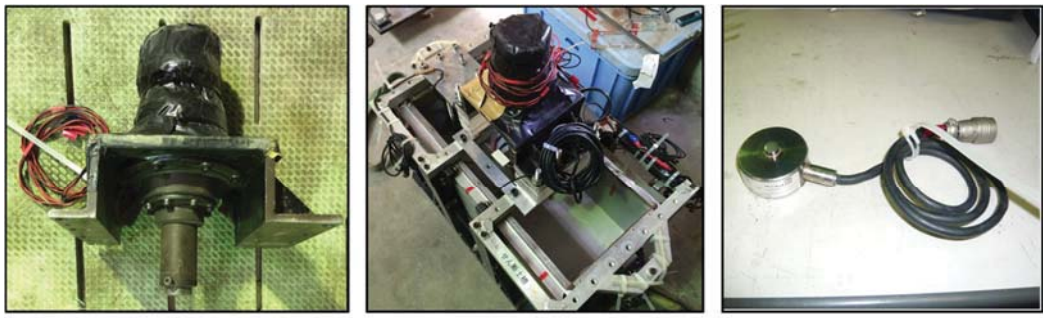

(a) Electrical Jack. (b) Jack mounted on top of the model. (c) One directional load cell.

Figure 3.16. Electrical Jack and load cell.

Figure 3.17. Sand hopper.

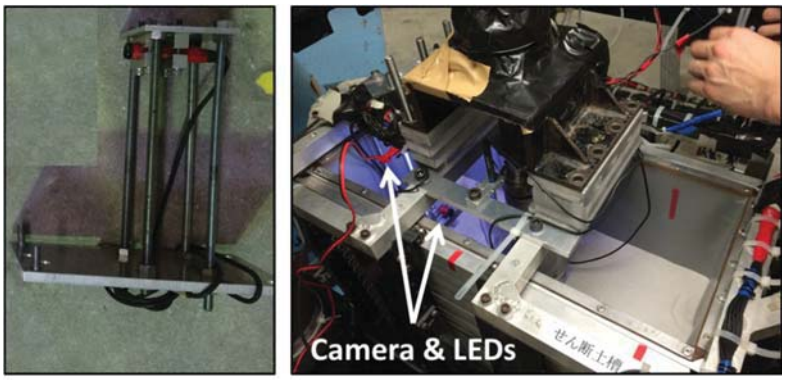

(a) Camera (b) Camera and LEDs inside the model container.

Figure 3.18. Camera and LED lights.

3.3.4.10. Earth Pressure Cell

Although different kind of earth pressure cells exist (Talesnick et al., 2014), as mentioned before five normal earth-pressure (EP) cells were utilized to record the ground pressure on the raft surface. The EPs were two types: non-built-in EPs (KYOWA-200kPa) and built-in EPs (KYOWA (PS-5KD)-500kPa) used in different test cases (Figure 3.4(a)).

3.4. Calibration Technique

3.4.1. Pile Calibration

The principle of strain gauges and the calibration method of the strain gauges attached to the top and bottom of piles are discussed in this section while the accuracy of the strain gauges is important for the study of piled raft foundation.

3.4.1.1. Principle of Strain Gauges

Based on the Hooke's law, the induced stress (σ) is proportional to the induced strain (ε) in the elastic limit of materials. The constant proportional property is called Young's modulus (E) as shown in equation (3.5).

$$E = \frac{\sigma}{\varepsilon} \tag{3.5}$$

So, if the Young's modulus of strain gauge material is known, stress can be calculated by this equation.

Generally, strain gauge is made by metallic resistive foil covered by laminate and plastic film. While, the strain gauge is attached to the measurement surface area, when the structure is subjected to the force, the strain gauge will contract or elongate along with the structure element

and undergo alter in electric resistance. The strain value can be measured by change in electric resistance by this equation:

$$\frac{\Delta R}{R} = K'\varepsilon \tag{3.6}$$

where ΔR = change of resistance of strain gauge (ohm), R = resistance of strain gauge, K' = gauge factor of strain gauge (depend on the material of strain gauge), ε = Induced strain.

Because the change of resistance is so small, a new circuit named Wheatstone bridge has been introduced to amplify the measured value. Wheatstone bridge has great importance while can detect small change of strain, especially in the model testing condition. The relationship in Wheatstone bridge's circuit is:

$$e = \frac{1}{4}\frac{\Delta R}{R}E = \frac{1}{4}K\varepsilon E \tag{3.7}$$

where, e = output voltage, E = input voltage.

In this way, the induced strain in each strain gauge can be obtained by in the current study by the following relation:

$$\varepsilon = \frac{2}{(1+\xi)}\frac{e}{KE} \quad \text{(For strain gauges with only measurement of axial force)} \tag{3.8}$$

The output voltage is zero in balance condition but when the condition is unbalanced, the resistance change will be measured using the variation of the e values.

3.4.1.2. Calibration Method

In order to find calibration factor of strain gauges (Tokyo Sekki), a special triangle plate

was made as shown in Figure 3.19(a). Three of the piles were fixed inside this setting while weights were hanged at plate center vertically to apply same vertical load evenly in the three piles. The weights were increased step by step in ten stages and after that decreased in the same steps until removal of all weights. This procedure was repeated three times for each group of piles to estimate the calibration factor precisely. The detail of calibration setting is shown in Figure 3.19. Also, the diagram of ratio between applied load and recorded voltage by strain gauges in three sample piles is presented in Figure 3.20. Using these values and calculating their average for each pile in three repetitions will give the calibration factor which is essential for calculation of axial force in the top and bottom of piles.

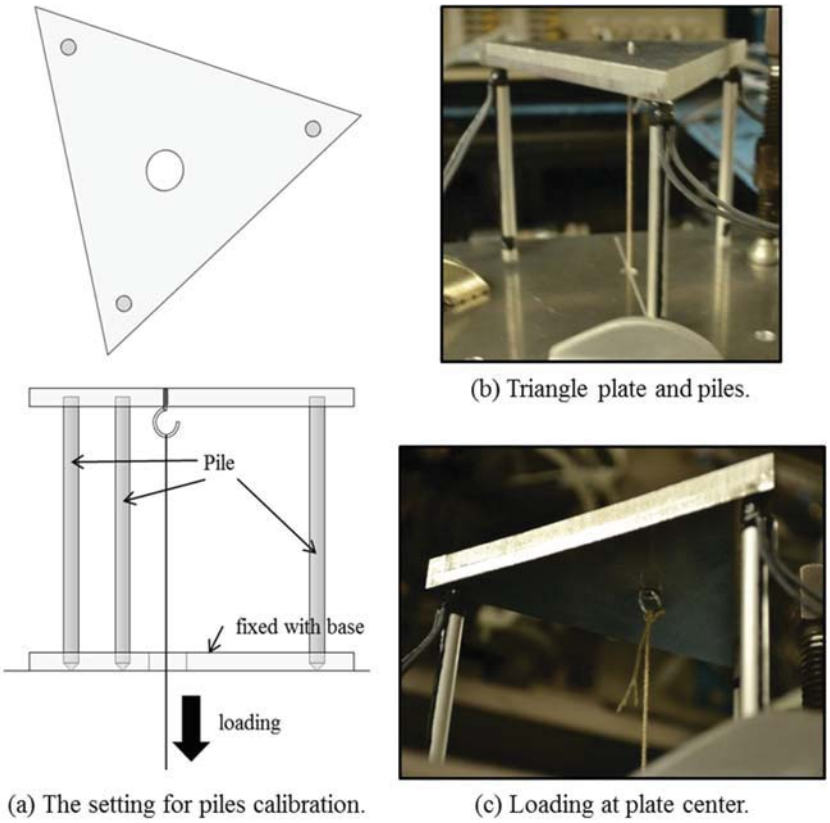

(a) The setting for piles calibration.

(b) Triangle plate and piles.

(c) Loading at plate center.

Figure 3.19. Piles calibration setting (Yamada, 2012).

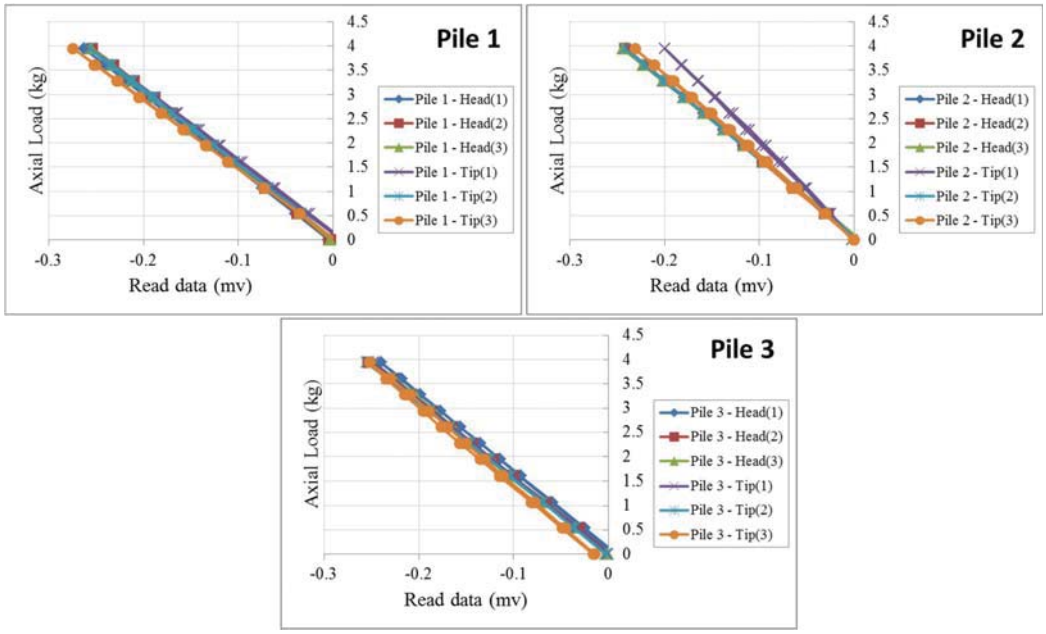

Figure 3.20. Piles calibration diagram.

3.4.2. Pore Water Pressure Transducer (PPT) and Earth-Pressure Cell Calibration

In order to calibrate and estimate calibration factor of earth-pressure cells (EP), they were attached on bottom of a rigid container as shown in Figure 3.21. Then the container was filled with water until a fixed height. Putting the container on the centrifuge basket the centrifuge acceleration was increased step by step (each step 5g) until 50g. Having the water pressure in each step and also by using the recorded values by EPs, the calibration factor was calculated for each step. The average value of calibration factors in all steps is the final calibration factor for each sensor (EP).

In case of pore pressure transducers (PPT), same trend was conducted but with some difference. In order to have more precise values firstly by using a small tank and applying air pressure in 1g step by step, the calibration was done for one PPT. Then, this PPT along with

others was calibrated in 50g condition in a same procedure of EP cells explained before. The result of this PPT was used as a valid instance for estimating the calibration factor of other PPTs which were calibrated in 50g condition.

3.4.3. Potentiometer (PTM) and Laser Displacement Transducer (LDT) Calibration

Using a micrometer, potentiometers (PTM) were calibrated. The calibration setup is shown in Figure 3.22(a). The potentiometers were held at one side and connected to a block. By rotating the micrometer, the screw jack was lengthened and pushed the block toward the potentiometers. This movement of the block was measured by the micrometer's scale. The movement increments were plotted to calculate the calibration factor.

Also, the same method was used for Laser displacement transducers (LDT) calibration (Figure 3.22 (b)). In this case, the movement increments of block were defined the calibration factor of LDT. While the LDT could not sense a transparent object, Opaque tape was pasted on the surface of block.

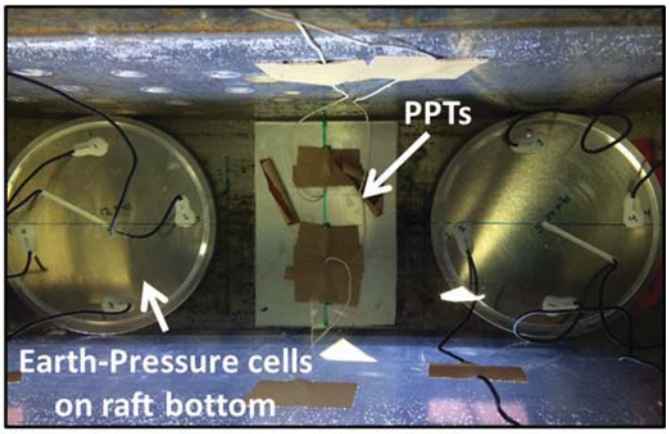

Figure 3.21. PPTs and EP cells Calibration.

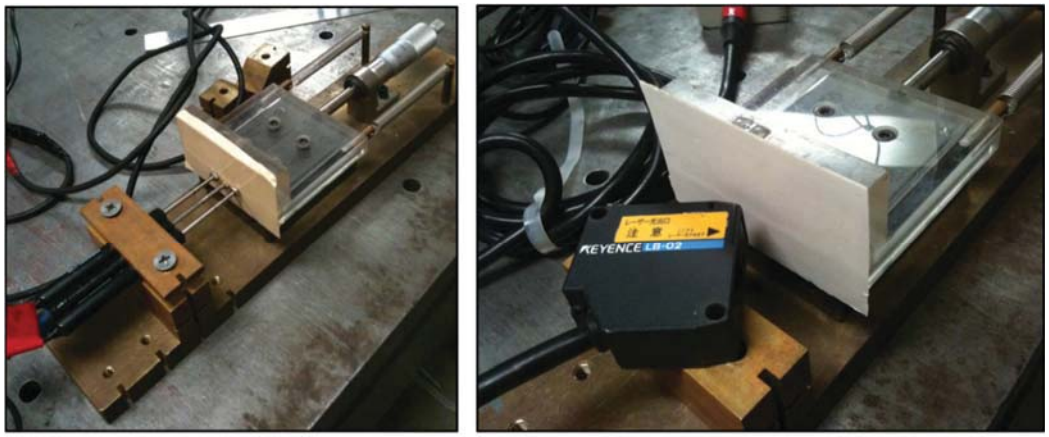

(a) Potentiometers (PTM) calibration. (b) Laser displacement transducer (LDT) calibration.

Figure 3.22. Potentiometer and LDT Calibration. (Boonsiri, 2015)

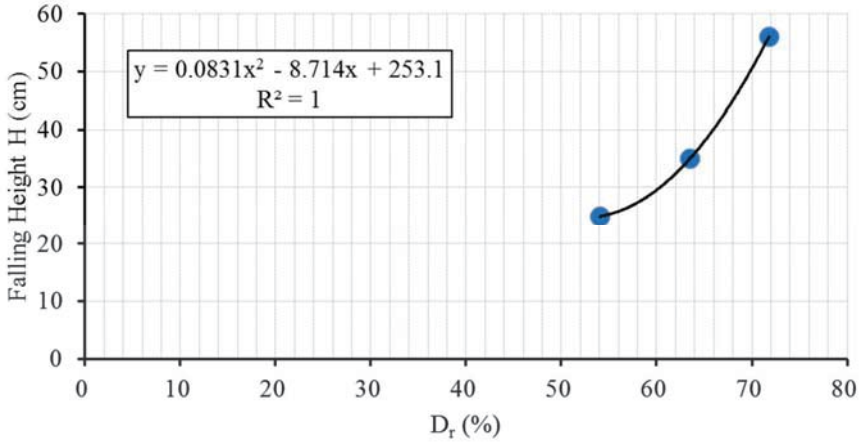

Figure 3.23. Sand hopper calibration diagram.

3.4.4. Sand Hopper Calibration

In order to calibrate the sand hopper, the ground model was made with different height of sand raining (elevation of sand hopper from model surface). Then the relative density of model ground was calculated and relationship between height of sand hopper and relative density was drawn as shown in Figure 3.23. Using this relationship, the required height of sand hopper for

making the ground with an intended relative density can be estimated.

3.4.5. Load Cell Calibration

The load cell calibration procedure was simple. The vertical load on the load cell was increased step by step in five stages and after that decreased in the same stages until removal of all weights. Using the applied weight in each step and the corresponding recorded values by sensor (load cell), the calibration factor was calculated for each stage. The final calibration factor is the average of calibration factors in all steps.

3.5. Test Procedure

3.5.1. Test Series

Totally, seven model tests were conducted in this study as presented in Table 3.8. The test cases can be divided in three main categories, tank with slab foundation, non-driven piled raft foundation and driven piled raft foundation. Also, in order to investigate the behavior of tank precisely, it was modelled not only on dry (non-liquefiable) sand but also on saturated (liquefiable) sand. In Case 1 and Case 2 a slab foundation (SF) and a non-driven piled raft foundation (PRF) were placed on dry sand respectively. The slab foundation was also modelled in Cases 3a & 3b on saturated sand. Case 3b was conducted in almost same conditions as Case 3a. A non-driven piled raft foundation (PRF) including 12 piles was placed on saturated sand in Case 4. To compare the behavior of oil tanks supported by PRFs with non-driven and driven piles on liquefiable sand, a driven piled raft foundation with 12 piles was modeled on saturated sand in Case 5. Based on a foundation design method, e.g. Meyerhof's method (Das, 2007) and using the φ' of Silica sand No.8 (Table 3.7), the bearing capacity of each pile and raft in the

prototype scale are about 1.2 and 107MN respectively in the static condition. Namely, the bearing capacity of 12 piles is about 14% of the bearing capacity of the raft. In order to increase the similarity of this foundation model with the real oil tank foundations in case of piles number, the driven piled raft foundation with larger piles number (24 piles) was modeled in Case 6. Due to the high density of piles in PRF with 24 piles and the difficulties in the modeling of the ground during sand pouring, the preparation of non-driven PRF with 24 piles was impractical and this case was not modeled.

Table 3.8. Test cases

Test code	Foundation	Ground	Details
Case 1	Slab	Dry sand (Dr=66%)	Slab w/o E.P.s
Case 2	Non-driven Piled Raft (12 Piles)	Dry sand (Dr=68%)	12 instrumented piles & raft w/o E.P.s
Case 3a	Slab	Saturated sand (Dr=65%)	Slab with 5 non-built-in E.P.s
Case 3b	Slab	Saturated sand (Dr=68%)	Slab with 5 built-in E.P.s
Case 4	Non-driven Piled Raft (12 Piles)	Saturated sand (Dr=69%)	12 non-instrumented piles & raft with 5 non-built-in E.P.s
Case 5	Driven Piled Raft (12 Piles)	Saturated sand (Dr=70%)	12 non-instrumented piles & 5 built-in EPs
Case 6	Driven Piled Raft (24 Piles)	Saturated sand (Dr=65%)	24 non-instrumented piles & 5 built-in EPs

3.5.1.1. Tank with Slab Foundation (SF)

In order to model tank with slab foundation on the ground (Cases 1, 3a and 3b), firstly, the model ground was made by dry Silica sand No.8 using air-pluviation method. The ground model depth was 220mm in total and the first 30mm at the bottom of the container was Silica sand No.3 as previously explained. The ground model target relative density was 65% but in

some cases, the final relative density had a few deviations from the target value as presented in Table 3.8. During the ground preparation, the sensors were placed in two different sections, first section at the center line of the model in the shaking direction and the second in the transverse direction. After pouring the sand into the container, the ground surface was flattened perfectly using a vacuum and the tank was put on the ground surface at the center of container. The model dimension and instrumentation details in Case 1 (SF on dry sand) are shown in Figure 3.24.

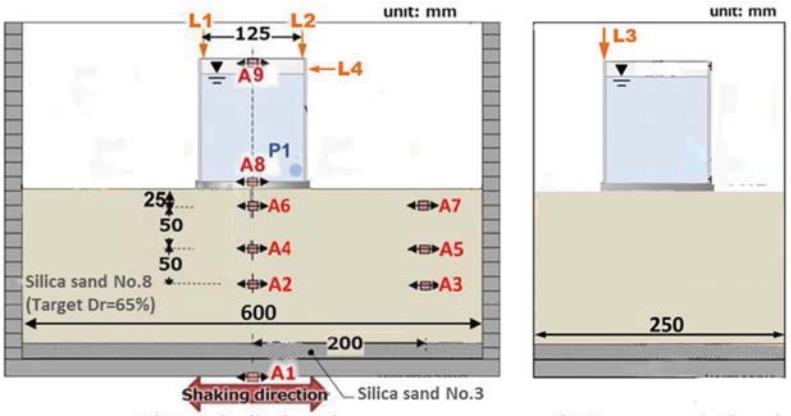

(a) Longitudinal section. (b) Transverse section.

Figure 3.24. Model setup and instrumentation in Case 1 (SF on dry sand).

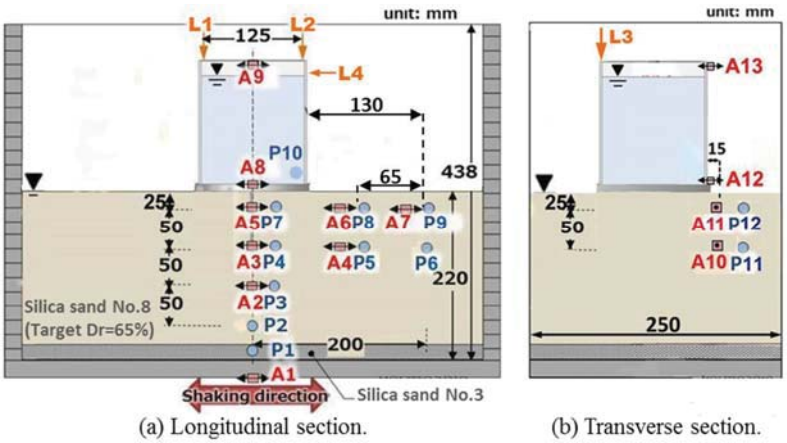

(a) Longitudinal section. (b) Transverse section.

Figure 3.25. Model setup and instrumentation in Cases 3a & 3b (SF on saturated sand).

In saturated cases (Cases 3a and 3b) after completion of ground modelling the saturation process was conducted as explained in section 3.3.3. The detailed model dimension and instrumentation in Cases 3a and 3b (tank with slab foundation on saturated sand) are shown in Figure 3.25. Furthermore, in order to measure the raft contact pressure, five external (non-built-in) earth-pressure (EP) cells were glued on the raft base in Case 3a (Figure 3.4). New raft models with 5 built-in earth-pressure cells covered by thin silicon rubber were employed in Case 3b, to improve the reliability of earth pressure measurements by eliminating the stress concentration on the attached EPs (Figure 3.4).

After completion of the ground modeling, saturation process (Cases 3a and 3b) and putting the tank on the ground model the preloading was applied on the tank to have a secure contact between the raft base and the ground surface. The preloading details will be explained in the later parts.

3.5.1.2. Tank with non-Driven Piled Raft Foundation (Non-Driven PRF)

The tank with non-driven piled raft foundation was modelled in Case 2 on dry sand and Case 4 on saturated sand. In these two cases, the piles were fixed in the center of the modeling box by an aluminum guide during sand pouring as shown in Figure 3.8 (b). The other parts of ground modelling were same as cases with slab foundation (section 3.5.1.1). Similarly, after completion of sand pouring in the container, the ground surface was flattened perfectly using a vacuum. In Case 4 (Non-driven PRF on saturated sand), same saturation procedure was used to saturate the ground. Then, the tank was put on the piles head at the center of container in both cases (Figures 3.26). The model dimension and instrumentation details in Case 2 (Non-driven PRF on dry sand) and Case 4 (Non-driven PRF on saturated sand) are presented in Figures 3.27 and 3.28 respectively. Afterwards, the preloading process was applied in both cases that will be

explained later.

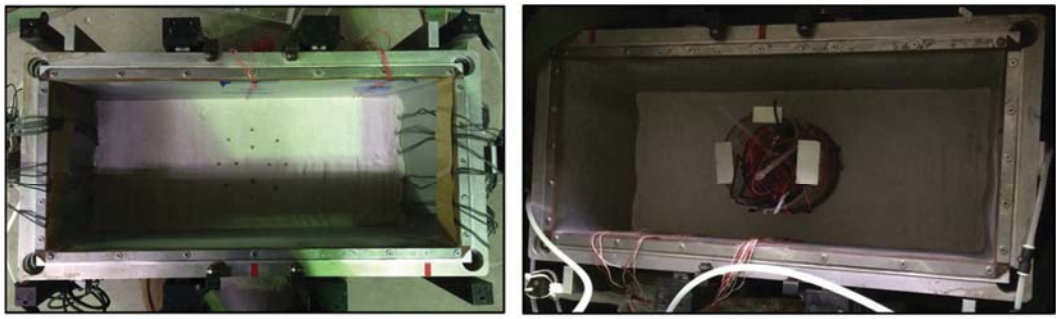

(a) Flattened surface of ground model. (b) Tank on the piles head at box center.

Figure 3.26. End of ground modeling in Cases 2 & 4 (Non-driven PRF).

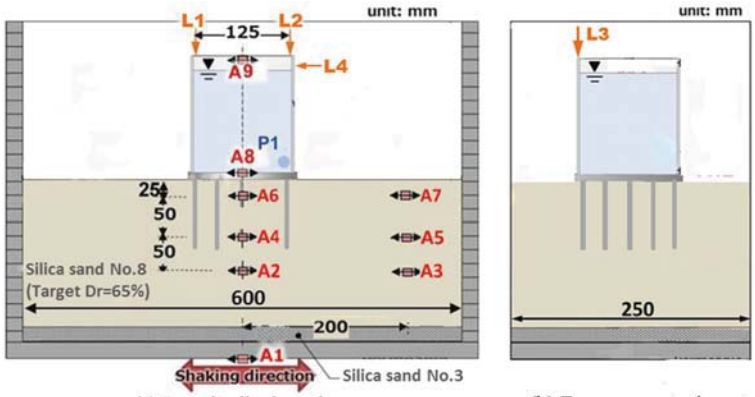

(a) Longitudinal section. (b) Transverse section.

Figure 3.27. Model setup and instrumentation in Case 2 (Non-driven PRF on dry sand).

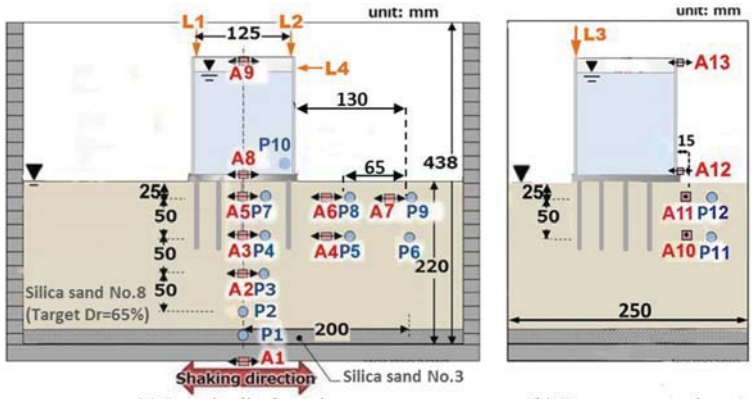

(a) Longitudinal section. (b) Transverse section.

Figure 3.28. Model setup and instrumentation in Case 4 (Non-driven PRF on saturated sand).

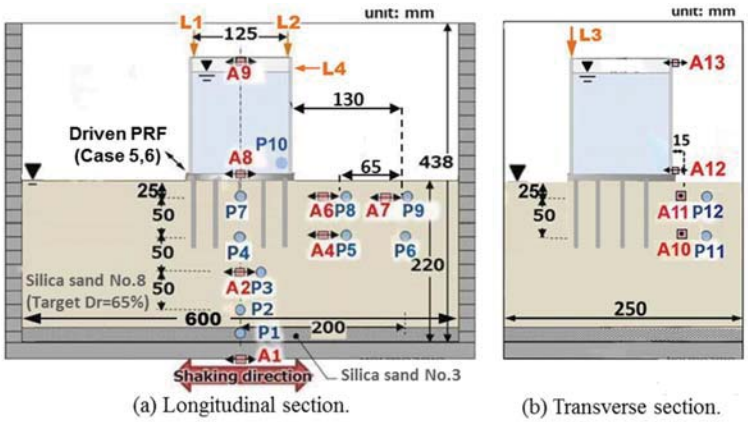

Figure 3.29. Model setup and instrumentation in Cases 5 & 6 (Driven PRF on saturated sand).

3.5.1.3. Tank with Driven Piled Raft Foundation (Driven PRF)

As previously mentioned, driven (displacement) piles displaces a large volume of soil during pile installation. Because it changes the soil density in pile border the installation procedure will affect the bearing capacity of piles. In this study, the piles are cylindrical with solid section which can be categorized as driven piles if the installation procedure displaces a large amount of soil. In this way, in order to study the difference between the behavior of piled raft foundation with non-driven and driven piles in saturated sand the driven PRF was also modeled in Cases 5 and 6. On other hand while the piles number has some effect on the behavior of PRF, the piles number was increased in Case 6 (24 piles) in order to study the behavior of oil tank piled raft foundation with higher density of piles under the raft.

In Case 5 (Driven PRF with 12 piles) and Case 6 (Driven PRF with 24 piles), the ground was modelled firstly. During sand pouring sensors were installed in different locations same as other cases. In these cases due to complicated pile installation procedure some sensors (A3 and A5) just beneath the tank was not utilized in order to prevent pile installation disturbance by sensors. The detail of instrumentation and model setup in Cases 5 and 6 are shown in Figure

3.29. After finishing sand pouring and making ground flat surface, the saturation process was conducted same as other saturated cases as discussed in section 3.3.3.

In order to model in-flight installation of the driven piles in Case 5 (Driven PRF with 12 piles) and Case 6 (Driven PRF with 24 piles), an 20mm thick acrylic guide plate (Figure 3.30 (a)) was used to hold the piles and tank during the pile installation at the center of the model ground. The plate has vertical holes with 6.5mm diameter at the locations of piles. To have upright positions of the piles inserted in the holes, small 10mm thick Styrofoam plates with 6mm diameter used as shown in Figure 3.30(a), (b). Setting all the piles and placing the tank model, the piles were pushed to the sand in 50g as the first pile installation stage using an electrical jack (Figure 3.30(g)) with a loading rate of 2mm/min. The jack loading was stopped before the tank bottom contacted to the guide surface (Figure 3.30(c)). Afterwards, the centrifuge was stopped and the tank and the guide were removed from the top of the piles and the tank was put again on the top of the piles (Figure 3.30(d) and (e)). Again in 50g centrifugal acceleration, the jack load was exerted to the tank to drive the piles into the sand model completely and to develop contact between the raft and the sand surface (Figure 3.30(f)). The replacement ratios defined by the total cross section of the piles to the raft base area are 1.9% and 3.8% for 12 and 24 piles model respectively. Assuming that the volume of piles is equivalent to the reduction of soil volume in the pile installation portion, relative density could be increased to 70% and 75% from the target sand density (Dr=65%). Due to the static pile installation procedure and the outward lateral displacement of sand, the actual increases of relative density by the pile driving should be smaller than those values. Furthermore, after completion of pile installation process, to have a secure contact of the raft base to the ground surface, preloading was applied on the tank in the same in-flight condition which will be discussed later.

3.5.2. Preloading

As indicated before, having made the model ground and placed the model tank on the ground; the tank was vertically loaded by an electrical jack to have a secure contact between the raft base and the ground surface. The preloading steps were different in slab and non-driven piled raft in comparison to driven piled raft which will be discussed in the next sections.

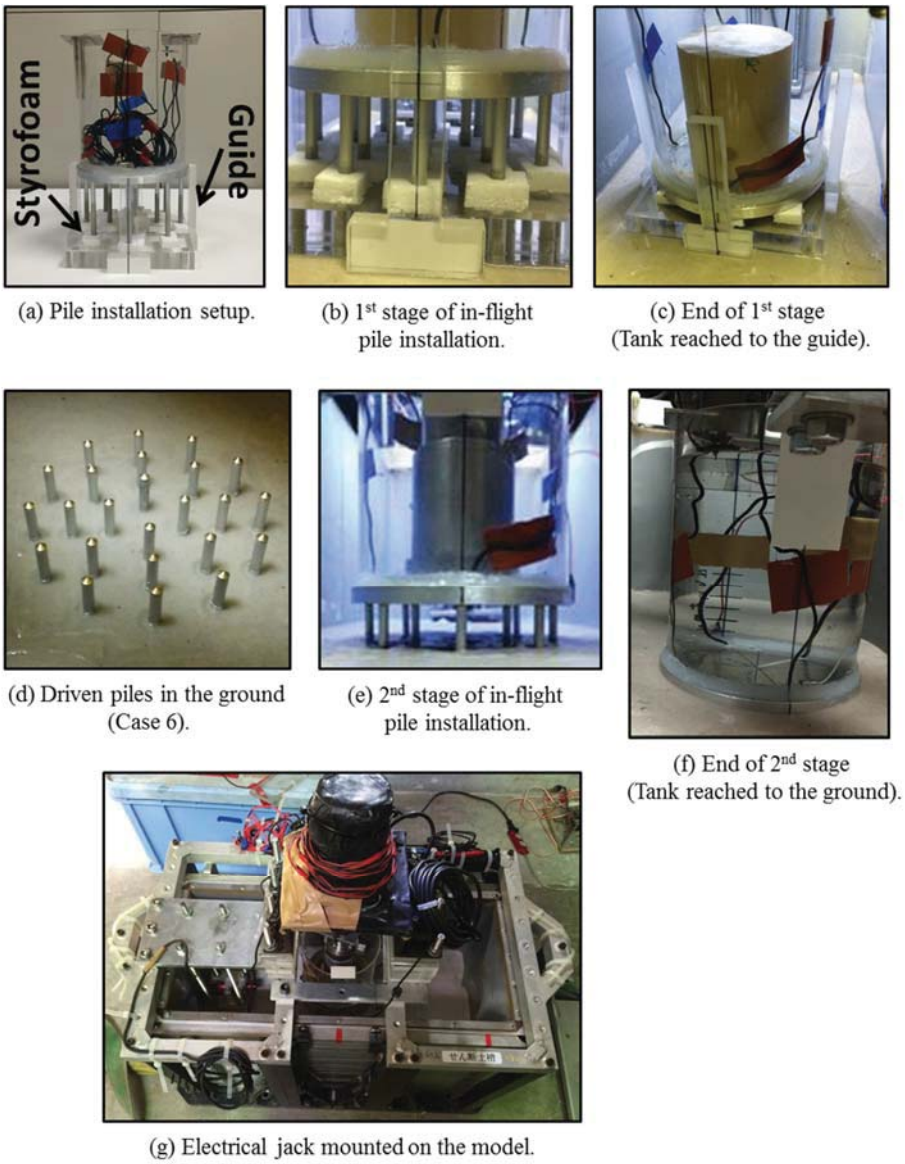

(a) Pile installation setup.
(b) 1st stage of in-flight pile installation.
(c) End of 1st stage (Tank reached to the guide).
(d) Driven piles in the ground (Case 6).
(e) 2nd stage of in-flight pile installation.
(f) End of 2nd stage (Tank reached to the ground).
(g) Electrical jack mounted on the model.

Figure 3.30. Pile installation process in Cases 5 & 6 (Driven PRF on saturated sand).

3.5.2.1. Preloading in Slab and non-Driven Piled Raft Foundation

After completion of the ground modeling, in slab foundation cases (Cases 1, 3a and 3b) and non-driven piled raft foundation cases (Cases 2 and 4), the model tank was placed on the ground in Cases 1, 3a and 3b or on top of piles head in Cases 2 and 4. Then, the tank was vertically loaded by an electrical jack in 1g condition to have a secure contact between the raft base and the ground surface. The load-displacement curves measured in the preloading for all cases except Cases 3a (the data were not recorded) are presented in Figure 3.31. The maximum preload for different cases was chosen based on the foundation type. In Cases 2 and 4 with the piled raft foundation, it was assumed that the raft load proportion (RLP) would be about 50% and the preload about twice that of slab foundation (Cases 1, 3a and 3b) was applied. Also, in saturated cases the preload was half of the dry cases due to the looseness of the saturated sand in comparison to the dry sand. In this way, the maximum preloads on the dry sand were 490 N and 980N for SF (Case 1) and PRF (Case 2) respectively, while in the saturated cases about halves of these loads were exerted on the foundations. The measured earth pressures in Case 3b with the built-in cells and Case 4 with the non-built-in cells during the preloading process are presented in Figure 3.32 together with the average raft contact pressure exerted by the jack. In Case 4, the pressure could not be recorded by E.P.5 (the raft center). In Case 4, all the earth-pressure cells recorded larger values than the calculated average pressure (25 kPa), which was calculated neglecting the load supported by the piles. These larger stresses can be attributed to the stress concentration on the non-built-in earth-pressure cells. However, the trends of variation in the measured contact pressures were well comparable to that of the average pressure, meaning that even those non-built-in cells could provide qualitative useful data during the test. In order to eliminate this undesirable stress concentration, the built-in earth-pressure cells were implemented at the raft base in Case 3b. Although the measured contact pressures by the built-in

cells showed a large difference, the average value of the measured pressures was much closer to the average exerted pressure. The inevitable uneven ground surface condition could be a reason for the large variation of the measured pressures.

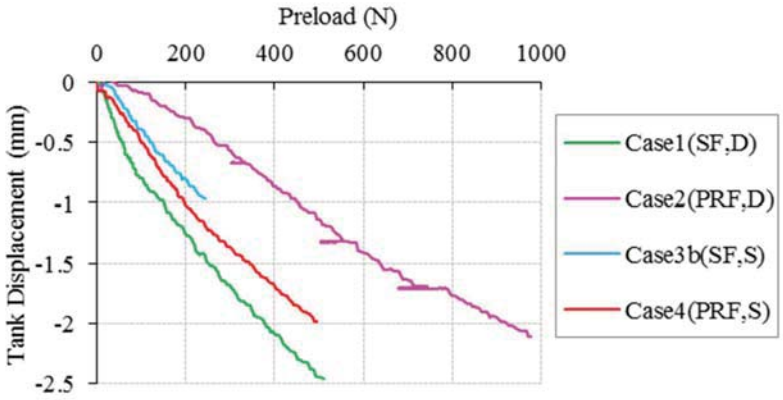

Figure 3.31. Exerted loads during preloading process.

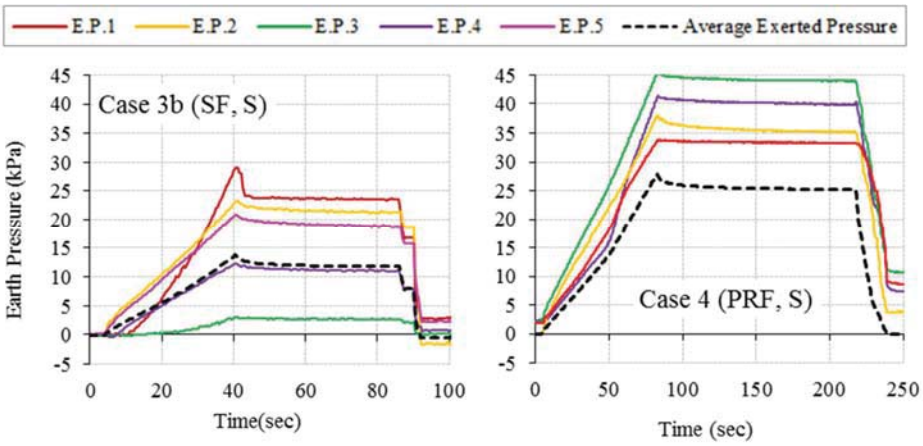

Figure 3.32. Raft base pressures during preloading process (Cases 3b and 4).

3.5.2.2. Preloading in Driven Piled Raft Foundation

Also, in cases of driven piled raft foundation (Cases 5 and 6) in order to have a secure contact of the raft base to the ground surface, preloading was applied on the tank by the electrical jack, in the same in-flight condition after the tank reached to the sand surface during the in-flight pile installation process.

The load-displacement relationships in the second installation and preloading process in these cases are presented in terms of total load and per pile load in Figure 3.33(a) and (b) respectively. The weight of the model tank and loading block (the cylindrical block inside the tank utilized for transfer of jack load to the tank bottom) put in the tank is included in the load. The raft base contacted to the sand surface at the displacement of about 25mm. The maximum preload was chosen to have a same maximum applied raft contact pressures neglecting the loads supported by the piles in the two cases, which was approximated by the load at the time of contact. Also, this value was selected considering the earth-pressure cells capacity (500kPa). In this way, the maximum preload in Case 5 and Case 6 were about 11.5kN and 13kN respectively and the maximum applied raft contact pressure in these cases neglecting piles load was about 650kPa in both cases. The per-pile load in Case 6 is almost the same as that in Case 5 at the end of penetration. However, the load displacement curves of the two cases are quite different. In the beginning, the per-pile load in Case 5 is larger than Case 6 and as the penetration increases the increment rate of Case 6 increases while that of Case 5 decreases. The larger per-pile load, in the beginning, could be attributed to group pile effect, that is, the pile end bearing capacity is relatively larger in the fewer piles case than the more pile case. But as the penetration increases, the larger shaft friction was mobilized for the latter case than the former due to the larger soil compaction and the larger horizontal stress. Although the maximum load in the preloading

process was different in driven-PRF cases (Case 5 and 6) comparing with SF cases on saturated sand (Cases 3a and 3b) and non-driven-PRF case on saturated sand (Case 4), the final penetration depth of raft during the preloading was not so much different for all the cases. In Case 3b and Case 4, the maximum settlement during preloading were 1 and 2mm respectively (Figure 3.31) while, they were 2.5mm in Case 5 and 2mm in Case 6 (Figure 3.33). The raft base pressures measured by the pressure cells and their average during the preloading process along with the average exerted pressure by the self-weight of the tank and the jack loading are presented in Figure 3.34. As this figure indicates in spite of some difference in the measured contact pressures by built-in cells, the average values of the recorded pressures are nearly compatible with the average applied stress with some exception, such as EP3 in the beginning of preloading of Case 5 and EP4 in the whole loading process of Case 6. As mentioned before, unavoidable uneven ground surface is a reason for significant variation of measured pressures especially in the beginning of the loading, which caused small pressures by poor contacts and large pressures by stress concentrations.

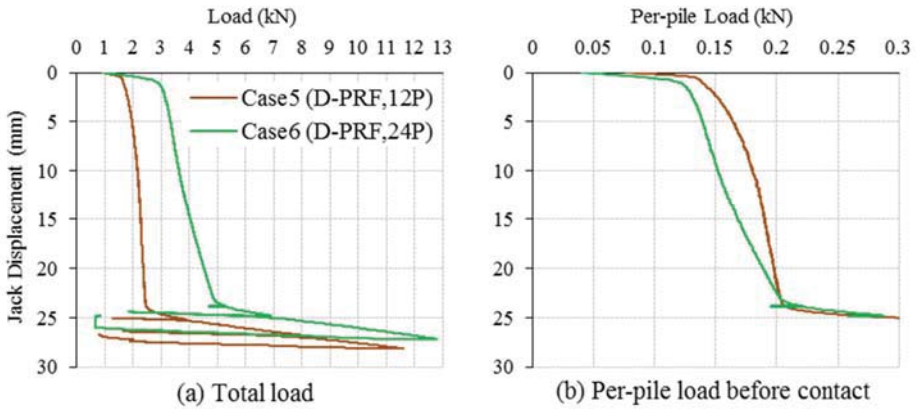

Figure 3.33. Jack loading during 2nd stage of piles installation and preloading (Cases 5 and 6).

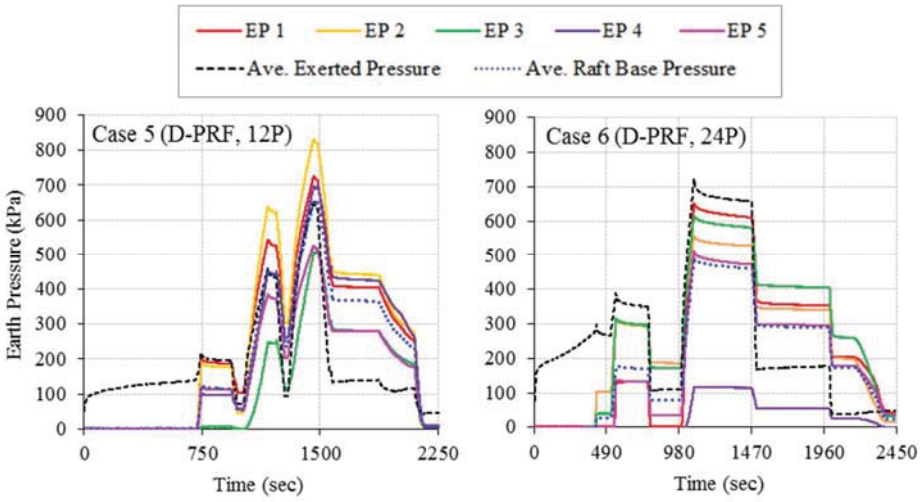

Figure 3.34. Raft base pressures during preloading process (Cases 5 and 6).

3.5.3. Shaking Tests

The centrifuge was stopped and the jack was detached after completion of the preloading in the driven PRF cases (Cases 5 and 6). Similarly, in the other cases (Cases 1, 2, 3a, 3b and 4) at the end of preloading process the jack was detached from top of the model and the whole setup was mounted on the shaking table on the swing platform of the centrifuge.

In the next step, the displacement sensors (LDTs) were set on the model (Figure 3.35(a)) and filling the tank with water (Figure 3.35(b)) with height of 14cm (water was used as the liquid inside the tank), the centrifugal acceleration was increased up to 50g. After confirming the steadiness of all sensors output, white noise vibration was inputted to the model for the dry sand cases but not for the saturated sand cases to avoid the change of structure of sand. In the continuation, the shaking tests were conducted. The target input wave in the tests is EW component of the acceleration recorded at Kurikoma, Kurihara city in 2008 Iwate-Miyagi Nairiku earthquake (JMA, 2008). The second shake with about fifteen percent higher amplitude was inputted to the model after the first shake. The comparison of target acceleration and its

Fourier spectrum with those of input motions in the tests are presented in the prototype scale in Figure 3.36. The high-frequency component of the target motion could not be inputted due to the limited performance of the shaker. Furthermore, there were some differences in the input acceleration, which can be clearly seen in the variation of Arias intensity of the input accelerations in Figure 3.37. Arias intensity (Ia) firstly proposed by Arias (1970) is a measure of intensity of shaking defined as (Kramer, 1996):

$$I_a = \frac{\pi}{2g}\int_0^{\infty}[a(t)]^2 dt \tag{3.9}$$

where *a(t)* is shaking acceleration and *t* is time. Also, further studies was done by Stafford et al. (2008) and some new predictive equations for the estimation of this value from crustal earthquakes in New Zealand has been developed for several horizontal components definitions.

In the dry sand cases (Cases 1 and 2), almost the same input motion could be exerted for the two test cases in each shake, but in the saturated sand cases, the different motions were inputted between the test cases depending on the first and second shakes. In Shake 1, the input motions of all cases are nearly similar, especially till 7sec, but in Case 3a, it was significantly larger than the others. In Shake 2, Case 3a and Case 3b had almost the same levels of the input motions, but they were remarkably larger than the other cases which had almost similar input motion levels mostly until 7sec. From the time variation of Arias intensity, it can be seen that the majority of major input acceleration had been exerted till 10 to 15sec and thereafter the input acceleration amplitudes were so small and the differences in all cases were negligible.

In the shaking tests, the ground and tank accelerations, the horizontal and vertical displacements of the tank, and the excess pore water pressures in the ground were measured as shown in section 3.5.1. Theses instrumentations were made not only in the longitudinal section of the shaking direction but also in the transverse section. In chapter 4, the results of the model

tests are given in the prototype scale unless otherwise stated.

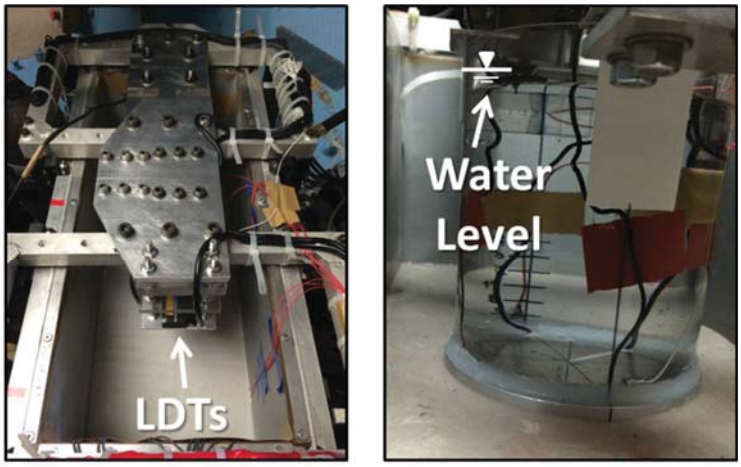

(a) LDTs attached to the model. (b) Tank filled with water.

Figure 3.35. Setting LDTs and filling the tank with water after preloading process.

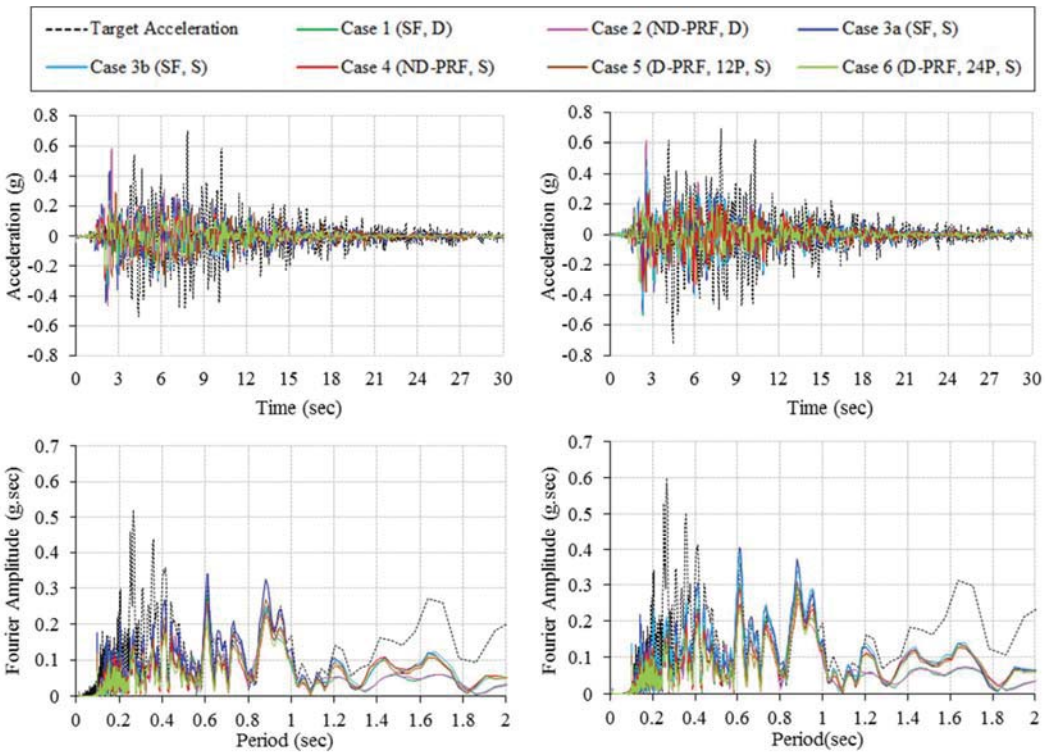

(a) Shake 1 (b) Shake 2

Figure 3.36. Input accelerations and their Fourier spectra.

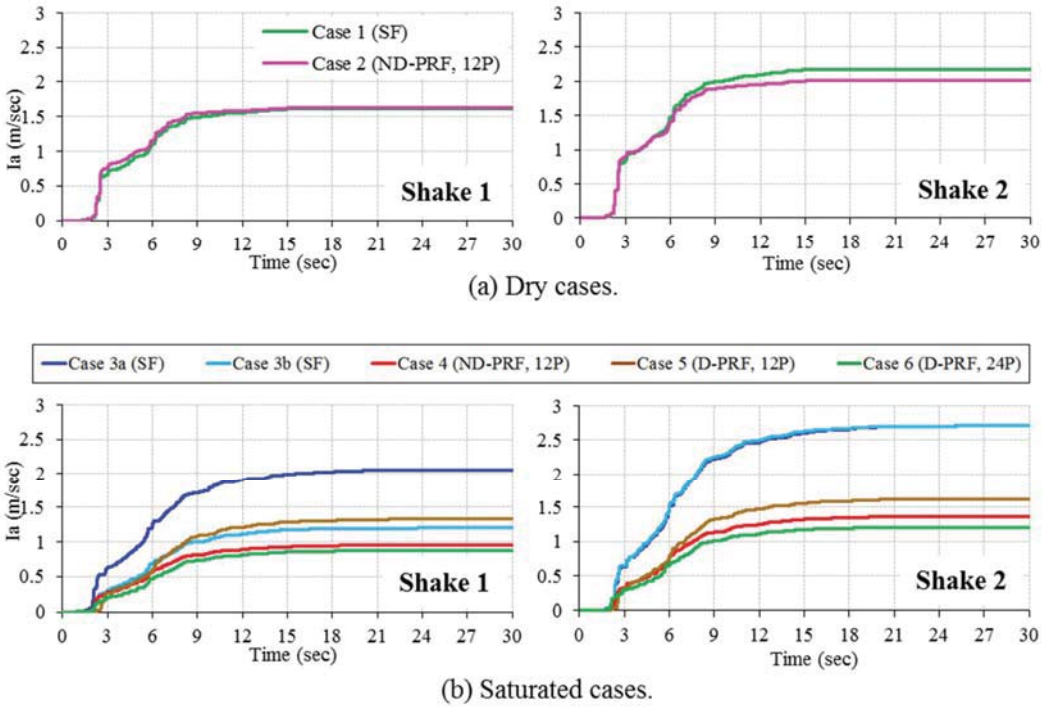

Figure 3.37. Arias intensity of input motions.

3.6. Summary

The basic principles of centrifuge modeling were explained in this chapter. Also, the details of model tests conducted in this study along with instruments and their calibration were described. Centrifuge modeling is a powerful procedure for simulation of piled raft foundation and the complicated soil-pile-raft interaction in this foundation system with prototype stress in model scale. In the previous studies on piled raft foundation, mostly this foundation was modeled for normal superstructures or buildings but in this study this foundation was modelled for storage tank. Also, this simulation was conducted on saturated (liquefiable) sand which was ignored in most of the previous researches due to the complexity of modeling of this system on the liquefiable ground.

On the other hand, in former investigations the piled raft foundation was modeled by non-driven (non-displacement) piles in which the piles are fixed in the container during the sand pouring but in the present study driven (displacement) piles were modelled. For this purpose, the model setup firstly was prepared and put on the model ground and during centrifuge rotation, in-flight pile installation was conducted and the driven piled raft foundation was modelled. By using this procedure, uniform contact condition between the raft and the ground surface can be developed. Furthermore, piles shaft friction which is necessary in the concept of piled raft foundation can be increased by this method in comparison to non-driven pile installation method. Also in order to study piles number effect on the behavior of foundation system, the piled raft foundation was modeled with two piles numbers.

Comparing the per-pile load during the piles installation showed that in the beginning the per-pile load in case with fewer piles number is larger than case with more piles due to group pile effect, that is, the pile end bearing capacity is relatively larger in the fewer piles case than the more pile case. But as the penetration increases, the larger shaft friction was mobilized for the latter case than the former due to the larger soil compaction and the larger horizontal stress.

Also, the results of earth pressure cells during the preloading process indicates better performance of built-in earth-pressure cells comparing to non-built-in earth-pressure cells due to the reduction of stress concentration on the built-in sensors.

Chapter 4 - Tests results and discussion

4.1. Introduction

The main objective of this chapter is to discuss on the model tests results and behavior of simulated tank with slab and piled raft foundation during dynamic loading. In the first part of this chapter, tank behavior on dry (non-liquefiable) sand is considered while in the second part, the behavior of tank on saturated (liquefiable) sand along with some introduction about soil liquefaction is explained.

In the shaking tests, the ground and tank accelerations, the horizontal and vertical displacements of the tank, and the excess pore water pressures in the ground were measured. Theses instrumentations were made not only in the longitudinal section of the shaking direction but also in the transverse section as shown in chapter 3. Despite careful instrumentations, some sensors could not measure the data, which are shown in Tables 4.1 and 4.2. In the following discussions, the results of the model tests are given in the prototype scale unless otherwise stated.

4.2. Tank Behavior on Dry Sand

As previously explained in Case 1 and Case 2 a slab foundation (SF) and a non-driven piled raft foundation (PRF) were modelled on dry sand respectively (Table 3.8). In this section the results of recorded data and tank behavior are discussed in detail. The tests information and list of malfunctioned sensors are presented in Table 4.1.

Table 4.1. Test cases on dry sand.

Test code	Foundation	Ground	Malfunctioned sensors
Case 1	Slab	Dry sand (Dr=66%)	---
Case 2	Non-driven Piled Raft (12 Piles)	Dry sand (Dr=68%)	L2, Piles 4 & 10

4.2.1. Ground Response

Ground accelerations observed beneath and beside the tank in the Shake 1 for the SF and PRF models on the dry sand are shown with the input accelerations in Figures 4.1 and 4.2. Fourier amplitudes of the acceleration beneath the tank (A6) are compared to those of the input motion in Figure 4.3. The input accelerations were amplified towards the shallow depth in both cases, but it was more amplified in low periods (high frequencies) in Case 1 with slab foundation. This behavior could be related to higher confinement pressure from the slab foundation in Case 1 in comparison to Case 2 with piled raft foundation which transferred some part of tank load to the deeper part. As shown in subsequent section, in Case 2 with PRF the majority of tank load was supported by piles and small portion of the tank load was directly transferred to the soil beneath the tank, therefore, the stiffness of the soil under the tank with large confine pressure in Case 1 was larger than that in Case 2, resulting in the large predominant frequency of the subsoil.

4.2.2. Tank Response

4.2.2.1. Tank Accelerations

Accelerations at the tank top and bottom in the shaking direction (A8, A9) during Shake 1 and their Fourier amplitude are shown in Figure 4.4. The tank top acceleration was larger than that of the bottom in Case 1 with slab foundation, implying a significant rocking motion. While

in Case 2 with piled raft foundation, the difference between the top and bottom accelerations and Fourier amplitudes are not as much as Case 1 which show the efficiency of the piled raft foundation in reducing rocking motion of the tank. The spectra of accelerations at the tank bottom and just beneath the tank are almost the same in Case 1, which in Case 2, the acceleration of tank bottom is larger than that beneath the tank, implying the shaking motion was transmitted through the piles and tank vibrated rather independently from the ground.

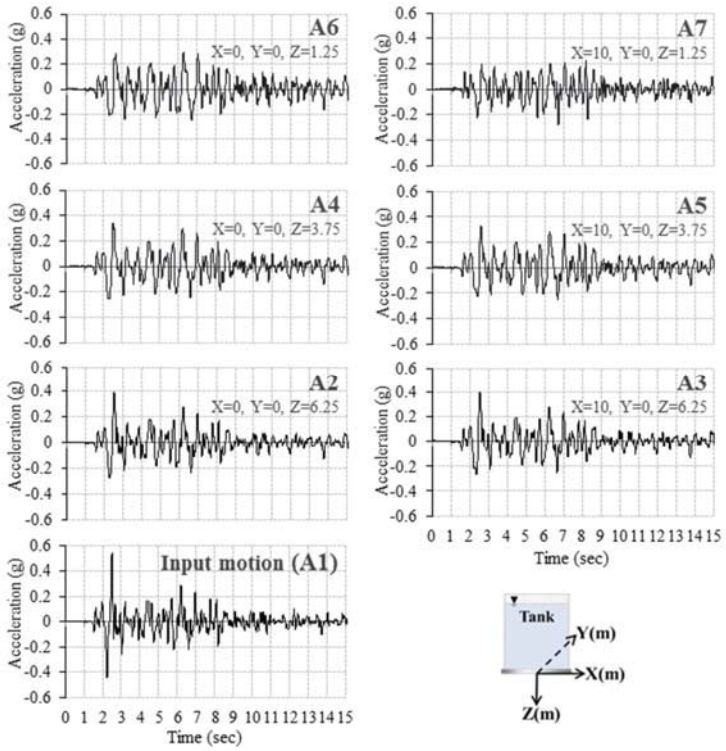

Figure 4.1. Ground accelerations during Shake 1 in Case 1 (SF).

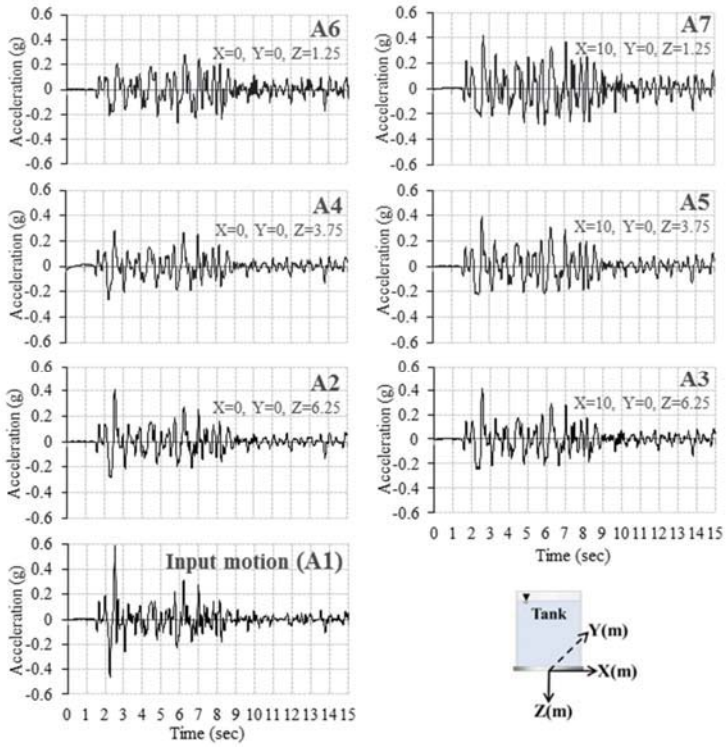

Figure 4.2. Ground accelerations during Shake 1 in Case 2 (PRF).

The raft contact condition to the ground caused the differences in the acceleration predominant period of the tank between the two foundations. The predominant period was smaller in Case 1 than Case 2 and the tank acceleration was largely amplified in this small period range (0.3-0.5sec). This tendency of tank response characteristics was also observed in the white noise vibration as shown in Figure 4.5. But the predominant period of the white noise vibration was shorter than that in the shaking test, which suggesting the reduction of soil stiffness by the large input motion in the latter than the former.

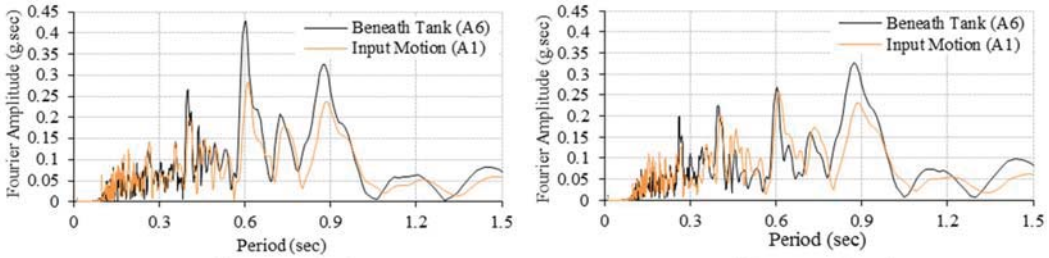

Figure 4.3. Ground responses in Shake 1 (Dry sand).

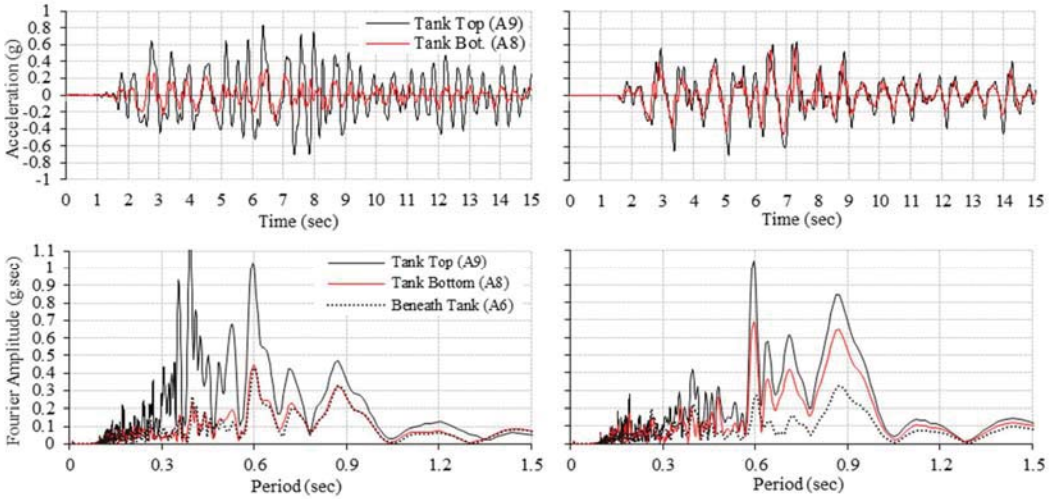

Figure 4.4. Tank responses in Shake 1 (Dry sand).

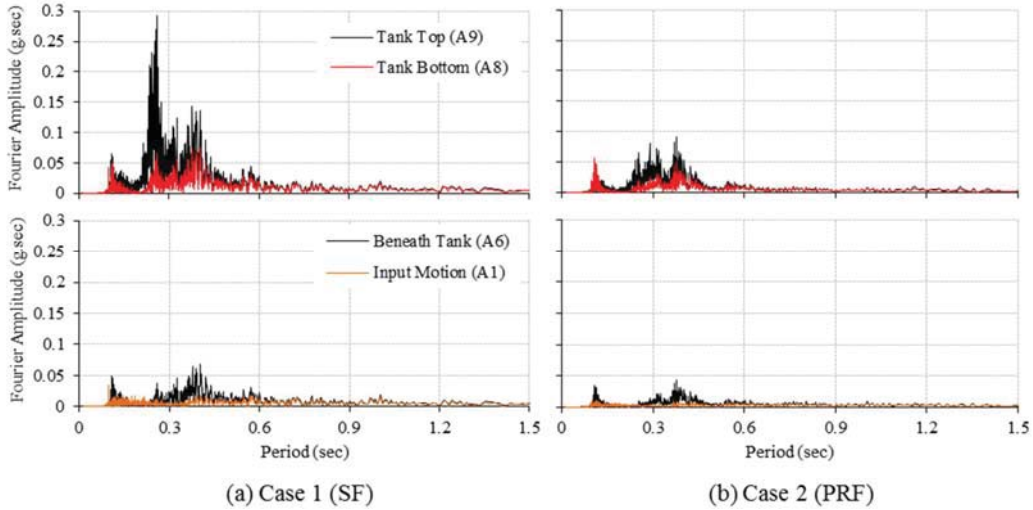

Figure 04.5. Ground and tank responses during White noise (Dry sand).

4.2.2.2. Tank Settlements

Tank settlements measured by three laser displacement transducers (L1, L2 and L3, Figures 3.22 and 3.25) are compared for the slab and piled raft foundations in Figure 4.6. In Figure 4.6(a), the settlements measured at the opposite top edges of the tank in the shaking direction (L1, L2) are shown, while in Figure 4.6(b) the tank edge settlements in the transverse direction (L3) are shown with the tank center settlement, that is, the average of L1 and L2. The tank center settlement and L2 are not plotted in the figures for Case 2 as the settlement could not be measured by L2 in this case due to the dislocation of the laser from the target plate. However, it is confirmed from the figures that the settlements of PRF are much smaller than those of SF, which is a good evidence of settlement reducer function of the piles. In the beginning of shaking till 2.5sec, although the input accelerations were not so large, both cases showed rapid settlements, which could be attributed to the densification of sand. After the initial settlement, the settlement rate once decreased in both cases, but in Case 1 the rate increased again from around 6 to 8sec and then the tank showed very small settlement increased until the end of the shaking. This large increase of settlement is not clearly seen in Case 2 in the figure. The difference in the trend of settlement from 6 to 8sec could be caused by the rocking motion enhanced during this period (Figure 4.4) and the load transfer by the piles to deep stiff layer. The LDTs data show dynamic variation in both cases, but the amplitude of variations and its duration is partly larger in the case of slab foundation which is another evidence of higher rocking motion in this case. Although the tank accelerations in the transverse direction were not measured in the dry sand cases, it can be confirmed from the small amplitude of L3 that the rocking should be smaller in the transverse direction than the shaking direction.

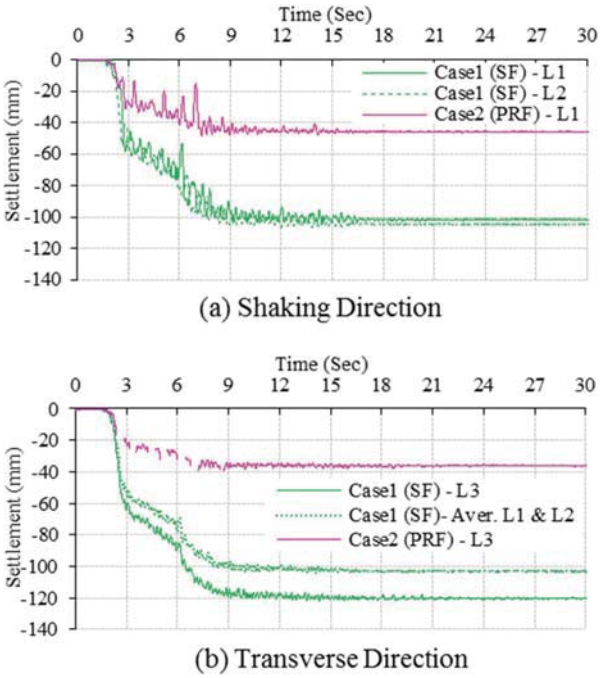

Figure 4.6. Tank settlements in Shake 1 (Dry sand).

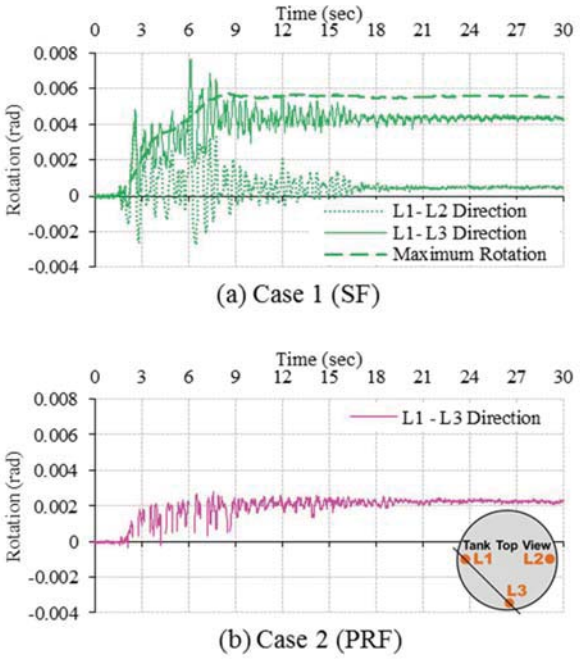

Figure 4.7. Tank rotations in Shake 1 (Dry sand).

4.2.2.3. Tank Rotation

The tank rotations in two cases are shown in Figure 4.7. The rotation of the tank in the shaking direction (L1-L2 direction) and L1-L3 direction are presented together with the maximum rotation for Case 1 while in Case 2 due to the absence of L2 data the rotation is presented only in L1-L3 direction. Considerable difference between the two foundations can be also seen in the rotational behavior. Both the rotation amplitude in dynamic response and the residual rotation of the slab foundation were much larger than those of the piled raft foundation, which verifying a better performance of piled raft foundation in reducing the tank rotation during dynamic loading. The rotation of slab foundation ceased at t=8sec and was kept constant, despite the further shaking at the later part of shaking. The same trend can be confirmed in PRF, but the time of becoming the constant rotation angle was earlier than SF. It should be noted that the rotation in the shaking direction was much smaller than that in L1-L3 direction. The rotational behavior will be discussed more in later section.

4.2.3. Piles and Raft Resistances

Using the instrumented piles in Case 2, the head axial load, tip resistance and shaft friction carried by each pile were measured. Figure 4.8 shows the axial forces time history of the three forces of all piles. The data could not be recorded in piles No. 4 and No. 10 due to broken strain gauges in these piles. Also the piles head load, tip resistance and shaft friction in static condition before the shaking are presented in Figure 4.9. The pile at the inner part of the raft (No. 9) had higher load bearing contribution in the static condition.

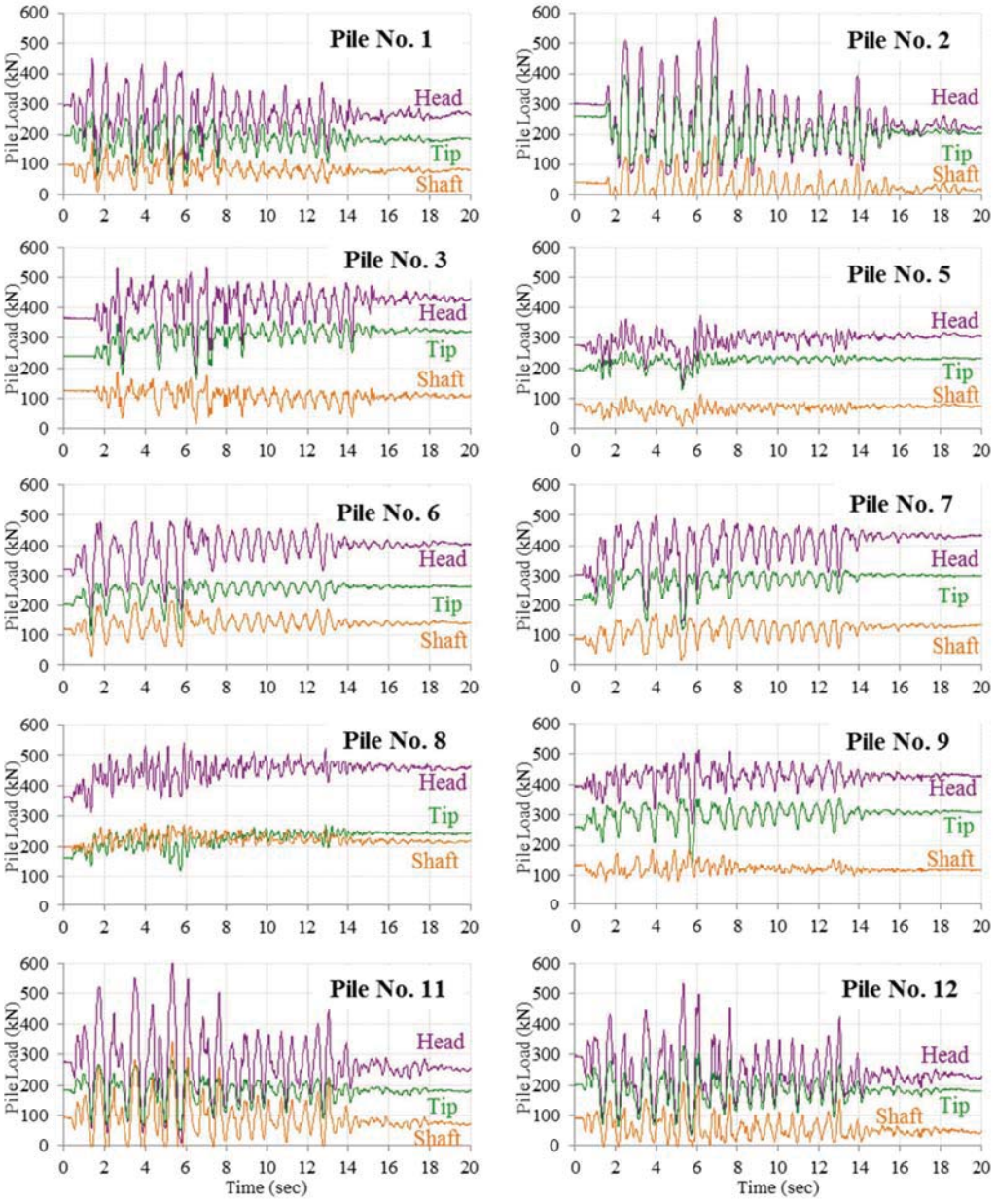

Figure 4.8. Variation of piles loads.

On the other hand, the piles at outer edge in the shaking direction (Piles No. 1, 2, 11 and 12) showed higher amplitude during the shaking, implying higher contribution of the pile resistance against the rotational moment from the tank as illustrated in Figure 4.12(a). In order

to discuss on the contribution of piles against dynamic loading, the piles head load, tip resistance and shaft friction are shown for three sample piles, No. 1 at outer edge of raft in shaking direction, No. 5 at outer edge of raft in transverse direction and No. 9 at center part of raft. These loads are calculated by eliminating static part of load from total one and presented in Figure 4.10. As this figure indicates pile No. 1 at the raft outer edge has higher contribution against dynamic loading in comparison to piles No. 5 at transverse direction and No. 9 at central part of raft.

Total loads carried by all piles are presented in Figure 4.11. In the figure, the measured pile head resistance, that is, the tank load carried by the piles, the pile tip, and shaft resistance components are shown together with the tank load. It should be noted that due to the interference of the moment strain to the axial strain measurement near the pile top, the measured total pile load was overestimated, which could be seen in the static and dynamic components. Namely, the measured static load was larger than the tank load, and the large amplitude measured during the shaking, though the shaking motion was applied in the horizontal direction, not vertical direction. However, the pile axial load bearing behavior can be discussed by the measurements and it can be said from the figure that the majority of the tank load was carried by piles in the static conditions for this particular piled raft foundation with frictional piles. About 67% of pile resistance was mobilized by the tips and 33% by the shaft in the static condition. By considering the average amplitude of dynamic loads of piles in Figure 4.10 and comparing this average amplitude in pile head, tip resistance and shaft friction, it is indicates that shaft friction contribution was increased to 40~45% during the shaking.

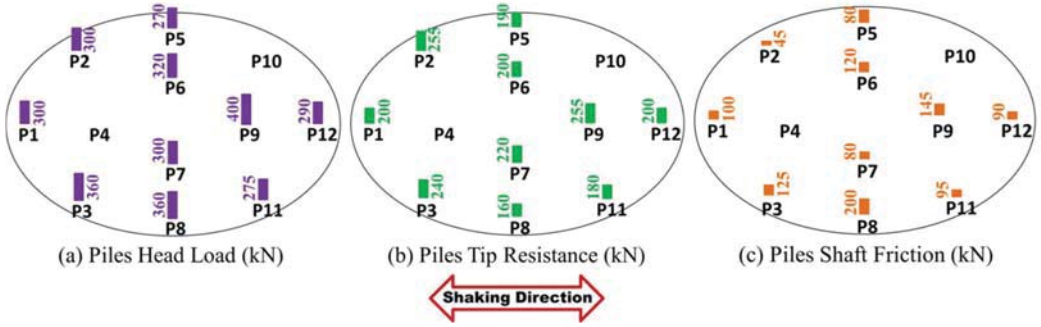

Figure 4.9. Piles loads before shaking (Static load).

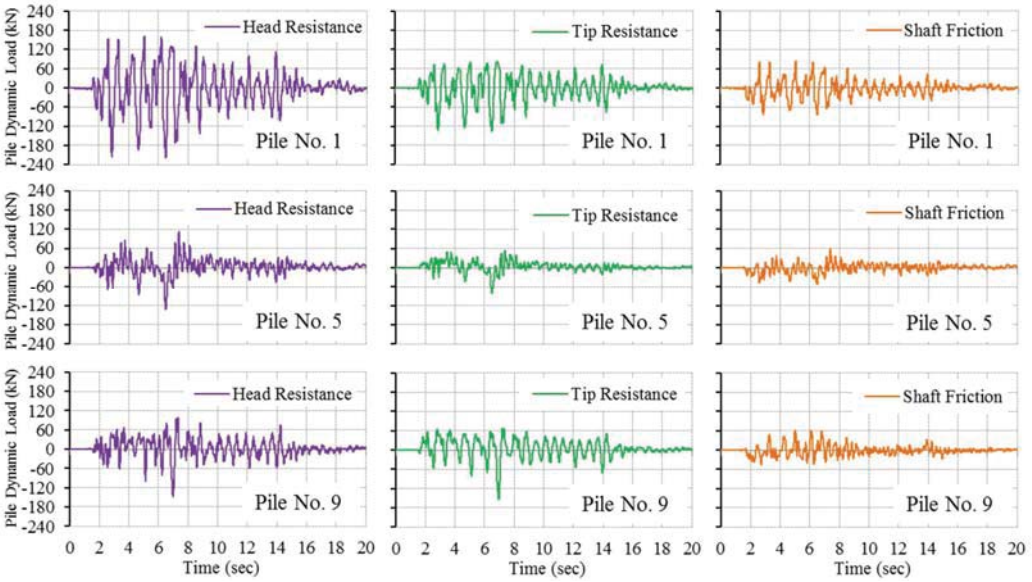

Figure 4.10. Piles dynamic loads during shaking.

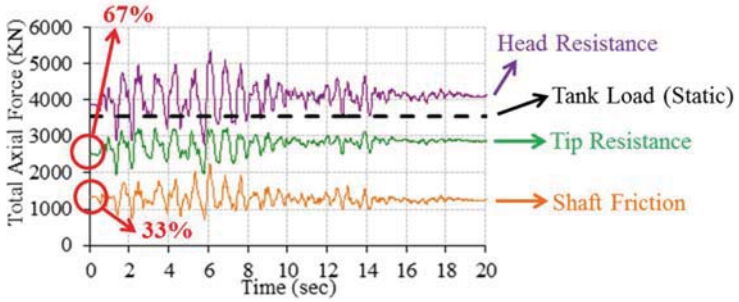

Figure 4.11. Total axial force carried by piles.

In order to verify the effects of piles and the raft on the rotational behavior of the tank, the tank rotational moment and the piles resistant moment are compared in Figure 4.12. The tank rotational moment and piles resistant moment are calculated from the tank inertia force and piles axial forces respectively around the center of the raft (Figure 4.12(a)). The difference between these two moments is the raft resistant moment. Although the error in the measurement of pile axial forces could cause the uncertainty (overestimation) in the approximation of the moment resistance, the mobilization trend of the resistance by the raft and piles can be confirmed in Figure 4.12(b). Both of the tip and shaft resistances almost evenly contributed in preventing the tank rotation. The piles resistant moment had the main role in bearing the tank rotational moment. However, despite very small raft contact pressure in the static condition, it is confirmed that the raft also resisted against the moment load (about 20%) especially when the large rotational moments were applied.

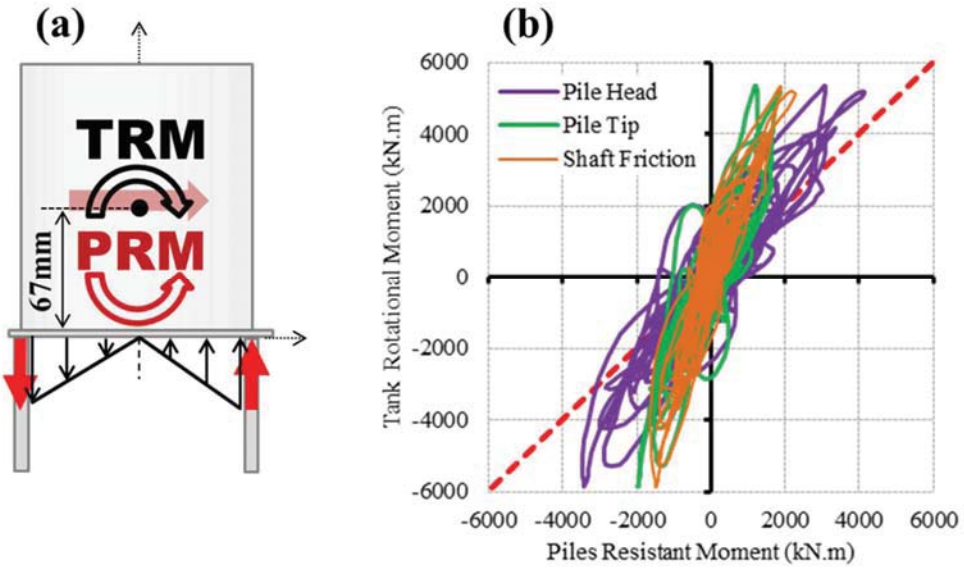

Figure 4.12. Tank rotational moment (TRM) and piles resistant moment (PRM) in Case 2 (PRF, Dry sand); (a) Diagram of PRM and TRM, (b) PRM vs. TRM.

4.3. Tank Behavior on Saturated (Liquefiable) Sand

4.3.1. Soil Liquefaction

One of the most important and complicated topics in geotechnical earthquake engineering is liquefaction. This destructive phenomenon attracted engineers consideration after huge successive earthquakes in Alaska (M_W=9.2) and Niigata (M_S=7.5) in 1964 which caused enormous liquefaction-induced damages (Figure 4.13). The damages include foundations failure, buried structures flotation, oil tanks and buildings overturning and slope failure (Figure 4.14). During these decades after those earthquakes, liquefaction has been investigated comprehensively by many researchers but the 2011 off the Pacific coast of Tohoku earthquake (Japan) and Christchurch (New Zealand) earthquakes in 2010 and 2011 indicated that this phenomenon still can make problem even in the countries where geotechnical earthquake engineering topics are pioneer (Figure 4.15).

Figure 4.13. Buildings overturning due to liquefaction during 1964 Niigata earthquake.

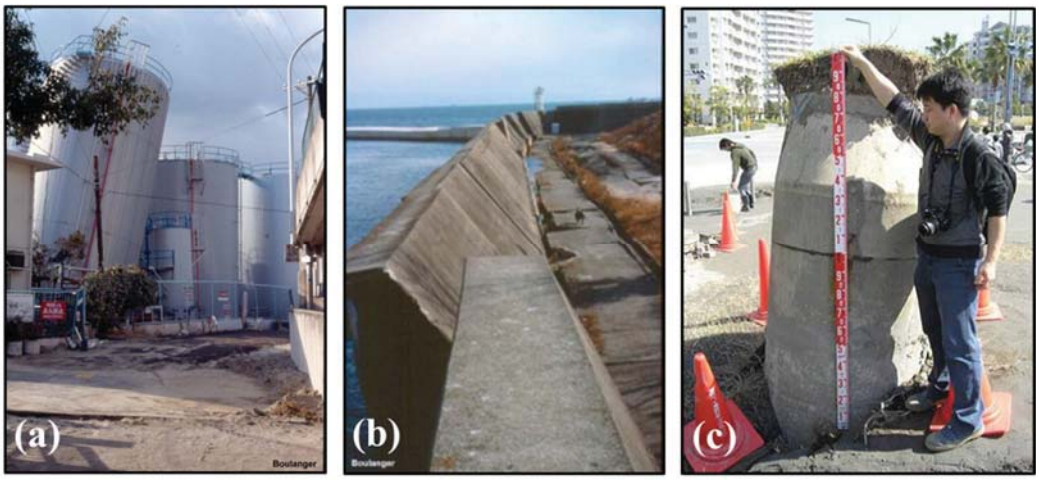

Figure 4.14. Soil liquefaction damages; (a) Tank overturning in 1995 Kobe earthquake (UC Davis website), (b) Quay wall overturning in 1995 Kobe earthquake (UC Davis website), (c) Buried structures flotation in 2011 Tohoku earthquake (Towhata, 2011).

Figure 4.15. (a) Liquefaction damages in 2011 Christchurch earthquake, (b) Liquefaction damages in 2011 Tohoku earthquake (Towhata, 2011).

Liquefaction is a kind of soil deformation triggered by cyclic loading of saturated cohesion-less soils under undrained condition. The generation of excess pore water pressure under undrained loading condition is a necessity for this behavior. Rapid loading by earthquakes induces undrained loading condition for saturated cohesion-less soils. During this loading, the tendency for densification causes increase of excess pore water pressure and reduction of

effective stress. Liquefaction initiated from this trend can be divided into flow liquefaction and cyclic mobility.

When the shear strength of a soil mass in its liquefied state is smaller than the shear stress required for static equilibrium of the soil, flow liquefaction can be triggered. In this condition the cyclic stresses is sufficient to drop soil strength and produce the flow failure. This failure occurs suddenly and the liquefied materials move in a large distance but it happens less frequently with severe effects comparing to cyclic mobility liquefaction.

On the other hand, cyclic mobility happens when the static shear stress is less than the shear strength of the liquefied soil in contrast to flow liquefaction. The induced deformations by cyclic mobility develop during earthquake shaking. The deformations in this type of liquefaction in contrast to flow type produce by not only cyclic but also static shear stresses. These deformations called lateral spreading (Figure 4.16) can happen on sloping ground or even almost flat ground next to water which can cause severe damages in presence of structures.

Level ground liquefaction is a kind of cyclic mobility liquefaction while static horizontal shear stresses which can develop lateral deformations do not exist. Despite of some ground oscillations, level ground liquefaction can develop small permanent lateral soil movement. This type of failures trigger by the upward flow of water which happen when the excess pore water pressure induced by earthquakes dissipate. This failure also can occur after the earthquake with some delay due to required time for dissipation of excess pore water pressure. Additional ground settlement and development of sand boiling are some characteristics of level ground liquefaction failures (Figure 4.17).

Figure 4.16. Damages induced by lateral spreading; (a) 2011 Christchurch earthquake, (b) 2011 Tohoku earthquake (Towhata, 2011).

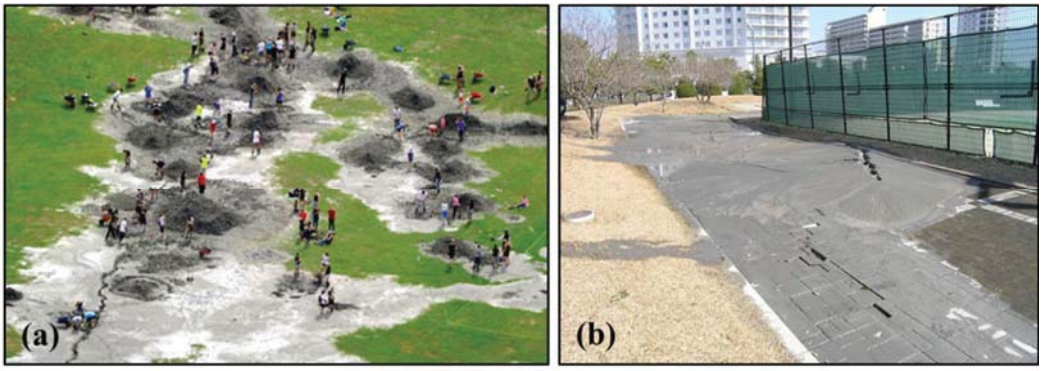

Figure 4.17. Damages induced by sand boiling; (a) 2011 Christchurch earthquake, (b) 2011 Tohoku earthquake (Towhata, 2011).

4.3.2. Tests Results in Saturated (Liquefiable) Cases

As indicated in section 3.5.1, five model tests were conducted on liquefiable sand in order to investigate the performance of piled raft foundation during liquefaction (Table 3.8). The tank

behavior in these model tests are discussed in this section. The tests information along with malfunctioned sensors in the tests is presented in Table 4.2.

Table 04.2. Test cases on saturated sand.

Test code	Foundation	Ground	Malfunctioned sensors
Case 3a	Slab	Saturated sand (Dr=65%)	EP3, L1, L2, L3 (Shake2)
Case 3b	Slab	Saturated sand (Dr=68%)	P2, P3
Case 4	Non-driven Piled Raft (12 Piles)	Saturated sand (Dr=69%)	A4, EP5
Case 5	Driven Piled Raft (12 Piles)	Saturated sand (Dr=70%)	P4, P11, P12
Case 6	Driven Piled Raft (24 Piles)	Saturated sand (Dr=65%)	P4, P5, P8, A11, A13

4.3.2.1. Ground Response

Figure 4.18 presents the ground acceleration responses in all the cases during Shake 1. Fourier amplitudes of the accelerations measured are compared with that of the input motion in Figure 4.19. Although there are some missing data due to the malfunctioning of accelerometers (Table 4.2), several points on the general behavior and the effects of foundation type can be observed from the figures. At the location of A2 (X=Y=0, Z=6.25m), 1.25m below the pile end, the input motions were propagated without attenuation for all the cases. However, above this depth, attenuation of input motion is clearly seen in the ground, especially for the short component, which is a clear evidence of soil stiffness reduction by liquefaction. The attenuation is more significant beside the tank than that beneath the tank, which can be attributed to the confinement effect of the tank load to the soil underneath. This prevents significant reduction of stiffness and increase of damping ratio as happening in the free ground beside the tank. However, the natural period of the ground became long due to the liquefaction, which could cause the amplification in the long period range as seen beneath the tank (A5). In Case 3a, because of

relatively large input motion, the attenuation was more than the other two cases. The acceleration response of A11 located at 0.75m out from the raft edge in the transverse section is similar to that of A5 beneath the tank center in Cases 3a, 3b and 4, implying that the tank load could affect the dynamic behavior at the location of A11. At the location of A6, 3m out from the raft edge, the attenuation level of PRFs (Cases 4, 5 and 6) are more than that of SF (Case 3b), implying the more effect of tank load for SF than PRF at this depth. This is because the tank loads were transmitted to the deep depth through piles of PRFs as compared to SF. In Case 3a, due to higher input motion, large attenuation also can be detected at this location. Comparing A10 (X=0, Y=4.5m, Z=3.75m) in Cases 5 and 6, more attenuation can be seen in Case 6 than Case 5, which also indicates the more tank load was carried by piles in Case 6 than Case 5. The details of proportion of the vertical load carried by the piles and the raft will be discussed later.

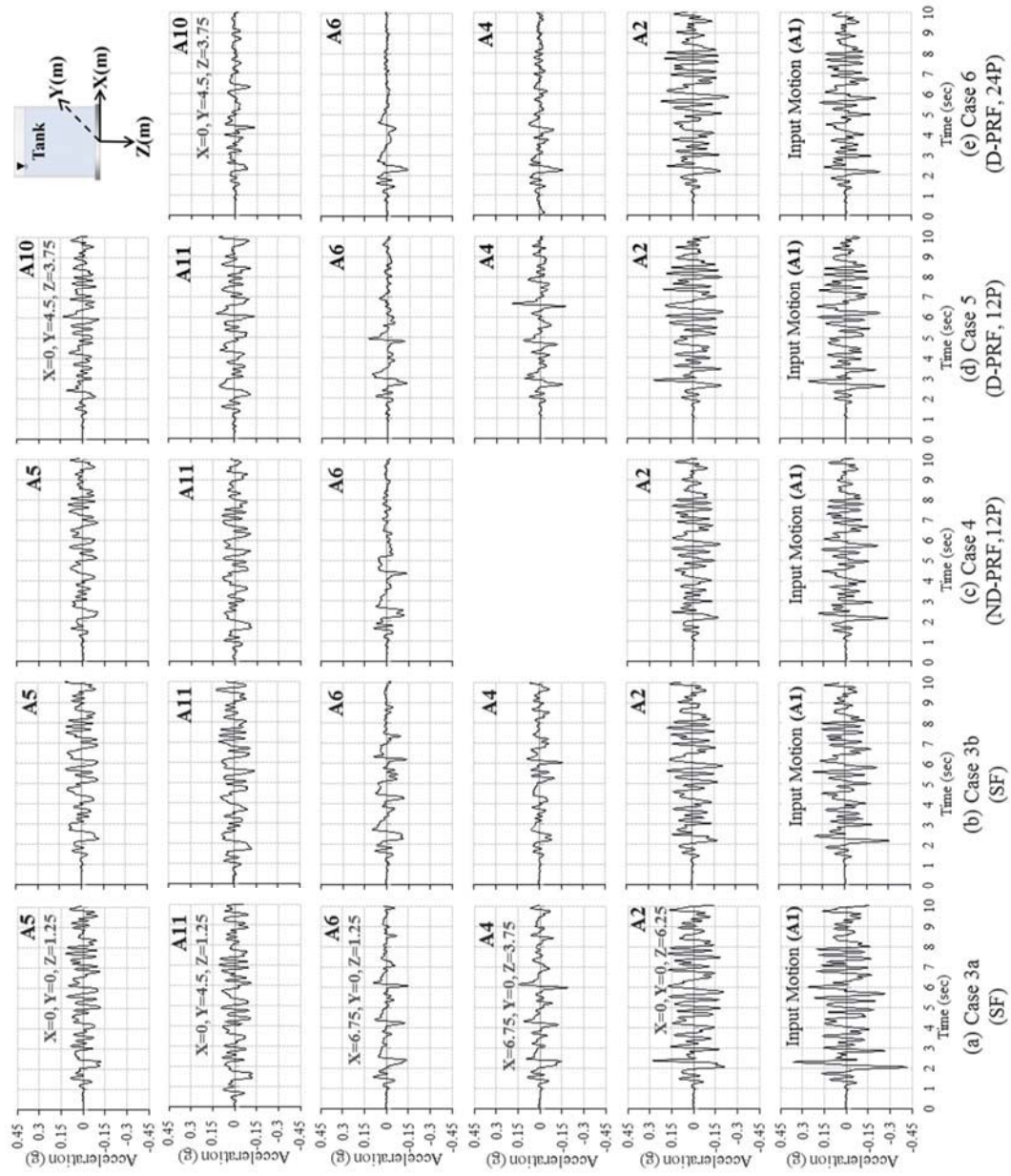

Figure 4.18. Ground accelerations in Shake 1 (saturated sand).

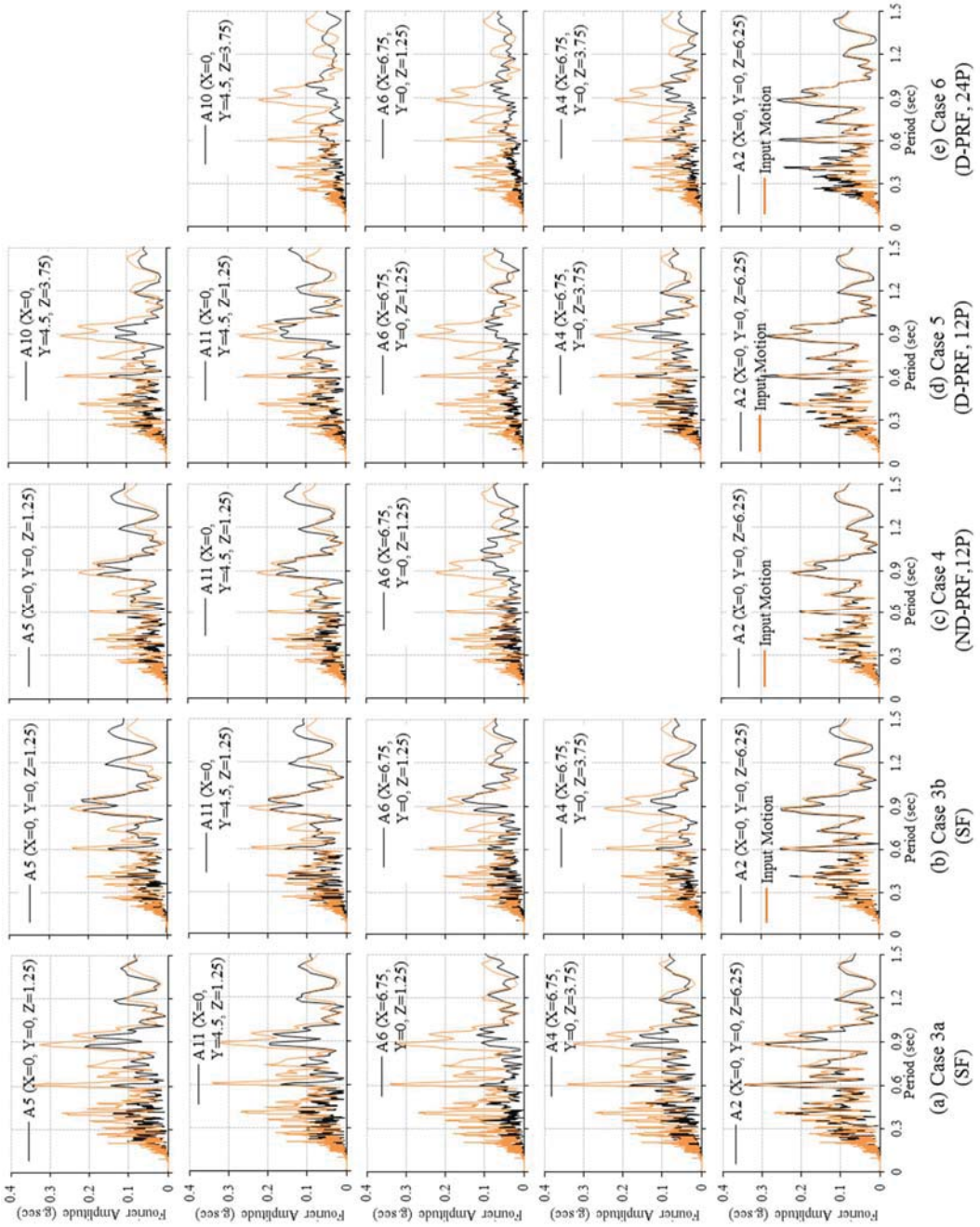

Figure 4.19. Ground response in Shake 1 (saturated sand).

4.3.2.2. Ground Excess Pore Water Pressures

The excess pore water pressures (EPWP) at different locations of the ground observed in Shake 1 are presented in Figure 4.20 (the detailed EPWPs in the ground are presented in Appendix A). The figure shows the EPWP in different depths in four vertical arrays, three in the longitudinal section at the tank center (P7, P4, P3 and P2: X=0m), near (P8 and P5: X=6.75m) and far (P9 and P6: X=10m) outside of the raft, and one in the transverse section (P12, P11: X=0, Y=4.5m). The EPWPs at P7 in the early stage of shaking is also shown in the figure. In Case 3b, P2 and P3, in Case 5, P4, P11 and P12 and in Case 6, P4, P5 and P8 could not be recorded (Table 4.2). In the figure, the initial overburden stress ($\sigma'_{v0} = z\gamma'$, γ': effective unit weight of sand) and the vertical stress (σ'_v) are presented. σ'_v is the sum of σ'_{v0} and the stress by the tank pressure, which is calculated by the elastic solution assuming the uniformly distributed raft pressure on an elastic half-space (Das, 2007). In the early stage of shaking, the EPWPs increased rapidly and then this rapid rise ceased and the water pressure either became almost constant or increased gradually during the shaking. Then the EPWPs started the dissipation. At the locations outside of the raft where the tank load did not affect σ'_v, the EPWP built nearly up to the σ'_v value, meaning almost zero effective stress. While at the location beneath and near the tank, where the tank load affected σ'_v, the EPWPs were smaller than the σ'_v values, reconfirming the confinement effect of the tank on the soil underneath. The larger the difference between σ'_v and σ'_{v0} is, the larger the remaining effective stresses, that is, σ'_v – EPWP, in particular at P7. However, it should be noted that the actual vertical stresses of PRF beneath the tank largely depend on the raft contact pressure. The pore water pressure behaviors of Cases 3b and 4 were almost the same from the beginning to the end, except of P7 and P4 at the tank beneath showing slightly larger EPWPs in Case 4 than Case 3b in the rapid EPWP rise period, which could be attributed to the increase of raft pressure in this period. Case 3a showed different behavior especially in the late start of the

dissipation. While for Cases 5 and 6 (driven-PRFs), the EPWP behaviors in the rapid rise period are also similar to those in Cases 3b and 4 in almost all locations. However, P7 shows quite a different behavior compared to that in Case 3a, Case 3b and Case 4. P7 in Case 6 shows two stage EPWP build-up until t=2sec and t=4–6sec and a gradual decrease immediately after the rapid build-up. In Case 5, P7 increased in one stage until t=3sec and also showed a gradual decrease from this point, which is different from the behaviors observed in Cases 3a, 3b and 4, where EPWP increased gradually after the rapid rise. These different behaviors of P7 in the different cases are considered as an effect of the pile driving. The pile driving process increased the density and lateral confinement of sand between piles, which could slower the EPWP increase and enhance the EPWP dissipation. This EPWP behavior also affected the pile resistance, resulting in the raft contact pressure, which will be discussed later. In contrast to the earlier dissipation beneath the tank, the slower dissipation of EPWP at other locations in Case 6 than the others is an evidence of smaller relative density in Case 6 (Table 4.2). In addition, the EPWP behavior in the area outside of the tank border is different in Cases 5 and 6 (driven PRFs) comparing to the other cases. Generally, the possible reason for this difference is slightly larger input motion in Case 5 and smaller relative density in Case 6 than the others. Similarly, the reason of the difference between Case 3a and the others can be the differences in the liquefaction level due to the larger input motion and smaller relative density in Case 3a (Figures 3.34 and 3.35 and Table 4.2). On the other hand, the residual EPWPs observed at the shallow depth after dissipation was due to the tank settlement at the location beneath the tank and the settlement of PPT due to the relatively large unit weight at the location out of the raft. In P7 of Cases 5 and 6, however, these positive EPWPs were not measured; even it lowered below zero at the end of shaking in Case 5. No clear reason could be found for this, but from the fact that this negative pressure finally became almost zero with a very slow increase, the large disturbance at the location of P7 or tension of the PPT

wire, both of which might be caused by the pile driving process, could be considered as possible reasons.

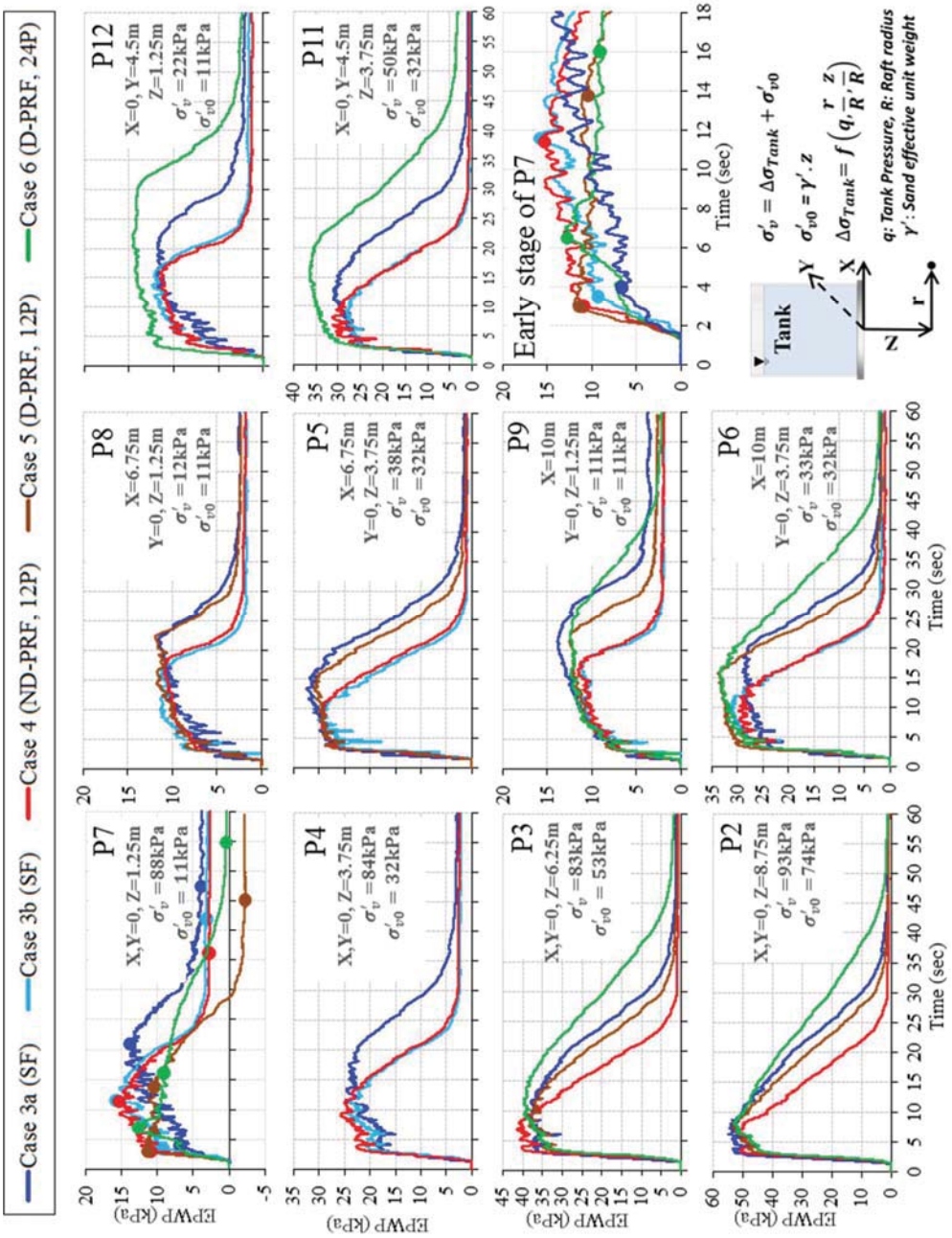

Figure 4.20. Excess pore water pressures of the ground in Shake 1 (saturated sand).

As above mentioned, the typical variation of EPWPs can be divided into three parts. The first part is until the end of rapid increase, which is called "build-up period" and t_1 is the end of this period. The second part is from t_1 to the time when the pore pressure starts the dissipation (t_2), which is named "liquefaction period". The third is the dissipation stage from t_2 until the end of this period (t_3). Determining the end of dissipation (t_3) is not straightforward due to the gradual decrease of EPWP and the residual EPWP. The end of dissipation was determined at the time when the decrease of EPWP from the maximum value became 99% of that at the end of the measurement. These three times are highlighted in the EPWP graphs of P7. In Figure 4.21, t_1, t_2 and t_3 obtained at four vertical arrays in Shake 1 and Shake 2 are shown for all cases. It should be noted that there is some uncertainty in the determination of t_2 of P7 for Cases 5 and 6. As the EPWP showed the gradual decrease from t_1, t_2 was determined by the time when a relatively large EPWP decrease rate was observed.

From Figure 4.21, the points discussed in Figure 4.20 can be confirmed. Focusing on t_1, that is, EPWP build-up time, they were almost the same, $t_1 \cong$ 4sec, regardless of test cases, the locations in the longitudinal or transverse sections, and Shake 1 or Shake 2, except P7, at Z=1.25m under the tank center. In Shake 1, t_1 in Case 6 was later than other cases also this value for Case 3a with relatively large input motion was larger than Cases 3b, 4 and 5 and the t_1s at P7 of Cases 3b and 4 were earlier than those at P4 (Z=3.75m), located below P7. While in Shake 2, t_1 at P7 in Case 6 became almost the same as those in Cases 4 and 5. However, t_1 of P7 in Case 3b, which had much larger input motion than that of Shake 1 (Figure 3.35) was later than those in the other cases. On the other hand, liquefaction duration time (t_2-t_1) and EPWP dissipation time (t_3-t_2) are quite different depending on the cases, the locations and the shaking history (Shake 1 or Shake 2). As a common behavior of liquefied layer, it can be seen that the deeper the location is, the shorter liquefaction time and the longer dissipation time are, due to early recovery of particle

contacts and slow dissipation near the undrained boundary, that is, the bottom of the model. As a result, at the depth deeper than 4m, the dissipation started at the time less than 10sec during the main shakings, while at the shallow depth Z=1.25m, the t_2s at most locations are longer than 15sec, meaning the dissipation or recovery of particle contact started after the main shaking. However, t_2 of P7 just beneath the tank at Z=1.25m showed relatively earlier dissipation compared to those outside the tank. Furthermore, t_2 of P7 is earlier than that of the lower position (P4) in Case 4 (PRF). This particular behavior at the shallow depth below the tank could be attributed to confinement effect of the tank load and the variation of raft load during the shaking, which is discussed in the later section. The earlier dissipation at the shallow depth (P7) than the deeper depth (P4) cannot be verified for Cases 5 and 6 in Shake 1 due to missed data in P4 and also the uncertainty in the determination of t_2 in Shake 1 as explained before. As an overall effect of the first shake on t_2 and t_3 in Shake 2, they became shorter than those in Shake 1, even though the input acceleration was larger in Shake 2 than Shake 1, which could be attributed to the densification of sand by the pre-shaking. But in Case 3b with the increase of input motion magnitude much larger than that in Shake 1, t_2 and t_3 at some locations out of the raft were longer than those in Shake 1. As for the comparison of EPWPs between the longitudinal and transverse sections, similar behaviors were observed in the two sections at the location outside of the tank.

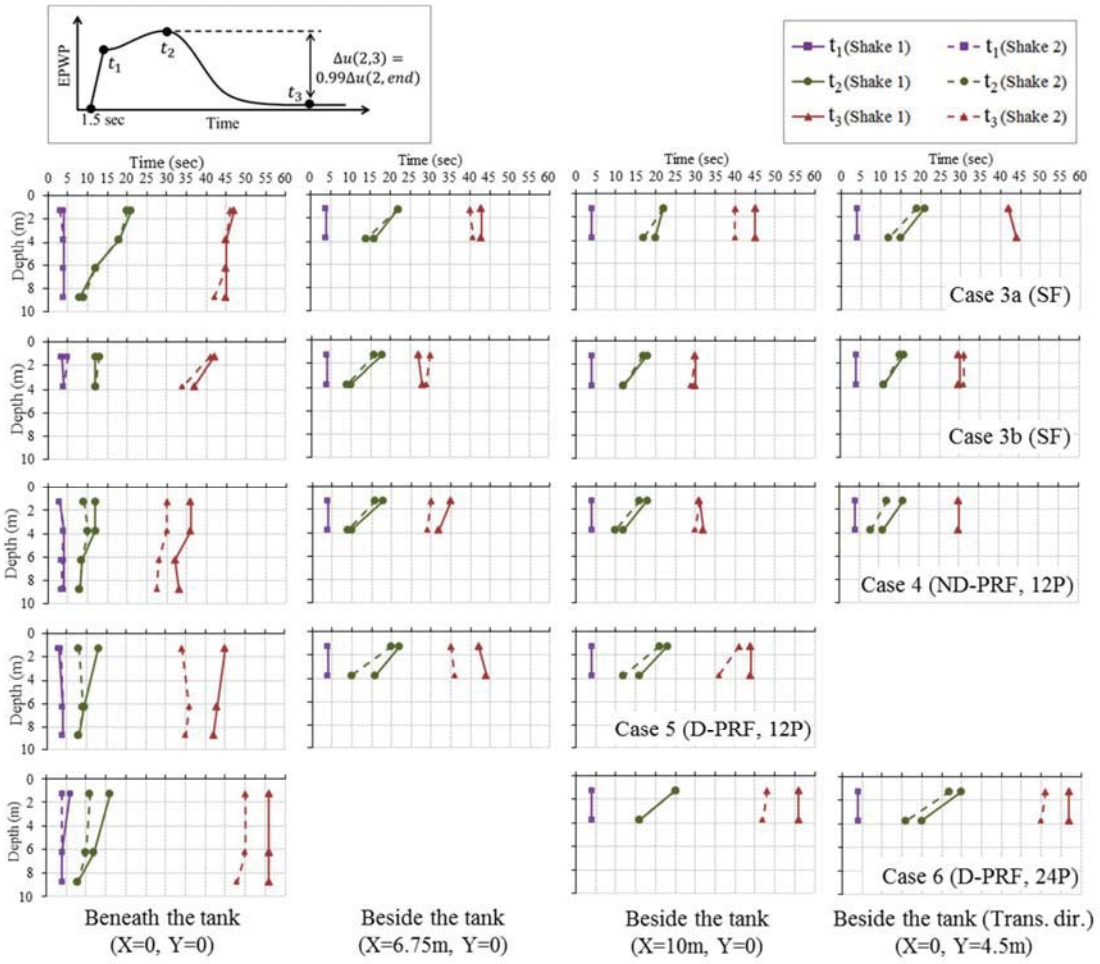

Figure 4.21. Times at the end of build-up (t_1), liquefaction (t_2) and dissipation (t_3) in the ground.

4.3.2.3. Piles and Raft Resistances

Figure 4.22 shows the variations of raft base contact pressures measured by five pressure cells during the two shakings. In Case 4, the cell at the tank center (EP5) and in Case 3a, EP3 could not measure the pressure. In the figure, the average raft contact pressure which is the average of the pressures recorded by five EP cells is also presented by dotted line for Cases 3b, 5 and 6 but not for Cases 3a and 4 due to the missed EP3 in Case 3a and EP5 in Case 4 measurements. The raft base pressures measured before and after the two shakings are also

presented in Figure 4.23. The measured base pressures in Cases 3a and 4 with the non-built-in cells were more uniform than those measured in Cases 3b, 5 and 6 with the built-in cells, which was partly because of the effect of initial surface undulation on the measured pressures. The effect was considered more significant for the built-in cells which created a more flat raft base than the no-built-in cells, which made a convex on the base. However, comparing the variations of Case 4 and 5 or 6, it can be confirmed that the built-in cells could measure the dynamic pressure better than the no-built-in cells. Also the variations in Case 3b shows that the average value of the five pressures measured by built-in cells during the shaking was close to the average tank pressure acting on the raft ($\boldsymbol{\sigma_T}$ =81kPa) while the non-built-in cells in Cases 3a and 4, almost all cells recorded the pressure more than $\boldsymbol{\sigma_T}$ not only during the shakes but also during the preloading stage (Figure 3.30). From these facts, it can be inferred that the built-in cells could give more precise pressure than the non-built-in ones. From the pressure distributions shown in Figure 4.23, it can be confirmed that average raft pressure (ARP) before and after the shaking were significantly different in Cases 5 and 6. Before Shake 1 the ARPs of Cases 5 and 6 were 44kPa and 11kPa respectively. Although there should be some difference between precise average raft pressure and the ARP, assuming they are quite similar, the vertical load was carried about 54% by the raft in the beginning of Shake 1 in Case 5, while in Case 6 only 14% of the vertical load was carried by the raft. This difference in the Raft Load Proportion (RLP) inevitably occurred due to the larger resistance of piles in Case 6 with 24 piles than that in Case 5 with 12 piles. However, the RLPs of the two cases became similar after the first shake, 20kPa (RLP=25%) in Case 5 and 17kPa (RLP=21%) in Case 6 respectively. In Shake 2 some change in ARP took place, but the change was small compared to Shake 1, from 20kPa to 25kPa (RLP=31%) in Case 5 and from 17kPa to 12kPa in Case 6.

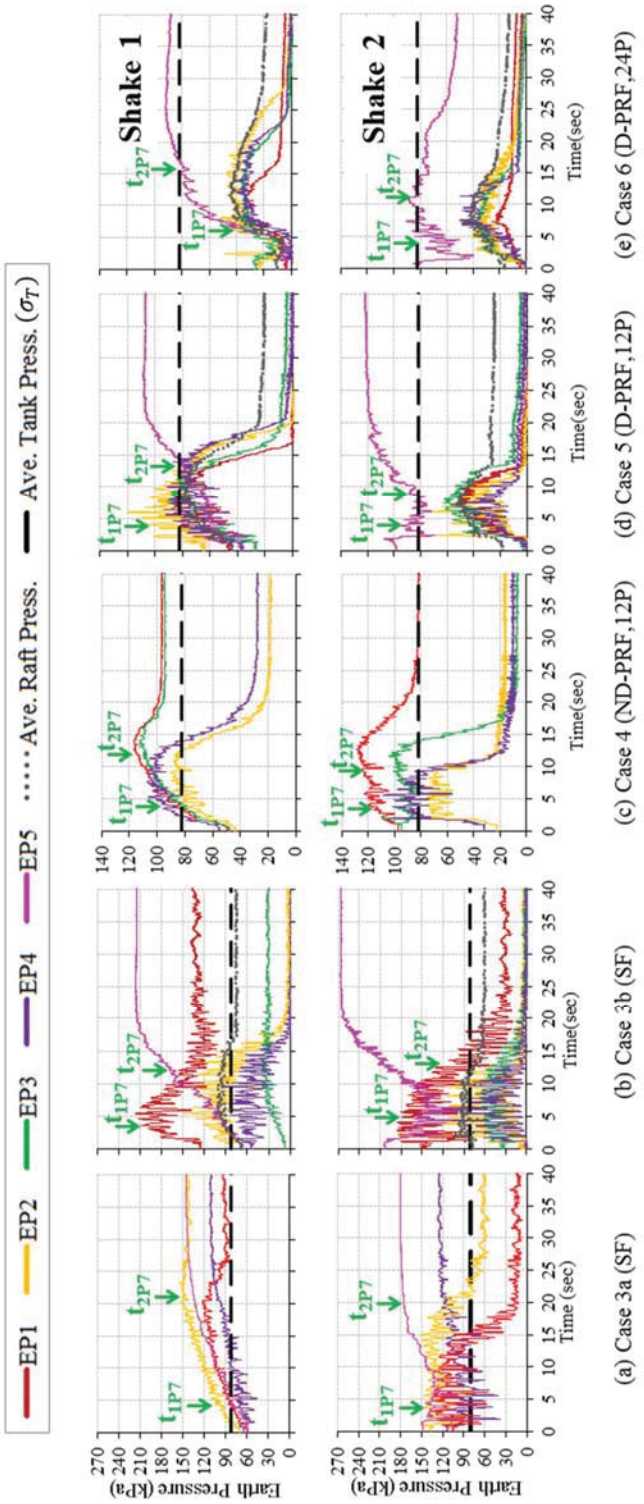

Figure 4.22. Variation of raft base contact pressures during the shakings (saturated sand).

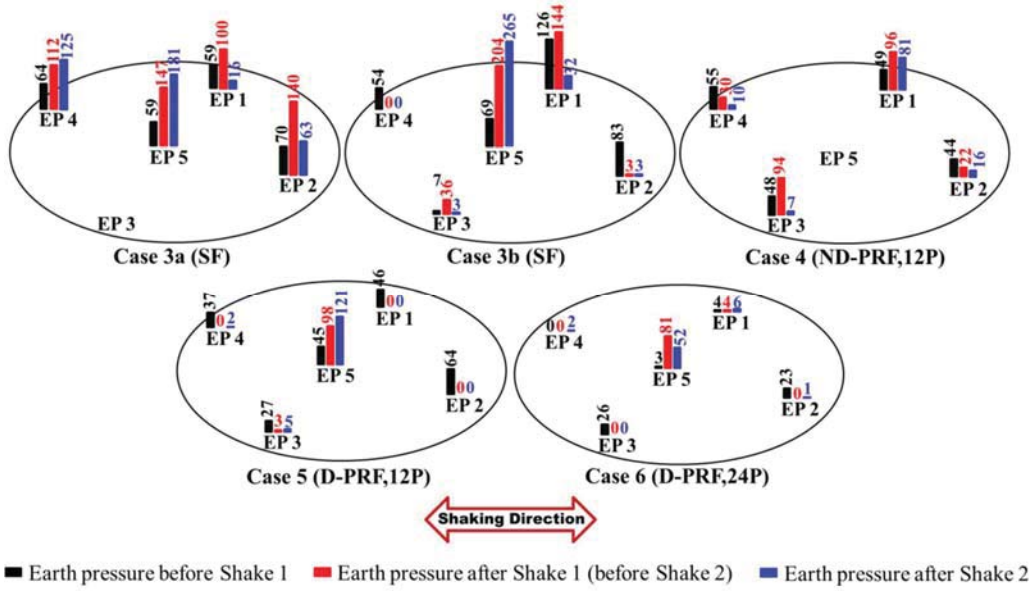

4.23. Raft base pressures before and after the shakes (saturated sand).

The raft base contact pressures showed even significant changes during the shaking with different patterns depending on the types of foundations, the locations and the shaking history, i.e., Shake 1 or Shake 2. As a common trend of PRF, the pressures all increased in the EPWP build-up stage (till t_1 of P7 shown in Figure 4.22). After that, the pressures showed different behaviors in different cases or shakings. For example, in Shake 1 of Case 5, all pressures reached to the average tank pressure ($\boldsymbol{\sigma_T}$) till t_2 in the liquefaction stage, and then all pressures near the perimeter of the raft and the ARP started decreasing, but EP5 at the center of the raft increased after t_2. This particular behavior implies that due to the liquefaction the piles lost almost all the vertical resistance and the vertical load was carried by the raft during the liquefaction stage. Then at the consolidation stage, the vertical load was redistributed to the inner part of the raft below which the soil had a relatively higher stiffness than the outer part of the raft and the piles which regained the vertical resistance due to dissipation of EPWPs, meaning more pile resistance mobilized than the initial value before the shaking. This trend in the base pressure variation can be

seen in Shake 1 of Case 6 to some extent. However, the behavior in details is quite different. In the beginning of the shake, the pressures did not increase till about 5sec and showed a rapid increase till t_1 but up to about the half of $\boldsymbol{\sigma_T}$. After t_1 the perimeter pressures became constant and then started decreasing at the time about t_2 while at the center of the raft the pressure (EP5) kept increasing after t_1 with a gradual decrease in the increasing rate till t_2 but showed the additional increase after t_2. In Case 6 with more driven piles, the piles vertical resistance could be maintained in the beginning and then decreased by the liquefaction, but about a half, not all like Case 5. In the consolidation stage the ARP decreased, in other words, the piles resistance was regained, but ARP at the end of shaking is larger than the initial value, meaning the mobilized pile resistance in the beginning, was not fully regained after the shake in Shake 1 of Case 6. It is also interesting to see that the amplitudes of dynamic component of the pressure are much larger for Case 5 than Case 6, which could be attributed to the smaller rocking motion in the latter than the former and more contribution of piles against dynamic load of tank for Case 6 than Case 5. The increase of the base pressure (EP5) or the stress concentration at the raft center by the shaking can be also confirmed in the slab foundations (Cases 3a and 3b). It should be also emphasized that the base pressures at the perimeter part of the raft, 1m from the raft edge, were all very small about 10% of $\boldsymbol{\sigma_T}$ with some exception even in SF. The level of stress concentration of SF (Case 3b) was much larger than PRF (Cases 5 and 6) and this concentration could be decreased by increasing the pile density, which is partly because of relatively less confined stress with less RLP for the large pile number case and also the more pile resistance. Almost same behavior as observed in Shake 1 occurred in Shake 2 with a slight difference. EP5 showed a rapid decrease at the beginning of Shake 2 even in SF (Cases 3a and 3b). The increases of ARP were smaller than Shake 1, which is the effect of densification by the first shaking. Furthermore in Case 6 EP5 show the reduction after t_2, that suggests relative large regaining of pile resistance in the consolidation part. From

these observations it is considered that these unstable or non-uniform pressures at the foundation base could be compensated by the additional resistance from the piles. Due to the fail in measuring EP5, the stress concentration at the raft center could not be confirmed in Case 4. However, overall trend in the pressure behavior at the perimeter part of the raft are similar to the others. Also because of the uncertainty by the no-built-in pressure cells used in Case 4, the effect of pile installation process on the raft base pressures could not be observed between Case 4 and Case 5.

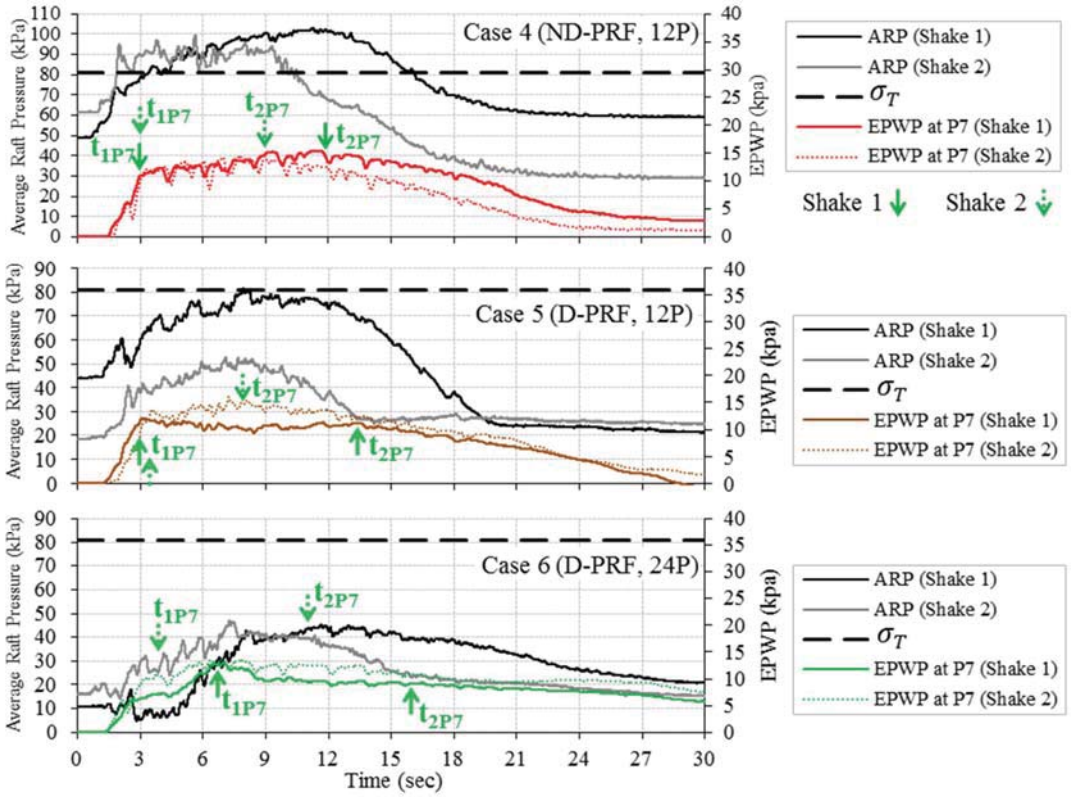

Figure 4.24. Variation of average raft pressure during the shakings (PRFs, saturated sand).

The average raft base pressure (ARP) measured by the pressure cells in Shake 1 and Shake 2 for three PRF models are shown together with EPWP at P7 in Figure 4.24. In Case 4, the average raft base pressure by the four outer pressure cells is shown in the figure. Much clearer trends can be confirmed from the figure, that is, the raft load proportion increased by the reduction of pile loads due to the liquefaction, but by the recovery of effective stresses of the soil due to the dissipation of EPWPs the raft load decreased, in other words, the pile load was regained gradually. The recovery of pile load was earlier in Shake 2 than Shake 1, which corresponds to the fact that t_2 in Shake 2 was earlier than that in Shake 1 for these cases (Figure 4.21). Comparing the behavior in the EPWP build-up stage till t_1, only Case 6 showed clear different behaviors between Shake 1 and Shake 2. In Shake 1 of Case 6, EPWP beneath the tank (P7) showed relatively slow and two-stages increase as discussed before (Figure 4.20) and the ARP did not increase till about 4.5sec, which could be an effect of large number of pile driving. However in Shake 2, the quick rise occurred in 3sec both in EPWP and ARP. From the behavior in Shakes 1 and 2, it can be inferred that the effects of pile driving by the static penetration, such as the increase of horizontal stress, could be eliminated by the large shaking.

In order to compare the behavior of piles and load sharing between piles tip and shaft in saturated condition with those in dry condition, the previous study by Takemura et al. (2014) was considered while in the current research the piles of piled raft foundation in saturated cases was not instrumented. Figure 4.25 shows the piles head load, tip resistance and shaft friction in static condition before the shaking. Based on this result, about 62% of pile resistance was mobilized by the tips and 38% by the shaft in the static condition.

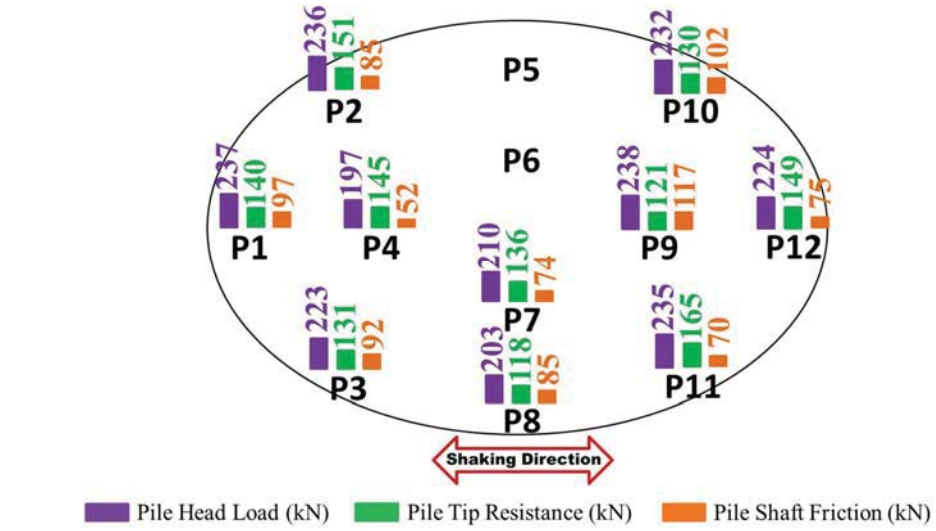

Figure 4.25. Piles loads before shaking (Static load-Saturated sand)(Takemura et al., 2014).

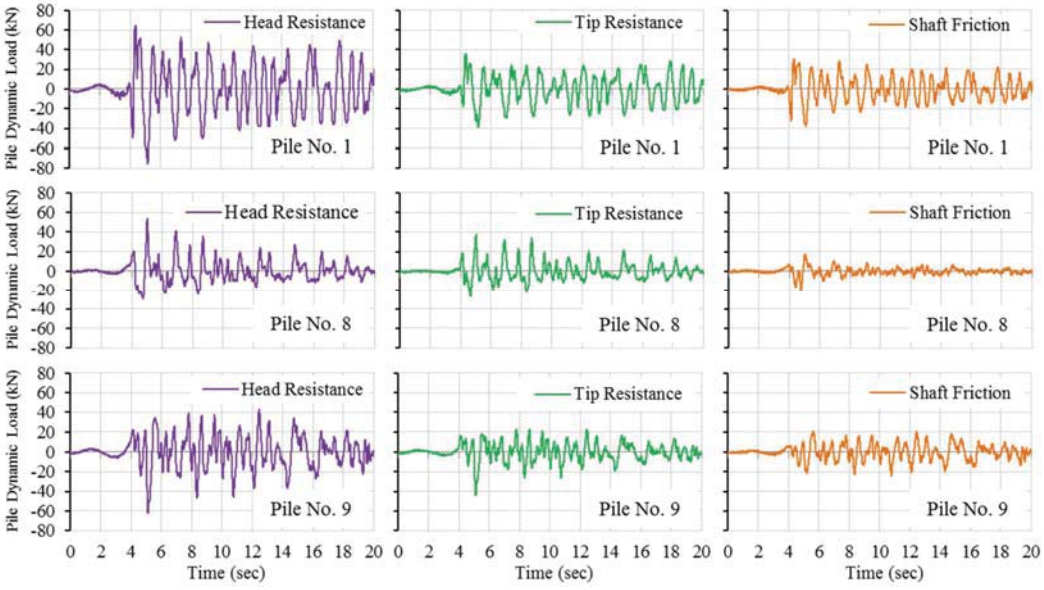

Figure 4.26. Piles dynamic loads during shaking (saturated sand)(Takemura et al., 2014).

Also, to discuss on the contribution of piles against dynamic loading, the piles head load, tip resistance and shaft friction are shown for three sample piles, No. 1 at outer edge of raft in shaking direction, No. 8 at outer edge of the raft in transverse direction and No. 9 at center part

of raft. These loads are calculated by eliminating static part of load from total one and presented in Figure 4.26. As this figure indicates similar to PRF on dry sand, pile No. 1 at the raft outer edge has higher contribution against dynamic loading in comparison to piles No. 8 at transverse direction and No. 9 at central part of the raft.

Also from this figure smaller contribution of piles against dynamic loading comparing to dry case (Figure 4.10) is detectable. On the other hand, by considering the average amplitude of dynamic loads of piles in Figure 4.26 and comparing this average amplitude in pile head load, tip resistance and shaft friction, it is indicated that in contrast to PRF on dry sand, the shaft friction contribution was not increased and slightly decreased from 38% to 36% during the shaking. Obviously the reason is looseness of sand in saturated ground comparing to dry condition. In other words, in case of PRF on dry sand during shaking due to densification of sand higher shaft fiction was developed in the piles but in case of PRF on saturated sand due to liquefaction and looseness of the ground this higher bearing capacity could not be developed in the piles.

4.3.2.4. Tank Response

4.3.2.4.1. Tank Accelerations

The accelerations at the top and bottom of the tank in the shaking direction (A9, A8) are shown with the input acceleration in Figure 4.27. In the figure, the tank accelerations in the transverse direction at the top (A13) and the bottom (A12) are also shown, but A13 couldn't be recorded in Case 6. The Fourier amplitude spectra of the tank accelerations both in the shaking and transverse directions are presented in Figure 4.28. In the shaking direction during the rapid increase of EPWP in the build-up period before t_l, the difference between the tank bottom and top accelerations were relatively small, but after t_l the bottom and top accelerations showed

difference, bigger at the top and smaller at the bottom than the input, resulting in the rocking motion of the tank. However, Case 6 had the less rocking motion and in particular, the spectra of the tank top and bottom accelerations are similar to that of input. This is a clear evidence for the effectiveness of higher pile density in reducing rocking motion of the tank. Also, despite the higher level of input motion in Case 5 comparing to Case 4, the driven PRF in Case 5 could reduce rocking motion of the tank to some extent. The rocking motion in Case 3a with the large input motion was higher than other cases, but Case 3b has less rocking motion in comparison with Cases 4 and 5 even though the input motion in this case was almost same till t=6sec and slightly larger after that time than Case 4 (Figure 3.35). In order to discuss precisely on the rocking motion of tank in Case 3b and compare with the results in Cases 4 (D-PRF) and 5 (ND-PRF), the tank response Fourier spectrum in these cases are compared in two phases, before and after end of liquefaction (t_2) in Case 3b (Figure 4.29). As the graphs indicate the rocking motion in Case 3b is slightly smaller not only during liquefaction period but also after that. It seems that the main reason for smaller rocking motion in Case 3b in comparison to Cases 4 and 5 is the higher contribution of raft against dynamic loading that will be discussed later. On the other hand, in Cases 3a, 3b, 4 and 5, short period components were significantly attenuated at the tank bottom but the long period components amplified. As a difference between SF and PRFs, it can be observed that the phase difference between the tank bottom and top accelerations were more significant in the late part of shaking in Cases 3a and 3b (SF) than Cases 4, 5 and 6 (PRFs).

In the transverse direction, the accelerations were much smaller than those in the shaking direction especially for Case 5 with driven piles. In particular, the bottom transverse acceleration is almost negligible and with no clear dominant frequency. But the top transverse accelerations showed a certain vibration with a clear dominant period of about 0.3sec, which is

about half of the dominant period in the acceleration of the shaking direction (0.6sec). This clear response of the tank top in the transverse direction can be attributed to the deflection of tank top due to the relatively small hoop stiffness at the top part of the tank wall.

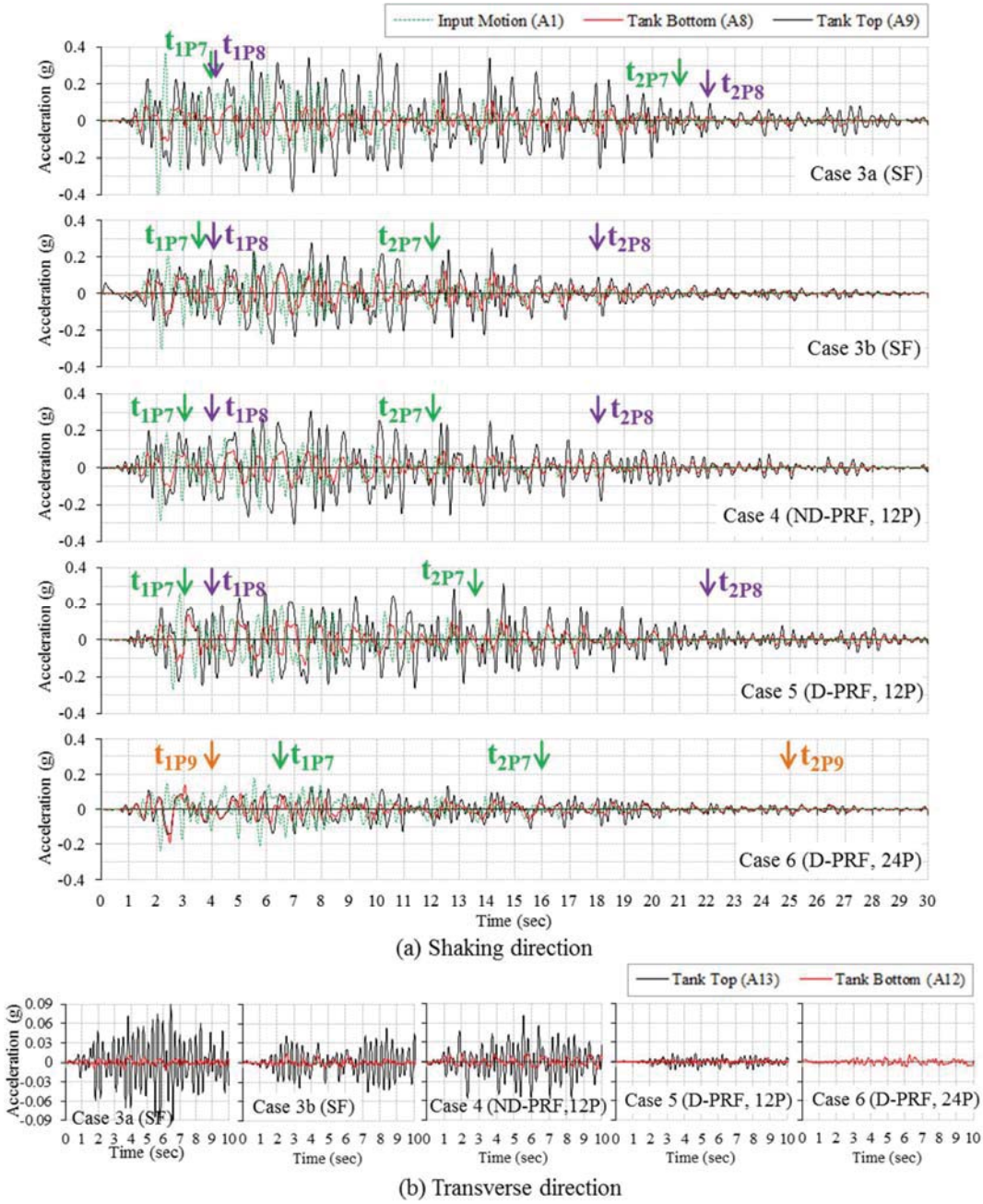

Figure 4.27. Tank response accelerations in Shake 1 (saturated sand).

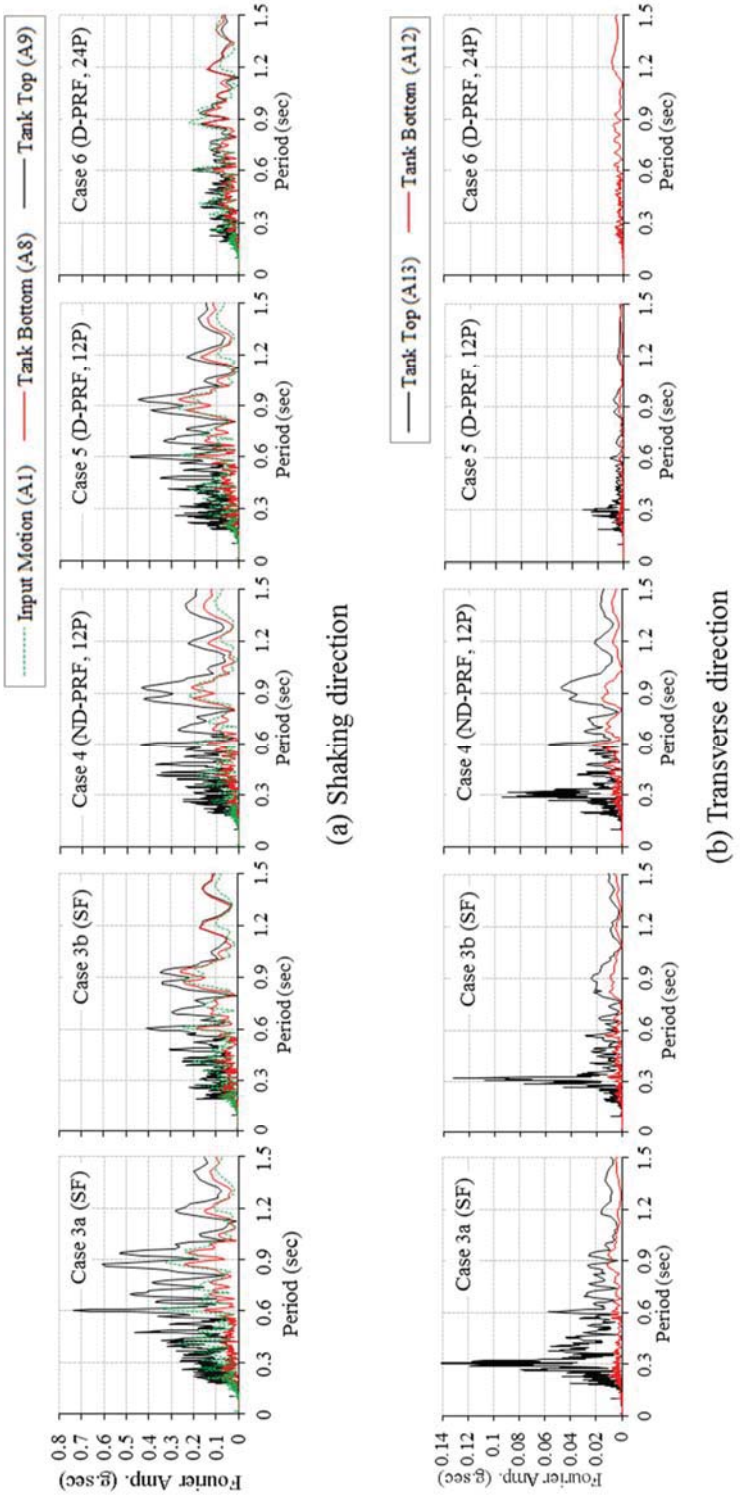

Figure 4.28. Tank response Fourier spectrum in Shake 1 (saturated sand).

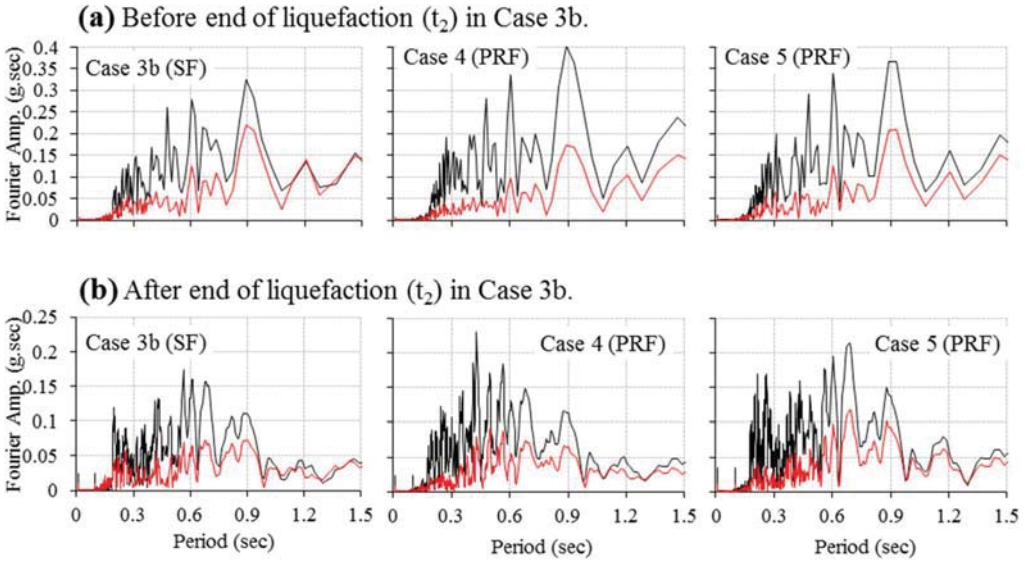

Figure 4.29. Tank response Fourier spectrum in Shake 1 of Cases 3b, 4 and 5; (a) before end of liquefaction (t_2) in Case 3b, (b) after end of liquefaction (t_2) in Case 3b.

4.3.2.4.2. Tank Settlements

Figure 4.30 shows the tank settlements measured by the three laser displacement transducers at the locations shown in the figure. The t_1 and t_2 obtained from P7 and P8 are also indicated in the figure. In Case 6, because P8 couldn't be recorded, P9 is substituted. In Shake 2 of Case 3a, as the LDTs could not record the data for certain time intervals, three sets of the settlement could be measured only till t=4sec and the measurements of L1 and L3 could be resumed near the end of the test as shown in the figure. The settlements increased gradually during the shaking in contrast to EPWPs behavior which showed a quick rise in a short time (Figure 4.20).

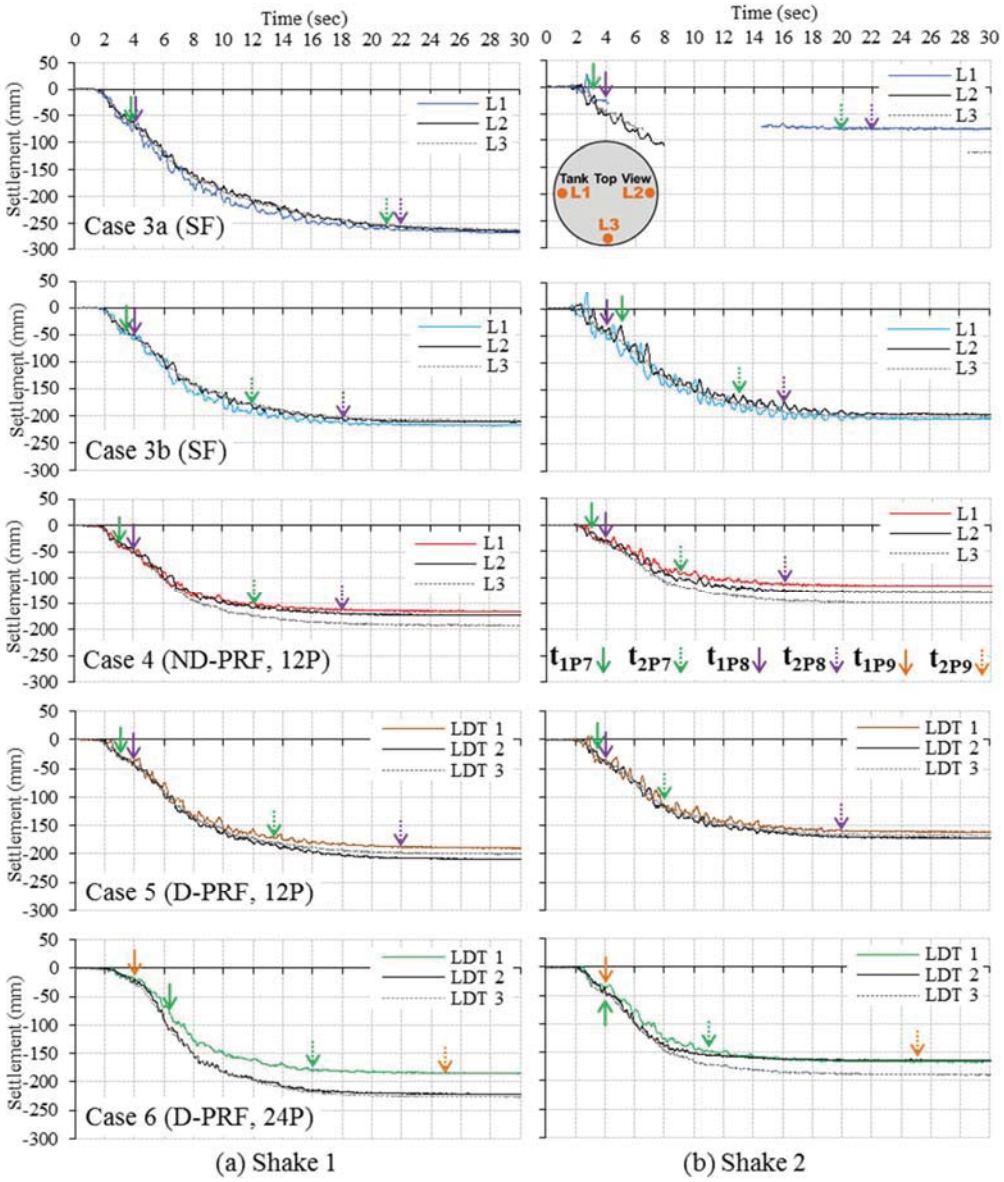

Figure 4.30. Tank settlements (saturated sand).

In Figure 4.31 the settlements at the tank center, which is the average of L1 and L2 are compared for the entire period and the early stage of shaking at the top and bottom figures with t_2 and t_1 of P7 and P8 or P9 (Case 6) respectively. Comparing the results in Shake 1 and Shake 2, the effect of densification by the first shake can be confirmed. Even though the input motion in

Shake 2 was larger than that of Shake 1, the settlements in the second shake were smaller than those of the first. The effect of pre-shaking was more significantly evidenced in the beginning. In Shake 1 of Cases 3a, 3b, 4 and 5, the tank started settling at time of about 1.5sec, which is the actual onset of the shaking in terms of Arias intensity (Figure 3.35), and the settlement rate increased with time until t=3sec while in Shake 2, there were no substantial settlement until t=2.3sec. The relatively large settlement of Shake 1 in the beginning of shaking could be attributed to the poor contact of the raft base to the ground surface, a kind of bedding error, which can be removed by the first shake. After this initial part, the settlement increased almost linearly with time until t=8sec at the time when EPWP dissipation started in the deep depth beneath the tank (t_2 of P2, Figure 4.21).

In Shake 1 of Case 6, the settlement started with delay at 2.5sec and increased slowly until about 4.5sec but after that, it increased rapidly until 8sec, the time that dissipation in deeper part started. This delay and slow increase of the settlement at the beginning can be attributed to the slow EPWP increase and remained pile resistance due to the effects of high density of driven piles as discussed before (Figure 4.24). But after 4.5sec the effect could be diminished by the shaking, that resulted in further EPWP generation and the reduction of piles resistance and the large settlement. Although the settlement rate decreased at 8sec, further settlement occurred even after, the time when EPWP just beneath the raft started decreasing (t_2P7), until the time when EPWP at the shallow depth beside the raft started decreasing (t_2P8 or t_2P9 (Case 6)). After this time, the minor settlement, which was mainly caused by small shaking and the consolidation of sand, took place. The residual settlement in the late stage of the tests seems smaller for Cases 4, 5 and 6 (PRFs) than Cases 3a and 3b (SF). Recovery of pile bearing load, which can be confirmed in Figure 4.24 could be a reason for the smaller settlement in the late stage of the shaking and after the shaking in the PRFs than the SF. In Shake 2, the particular

difference between Case 6 and the other cases observed in Shake 1 was no more observed, which is also an evidence that indicates the effects of pile driving could be diminished by the first shaking.

As for the overall effect in reducing the settlement, simple direct comparisons cannot be done because of different input acceleration and initial density of the sand. To discuss these effects, the EPWP behavior could be a reference, especially liquefaction time (t_2) and consolidation time (t_3) at the ground outside of the tank, because the liquefaction and compression after liquefaction will be longer for the less dense sand and the larger shaking if the shaking time is the same. From Figures 4.20 and 4.21, the level of liquefaction is considered the most in Case 6 and the second in Cases 3a and 5 while Cases 3b and 4 had almost same liquefaction level. Considering the relative significance of the liquefaction or shaking, the effect of piles of PRF as a settlement reducer can be confirmed from the results of Case 3b and Case 4. While for the effects of pile driving and the pile number, they can be seen in the beginning of Shake 1 between Cases 4 and 5 and Cases 5 and 6 respectively. However, the effects of pile driving and pile number on the settlement reduction cannot be confirmed in the later part of Shake 1 and in Shake 2 due to the elimination of the driving effects by the shaking and incomparableness of the test conditions. Beside the above mentioned effects, such as, sand density, input motion, pile installation method, load proportion between the raft and pile could be a critical factor. Before Shake 1 in Case 6, the majority of the vertical load was carried by the piles (Figures 4.23 and 4.24) and before losing the pile resistance till t~4.5sec, the settlement was very small. But once the piles lost the resistance and load transferred to the raft, a large settlement occurred.

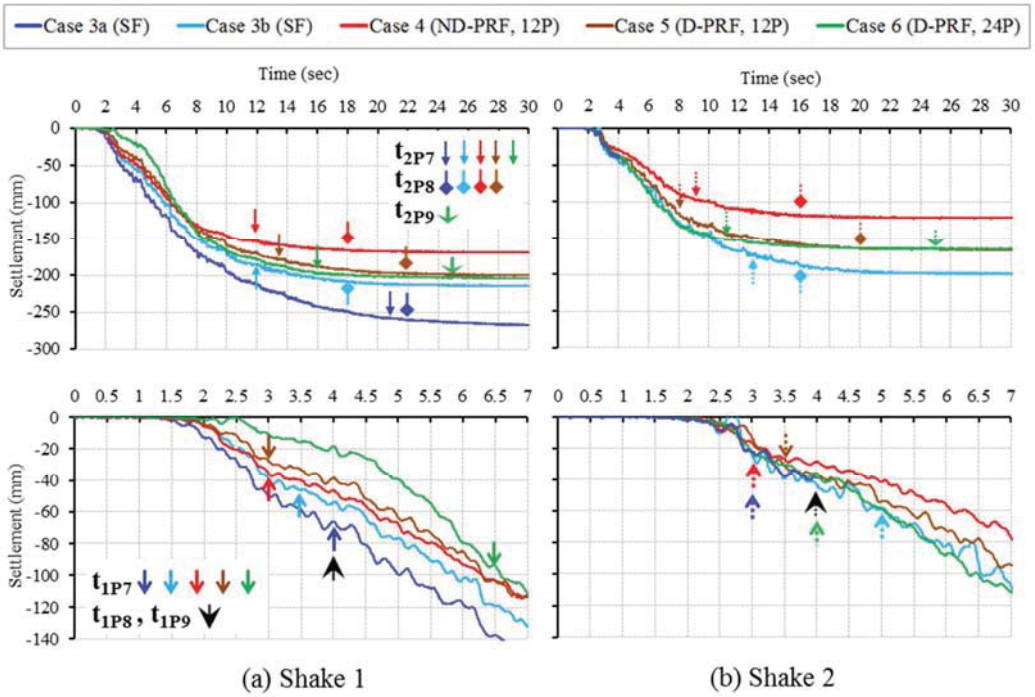

Figure 4.31. Tank center settlements (saturated sand), top: entire shaking period with t_2, bottom: earlier stage of shaking with t_1.

4.4. Tank Maximum Rotation and Maximum Rotation Direction (Dry and Saturated Cases)

In the safety assessment of tank foundation, the uneven settlement is a critical concern. For the relatively small diameter tank supported by a rigid slab or raft, the uneven settlement is equivalent to the rotation of the foundation. In the previous dynamic model tests of foundation using the one directional shaking table, e.g., (Takemura et al., 2014), the rotation of tank foundation was only measured in the shaking direction. In this study, with the settlement at three locations (Figure 4.30), the maximum rotation and its direction were measured.

Figure 4.32 shows the revolution of the maximum rotation in Case 1 during the shaking for the entire period and the early stage of shaking in the top and bottom figures. The same trends

are presented in Figure 4.33 for cases on saturated sand (Cases 3a, 3b, 4, 5 and 6) along with t_2 and t_1 of P7 and P8 or P9 (Case 6). In the figures results of Case 2 is missed, because L2 could not be measured. Also for Shake 2 of Case 3a, limited results are shown, as the three settlements could be obtained till t=4sec and L1 and L3 could give the data at the end of the shaking (Figure 4.30). In the beginning of shaking, the rotation gradually increased with time in all the cases until t_1 of P7. The increase of rotation, in the beginning, is earlier and much larger for Shake 1 and Shake 2 of Case 1 (SF, Dry sand), Case 6 (Driven PRF, 24Piles) and Shake 2 of Case 3a than the other cases.

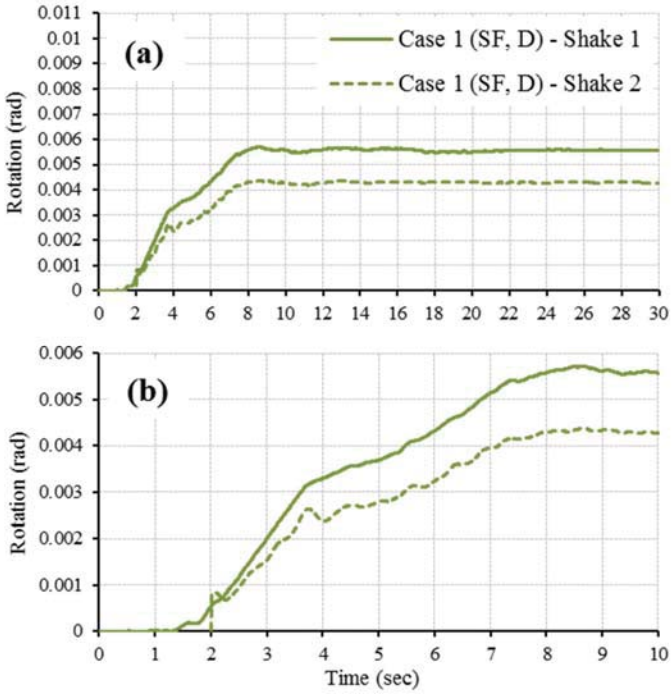

Figure 4.32. Tank maximum rotation (Dry sand), (a) entire shaking period with t_2, (b) earlier stage of shaking with t_1.

Although $t_{l\,p7}$ in Shake 1 of Case 6 was longer than those of the other cases, the increase of rotation in the early stage (during build-up period) was much larger both for Shake 1 and Shake 2. In Shake 1, the rapid increase in the rotation started from t=3.5sec, but in Shake 2 the increase started from t=2sec. The time of the large rapid rotation increase in Shake 1 of Case 6 is close to the time of the onset of the average raft pressure (ARP) increase from a very small value (Figure 4.24) and the time of the onset of increase in the settlement (Figure 4.31). It is considered that in Case 6 in the beginning of Shake 1(until 5sec as shown in Figure 4.24) almost vertical load was carried by the piles (as discussed in section 4.3.2.3 and Figure 4.24) and the raft base contact condition to the ground surface could not be uniform with some local gaps due to the small raft load. This initial condition caused large and relatively non-uniform settlement by the reduction of pile resistance, resulting in very large rotation from the beginning. The earlier large rotation in Shake 2 of Case 6 could be a result of the initially existing inclination of the foundation. This large settlement and rotation could also be enhanced by the relatively large level of liquefaction in Case 6 as compared to the others as discussed in the previous section.

The large tank accelerations of dry sand (Case 1) from the beginning (Figure 4.4) can be a reason for the earlier and much larger rotation in Case 1. As discussed in Figure 4.7, the rotation of SF on dry sand ceased at t=8sec and was kept constant and the same trend was observed in Case 2 (PRF, Dry sand). The tank accelerations measured in the beginning of Shake 2 are depicted for the saturated cases in Figure 4.34. A large amplification was observed at the tank top from the very beginning in Case 3a as compared to the two other cases which can be the reason for the large rotation in Shake 2 of Case 3a.

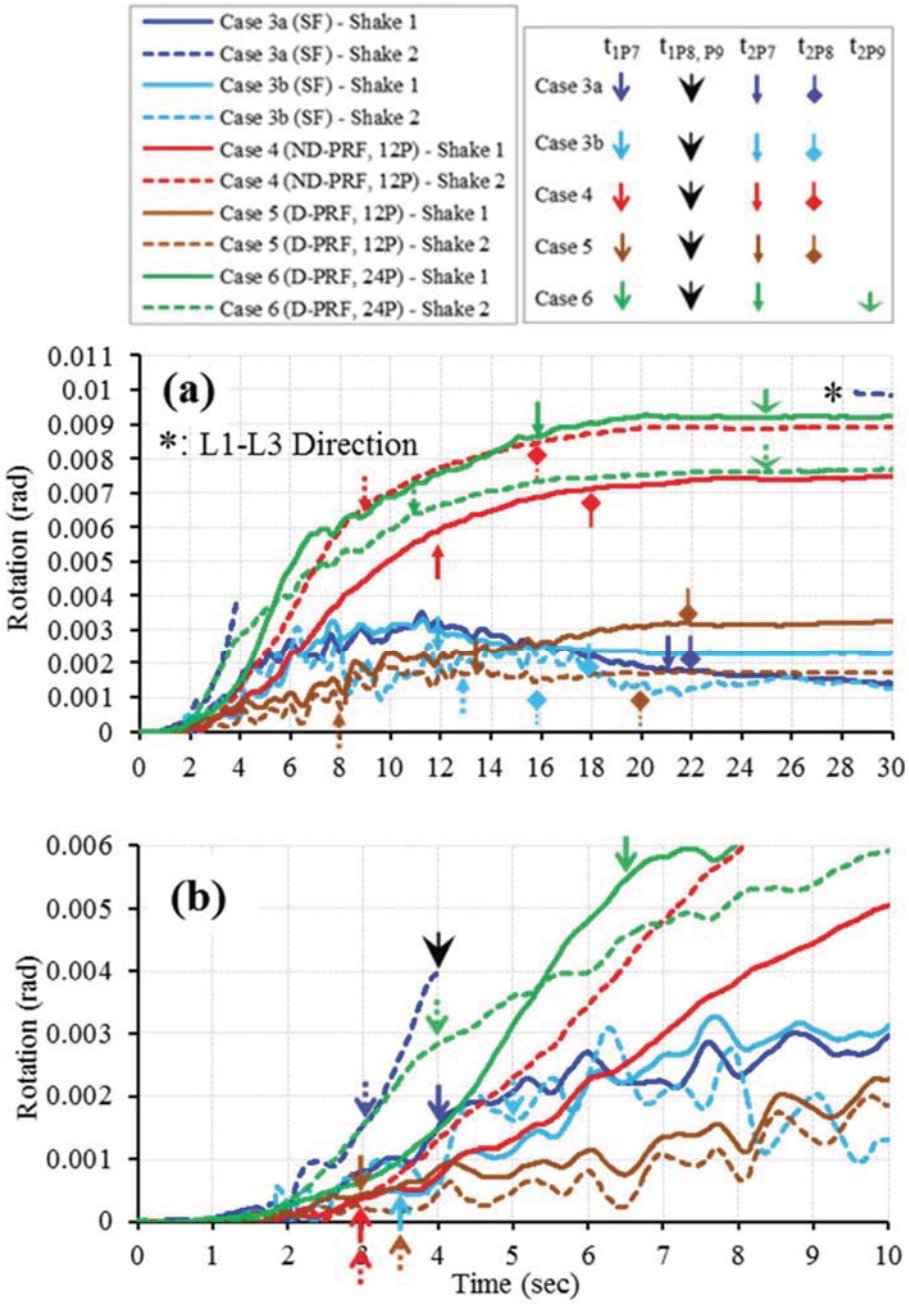

Figure 4.33. Tank maximum rotation (Saturated sand), (a) entire shaking period with t_2, (b) earlier stage of shaking with t_1.

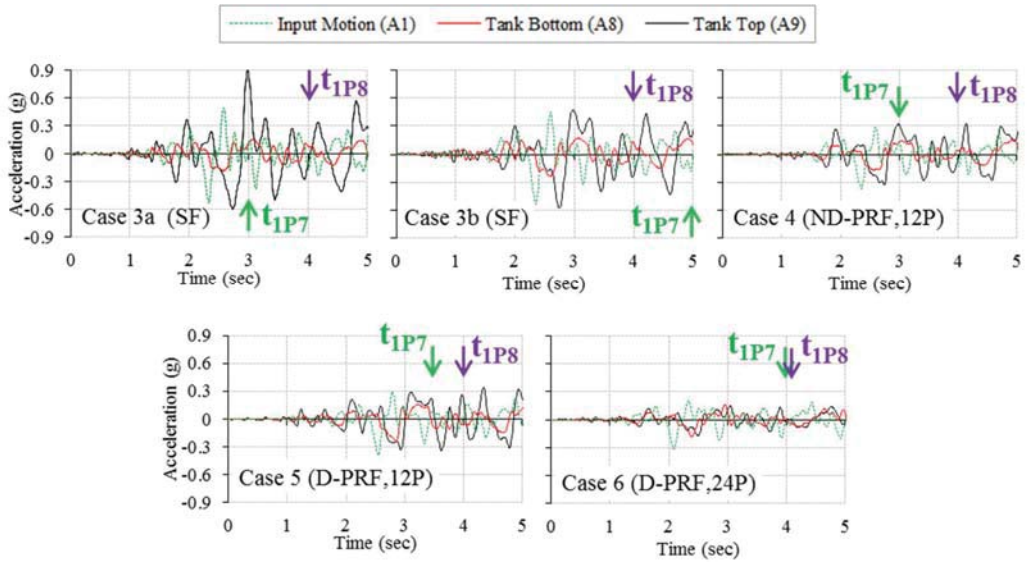

Figure 4.34. Tank response accelerations in the beginning of Shake 2 (saturated sand).

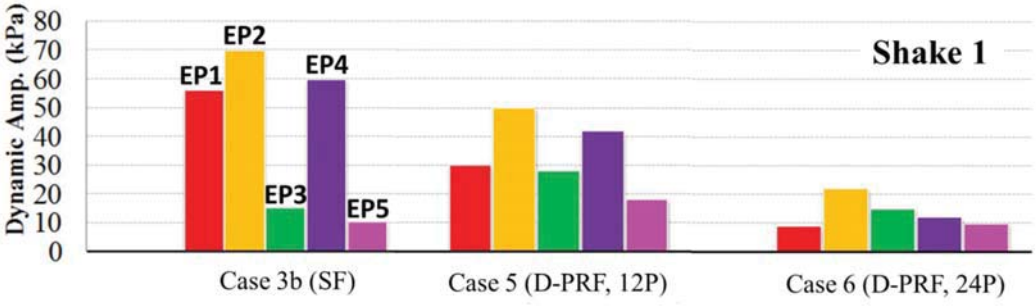

Figure 4.35. Average of earth pressures amplitudes in Cases 3b, 5 and 6.

Beside Case 6, the behaviors of the tank on liquefied sand in the other cases are also quite complicated and different in different cases. In Case 4 (non-driven PRF, 12Piles), the rotation increased monotonically in the liquefaction stage (from t_1 to t_2) both for Shake 1 and Shake 2. While in Shake 1 of Cases 3a and 3b, the rotation increased after t_1 but turned to decrease in the liquefaction period. In Shake 2 of Case 3b, the rotation behavior was more fluctuated during the shaking. In both shakes of Case 5, the rotation increased monotonically in the liquefaction

period but not as much as Cases 4 and 6. As a result, the tank rotations after the shaking were larger for Cases 4 and 6 (PRFs) than Cases 3a and 3b (SF), except for Shake 2 of Case 3a, which showed the large rotation from the beginning and those for Case 5 (PRF) were similar to Case 3b. The large dynamic base pressure amplitudes can be pointed out as a common behavior of Case 3b and Case 5 as compared to relatively small amplitudes in Case 6, especially in Shake 1 (Figure 4.22). Average of earth pressures dynamic amplitudes are presented for Cases 3b, 5 and 6 with built-in earth-pressure cells in Figure 4.35. This figure indicates larger average of dynamic amplitude of earth pressures for Cases 3b and 5 comparing to Case 6. This large reaction from the raft against the dynamic load could also positively work for reducing the rotation.

From these results, the effect of piled raft foundation in preventing uneven settlement cannot be confirmed when liquefaction occurs in the entire depth of piles. However, in the beginning of the shaking in the period of EPWP build-up, the rotations of piled raft foundations were smaller than those of slab foundation except in Case 6, showing the effectiveness of piled raft foundation for the condition that the pile vertical bearing resistance could be mobilized (before start of liquefaction).

Figure 4.36 shows revolutions of the direction of maximum rotation, θ, during the shaking. The definition of θ is given in the figure. By using plane equation in geometry and coordinates of three points on the tank (L1, L2 and L3), point D on the tank raft with maximum settlement is estimated and maximum rotation of tank which occurred at point D is calculated. As there was some inevitable error in the estimation of direction from the measured settlement, especially in the beginning of shaking when the settlement was very small, the first part of the data with large fluctuation is eliminated in the figure. From the figure, the observed behavior in the direction of

maximum rotation can be divided into some groups. In Cases 1, 4, 6 and Shake 2 of Case 3a, the direction suddenly changed from the shaking direction (θ=0 or 180°) to the different direction and became constant to a certain direction more transverse than the shaking direction. While in Case 5, although some fluctuation in the direction took place in the beginning, the maximum rotation directed to the shaking direction (θ ~ 180°). On the other hand in Case 3b and Shake 1 of Case 3a, the direction showed unstable behavior, gradually changed from the shaking direction until the end of the shaking, which corresponds to the change of rotation during the shaking shown in Figure 4.33. It can be also seen by comparing Figure 4.36 with Figures 4.32 and 4.33 that the rotation trends to be larger for the cases (Cases 1, 4, 6 and Shake 2 of Case 3a) with maximum rotation direction more to the transverse direction than the shaking one. From these observations, it can be inferred that once the direction of the rotation is fixed to a direction diverted from the shaking direction, the rotation will be accumulated by shaking. But while the rotation mainly takes place in the shaking direction in the beginning of shaking, the monotonic increase in the rotation may not easily occur and the rotation behavior becomes very complicated as seen in the slab foundation cases (Figure 4.33). However, it should be noted that even for the slab foundation, once a relatively large tilting to the diverse (transverse) direction was triggered by a large rocking motion of the tank, a large rotation occurred inevitably by the shaking as shown in Shake 2 of Case 3a. This unstable behavior (large and transverse direction rotation) could be prevented by the additional support from the piles in PRF in Case 5. There could be a several reasons why Cases 1, 4 and 6 (PRFs) tilted in the diverse direction, such as inevitable difference of bearing resistance of each pile, non-uniformity of raft base contact condition to the ground, which could cause the rotation of the tank occur in the area with small pile resistances and poor contact of the raft base to the ground. The effects of these inevitable and uncontrollable factors could be very much enhanced for the condition that the liquefaction

takes place in entire depth where piles are installed.

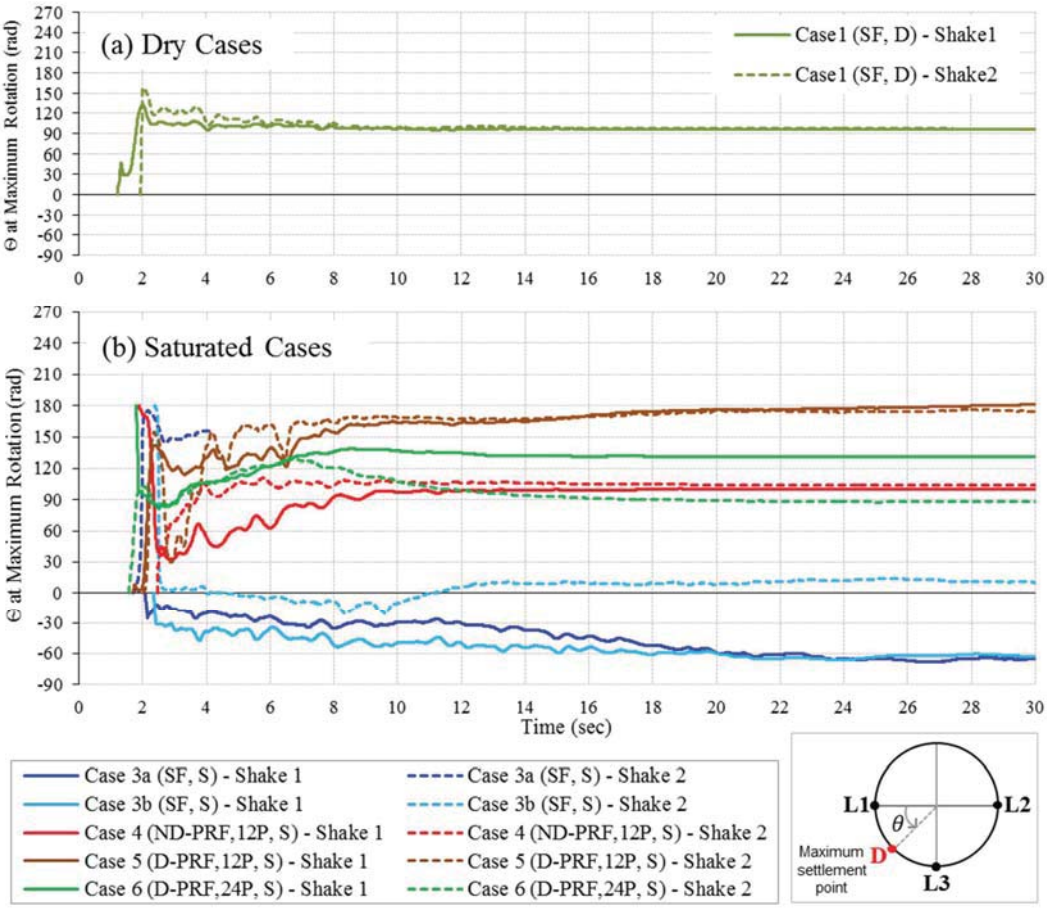

Figure 4.36. Direction of tank maximum rotation.

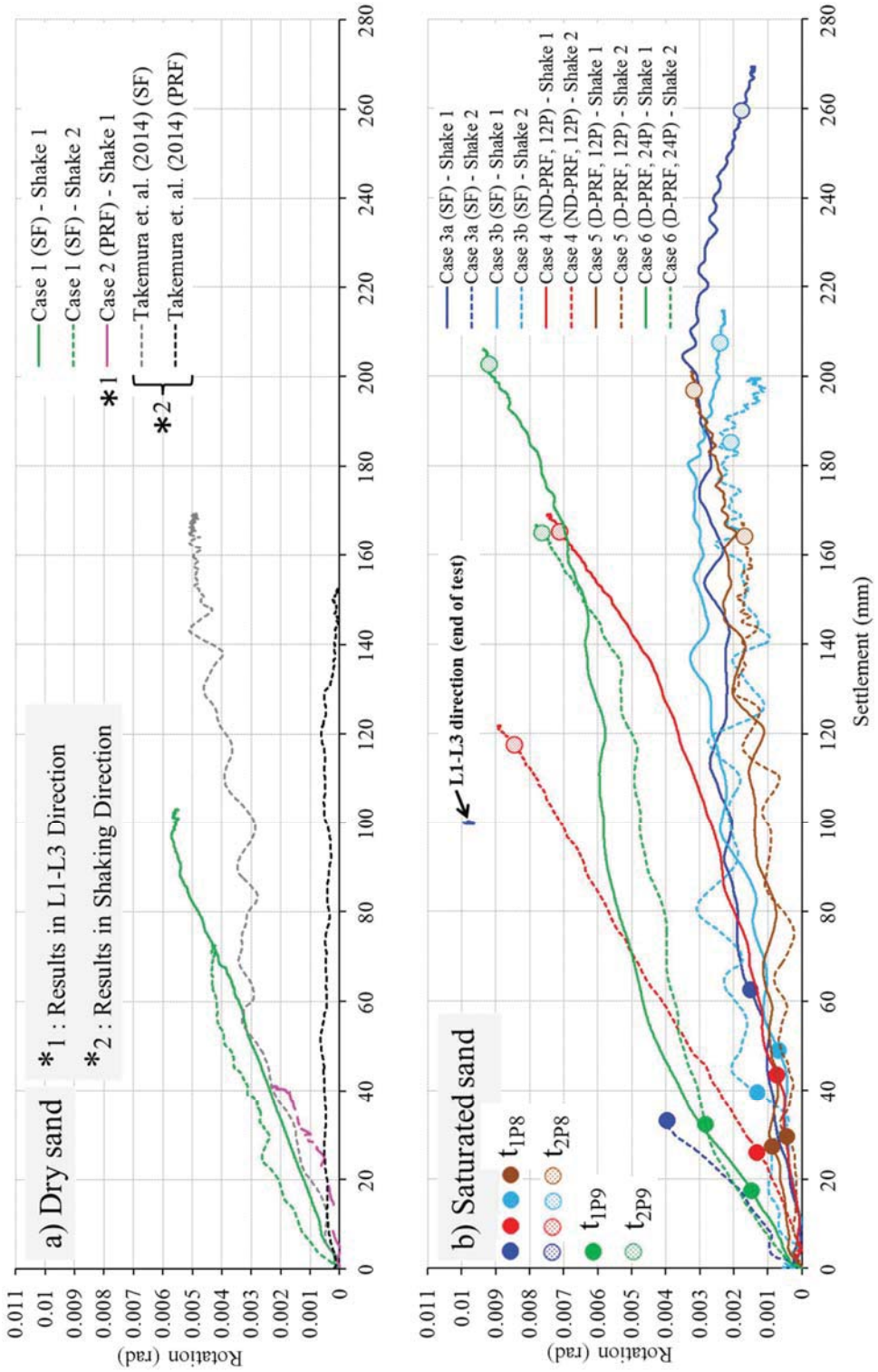

Figure 4.37. Tank maximum rotation vs settlements.

The relationships between the tank maximum rotation and the tank center settlement were presented in Figure 4.37. In the top figure, the relationship obtained from the dry ground cases are shown with the results of the previous study (Takemura et al., 2014). In the previous results (Takemura et al., 2014), the tank rotation is in the shaking direction. In the bottom figure, the same relationship was plotted for the saturated cases with the marks at the time of EPWP buildup end (t_1) and liquefaction stage end (t_2) obtained from the PPTs (P8 or P9 (Case 6)) at the shallow depth beside the tank. These times are considered as indicators of the partial liquefaction and complete liquefaction. Due to the lack of settlement data, the rotations of L1-L3 direction are used for some cases, as shown in the figures, but in Shake 2 of Case 2, even this data could not be recorded. In dry cases, the trend of relation is almost the same for SF and PRF, except the PRF of the previous tests (Takemura et al., 2014), which shows much smaller uneven settlement than the others. This small rotation could be considered as an advantage of PRF. However, the advantage may be overestimated because of the uncertainty about the rotation in the diverse direction and the non-monotonic increase of the rotation. Nonetheless, the effectiveness of PRF in the dry sand cases (Case 1 and Case 2) for preventing the uneven settlement can be confirmed. Namely, the tank settlement caused by the shaking can be reduced by PRF, which resulting in the smaller rotation as compared to SF.

In the saturated cases, the relationships are so various for the different cases and between the first and second shakings. As an overall trend of the relations, the followings can be pointed out: 1) majority of the settlement and rotation took place in the liquefaction stage. 2) in the early stage till t_1, the rotations of PRFs except for Case 6, were smaller than or equal to those of SF. 3) Neglecting the large settlement and tilting caused by poor raft contact in Case 6, the effectiveness of driven PRF compared to non-driven PRFs in reducing uneven settlement can be seen from the results of Cases 5 and 4.

As discussed in the previous sections, the dynamic behaviors of PRF and SF resting on liquefiable sand are so complicated, which are affected by various factors. Therefore the effectiveness and limitation of PRFs should be studied more for different conditions, i.e., on the ground with partial liquefaction, such as, the liquefaction in partial depth, not entire depth or ground with non-liquefied soil layer, and the ground and tank with artificial asymmetric conditions, to clarify the conditions of positive application of PRF, including the dynamic and static pile installation methods and pile head fixity.

4.5. Liquid Behavior inside the Tank (Sloshing)

Sloshing can be developed in tanks by long-period ground motions. The fluctuation of tank liquid can affect the overall behavior of oil tanks and its stability by enhance of tank vibration and its uneven settlement. Also, it can damage the roof and the top of tank wall. The liquid mass inside tank is separated into two parts: (1) the impulsive mass near the base of the tank which moves with the tank wall, and (2) the convective (sloshing) mass near the top experiences free-surface sloshing (Figure 4.38). The impulsive mass has large acceleration; therefore, it controls the seismic loads like shear and overturning moment in the tank. The convective mass tolerate small acceleration, therefore, it contributes insignificantly to the seismic loads in the tank. However, the convective mass requires space to slosh freely in the tank. In case of large diameter tanks, the essential freeboard is large. Also when tanks rest on soft soil deposits or exposed to near-field earthquakes, due to low-frequency ground motions freeboard requirement increase. Inadequate freeboard may cause upward load on the roof and increase of impulsive mass because of the constraining effect of the roof. The upward force on top of tank wall and roof may cause some damages in the joints or tear the tank shell (Figure 4.39).

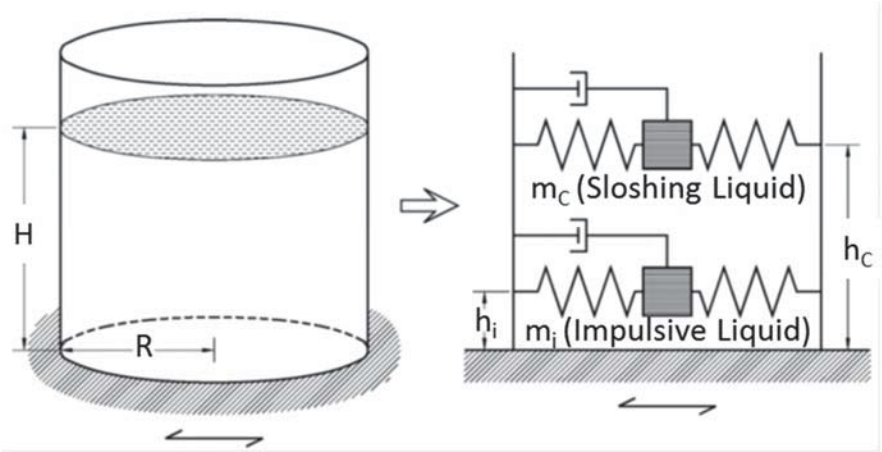

Figure 4.38. Simple model of liquid-filled tank (Malhotra et al., 2000).

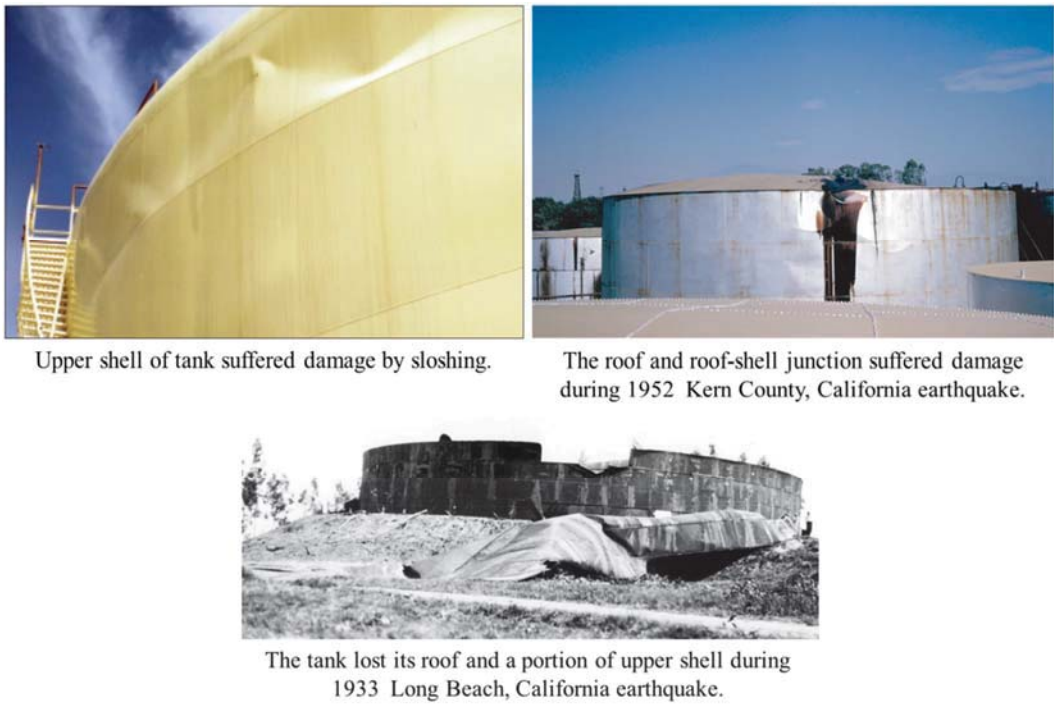

Upper shell of tank suffered damage by sloshing.

The roof and roof-shell junction suffered damage during 1952 Kern County, California earthquake.

The tank lost its roof and a portion of upper shell during 1933 Long Beach, California earthquake.

Figure 4.39. Sloshing damages to the tanks (Malhotra et al., 2000), (Malhotra, 2006).

Regarding API (2007), the impulsive period of the tank can be estimated by equation 4.1. Also, the first mode sloshing wave period may be calculated by equation 4.2, where K_S is the sloshing period coefficient.

$$T_i = \frac{1}{\sqrt{2000}} \frac{C_i H}{\sqrt{\frac{t_u}{D}}} \frac{\sqrt{\rho}}{\sqrt{E}} \tag{4.1}$$

$$T_C = 1.8 K_S \sqrt{D} \qquad K_S = \frac{0.578}{\sqrt{tanh\left(\frac{3.68H}{D}\right)}} \tag{4.2}$$

where, C_i: coefficient for determining impulsive period of tank system, H: liquid height inside the tank (m), ρ: liquid density (kg/m^3), t_u: tank shell thickness (mm), D: tank diameter (m), E: elastic modulus of tank material (MPa). Also, the sloshing period of liquid inside circular tanks in different modes can be calculated by following equation (Housner, 1963):

$$f = \frac{1}{T} = \frac{1}{2\pi} \sqrt{\frac{\lambda g}{R} tgh\left(\frac{\lambda H}{R}\right)} \tag{4.3}$$

where, f: sloshing frequency (Hz), H: height of liquid inside tank (m), R: tank radius (m), g: acceleration of gravity (m/s^2), λ: a factor for different modes (λ_1=1.841, λ_2=5.331, λ_3=8.536, λ_4=11.706).

Using these equations the impulsive period (equation 4.1) of tank is T_i = 0.117sec and the first mode of sloshing wave period (equation 4.2) is T_C = 2.75sec which is almost same as calculated value by equation 4.3 for the first mode. Based on equation 4.3 the sloshing period of water surface in modes 1 to 4 is 2.77, 1.61, 1.28 and 1.09 respectively.

As these equations indicate, type of liquid inside the tank just affect the impulsive period of tank due to existence of liquid density in the equation while the sloshing wave period just depends on the tank dimension. If the modelled liquid will be changed to oil with density range of 900-930kg/m^3 (differ for different temperatures), tank impulsive period will change to T_i = 0.111-0.113sec which the difference is almost negligible in comparison to value calculated for water inside the tank (T_i = 0.117sec). This means that modeling of inside liquid by water instead of oil is not affected the tank response.

As mentioned before a pore pressure transducer (PPT) was located inside the tank to record water pressure during the shakings (Figure 3.22). The Fourier amplitude of tank acceleration at center of gravity and tank water pressure increment are presented in Figure 4.40 for dry and saturated cases. As these graphs depict the predominant period of both tank center of gravity acceleration and water pressure increment are almost compatible which declare the dependence of tank water fluctuation on the tank acceleration. However predominant periods range is 0.4~0.9sec which is smaller than sloshing period in different modes calculated by equations 4.2 and 4.3 (1.09-2.77sec). It means that tank acceleration may not amplified long period sloshing of liquid mass.

Table 4.3 shows maximum water height inside the tank during sloshing of liquid. As this result indicates because of the amplification of input motion through the ground in dry cases (Cases 1 and 2) the tank acceleration could be increased comparing to the input motion level. Consequently the sloshing behavior can be more critical in case that oil tank rests on dry sand. Regarding these results the maximum of liquid height during the sloshing of the tank liquid is 3.77m in prototype scale in case of tank with slab foundation while thanks to application of piled raft foundation in Case 2 this could be reduced to 1.83m.

On the other hand, in saturated cases by attenuation of input motions through the ground the tank acceleration is reduced and as a result sloshing waves may decrease. But positive performance of piled raft foundation in reducing waves height cannot be confirmed while the piles effect was diminished during the shaking and sloshing by liquefaction.

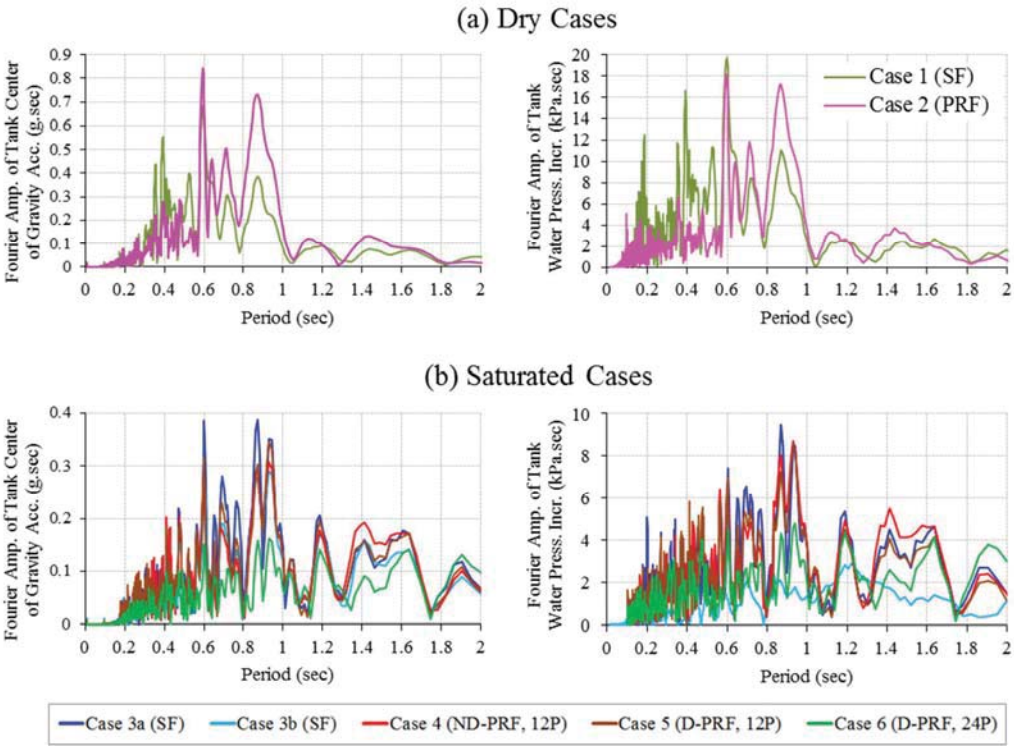

Figure 4.40. Fourier amplitude of tank center of gravity acceleration and tank water pressure increment (Shake 1).

Table 4.3. Maximum of water height during sloshing of liquid

	Maximum of water height (m) during sloshing	
	Shake 1	Shake 2
Case 1 (SF, Dry)	3.26	3.77
Case 2 (PRF, Dry)	1.6	1.83
Case 3a (SF, Saturated)	0.69	1.28
Case 3b (SF, Saturated)	0.43	1.38
Case 4 (Non-driven PRF, Saturated)	0.76	0.89
Case 5 (Driven PRF, Saturated, 12Piles)	0.68	0.86
Case 6 (Driven PRF, Saturated, 24Piles)	0.55	0.63

Another concern in the sloshing behavior of liquid inside the tanks is liquid viscosity. Although regarding equations 4.1, 4.2 and 4.3, the sloshing and impulsive period of liquid inside the tank are not dependent on liquid viscosity, this parameter may have some effect on the sloshing behavior of liquid. Based on previous study by Uras (1995), liquid viscosity behaves as a damping effect. By increase of viscosity, the amplitude of liquid surface displacement and magnitude of dynamic pressures decrease. However, wave form of sloshing and pressure distribution in the liquid may not be affected. Based on this result, similar to equations 4.1-4.3, fundamental sloshing frequencies will not change by viscosity increase. Considering this fact different types of liquid can be stored in the cylindrical storage tanks.

Cylindrical storage tanks can be divided into two groups: fixed roof tanks and floating roof tanks. Fixed roof tanks are used for substances with high flash point e.g. fuel oil, water, bitumen etc. Floating roof tanks are divided to external floating roof tanks (FR) and internal floating roof tanks (IFR). IFR tanks are used for liquids with low flash points (gasoline, ethanol, MS, ATF) and the floating roof objective is to trap the vapor from low flash-point fuels. Floating roofs are supported with legs or cables on which they rest. FR tanks do not have a fixed roof at the top and has a floating roof only. Medium flash point liquids such as Naphtha, Kerosene, Diesel, and Crude oil are stored in these tanks. Another type of storage tanks which mostly are used in mining area is open roof type tank to store ore slurries. This type is the easiest one in order to build. While flash points of some fuels (LPG, Hydrogen, Hexane, Nitrogen, Oxygen etc.) are so low, those storage tanks are usually spherical.

4.6. Effect of Input Motion Type on the Tank Behavior

Two main types of strong ground motion, far-fault and near-fault earthquakes are defined. The ground motions recorded in near-fault region are qualitatively different from the usual far-fault earthquake ground motions. In near-fault earthquakes the acceleration history includes a long period pulse which is related to the pulse in the velocity history. Such a significant pulse does not exist in the far-fault recorded ground motions as is shown in Figure 4.41. This long period pulse affects structures response significantly.

On the other hand, ground motions can be categorized regarding different parameters e.g. amplitude, frequency content and duration of acceleration history. The duration of ground

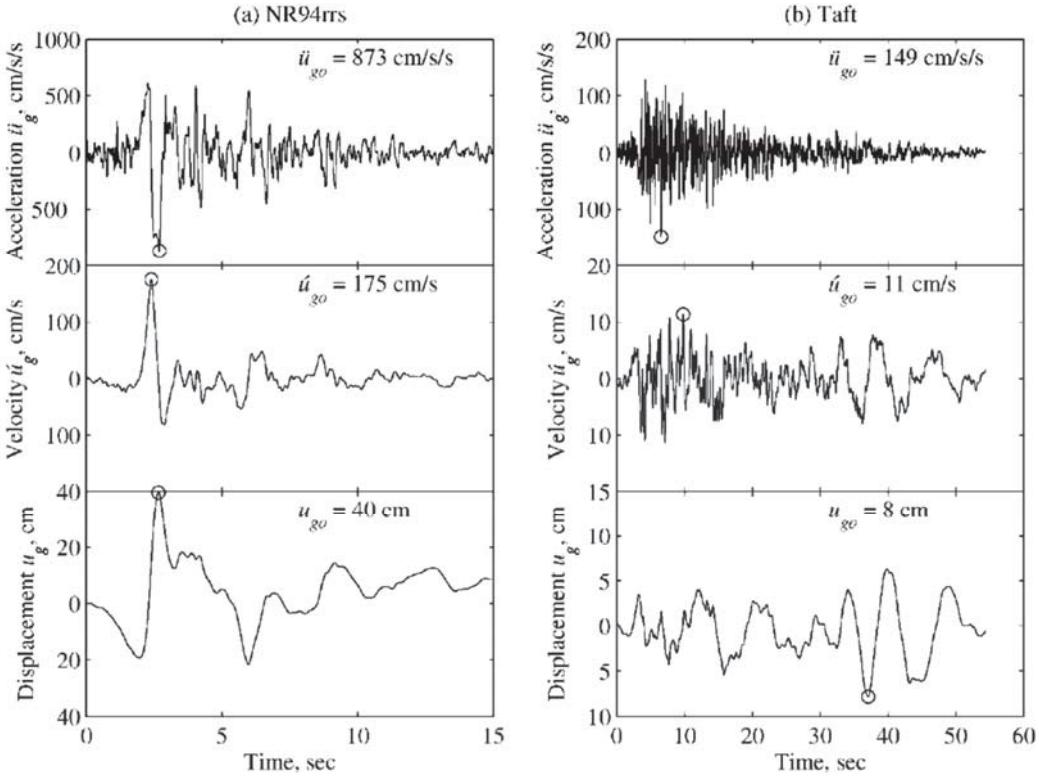

Figure 4.41. Recorded ground motions (a) Near-fault region of Northridge 1994 California earthquake (b) Far-fault region of 1952 Kern county earthquake (Chopra et al., 2001).

motions may have a significant effect on earthquake response and damage. The build-up of pore water pressure in saturated sands is depended on the number of load cycles that happen during an earthquake. A short duration motion may not have enough load reversals to produce liquefaction in a ground even if the acceleration amplitude is large. In the other words, acceleration with long duration and moderate amplitude can develop sufficient stress cycles to trigger liquefaction in a prone ground.

In this research the input motion is East-West component of the acceleration recorded at Kurikoma city in 2008 Iwate-Miyagi Nairiku earthquake. This ground motion is a near-fault strong motion and the input acceleration contain a pulse at the beginning in both dry and saturated cases as shown in Figure 4.42. As the figure indicates this pulse is attenuated through the both dry and saturated ground and could not affect the tank. But this pulse could affect the saturated ground and caused rapid increase of P_L value as shown in Figure 5.11.

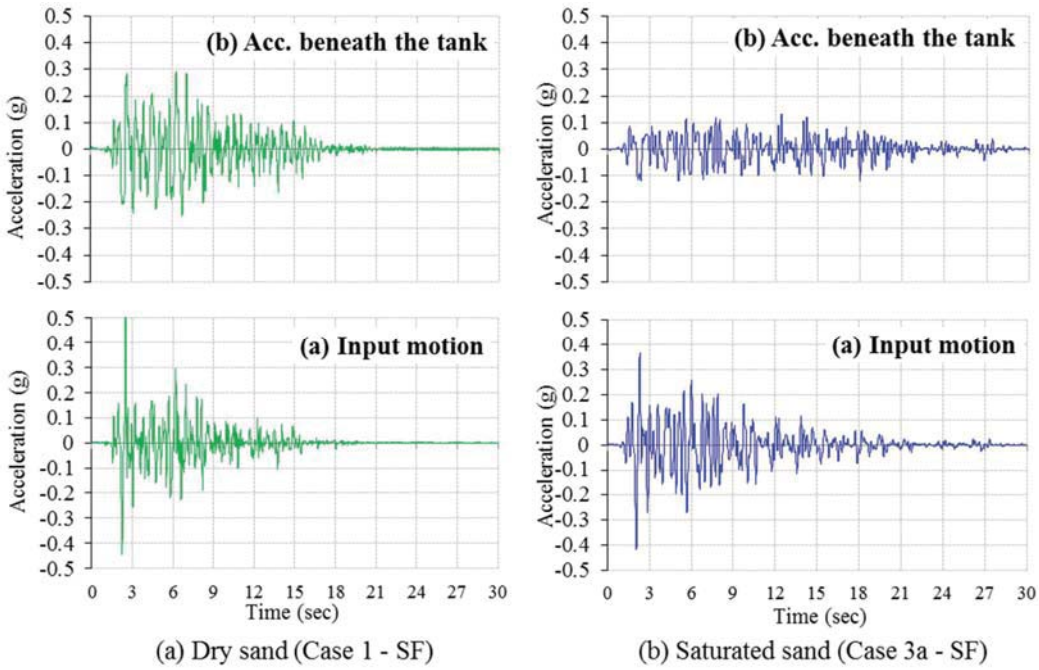

Figure 4.42. Input motion and recorded acceleration beneath the tank in dry and saturated sand.

Since the main purpose of this research is investigation about general behavior of piled raft foundation of oil tanks against seismic loading, using a sample real input motion is reasonable. But if the detail effect of input motion types will be the main objective, different types of accelerations should be utilized to study the performance of the structure and its foundation during those excitations. This purpose can be obtained using not only physical modeling but also numerical modeling.

4.7. Effect of Tank Liquid Level on the Tank Behavior

Liquid level may affect the tank behavior remarkably because of the change in the tank total weight. In the dry sand cases, by reduction of liquid level and tank total weight, its settlement will decrease. Also by reduction of tank center of gravity height and inertial force, tank rotational moment will decrease. Obviously, due to less liquid height, sloshing waves and its critical effect on the tank behavior will be attenuated. In this way, by reduction of settlement, tank rotational moment and sloshing waves, tank rotation also may be controlled and attenuated.

On the other hand, the condition when the tank is located on the liquefiable ground (saturated sand) will be more complicated. While by reduction of liquid level, the tank weight will be decreased and the settlement level will be affected but on the contrary, by reducing tank confinement effect on the subsoil, liquefaction potential of ground just beneath the tank will increase. So, the positive effect of tank on the subsoil for reduction of liquefaction potential of the ground will decrease and the ground beneath the tank will experience larger liquefaction and consequently looseness which may affect the piles bearing capacity more seriously. In this way additional settlement and uneven settlement may trigger. Similar to dry cases by reducing liquid level the sloshing waves and tank rotational moment will reduced which can positively affect the tank behavior.

4.8. Tank Horizontal Displacement during Dynamic Loading

Using the horizontal LDT4 (Figures 3.22 and 3.23), horizontal displacement of tank during shakings are recorded and presented for all cases in Figure 4.43. While the data could not be recorded in Shake 2 of Case 2 and the recorded data for Shake 2 of Case 3a was not reliable these results are not presented in this figure. Although in contrast to laterally spreading grounds (Brandenberg et al., 2005), the ground beneath the tank in this study was flat, as the figure indicates in all cases dynamic and residual horizontal displacement occurred in the tank.

In dry sand cases (Figure 4.43(a)), the residual displacement is a little smaller for both shakes of Case 1 with slab foundation in comparison to Case 2 with piled raft foundation. Considering the results in saturated sand cases (Figures 4.43(b), (c)) these observations can be pointed out: 1) similar to dry cases, the residual displacement in SF cases is smaller than in PRF cases, 2) in all cases the displacement in Shake 2 is less than Shake 1 despite of larger input motion in Shake 2. The densification of ground during the first shake can be the reason while it

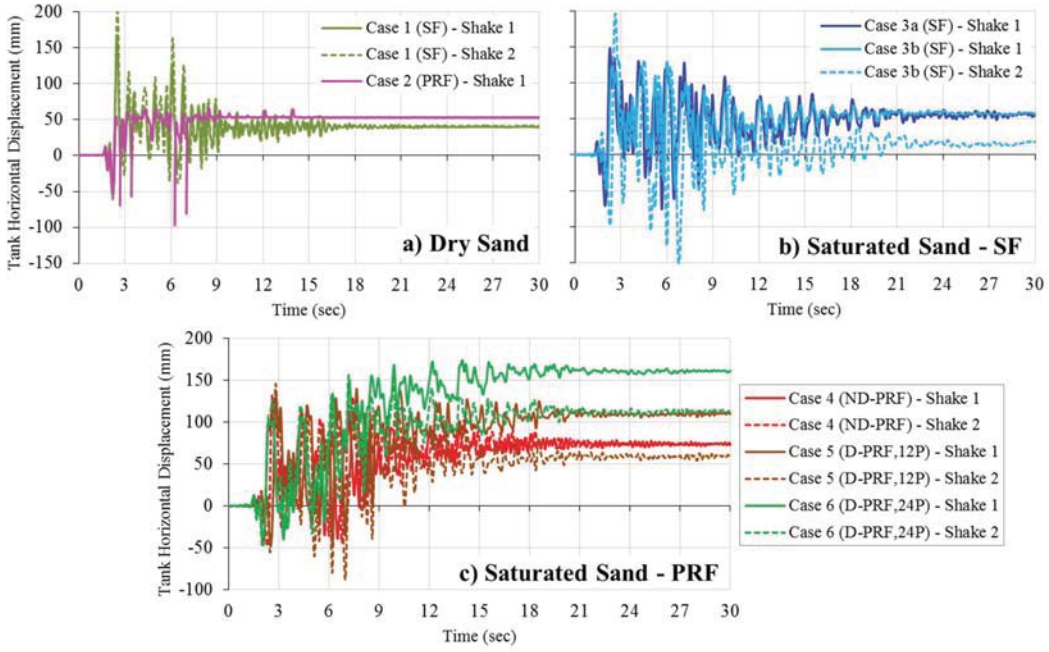

Figure 4.43. Tank horizontal displacement during shaking.

might increase the friction between tank and the ground. 3) Case 6 with large number of piles had the maximum horizontal displacement in both shakes comparing to all cases. Regarding this results, it seems that raft friction has the main contribution against horizontal displacement. Due to small raft average pressure in Case 6 (Figure 4.24) and also as discussed before uneven contact between the raft and subsoil, larger displacement happened in both shakes of this case. Also, in dry cases almost larger displacement in PRF case (Case 2) might be due to smaller raft contact pressure. On the other hand, the larger horizontal displacement in saturated cases may be attributed to the smaller raft friction in saturated sand cases. In addition, despite of larger input motion in SF cases on saturated sand (Figure 3.35), PRFs have larger displacement which is another evidence for this behavior.

In conclusion, piled raft foundation of oil tank with pin connection between the raft and piles may not be so effective in reducing horizontal displacement of tank during dynamic loadings. Enough and uniform raft contact pressure in this foundation system is more important against horizontal displacement. On the other hand, fixed pile to raft connection might affect the horizontal displacement of tank and should be studied in the future researches.

4.9. Summary

In this chapter, the results of centrifuge model tests on the piled raft and slab foundation of oil tanks was discussed. In the first part of chapter, the behavior of modelled oil tank on the non-liquefiable (dry) sand was considered. In this section tank behavior with slab foundation and non-driven piled raft foundation on dry sand were compared. In the second part of the chapter the tank behavior with slab, non-driven and driven piled raft foundation with different piles number on the liquefiable (saturated) sand was studied. Also some introduction about soil liquefaction was included in the second part of the chapter.

The ground response, tank accelerations, tank settlements, tank rotation, ground excess pore water pressures in saturated ground, piles and raft resistances, tank maximum rotation and direction of maximum rotation along with liquid behavior inside the tank were explained and discussed in detail in this chapter. Based on the discussions the followings can be pointed out:

1. In dry sand ground, the input motions were amplified in both types of foundation, but the amplification for the slab foundation case was more in low periods range than the PRF. The less confinement effect of the raft stress of PRF than that of SF made the natural period of the subsoil longer for the PRF than the SF.

2. Because to the contribution of piles of the piled raft foundation, this foundation system could effectively reduce the tank rocking motion, settlement and uneven settlement when the tank was modelled on the dry sand.

3. In case of tank with piled raft foundation on the dry sand, despite of larger piles load sharing, in this piled raft foundation with frictional piles, not only the pile resistance but also the raft resistance bears the loads and rotational moment.

4. Because of the large soil stiffness reduction by the liquefaction, the input motion is significantly attenuated especially in short period range and at the ground beside the tank where less confinement pressure is transmitted from the tank. While at the ground beneath or just beside the tank, due to the confinement effect of the tank load, the attenuation level is relatively small compared to the further outside ground and some amplification of motion could occur in long period range.

5. The pile driving process could increase the density and lateral stresses of sand between piles, which could slower the excess pore water pressure (EPWP) increase and enhance

the EPWP dissipation beneath the tank. This effect becomes more significant as the number of pile increases.

6. As a common trend of PRF without shaking history, the base contact pressures at all location increase in the EPWP build-up stage. At the outer part of the raft base, the pressures are kept almost constant during the liquefaction stage and then start decreasing in the consolidation stage, while in the central part the pressure increases even in the consolidation stage, showing the stress concentration due to the relatively large stiffness by the raft pressure. The increase of raft load proportion (RLP) of PRF is caused by the reduction of piles resistance due to the liquefaction, but the RLP decreases gradually with the recovery of piles resistance by the EPWP dissipation. The concentration of base pressures at the center is more significant for SF than PRFs and as the number of piles increases, the concentration could be reduced by the additional support from the piles.

7. The reduction of pile resistance could be slowed by the pile driving to some extent, but the effect could not be expected after a large shaking.

8. Driven PRF could reduce the rocking motion of tank during shaking in comparison to non-driven PRF, especially for the Driven PRF with a larger number of piles.

9. Piled raft foundation was somewhat effective in reducing tank settlement but relatively large raft load proportion (RLP) is a necessity for preventing a large settlement and uneven settlement during the liquefaction.

10. Once the direction of the maximum rotation is fixed to a direction diverted from the shaking direction, the rotation will be accumulated by shaking. But while the rotation mainly takes place in the shaking direction, the monotonic increase of the rotation may

not easily occur and the rotation behavior becomes very complicated for the slab foundation.

11. The liquid behavior (sloshing) inside the tank is directly related to the acceleration level at the tank center of gravity. Because of the higher tank acceleration in dry cases due to the amplification of input motion in the ground the water pressure increment inside the tank was larger in dry cases.

Chapter 5 – Practical application of the study

5.1. Introduction

There are some typical differences between oil tank foundation and other infrastructures. Circular shape of foundation, uniformly distributed load of a huge mass of liquid and the complex movement of liquid inside the tank during dynamic loads make this infrastructure foundation unique in comparison to other structures foundation.

Different kind of foundations has been used for oil storage tanks in the real projects and a wide range of foundations are permitted based on the design codes (API 650 (2007), Design recommendation for storage tanks (2011)). The most common foundation system for this infrastructure is earth foundation (Figure 5.1(a)). Also slab foundation is commonly utilized for oil tanks when the bearing capacity of subsoil is not satisfactory (Figure 5.1(b)). Furthermore, sometimes a deep foundation like pile groups is necessary in order to enhance the performance of foundation (Figure 5.1(c)). In this situation utilization of an appropriate slab underneath the tank is inevitable in order to afford suitable connection between the tank structure and the piles group while using the common pile caps is not practical due to punching effect on the tank bottom shell. The design strategy of the piles depends on the ground condition. In some cases the piles are designed to contribute against the loads by not only shaft friction but also tip resistance. But in some other cases the contribution of both is not possible and design is just based on one of them. In the normal pile foundation design method of ordinary storage tanks, the raft contribution against loads is ignored. While existence of raft is necessary for placing the tank on the ground, by taking into account the raft capacity the foundation performance will be affected and the required number and length of piles will be changed (Figure 5.1(d)).

In the past few years, it is common to account the raft bearing capacity of pile foundation of normal structures (buildings) as a part of foundation system, while the raft is necessary as a base beneath the structure (Abdel-Fattah et al., 2016). In this way the structures construction cost will be decreased by reduction of required piles number and length. Furthermore, the foundation system performance will be enhanced by controlling settlement and uneven settlement of the structure. The main problem is a comprehensive design procedure, estimation of loads applied to the structure and its components which depends on the sophisticated interaction between the soil and structure and also specification of the situations (e.g. ground condition, structure and loading type) in which piled raft foundations have acceptable and preferable performances. Due to this limitations and ambiguities this foundation system has been considered only for normal structures like buildings and its application for other kind of structures is almost ignored in previous studies and real projects. Some sample application of piled raft foundation for buildings in different countries are presented by Poulos (2001) also some other projects constructed in Japan are discussed by Yamashita (2012).

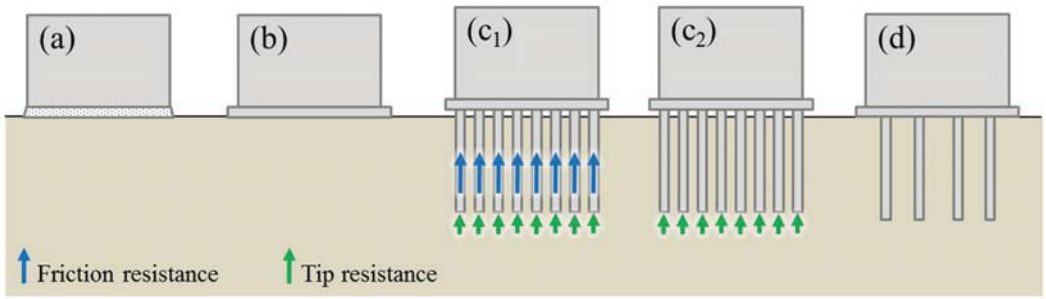

Figure 5.1. Oil tank foundation types; (a) Earth foundation, (b) Slab foundation, (c_1) Pile foundation with end bearing and frictional piles, (c_2) Pile foundation with end bearing piles (d) Piled raft foundation.

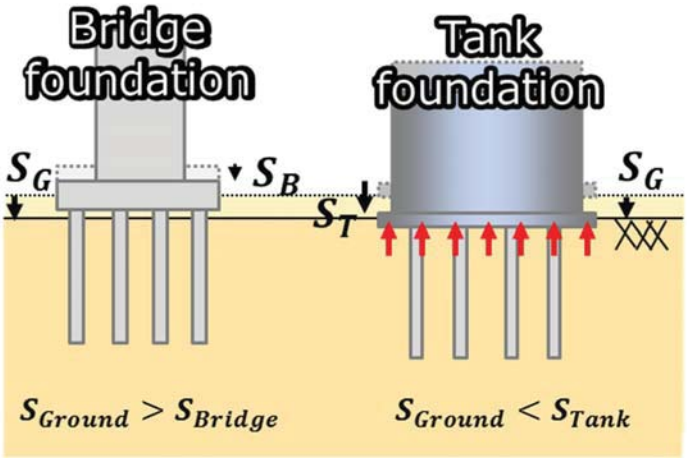

Figure 5.2. Comparison of oil tank foundation and bridge foundation.

One of the most important points in the behavior of piled raft foundation is secure contact between the raft and the subsoil. The raft contribution and consequently full capacity of piled raft foundation system cannot be developed without uniform and sufficient raft contact pressure. In oil storage tanks same as other infrastructures large settlement is prohibited due to disturbance of tank and its attachments (e.g. valves) performances. But thanks to flexible pipes some level of settlements is acceptable for oil storage tanks in contrast to other infrastructures that restricted the allowable settlement range (e.g. bridges). Due to this acceptable level of settlement, secure contact between the raft and ground can be expected in oil tanks and concept of piled raft foundation could be reasonably assured for these structures (Figure 5.2). Another important point in the concept of piled raft foundation is piles type (end bearing or friction pile). In the end bearing piles because of large tip resistance, enough structure settlement cannot be afforded and the secure contact of raft and subsoil may not be developed. So the concept of piled raft foundation is not possible for this kind of piles. In the other words, only friction piles can participate as a part of piled raft foundation system (Figure 5.1(c_1)).

The main objective of this chapter is to clarify some hindered aspects of piled raft

foundations of storage tanks using the results obtained in the previous chapter. Also, for this purpose the previous studies will be considered and the required points will be indicated.

5.2. Pile and Piled Raft Foundation Differences

In the engineering design of foundations it is usual to consider firstly a shallow foundation like a slab foundation to sustain the structure load. If the capacity of the shallow foundation will not satisfy the structures load or stability, deep foundation will be utilized to enhance bearing capacity and stability of the foundation. Pile foundation is a kind of deep foundation in which total structural load is carried by the piles and bearing capacity of the raft or piles cap is ignored. In case of piled raft foundation, raft behaves as a part of the foundation system and this contribution will affect the foundation behavior and its bearing capacity. Due to the contribution of raft, a complicated interaction between soil, pile and raft will be mobilized against loads in comparison to a fully piled foundation (Figure 5.3).

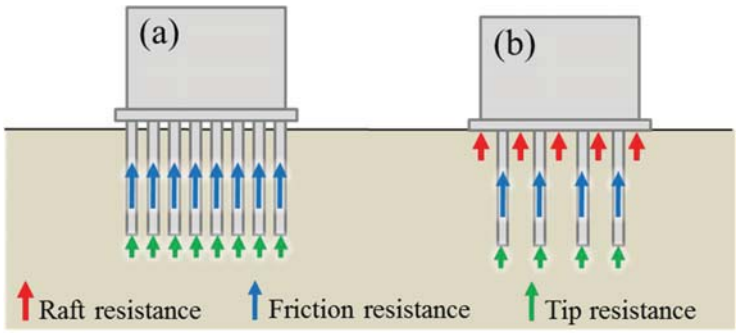

Figure 5.3. (a) Pile foundation, (b) Piled raft foundation.

5.3. Special Considerations for the Rational Design of Piled Raft Foundation

Design of piled raft foundation similar to other foundation systems needs precise attention on the some considerations like: 1) maximum settlement, 2) uneven settlement, 3) load capacity for vertical and lateral loads, 4) pile and raft load share, 5) piles load and moments for the structural design, 6) raft moments and shears for the its structural design.

Based on the previous study by Randolph (1994), three types of design strategies are presented for the piled raft foundations:

1) In the first one, the piles are assumed as a group to sustain main part of the load and a few contributions by raft against loads is presumed.

2) In the second strategy, piles are designed to work at a load which is about 70-80% of the ultimate load capacity. In this method, required numbers of piles are utilized in order to reduce contact pressure between the raft and the subsoil.

3) In the third type, the piles are located in the essential locations in order to reduce the uneven settlement instead of decreasing total settlement.

Moreover, in the second approach it is possible to utilize the full load capacity of the piles which means some or all piles operate at total (100%) of their ultimate load capacity. This strategy enhances the concept of using piles as settlement reducers while the piles can also increase the ultimate load capacity of foundation system.

The load-settlement relation of piled raft foundations designed based on the illustrated strategies during static loading are shown in Figure 5.4. The raft foundation behavior is presented by curve number 0 which shows large settlement during design load. The behavior for

first strategy in which the behavior of foundation system is mostly depended on the pile group performance is presented by curve number 1. In this case the relation is linear during the design load and the piles carry the main part of loads. The trend of the second strategy is presented by curve number 2. In this condition the piles work with smaller safety factor while there are fewer piles, but the raft contribution is larger. Curve 3 shows the concept of using the piles as settlement reducers and utilizing full capacity of piles at the design load. As a result, despite of non-linear load-settlement relation at design load, the foundation system has enough factor of safety and the settlement criterion is assured. Consequently, the design strategy presented by curve 3 is reasonable and more economical than the others.

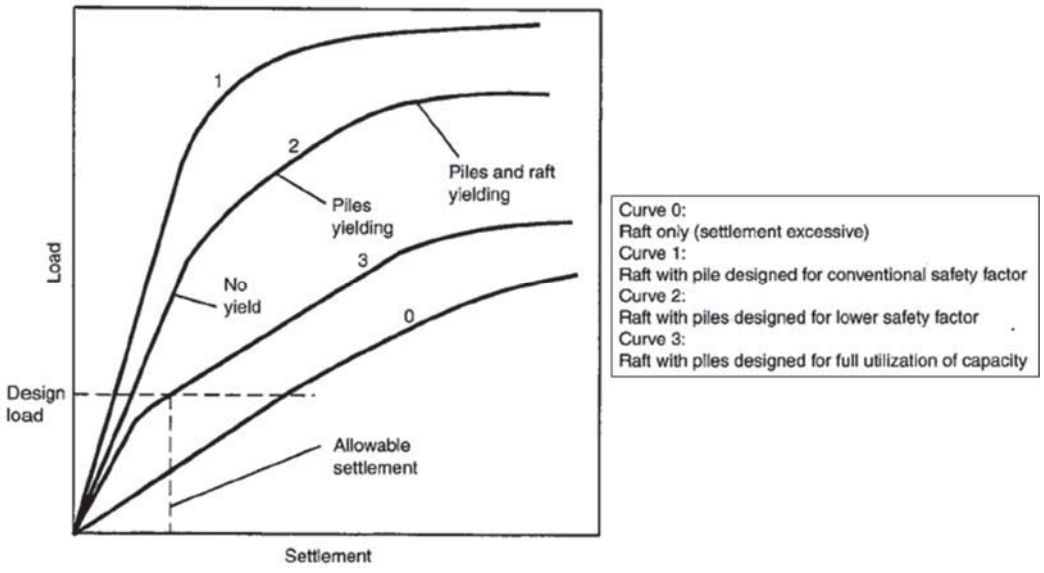

Figure 5.4. A general load-settlement curves for piled raft foundations based on different design strategies (Poulos, 2001).

The most important difficulty in the design of piled raft foundation of oil tanks is estimation of pile and raft load proportion especially in case of dynamic loading. As Figure 5.5 indicates raft and piles load proportion can be estimated during static loads using these formulations: $LP = \frac{\int q_{raft}}{Q_V}$, $PLP = \frac{\Sigma q_{pile}}{Q_V}$. The estimated values of RLP and PLP will be between 0 and 100 percent. But during the dynamic loading the estimation is more complicated while the dynamic horizontal loads (Q_d) will add or reduce some part of loads (△q) on the raft or piles which depends on the location of pile and raft element. So, it is very difficult to precisely determine pile and raft design load due to variability of raft load proportion (RLP) and pile load proportion (PLP). On the other hand regarding the test results of piled raft foundation of oil tank on dry (non-liquefiable) and saturated (liquefiable) sand presented in chapter 4, PLP was large in the beginning and increased after shaking in case that tank was resting on non-liquefiable sand. While in case of liquefied ground the PLP had a value in range of 0~100% before shaking (static loading) but during the shaking and the liquefaction it was reduced even until 0% and again after the shaking bearing capacity of piles was regained and PLP had a value in range of 0~100%. Because of this complexity in the assessment of PLP and piles load, critical conditions should be determined to design piled raft foundation of oil tanks.

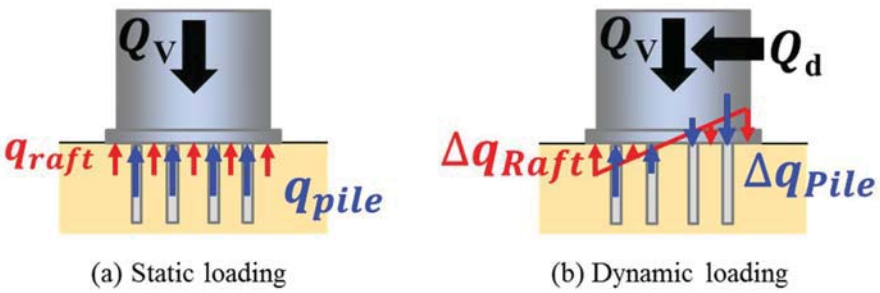

Figure 5.5. Piles and raft contribution during static and dynamic loading.

The main design concerns in the piled raft foundation of oil tanks during various loading condition are tank overall stability (bearing capacity of foundation, settlement and uneven settlement), structural components strength (piles and raft) and sloshing of liquid inside the tank which may affect the foundation performance. In the continuation, some practical application of this research in order to implement piled raft foundation system for oil storage tanks will be discussed in cases that tank is located on non-liquefiable or liquefiable sand.

5.3.1. Non-Liquefiable Sand

Regarding the previous investigations piled raft foundations are more effective when adequate load capacity can be developed by the raft. Some different soil profiles are examined by Poulos (1991) and indicated that these ground conditions are the best for appropriate performance of piled raft foundation of normal buildings during static loading: (a) soil profiles consisting of relatively stiff clays, (b) soil profiles consisting of relatively dense sands. In these ground conditions the raft can develop the required bearing capacity and using the piles; the foundation system performance will be enhanced in the other aspects like uneven settlement.

On the other hand the results of current research show that performance of piled raft foundation of oil tank was acceptable according to its performance in various contexts e. g. rocking motion, settlement and uneven settlement. In the next sections some aspects will be considered more and discussed in detail.

5.3.1.1. Bearing Capacity and Overall Stability of Foundation

The importance of accurate evaluation of the stability of oil storage tanks is proved during

the decades due to the failures happened for this kind of infrastructures (Duncan et al., 1984). Usually, this failure cause large non-uniform settlements and tilting of the tank and may lead to tank rupture and loss of the inside liquid. This may cause disasters like contamination of environment or huge fires.

Two types of foundation instability have been recorded in the storage tanks foundation; base shear (Figure 5.6(a)) and edge shear failure (Figure 5.6(b)). The failure of entire tank which acts as a unit is named base shear. On the other hand, edge shear involves local failure of a section of the tank perimeter and the adjacent part of the subsoil. Using available bearing capacity formulas that take into account the thickness of the weak soil layer underneath the tank comparing to the tank width, both of the stability failure modes can be assessed (Duncan et al., 1984).

According to these failure modes, it seems that by locating piles under the tank in the piled raft foundation system there are possibility to increase the shear failure surface and consequently enhance the factor of safety against these failures especially edge shear failure mode which can be developed near the ground surface and piles area (Figure 5.7).

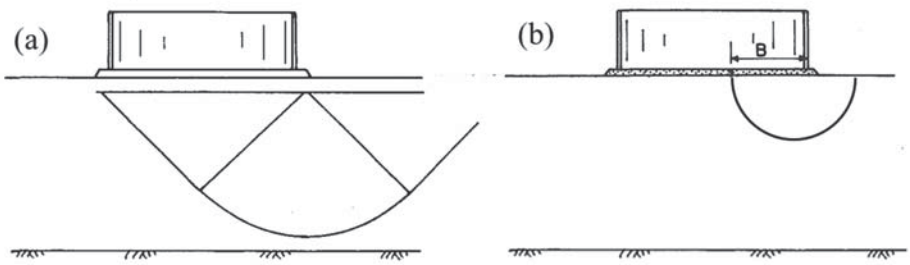

Figure 5.6. Tank stability failure mechanism, (a) Base shear failure, (b) Edge shear failure (Duncan et al., 1984)

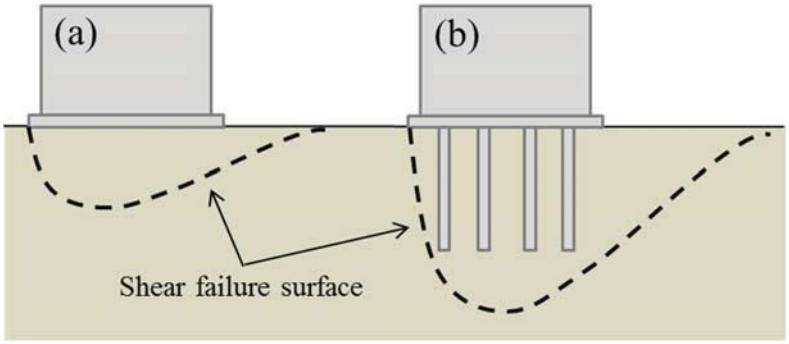

Figure 5.7. Shear failure surface, (a) Raft foundation, (b) Piled raft foundation.

On the other hand, based on the results of the pile loads in case of piled raft foundation of oil tank on non-liquefiable ground (Figure 4.11), the majority of the tank load had transferred to the piles of the piled raft system. Since almost significant settlement was developed in the tank (Figure 4.6) reasonable performance of the Piled raft system or in the other words the contribution of the raft against the loads can be taken place. So thanks to enough bearing capacity of the raft and the piles especially in a sandy soil ground with sufficient relative density and non-liquefiable condition, the piled-raft bearing capacity cannot be the main concern and other critical issues like settlement or uneven settlement of the foundation should be considered precisely.

5.3.1.2. Settlement and Uneven Settlement of Tank

Storage tanks made by steel are flexible structures and can sustain some level of uneven settlement. But if this settlement exceeds the structure capacity, the catastrophe may happen due to distortion and rupture of the tank shell and spill of the tank contents.

For small size tanks as was modelled in this research, the slab commonly is assumed to be rigid, in this way uneven settlement of foundation is equal to foundation rotation. According to

trend presented in Figure 4.37, tank center settlement and tank rotation (uneven settlement) has approximately linear relation when it is resting on a dry sandy ground. Based on the previous chapter results, using piled raft foundation system can effectively reduce not only tank settlement but also tank uneven settlement (Figures 4.6, 4.7 and 4.37). On the other hand, in contrast to majority of oil tanks resting on earth foundations (API650, 2007), construction of a raft beneath the tank can positively create a flat surface underneath the tank which is effective in developing a uniform settlement under the tank. So due to existence of raft in piled raft system some part of local settlements beneath the tank which may cause rupture and leakage of inside liquid, can be reduced.

5.3.1.3. Structural Components (Piles and Raft)

As previously was explained piled raft foundation system in comparison to normal pile foundation requires less number of piles and smaller pile length. This reduction in pile length and number is so vital especially in point of view of real projects expenses. But this reduction in the piles number and length causes increase of static and dynamic load portion that each pile should carry. On the other hand as Figure 4.11 indicates in piled raft of oil tank located on non-liquefiable sand with sufficient resistance of soil, despite of raft contribution, the main part of static and dynamic loads is transferred to the piles. In this condition, more attention is essential for design of piles while they have main contribution against loads. Furthermore, during the dynamic loading higher piles load is expected due to contribution of them against dynamic loads and tank rotational moment (Figures 4.10 and 4.12). In this complicated situation the design of piles is a critical issue in order to have enough structural strength and factor of safety against failure. Another concern is punching of the raft by the piles. Because the piles has

considerable load share especially during dynamic loading, there is possibility of raft punching by the piles and rupture of tank shell and leakage of the liquid. Considering these issues precise pile and raft design procedure which is including reasonable design loads and factor of safety is inevitable. For this purpose as shown in Figure 4.10, piles location is also important. Although the static part of load is distributed to some extent evenly between the piles, the distribution of dynamic part depends on the piles location while the piles at the raft perimeter have larger contribution against dynamic loads in comparison to the piles at the raft center (Figure 5.8 and 4.10).

Considering these points, as a remedy in order to reduce the failure risk of piles it is recommended to estimate piles design loads with assumption of raft load proportion equal zero. Also, a designer can use different factor of safety for the interior and exterior piles; a larger one for the outer piles and a smaller one for the inner piles. Also the piles can be designed for a design load included the static load (q_s) plus maximum of amplitudes of dynamic loads (q_d) as shown in Figure 5.8(a). Obviously, by using this method the raft thickness should be estimated based on the punching effect of perimeter piles with larger pile load, bending moment and shear of the raft.

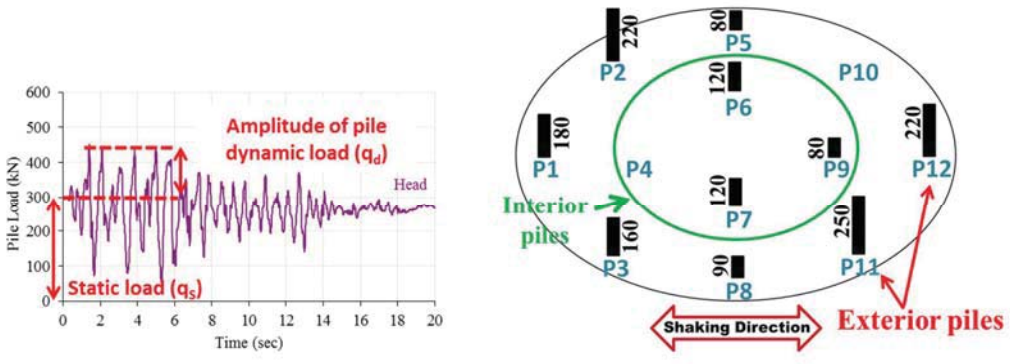

(a) Sample pile load (b) Amplitude of piles dynamic load

Figure 5.8. Piles with larger loads at the raft perimeter.

5.3.1.4. Sloshing

As explained before sloshing behavior of liquid inside the tank is one of the key issues in the oil tank structures. The fluctuation of tank liquid can affect the overall behavior of oil tanks and its stability by enhance of tank vibration and its uneven settlement. Also, it can damage the roof and the top of tank wall.

According to the detailed discussion presented in chapter 4, liquid sloshing is related to the tank center of gravity acceleration. Due to the amplification of input motion through the ground the tank acceleration could be increased comparing to the input motion level. Consequently the sloshing behavior can be more critical in case that oil tank rests on a non-liquefiable ground. Based on the results of this research the maximum of liquid height during the sloshing of the tank liquid is 3.7m in prototype scale in case of tank with slab foundation while this could be reduced to 1.8m in case of oil tank with piled raft foundation. This reduction is so important in the tanks with floating and non-floating roof while this free-surface wave height determines the freeboard requirements of tank and it can reduce the forces on the roof.

5.3.2. Liquefiable Sand

According to previous investigations (Poulos, 2001), there are some unfavorable ground conditions for the application of piled raft foundation. Some of them are: 1) soil profile including soft clays near the surface, 2) soil profiles containing loose sands near the surface, 3) soil profiles which contain soft compressible layers at shallow depth, 4) soil profiles that probably may experience consolidation settlements, 5) soil profiles that may possibly suffer swelling movements due to external causes.

Liquefiable sandy ground can be categorized as the second group. In the first two cases including liquefiable sand, the raft may not be able to provide significant load capacity and stiffness. In the third one due to long-term settlement of the compressible layers the raft contribution may not be developed quickly. The last two cases are also so risky in case of piled raft foundation while consolidation settlement may cause loss of contact between the raft and the subsoil. On the other hand, in case of swelling soils due to action of them on the raft, additional tensile force may be exerted in the piles.

In the current research also the behavior of modelled piled raft foundation of oil tank was not so positive in cases which the tank was modelled on the liquefiable ground. In order to discuss more on the behavior of foundation on liquefied sand some detailed discussion are presented in the continuation.

5.3.2.1. Bearing Capacity and Overall Stability of Foundation

In contrast to piled raft foundation of oil tanks on the non-liquefiable sandy ground, PRF bearing capacity on liquefiable sand need more consideration. Obviously, due to less strength of saturated sand and looseness of liquefied ground the bearing capacity of foundations on this kind of subsoil is an important concern. In case of piled raft foundation of storage tanks as the result of chapter 4 indicates (Figures 4.22 and 4.24) during liquefaction the bearing capacity of the piles is seriously affected by the increase of excess pore water pressure. In the other words, due to increase of excess pore water pressure, the bearing capacity of piles is reduced partially or even completely diminished during the liquefaction period (Figure 5.9). In this situation piles bearing capacity cannot be taken into account for design of foundation system and the slab alone should satisfy the bearing capacity criteria.

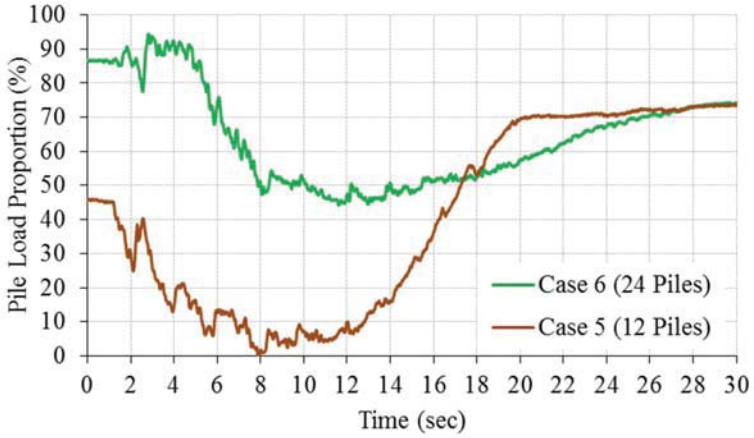

Figure 5.9. Pile load proportion during the shaking.

Another concern in the concept of overall stability of tanks is lateral spreading of ground especially in cases the tank is constructed on the fields that are prone to lateral spreading. Although the storage tank fields are not constructed on the sloping ground, this kind of catastrophic situation can happen when the tank field is located next to the ports as occurred during the Kobe earthquake (1995) (Cubrinovski et al., 2001). In this condition lateral movement of quay walls toward the sea may trigger lateral spreading of the backfill ground where the storage tanks are located. This large lateral ground displacement is a key factor affecting piles response significantly and may cause disturbance in the piled raft performance and damage to the piles.

5.3.2.2. Settlement and Uneven Settlement of Tank

According to the results of this research, settlement and uneven settlement of tank piled raft foundation resting on the liquefiable sand is almost considerable (Figures 4.31 and 4.33). The most critical issue same as non-liquefiable ground condition is enough and uniform contact

between the raft and the subsoil. As the results indicate despite of large number of piles beneath the raft, when enough contact pressure between the raft and soil could not be developed, large settlement and uneven settlement happened. So, the most important criteria which should be considered during the construction of piled raft is development of this desirable contact condition. The desirable contact condition includes not only the enough contact pressure between the raft and ground but also uniform pressure and contact condition. Clearly, any kind of unevenness in the structure load or contact condition can trigger uneven settlement which should be avoided. On the other hand as shown in Figure 4.36 when the uneven settlement triggered in the transverse direction, its large and monotonic increase may be continued until end of shaking but when this uneven settlement happened in the shaking direction, the tank can return to its main position and large uneven settlement may be avoided. In this way, by eliminating any kind of non-uniformity in the structural condition and raft contact especially in case of small size tanks, tank rotation can be limited to the main shaking direction and the large rotation in the other directions can be eluded.

According to the relationship between the tank settlement and uneven settlement presented in Figure 4.37, it seems that piled raft foundation could have acceptable performance in comparison to slab foundation in some duration by controlling uneven settlement of tank. In order to categorize and identify the condition in which piled raft foundation of oil storage tanks on liquefiable sand has better performance, the severity of ground liquefaction should be understood. While the structural damages by soil liquefaction are extremely affected by liquefaction intensity this parameter is also so important for judgment about the performance of oil tank piled raft foundation. For this purpose, P_L value firstly introduced by Iwasaki et al. (1978) can be utilized. This liquefaction potential index (P_L) is defined by equation 5.1 in order to approximate the intensity of liquefaction extent at a given site for a seismic motion.

$$P_L = \int_0^{20} F.w(z)dz \quad (5.1)$$

where F = 1 - F_L for $F_L \leq 1$ and F = 0 for $F_L > 1$, and w(z) = 10 - 0.5z (z: depth in m), as shown in Figure 5.10. The w(z) function is a weight function of the depth and give bigger weight to the shallow portion. Its triangular shape along with 20m maximum of depth is chosen based on the liquefaction phenomena in the previous earthquakes. The P_L value will takes values between 0 and 100 in general cases while it will be equal 0 in cases $F_L \leq 1$ for the entire depth and 100 for cases $F_L = 0$ for the entire depth. As mentioned before this value (P_L) can be utilized for assessment of liquefaction potential for a given site. So, Iwasaki (1986) calculated P_L value for many liquefied and non-liquefied sites during some huge previous earthquakes and finally proposed a simple method for determining soil liquefaction potential in terms of P_L as follow:

$P_L = 0$: Liquefaction risk is very low, $0 < P_L \leq 5$: Liquefaction risk is low, $5 < P_L \leq 15$: Liquefaction risk is high and $P_L > 15$: Liquefaction risk is very high.

The P_L value during the shaking is calculated for the test cases of tank on liquefiable sand mentioned in chapter 4. In this calculation F_L is estimated using the simplified method explained by Annaki et al. (1977) and Yoshimi (1980). The results are presented in Figure 5.11 for all the cases during the shaking. On the other hand as indicated before and shown in Figure 4.37, almost in all piled raft foundation cases (Cases 4, 5 and 6), the piled raft foundation system could reduce settlement and uneven settlement of tank comparing to slab foundation cases (Case 3a and 3b) at the beginning before t_l (start of liquefaction stage beside the tank). While t_l is 4sec for all cases (Figure 4.21) the P_L value for t=4sec as the figure indicates is 9 for Case 6, 15 for Case 4 and 17 for Case 5. Regarding these results, if the special behavior in Case 6 will be neglected and P_L in Cases 4 and 5 will be considered, it seems that if the ground condition and design seismic motion of a given site can confine the P_L value to 15 or less, a better performance

for piled raft foundation of tank on liquefiable sand can be expected.

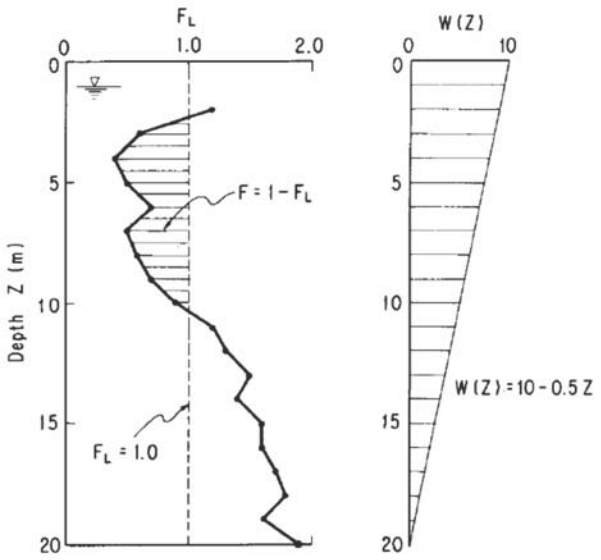

Figure 5.10. Example of F_L value and weight function w(z) (Iwasaki, 1986).

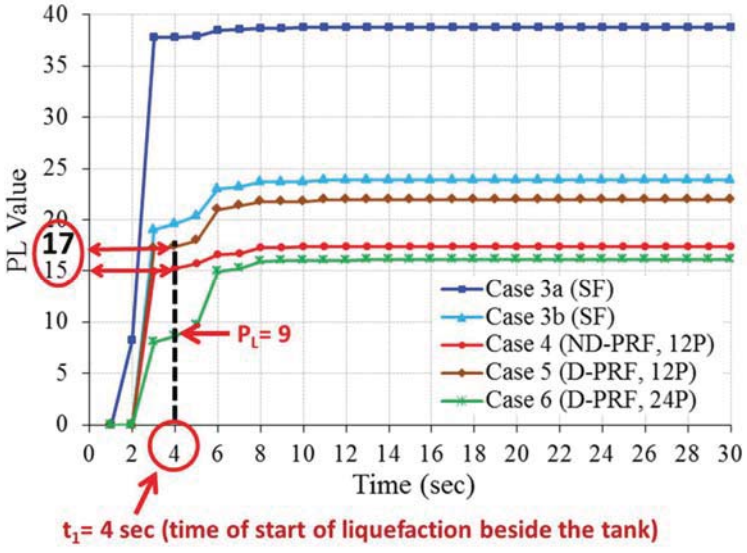

Figure 5.11. P_L value during the shaking.

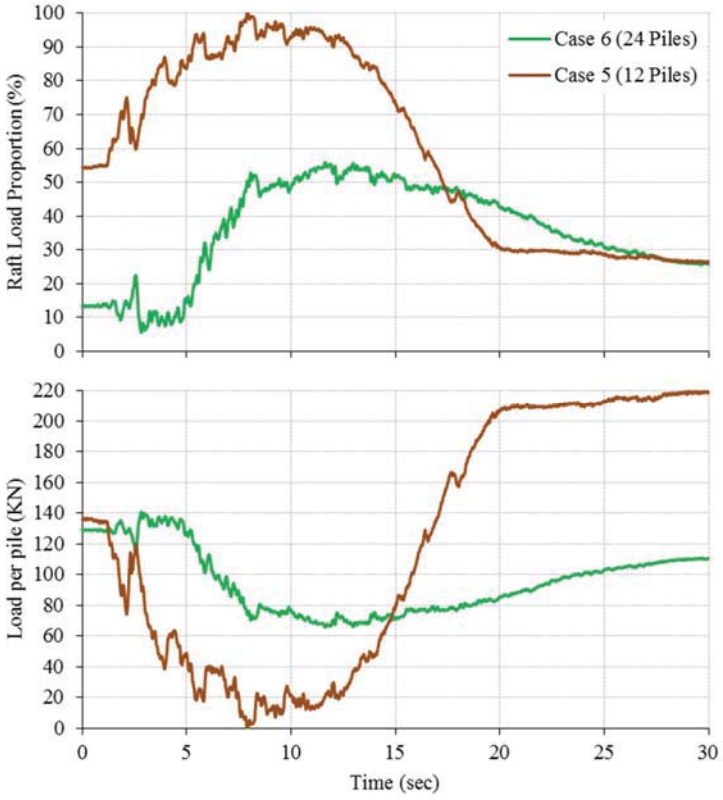

Figure 5.12. Raft load proportion and load per pile in PRF on liquefiable sand (Cases 5 & 6)

5.3.2.3. Structural Components (Piles and Raft)

Regarding Figure 4.24 in contrast to behavior of PRF on dry sand, pile load is not the main concern while raft has contribution against loads before start of shaking until the end. Raft load proportion of the piled raft in two piled raft cases with 12 and 24 piles are presented in Figure 5.12. As the figure indicates the raft has persistent contribution against the loading during the shaking in both cases. The contribution of raft is not diminished during the shaking even in case with large number of piles (Case 6) that the main part of load was transferred to the piles at the beginning. This continuous contribution of raft reduces the piles load and risk of failure of piles and punching effect on the raft. Also the load of each pile during the shaking is shown in this

figure. As previously indicated the graphs show that the piles bearing capacity is diminished completely or partly during the liquefaction period. This behavior affects strongly the performance of piled raft foundation and its concept which demands contribution of both raft and piles.

Consequently by disturbing simultaneous contribution of raft and piles some instability may happen in the piled raft foundations of oil tanks located on the liquefiable ground and significant settlement and uneven settlement may occur.

5.3.2.4. Sloshing

Because the sloshing of liquid inside the tank is directly related to the tank acceleration, in liquefiable sandy ground in contrast to non-liquefiable ground by attenuation of input motion through the ground the tank acceleration is reduced and as a result sloshing waves may decrease. Regarding the results of this study the maximum of liquid height during the sloshing in cases with piled raft foundation on the liquefiable sand are 0.9m (Case 4), 0.85m (Case 5) and 0.63m (Case 6) which are inconsiderable in comparison to the tank dimension and also so smaller than oil tank PRF on dry sand.

On the other hand due to loose condition of liquefied sand and its long natural period there is possibility for amplifying sloshing waves of liquid inside the tank. As Figure 4.40(b) indicates the predominant periods of water pressure increments inside the tank are smaller than sloshing period of water surface in different modes (2.77, 1.61, 1.28, and 1.09) inside the tank so this amplification may not happen for this small size tank with this special dimension.

In conclusion, sloshing behavior of liquid inside the oil tanks with piled raft foundation on

liquefiable sand is not a main concern but the tank dimensions should be designed in a way that confines the possibility of amplification of liquid waves inside the tank by long period movements of ground.

5.4. Long-term behavior of piled raft foundation

The most important concern about long-term behavior of piled raft foundation is change in the load sharing of piles and raft. This change can happen by long-term settlement of ground and foundation after construction of the structure especially when the ground and foundation subsidence is not equal. In such a condition some gap between the raft and subsoil may affect the load sharing between the piles and raft. In this way increase of piles load proportion may exceed its bearing capacity and cause damage in the piles. Even uneven settlement may happen due to non-uniform contact condition between the raft and subsoil. So, this kind of situation should be considered as a critical condition during the foundation design.

One solution for this critical condition is using just frictional piles instead of end bearing piles while the end bearing type of piles may prevent settlement of piles and cause difference in settlement of foundation and subsoil. Also as it was recommended in this chapter it is better to satisfy the bearing capacity criteria of piled raft foundation of oil tank located on non-liquefiable sand with assumption of no contribution from the raft. In this way this critical condition will be considered during the foundation design.

On the other hand, Yamashita et al. (2011, 2012, 2014) presented the results of some case studies of piled raft foundation located on non-liquefiable and liquefiable ground. They considered the settlement and load sharing of piled rafts by monitoring the full-scale structures during a long period after the end of construction. Based on their measurement results, the

maximum vertical ground displacements just below the raft were approximately same as the foundation settlement. Also the foundation settlement and the load sharing found to be stable for a long period after the end of the construction. Furthermore, some of the building sites were struck by the 2011 off the pacific coast of Tohoku earthquake. Also, in those case studies, based on the static and dynamic measurement results, no significant changes were observed in the foundation settlement and the load sharing after the strong ground motion. So, theirs behavior was quite stable and considering these case studies results, it seems that by taking into account all the critical conditions during the foundation design, reasonable performance of foundation system can be expected.

5.5. Behavior of piled raft foundation of oil tank on clay

Although large number of structures is constructed on the soft ground, there is disinclination to use piled raft foundation on soft clay ground due to concerns about excessive and delayed settlement and inadequate bearing capacity. In the other words this foundation system is considered as an undesirable foundation type in soft clay (Poulos, 2001). Despite these concerns and ambiguities, a few successful application of piled raft foundation on soft clay have been reported (Yamashita et al., 2012). Also, some researchers studied performance of piled raft foundation on clay soils using numerical modeling (Cho et al., 2012; Fattah et al., 2013; Lee et al., 2010; Ragheb et al., 2015; Sanctis et al., 2006; Seo et al., 2004; Small et al., 2008). Furthermore, Reul et al. (2003) compared the in situ measurements of piled rafts behavior in over-consolidated clays by numerical analysis. In addition, Badry et al. (2015) presented a case study of oil storage tank with pile group foundation on marine clay.

The main difference in clay ground is the long consolidation settlement in this type of soil

especially in saturated condition. Due to structure load and immediate settlement of foundation, the excess pore water pressure increases beneath the foundation. The EPWP start to dissipate slowly by flowing water from areas with high EPWP toward regions of lower water pressure. By reduction of EPWP, the effective stress in the soil increases and leads to further settlement of the foundation during a long period. This consolidation settlement may cause reduction of contact between the raft and subsoil which enhances the piles load and consequently increase of foundation settlement. So this condition should be treated with remarkable caution.

On the other hand, due to large natural period of soft clay ground, the long period sloshing of liquid inside the tank may be amplified. So special consideration for tank liquid sloshing is inevitable in cases that storage tank is resting on soft clay.

5.6. Summary

The results of this study were employed in this chapter in order to present some practical hints for the application of piled raft foundation for oil storage tanks on non-liquefiable and liquefiable sand. Different aspects of performance of tank piled raft foundation were discussed based on the centrifuge test results conducted in the current research. In the discussions some design considerations for piled raft foundations were explained. Also some practical points about overall stability, bearing capacity, settlement, uneven settlement and structural components of piled raft foundation of oil tanks were considered. Some key issues of the discussions are pointed out in the following charts:

a) Oil tanks with piled raft foundation on non-liquefied sand

	Tank Overall Behavior			Structural Components		Sloshing
	Bearing Capacity	Settlement	Uneven Settlement	Piles	Raft	
Critical Conditions	-	-	-	Large axial load	Punching of the raft	Large
Remedies	-	-	-	1. Classifying piles to interior and exterior piles. 2. Using different safety factors for interior and exterior piles. 3. Assuming RLP=0 for pile design load estimation. 3. Design o piles for static load plus maximum amplitude of dynamic loads.	Checking the raft punching failure by the piles in the raft perimeter.	Considering the large free-surface liquid waves height to determine freeboard requirement of tank.

b) Oil tanks with piled raft foundation on liquefied sand

	Tank Overall Behavior			Structural Components		Sloshing
	Bearing Capacity	Settlement	Uneven Settlement	Piles	Raft	
Critical Conditions	Piles Bearing capacity will diminish during the liquefaction	Is significant	Is significant			Amplification of liquid waves by long period movements of ground.
Remedies	Raft alone should satisfy the bearing capacity criteria	PRF may have better performance if P_L value of the site is less than 15.				Tank dimensions should be designed to confine this possibility.

Chapter 6 – Conclusions and recommendations

The main objective of this research was to study mechanical behavior of oil storage tanks with piled raft foundation which are resting on non-liquefiable and liquefiable sand during dynamic (earthquake) loading. Also another concern was the difference between performance of piled raft foundation of oil tanks with different pile installation procedures (driven and non-driven pile installation). Furthermore number of piles was another key issue in oil tank piled raft foundations which must be considered. For this purpose, centrifuge model tests were conducted to answer these questions. Piled raft foundation was modelled in small scale to employ during the centrifuge tests also a special setup was developed to model driven (displacement) piled raft foundations for storage tanks with different piles number. The following findings were concluded from the present research.

6.1. Main Conclusions

In **chapter 2,** the prior research on piled raft foundation is indicated. This foundation system has been investigated under different loading mechanisms e. g. static and dynamic horizontal and vertical loadings and real seismic loadings. Also analytical methods along with physical simulation were used to investigate about the performance of this foundation in different conditions. Furthermore some field studies were conducted to check the application of this system in real projects and during real previous earthquakes.

This foundation has been considered mostly on the ground with stable and enough bearing capacity (dry sand and hard clay). Also, it has been investigated mainly for normal building

structures no other infrastructures like oil storage tanks. The reason is the complex soil-structure interaction between raft, ground and piles during the earthquakes and the difficulties for calculation of pile and raft load proportion in such a complicated condition. Furthermore despite of some studies about pile installation procedure effect on the performance of the piles, this topic is almost ignored in case of piled raft foundation.

Therefore, in this thesis the main objective was developing a system with proper instrumentation devices for centrifuge modeling of oil tank with slab, driven and non-driven piled raft foundation. In order to study the mechanical behavior of oil tank supported by piled raft, the modeling was conducted on both dry (non-liquefiable) and saturated (liquefiable) sand.

In **chapter 3**, the basic principles of centrifuge modeling were addressed. The details of model tests conducted in this study along with instruments and their calibration were explained. Centrifuge modeling is a powerful procedure for simulation of piled raft foundation while the complicated soil-pile-raft interaction with prototype stress in model scale can be simulated. In contrast to the previous studies this foundation system was modelled for storage tanks. Also, the modeling was conducted on saturated (liquefiable) sand which was ignored in most of the previous researches.

By developing a particular setup, in-flight installation of piles was simulated and driven piled raft foundation with different piles number was also modelled for storage tank. Thanks to this complex installation method, shaft friction of piles which is necessary in the concept of piled raft foundation could be enhanced comparing to non-driven pile installation method.

Comparing the per-pile load during the piles installation indicated that in the beginning the per-pile load in case with fewer piles number is larger than case with more piles due to group pile effect, that is, the pile end bearing capacity is relatively larger in the fewer piles case than

the more pile case. But as the penetration increases, the larger shaft friction was mobilized for the latter case than the former due to the larger soil compaction and the larger horizontal stress.

Furthermore, in order to calculate load share in the raft and piles, two types of earth pressure cells (non-built-in and built-in) were utilized on the raft surface. The results during the preloading process testified the better performance of built-in earth-pressure cells comparing to non-built-in one due to the less stress concentration effect on the built-in sensors.

In **chapter 4**, the results of centrifuge model tests on the piled raft and slab foundation of oil tanks was discussed. The ground response, tank accelerations, tank settlements, tank rotation, ground excess pore water pressures in saturated ground, piles and raft resistances, tank maximum rotation and direction of maximum rotation along with sloshing of liquid inside the tank were discussed in detail in this chapter. Some of the findings are pointed out in the following:

In dry sand ground, the input motions were amplified in both types of foundation, but the amplification for the slab foundation case was more in low periods range than the PRF. The less confinement effect by the raft in PRF than that of SF made the natural period of the subsoil longer for the PRF than the SF.

Due to the contribution of piles of the piled raft foundation, this foundation system could effectively reduce the tank rocking motion, settlement and uneven settlement when the tank was modelled on the dry sand.

In case of tank with piled raft foundation on dry sand, despite of larger piles load sharing, in this piled raft foundation with frictional piles, not only the pile resistance but also the raft resistance carried the loads and rotational moment.

In the cases that tank was modelled on the saturated sand, due to the large soil stiffness reduction by the liquefaction, the input motion was significantly attenuated especially in short period range and at the ground beside the tank where less confinement pressure was transmitted from the tank. While at the ground beneath or just beside the tank, due to the confinement effect of the tank load, the attenuation level was relatively small compared to the further outside ground and some amplification of motion could occur in long period range.

The pile driving process could increase the density and lateral stresses of sand between piles, which could slower the excess pore water pressure (EPWP) increase and enhance the EPWP dissipation beneath the tank. This effect became more significant as the number of pile increased. However, within the condition adopted in the tests, that is, the static driving with pile replacement ratio of about 4% for relatively small raft diameter (7.5m), the effects could be eliminated by a large shaking.

The raft base contact pressures significantly change during the shaking with different patterns depending on the types of foundations, the locations and the shaking history. As a common trend of PRF without shaking history, the base contact pressures at all location increase in the EPWP build-up stage. At the outer part of the raft base, the pressures are kept almost constant during the liquefaction stage and then start decreasing in the consolidation stage, while in the central part the pressure increases even in the consolidation stage, showing the stress concentration due to the relatively large stiffness by the raft pressure. The increase of raft load proportion (RLP) of PRF is caused by the reduction of piles resistance due to the liquefaction, but the RLP decreases gradually with the recovery of piles resistance by the EPWP dissipation. The concentration of base pressures at the center is more significant for SF than PRFs and as the number of piles increases, the concentration could be reduced by the additional support from the

piles.

The reduction of pile resistance could be slowed by the pile driving to some extent, but the effect could not be expected after a large shaking. The change of RLP during and after the shaking depends on the number of piles and level of liquefaction. The less the pile number and the more the liquefaction significance are, the larger the RLP during the liquefaction and the later the RLP reduction after the liquefaction.

Driven PRF could reduce the rocking motion of tank during shaking in comparison to non-driven PRF, especially for the Driven PRF with a larger number of piles.

The piled raft foundation is effective in reducing tank settlement compared to the slab foundation. Even for the very small RLP, the PRF with a large number of driven piles could reduce the tank settlement at the beginning due to the slow EPWP increase and remained piles resistance. But the effects of the driven piles could be diminished by the shaking, which results in large settlement and uneven settlement for poor and non-uniform contact between the raft and ground surface. Therefore relatively large raft load proportion, which can secure the good raft base contact, is a critical condition for preventing a large uneven settlement of the foundation.

Once the direction of the maximum rotation is fixed to a direction diverted from the shaking direction, the rotation will be accumulated by shaking. There could be a several reasons of the rotation to more transverse direction, such as inevitable difference of bearing resistance of each pile, non-uniformity of raft base contact condition to the ground. On the other hand, while the rotation mainly takes place in the shaking direction, the monotonic increase of the rotation may not easily occur and the rotation behavior becomes very complicated for the slab foundation. This unstable behavior could be attributed to the stress concentration in the central part of the raft base, which could be prevented by the additional support from the piles.

The liquid behavior (sloshing) inside the tank is directly related to the acceleration level at the tank center of gravity. Because of the higher tank acceleration in dry cases due to the amplification of input motion in the ground the water pressure increment inside the tank was larger in dry cases. But the piled raft foundation in dry case could effectively reduce sloshing of liquid mass while it was not so effective in saturated cases.

In **chapter 5**, some practical points for the application of piled raft foundation for oil storage tanks on non-liquefiable and liquefiable sand were presented by employing the results of study. Considering overall stability, bearing capacity, settlement, uneven settlement and structural components of piled raft foundation system of oil tanks, some key issues were discussed.

Due to large contribution of piles in carrying of loads when oil tank with piled raft foundation is located on non-liquefiable sand, special consideration and attention is necessary for design of piles and their punching effect on the raft. It is recommended to divide piles regarding their location and to use different safety factors for interior and exterior piles. Also, in order to estimate piles design load, it is reasonable to assume raft load proportion equal zero. Furthermore, it is recommended to design piles for static load plus maximum amplitude of dynamic loads. On the other hand, it is essential to check punching effect of piles located in the raft perimeter.

Special considerations are inevitable for freeboard requirements of tank while the sloshing waves are almost significant in case of oil tank on dry sand in contrast to saturated sand.

In conditions that piled raft foundation are used for oil tanks on liquefiable sand, bearing capacity of foundation should be checked ignoring the piles capacity. Also this point should be considered that this foundation system may have better performance for controlling settlement

and uneven settlement when PL value of the site is less than 10.

6.2. Recommendations for Future Studies

Although the typical and interesting behavior of pile raft foundation in the liquefiable sand have been observed in the tests, the dynamic behaviors are so complicated, which are affected by various factors. Furthermore for the conditions of complete liquefaction in the entire ground, the better performance of piled raft foundation could not be expected. Therefore the effectiveness and limitation of piled raft foundations should be studied more for different conditions, i.e., on the ground with partial liquefaction, such as, the liquefaction in partial depth, not entire depth or ground with non-liquefied soil layer, and the ground and tank with artificial asymmetric conditions, to clarify the conditions of positive application of piled raft foundation, including the dynamic and static pile installation methods and pile head fixity.

The pile head fixity may reduce the tank rotation and its horizontal displacement which can positively reduce the sloshing effect of the liquid inside the tank. On the other hand, this type of connection may enhance moment in the pile and increase of pile dimension. Also, while the dynamic pile installation procedure is mostly utilized in real projects, this type of pile installation method should be modeled in the future studies to compare the difference between the application of dynamic driven piles and non-driven piles. These topics affect significantly the behavior of oil storage tanks due to not only changing of soil-pile-raft interaction but also altering the sloshing behavior of tank liquid. So these issues should be investigated more to consider various effective conditions on the seismic performance of oil storage tanks on liquefiable and non-liquefiable ground.

References:

1) Abdel-Fattah, T.T., and Hemada, A.A. (2016). Evaluation of the existing piled foundation based on piled–raft design philosophy. Innov. Infrastruct. Solut. *1*, 1–11.

2) Adejumo, T.W., and Boiko, I.L. (2013). Effect of installation techniques on the allowable bearing capacity of modeled circular piles in layered soil. Int. J. Adv. Technol. Eng. Res. *2*, 1536–1542.

3) Alnuiam, A., El Naggar, H., and El Naggar, M.H. (2013). Performance of Piled-Raft System under Axial Load. In Proceeding of the 18th Inter. Con. on Soil Mechanics and Geotechnical Engineering, (France, Paris), pp. 2663–2666.

4) Annaki, M., and Lee, K.L. (1977). Equivalent Uniform Cycle Concept for Soil Dynamics. J. Geotech. Eng. Div. *103*, 549–564.

5) Arias, A. (1970). A measure of earthquake intensity. In Hansen RJ (Ed) Seismic Design for Nuclear Power Plants., (Cambridge, MA: MIT Press), pp. 438–483.

6) Badry, P., and Satyam D., N. (2015). Interaction analysis for oil storage tank on marine clay. Int. J. GEOMATE *8*, 1123–1129.

7) Baziar, M.H., Ghorbani, A., and Katzenbach, R. (2009). Small-Scale Model Test and Three-Dimensional Analysis of Pile-Raft Foundation on Medium-Dense Sand. Int. J. Civ. Eng. *7*, 170–175.

8) Bloomquist, D., Feld, T., Townsend, F.C., Gravgaard, J., and Gill, J. (1991). Development of a multiple pile driver/load test device for pile group studies. In Centrifuge 91, (Colorado, USA), pp. 355–359.

9) Boonsiri, I. (2015). A centrifuge model study on behavior of ground movement and pile group response to tunneling in sand. Doctor of Philosophy. Tokyo Institute of Technology.

10) Brandenberg, S.J., Boulanger, R.W., Kutter, B.L., and Chang, D. (2005). Behavior of Pile Foundations in Laterally Spreading Ground during Centrifuge Tests. J. Geotech. Geoenvironmental Eng. *131*, 1378–1391.

11) Burland, J.B., Broms, B.B., and DeMello, V.F.B. (1977). Behaviour of foundations and structures. In Proceedings of 9th ICSMFE, (Tokyo, Japan), pp. 496–546.

12) Chaithra, T.P., and Manogna, H.N. (2015). Dynamic soil structure interaction analysis for piled raft foundation. Int. J. Eng. Comput. Sci. *4*, 13601–13605.

13) Chaudhary, M.T.A. (2007). FEM modelling of a large piled raft for settlement control in weak rock. Eng. Struct. *29*, 2901–2907.

14) Cho, J., Lee, J. H., Jeong, S., and Lee, J. (2012). The settlement behavior of piled raft in clay soils. Ocean Eng. *53*, 153–163.

15) Chopra, A.K., and Chintanapakdee, C. (2001). Comparing response of SDF systems to near-fault and far-fault earthquake motions in the context of spectral regions. Earthq. Eng. Struct. Dyn. *30*, 1769–1789.

16) Cooke, R.W. (1986). Piled raft foundations on stiff clays-a contribution to design philosophy. Geotechnique *36*, 169–203.

17) Cubrinovski, M., and Ishihara, K. (2001). Analysis of the performance of an oil-tank pile foundation in liquefied deposits. In Proceeding of XV ICSMGE TC4 Satellite Conference on "Lessons Learned from Recent Strong Earthquakes," (Istanbul, Turkey), pp. 339–344.

18) Das, B.M. (2007). Fundamentals of Geotechnical Engineering (Chris Carson).

19) Duncan, J.M., and D'Orazio, T.B. (1984). Stability of Steel Oil Storage Tanks. J. Geotech. Eng. *110*, 1219–1238.

20) Eslami, A., Veiskarami, M., and Eslami, M.M. (2012). Study on optimized piled-raft foundations (PRF) performance with connected and non-connected piles-three case histories. Int. J. Civ. Eng. *10*, 100–111.

21) Fattah, M.Y., Al-Mosawa, M.J., and Al-Zayadi, A.A.O. (2013). Time dependent behavior of piled raft foundation in clayey soil. Geomech. Eng. J. *5*, 17–36.

22) FDMA (1974). Notification of technical specifications regarding to the regulations on hazardous materials.

23) Fellenius, B.H., Tech, and Ochoa, M. (2013). Large liquid storage tanks on piled foundation. In Proceeding of Inter. Conf. on Foundation and Soft Ground Engineering-Challenges in the Mekong Delta, (Hochiminh, Vietnam), pp. 3–17.

24) Flynn, K.N., and McCabe, B.A. (2015). Shaft resistance of driven cast-in-situ piles in

sand. Can. Geotech. J. *53*, 49–59.

25) Hamada, J. (2016). Bending moment of piles on piled raft foundation subjected to ground deformation during earthquake in centrifuge model test. Jpn. Geotech. Soc. Spec. Publ. *2*, 1222–1227.

26) Hamada, J., Tsuchiya, T., Tanikawa, T., and Yamashita, K. (2012). Lateral loading model tests on piled rafts and their evaluation with simplified theoretical equations. In Proceedings of the 9th Inter. Conf. onTesting and Design Methods for Deep Foundations (IS-Kanazawa 2012), (Japan, Kanazawa), pp. 467–476.

27) Hirakawa, K., Hamada, J., and Yamashita, K. (2016). Settlement behavior of piled raft foundation supporting a 300m tall building in Japan constructed by top-down method. Jpn. Geotech. Soc. Spec. Publ. *2*, 166–169.

28) Horikoshi, K., and Randolph, M.F. (1994). Settlement of piled raft foundations on clay. In Proceedings of Centrifuge 94, pp. 449–454.

29) Horikoshi, K., and Randolph, M.F. (1996). Centrifuge modelling of piled raft foundations on clay. Géotechnique *46*, 741–752.

30) Horikoshi, K., and Randolph, M.F. (1998). A contribution to optimum design of piled rafts. Géotechnique *48*, 301–317.

31) Horikoshi, K., Watanabe, T., Fukuyama, H., and Matsumoto, T. (2002). Behavior of piled raft foundations subjected to horizontal loads. In Proceeding of Inter. Conf. of Physical Modelling in Geotechnics, pp. 715–721.

32) Horikoshi, K., Matsumoto, T., Hashizume, Y., Watanabe, T., and Fukuyama, H. (2003). Performance of Piled Raft Foundations Subjected to Static Horizontal Loads. Int. J. Phys. Model. Geotech. *3*, 37–50.

33) Housner, G.W. (1963). Dynamic analysis of fluids in containers subjected to acceleration. Nuclear reactors and earthquakes, Report No. TID 7024.

34) Imamura, S., Yagi, T., and Takemura, J. (2010). Dynamic stability of oil tank supported by piled-raft foundation on liquefiable sand. In Physical Modelling in Geotechnics, (Zurich, Switzerland), pp. 1409–1414.

35) Ishihara, K., Kawase, Y., and Nakajima, M. (1980). Liquefaction characteristics of sand

deposits at an oil tank site during the 1978 Miyagiken-oki earthquake. Soils Found. *20*, 97–111.

36) Ishimatsu, S., Yagi, T., Yoshimi, T., and Takemura, J. (2009). Filed observation of pile behavior during the liquid level variation in an oil tank. Kisoko *37*, 76–79.

37) Iwasaki, T. (1986). Soil liquefaction studies in Japan: state-of-the-art. Soil Dyn. Earthq. Eng. *5*, 2–68.

38) Iwasaki, T., Tatsuoka, F., Tokida, K., and Yasuda, S. (1978). A practical method for assessing liquefaction potential based on case studies at various sites in Japan. In 5th Japan Symposium on Earthquake Engineering. (Japan).

39) JMA (2008). http://www. seisvol.kishou.go.jp/eq/kyoshin/jishin/080614_iwate-miyagi/index.html.

40) Klotz, E.U., and Coop, M.R. (2001). An investigation of the effect of soil state on the capacity of driven piles in sands. Géotechnique *51*, 733–751.

41) Kramer, S.L. (1996). Geotechnical earthquake engineering. In Geotechnical Earthquake Engineering, (Prentice Hall).

42) Lee, S., and Moon, J. S. (2016). Effect of interactions between piled raft components and soil on behavior of piled raft foundation. KSCE J. Civ. Eng. 1–10.

43) Lee, J., Kim, Y., and Jeong, S. (2010). Three-dimensional analysis of bearing behavior of piled raft on soft clay. Comput. Geotech. *37*, 103–114.

44) Liew, S., Gue, S., and Tan, Y. (2002). Design and instrumentation results of a reinforcement concrete piled raft supporting 2500 ton oil storage tank on very soft alluvium deposits. In Proceeding of the 9th Inter. Conf. on Piling and Deep Foundations, (Nice, France).

45) Long, P.D., President, V., and Vietnam, V.W. (2010). Piled Raft-A Cost-Effective Foundation Method for High-Rises. Geotech. Eng. J. SEAGS AGSSEA *41*.

46) Malhotra, P.K. (2006). Earthquake Induced Sloshing in Tanks with Insufficient Freeboard. Struct. Eng. Int. *16*, 222–225.

47) Malhotra, P.K., Wenk, T., and Wieland, M. (2000). Simple procedure for seismic analysis of liquid-storage tanks.

48) Marshall, A.M., Cox, C.M., Salgado, R., and Prezzi, M. (2014). Centrifuge modelling of non-displacement piles and pile groups under lateral loading in layered soils. (Australia, Perth),

p. 847.

49) Matsumoto, T., Fukumura, K., Pastsakorn, K., Horikoshi, K., and Oki, A. (2004a). Experimental and Analytical Study on Behaviour of Model Piled Rafts in Sand Subjected to Horizontal and Moment Loading. Inter J. Phys. Model. Geotech. *4*, 1–19.

50) Matsumoto, T., Fukumura, K., Horikoshi, K., and Oki, A. (2004b). Shaking Table Tests on Model Piled Rafts in Sand Considering Influence of Superstructures. Inter J. Phys. Model. Geotech. *4*, 21–38.

51) Matsumoto, T., Nemoto, H., Mikami, H., Yaegashi, K., Arai, T., and Kitiyodom, P. (2010). Load Tests of Piled Raft Models with Different Pile Head Connection Conditions and Their Analyses. Soils Found. *50*, 63–81.

52) Nicola, A.D., and Randolph, M.F. (1999). Centrifuge modelling of pipe piles in sand under axial loads. Géotechnique *49*, 295–318.

53) Pan, S., Pu, J., Yin, K., and Liu, F. (1999). Development of pile driver and load set for pile group in centrifuge. Geotech. Test. J. *22*, 317–323.

54) Pastsakorn, K., Hashizume, Y., and Matsumoto, T. (2002). Lateral load tests on model pile groups and piled raft foundations in sand. In Proceeding of Inter. Conf. of Physical Modelling in Geotechnics, (St. Johns, Newfoundland, Canada), pp. 709–714.

55) Poulos, H.G. (1991). In Computer methods and advances in geomechanics. In Computer Methods and Advances in Geomechanics, (Rotterdam: Balkema), pp. 183–191.

56) Poulos, H.G. (2001). Piled raft foundations: design and applications. Géotechnique *51*, 95–113.

57) Poulos, H.G., and Grahame, B. (2008). Foundation design for the burj Dubai-the worlds tallest building. In 6th International Conference on Case Histories in Geotechnical Engineering, (Arlington, VA).

58) Poulos, H.G., Small, J.C., and Chow, H. (2011). Piled raft foundations for tall building. Geotech. Eng. J. SEAGS AGSSEA *42*, 78–84.

59) Prakoso, W.A., and Kulhawy, F.H. (2001). Contribution to Piled Raft Foundation Design. J. Geotech. Geoenvironmental Eng. *127*, 17–24.

60) Ragheb, A.M., Abdelaziz, T.M., and Ayad, E.N.A. (2015). Load sharing of piled-raft foundations embedded in soft to medium clay subjected to vertical loads. Int. J. Sci. Eng. Res. *6*, 989–1009.

61) Randolph, M.F. (1994). Design methods for pile groups and piled rafts. XIII ICSMFE 61–82.

62) Randolph, M.F., Carter, J.P., and Wroth, C.P. (1979). Driven piles in clay—the effects of installation and subsequent consolidation. Géotechnique *29*, 361–393.

63) Randolph, M.F., Dolwin, R., and Beck, R. (1994). Design of driven piles in sand. Géotechnique *44*, 427–448.

64) Reul, O., and Randolph, M.F. (2003). Piled rafts in overconsolidated clay: Comparison of in situ measurements and numerical analyses. Géotechnique *53*, 301–315.

65) Sahraeian, S.M.S., Takemura, J., and Sakae, S. (2015). A study on seismic behavior of piled raft foundation for oil storage tanks using centrifuge model tests. In 6th International Conference on Earthquake Geotechnical Engineering, (Christchurch, New Zealand).

66) Sanctis, L. de, and Mandolini, A. (2006). Bearing Capacity of Piled Rafts on Soft Clay Soils. J. Geotech. Geoenvironmental Eng. *132*, 1600–1610.

67) Sawada, K., and Takemura, J. (2014). Centrifuge model tests on piled raft foundation in sand subjected to lateral and moment loads. Soils Found. *54*, 126–140.

68) Sento, N., Yasuda, S., Yoshida, N., and Harada, K. (2004). Case studies for oil tank on liquefiable sandy ground subjected to extremely large earthquakes and countermeasure effects by compaction. In Proceeding of 13th World Conference on Earthquake Engineering, (Canada, Vancouver).

69) Seo, Y., and Jeong, S. (2004). Parametric study of piled raft foundation on soft clay. J. Ocean Sci. Technol. *1*, 147–152.

70) Shukla, S.J., Desai, A.K., and Solanki, C.H. (2011). Behavioural study of piled raft foundation in layered soil deposits. Int. J. Adv. Eng. Technol. *2*, 191–195.

71) Shukla, S.J., Desai, A.K., and Solanki, C.H. (2013). A dynamic behavioural study of 25 storey building with piled raft foundation with variable subsoils. Int. J. Struct. Civ. Eng. Res. *2*, 119–130.

72) Shukla, S.J., Desai, A.K., and Solanki, C.H. (2015). A behavioural study of dynamic soil structure interaction for piled raft foundation with variable sub soils by time history FEM model. Int. J. GEOMATE *8*, 1288–1292.

73) Singh, N.T., and Singh, B. (2008). Interaction analysis for piled rafts in cohesive soils. In 12th International Conference of International Association for Computer Methods and Advances in Geo-Mechanics (IACMAG), Goa, pp. 3289–3296.

74) Small, J.C., and Liu, H.L.S. (2008). Time-settlement behaviour of piled raft foundations using infinite elements. Comput. Geotech. *35*, 187–195.

75) Stafford, P.J., Berrill, J.B., and Pettinga, J.R. (2008). New predictive equations for Arias intensity from crustal earthquakes in New Zealand. J. Seismol. *13*, 31–52.

76) Takemura, J., Kondoh, M., Esaki, T., Kouda, M., and Kusakabe, O. (1999). Centrifuge Model Tests on Double Propped Wall Excavation in Soft Clay. Soils Found. *39*, 75–87.

77) Takemura, J., Yamada, M., and Seki, S. (2014). Dynamic response and settlement behavior of piled raft foundation of oil storage tank. In Physical Modelling in Geotechnique, (Perth, Australia), pp. 613–619.

78) Talesnick, M.L., Ringel, M., and Avraham, R. (2014). Measurement of contact soil pressure in physical modelling of soil–structure interaction. Int. J. Phys. Model. Geotech. *14*, 3–12.

79) Tan, Y.C., and Chow, C.M. Design of piled raft foundation on soft ground.

80) Thaher, M., and Jessberger, H.L. (1991). The behaviour of pile-raft foundations investigated in centrifuge model tests. Proc. Centrifuge 91 225–234.

81) Towhata, I. (2011). Geotechnical damage caused by the recent gigantic earthquake in Japan (Semarang, Indonesia).

82) Uras, R.A. (1995). Sloshing analysis of viscous liquid storage tanks.

83) Yamada, M. (2012). A study on dynamic response and seismic settlement behavior of piled raft foundation for oil storage tank. Master Thesis. Tokyo Institute of Technology.

84) Yamashita, K. (2012). Field measurements on piled raft foundations in Japan. In Proceedings of the 9th Inter. Conf. onTesting and Design Methods for Deep Foundations

(IS-Kanazawa 2012), (Japan, Kanazawa), pp. 79–94.

85) Yamashita, K., Yamada, T., and Hamada, J. (2011). Investigation of Settlement and Load Sharing on Piled Rafts by Monitoring Full-Scale Structures. Soils Found. *51*, 513–532.

86) Yamashita, K., Hamada, J., Onimaru, S., and Higashino, M. (2012). Seismic behavior of piled raft with ground improvement supporting a base-isolated building on soft ground in Tokyo. Soils Found. *52*, 1000–1015.

87) Yamashita, K., Hashiba, T., Ito, H., and Tanikawa, T. (2014). Performance of Piled Raft Foundation Subjected to Strong Seismic Motion. Geotech. Eng. J. SEAGS AGSSEA *45*.

88) Yoshimi, Y. (1980). Liquefaction of sand (Japan: Gihodoshupan).

89) Ziaie-Moayed, R., Kamalzare, M., and Safavian, M. (2010). Evaluation of piled raft foundations behavior with different dimensions of piles. J. Appl. Sci.

90) (2007). API 650: Welded steel tanks for oil storage.

91) (2011). Design recommendation for storage tanks and their supports with emphasis on seismic design (2010 edition).

Appendix

Appendix A: Excess pore water pressure of the ground

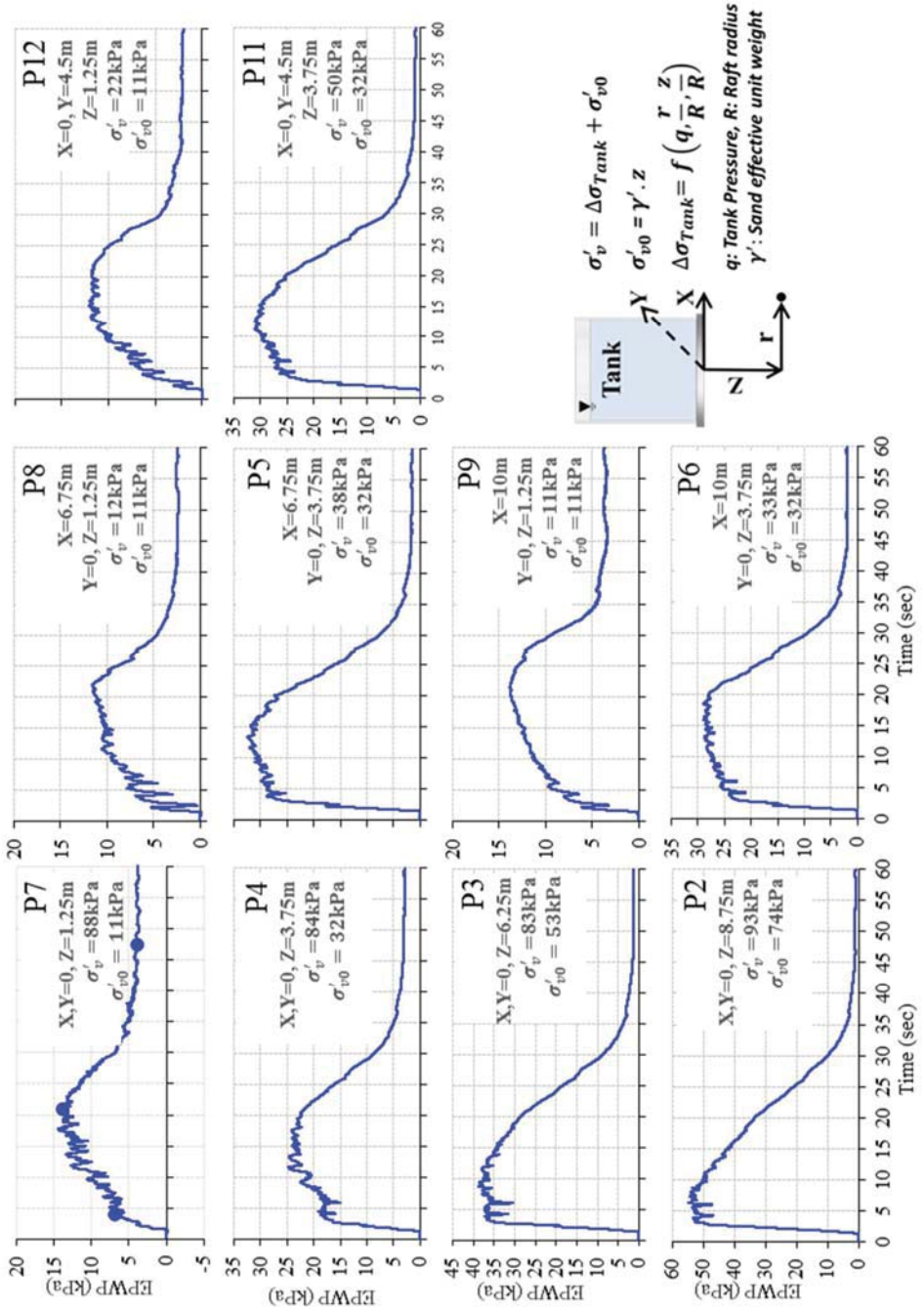

Figure A.1. Excess pore water pressures of the ground in Case 3a (Shake 1).

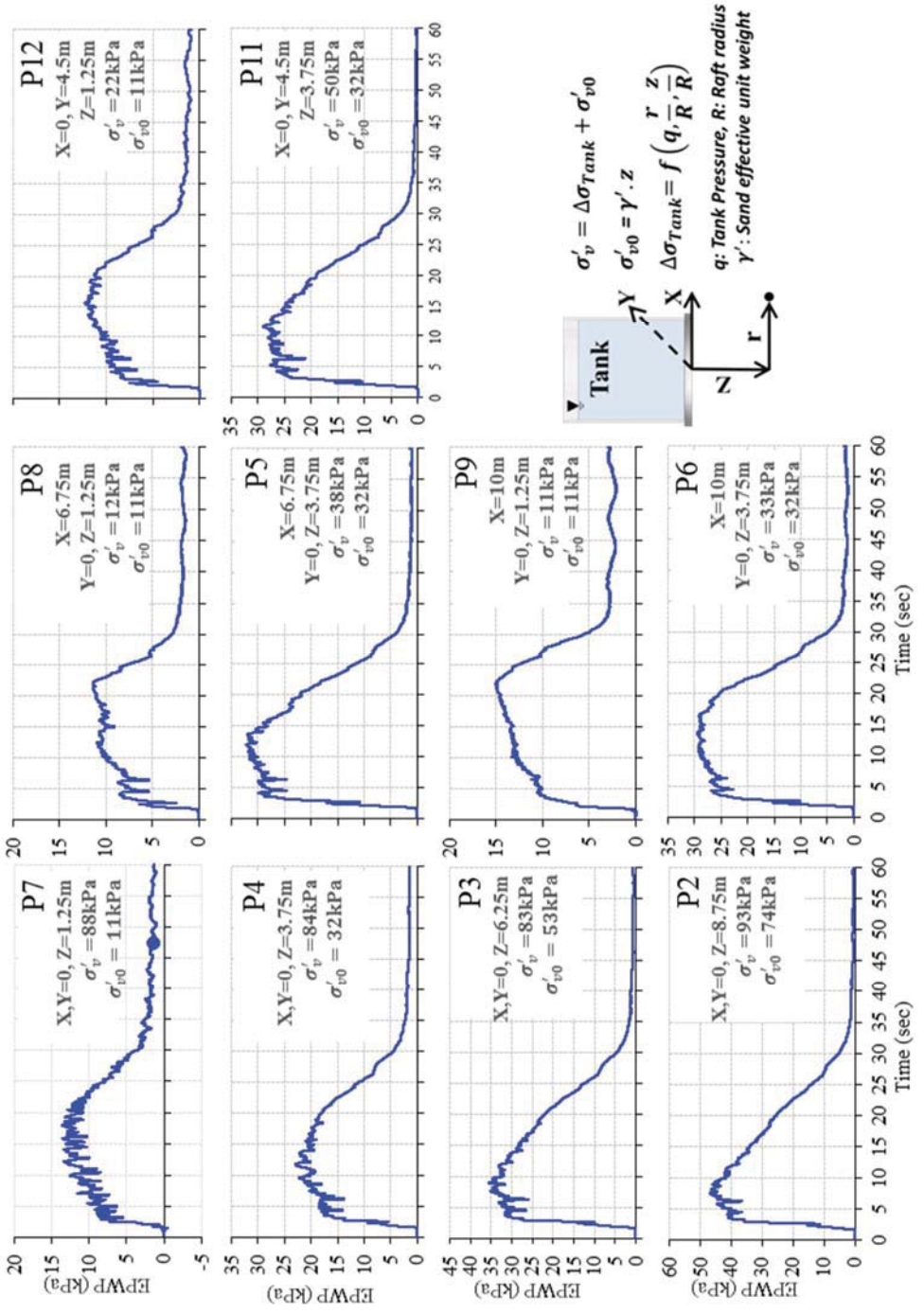

Figure A.2. Excess pore water pressures of the ground in Case 3a (Shake 2).

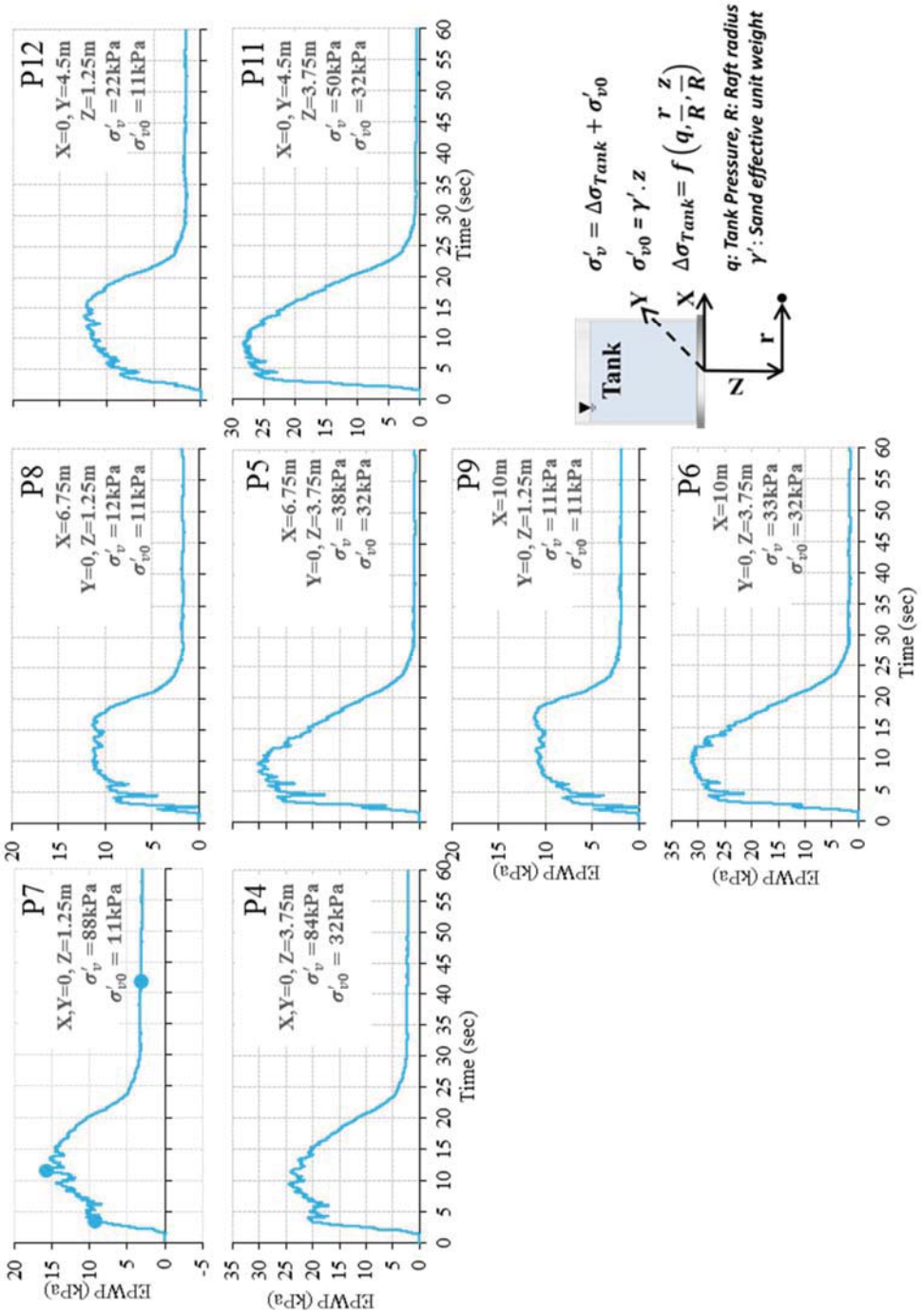

Figure A.3. Excess pore water pressures of the ground in Case 3b (Shake 1).

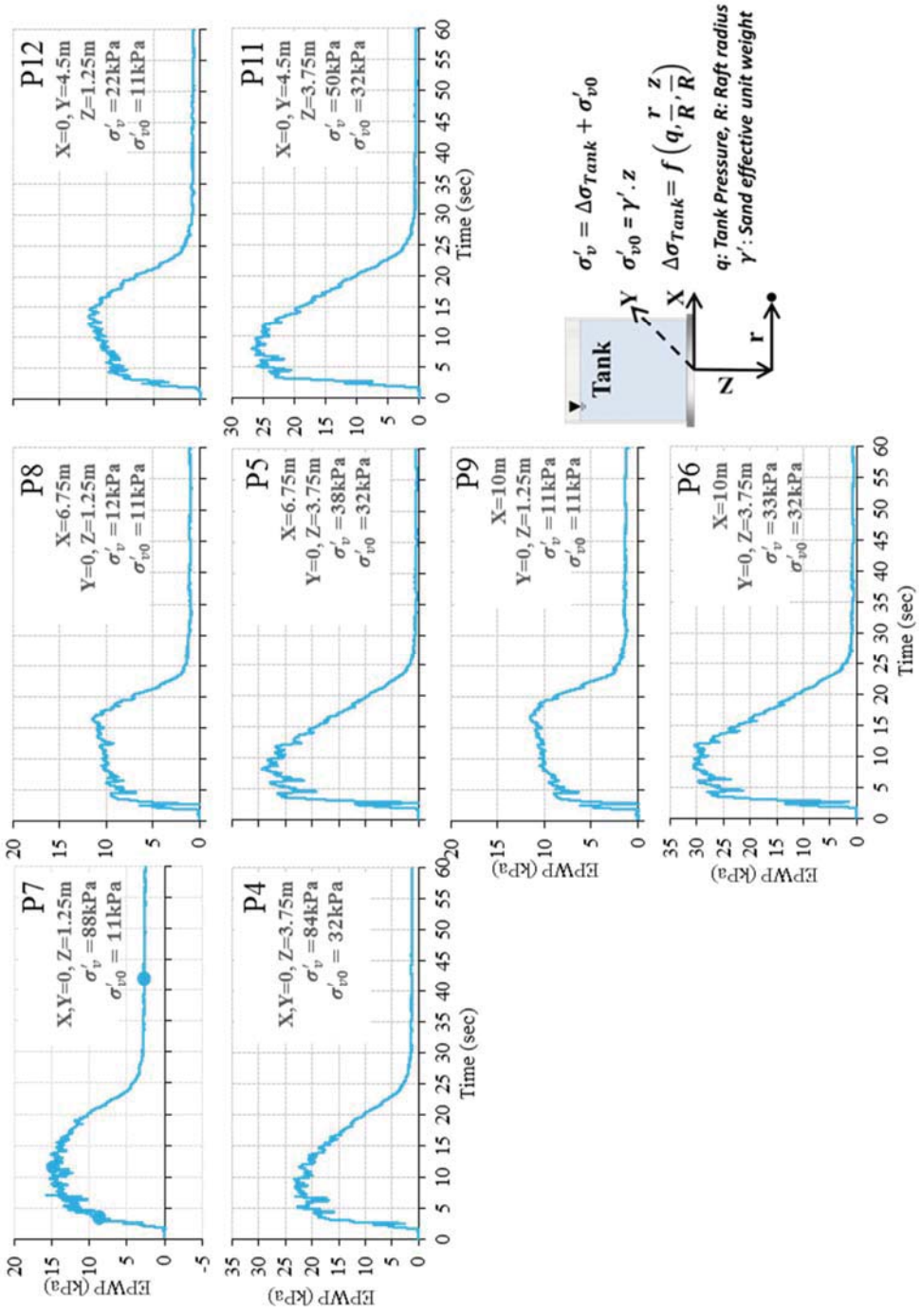

Figure A.4. Excess pore water pressures of the ground in Case 3b (Shake 2).

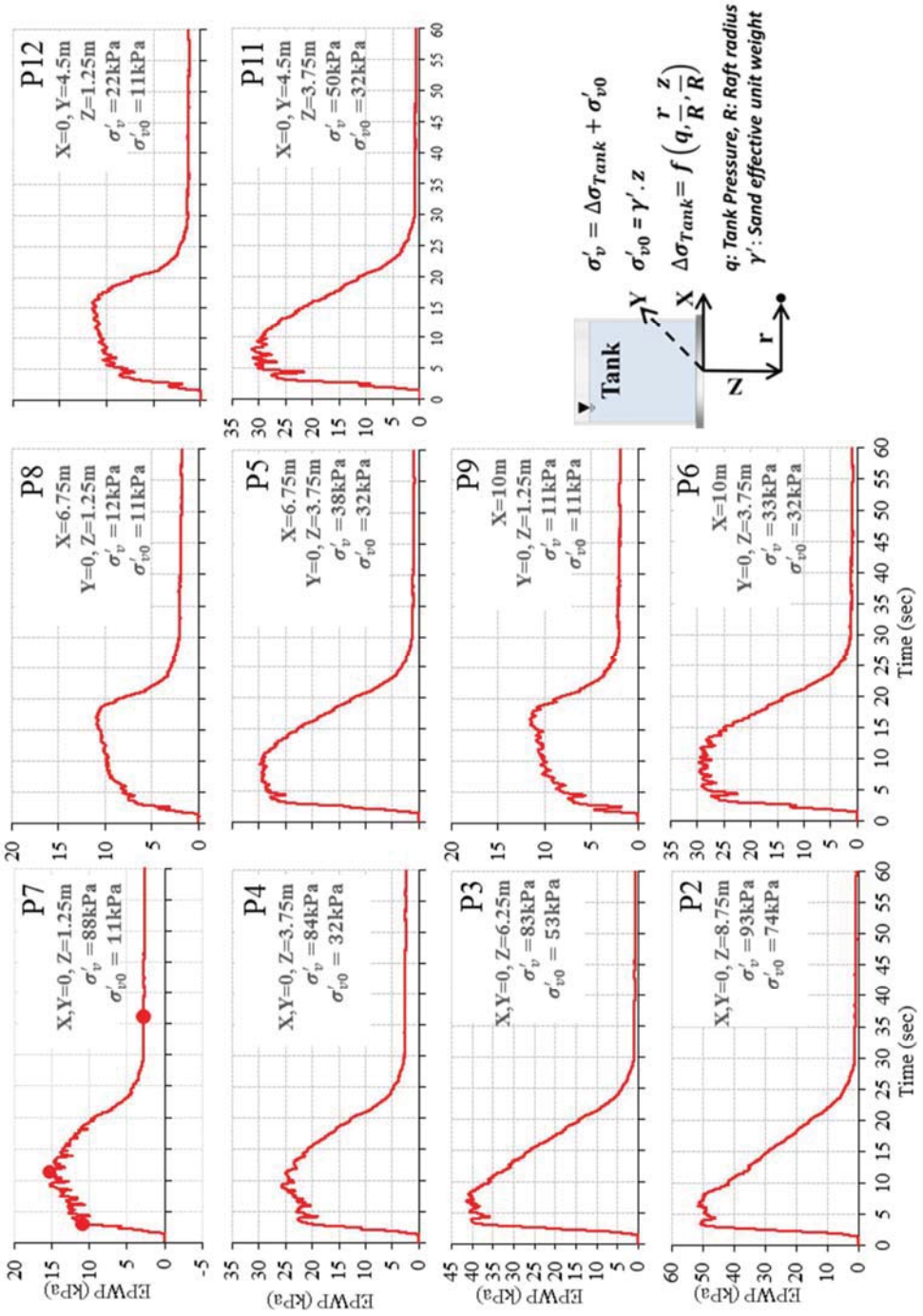

Figure A.5. Excess pore water pressures of the ground in Case 4 (Shake 1).

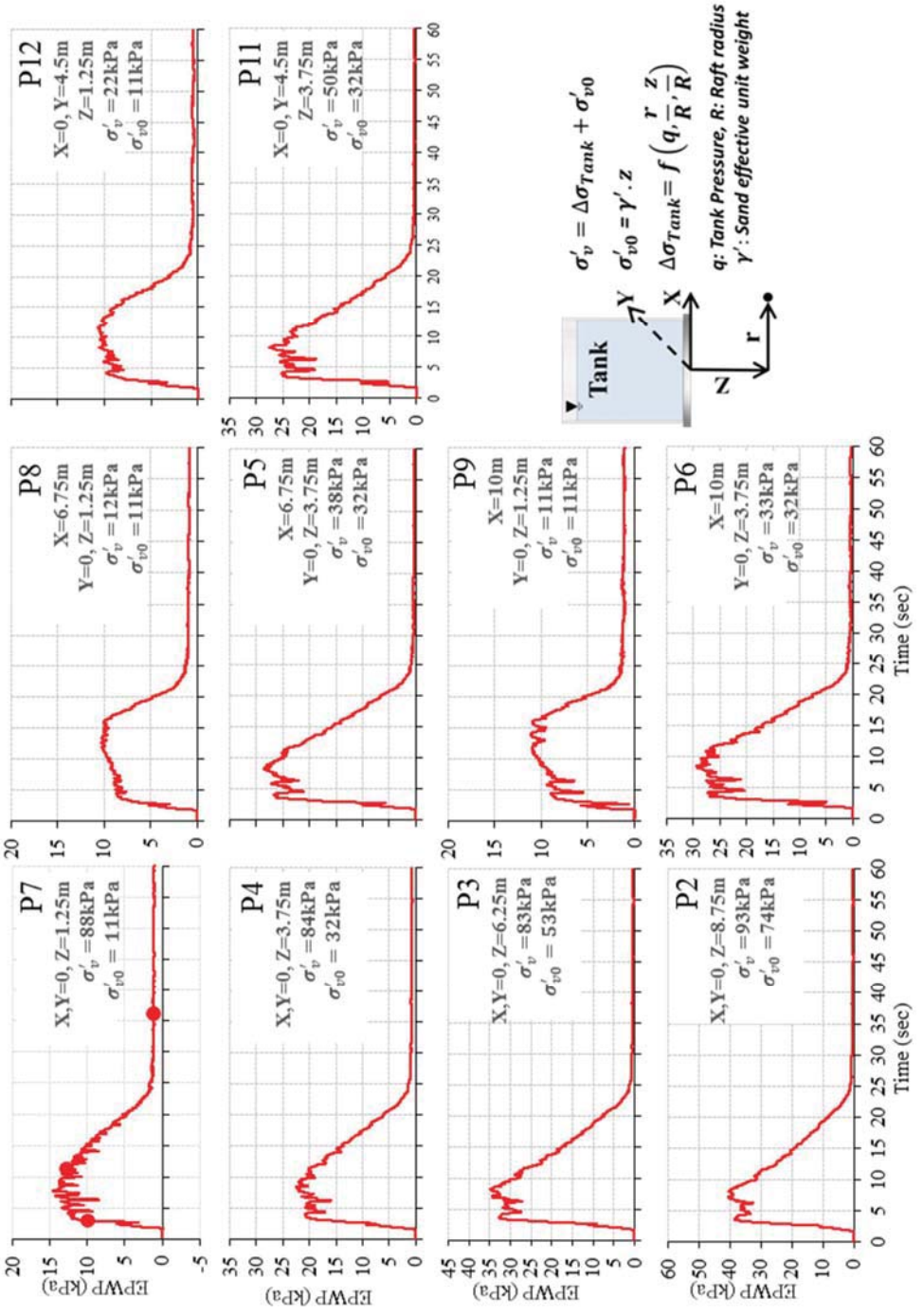

Figure A.6. Excess pore water pressures of the ground in Case 4 (Shake 2).

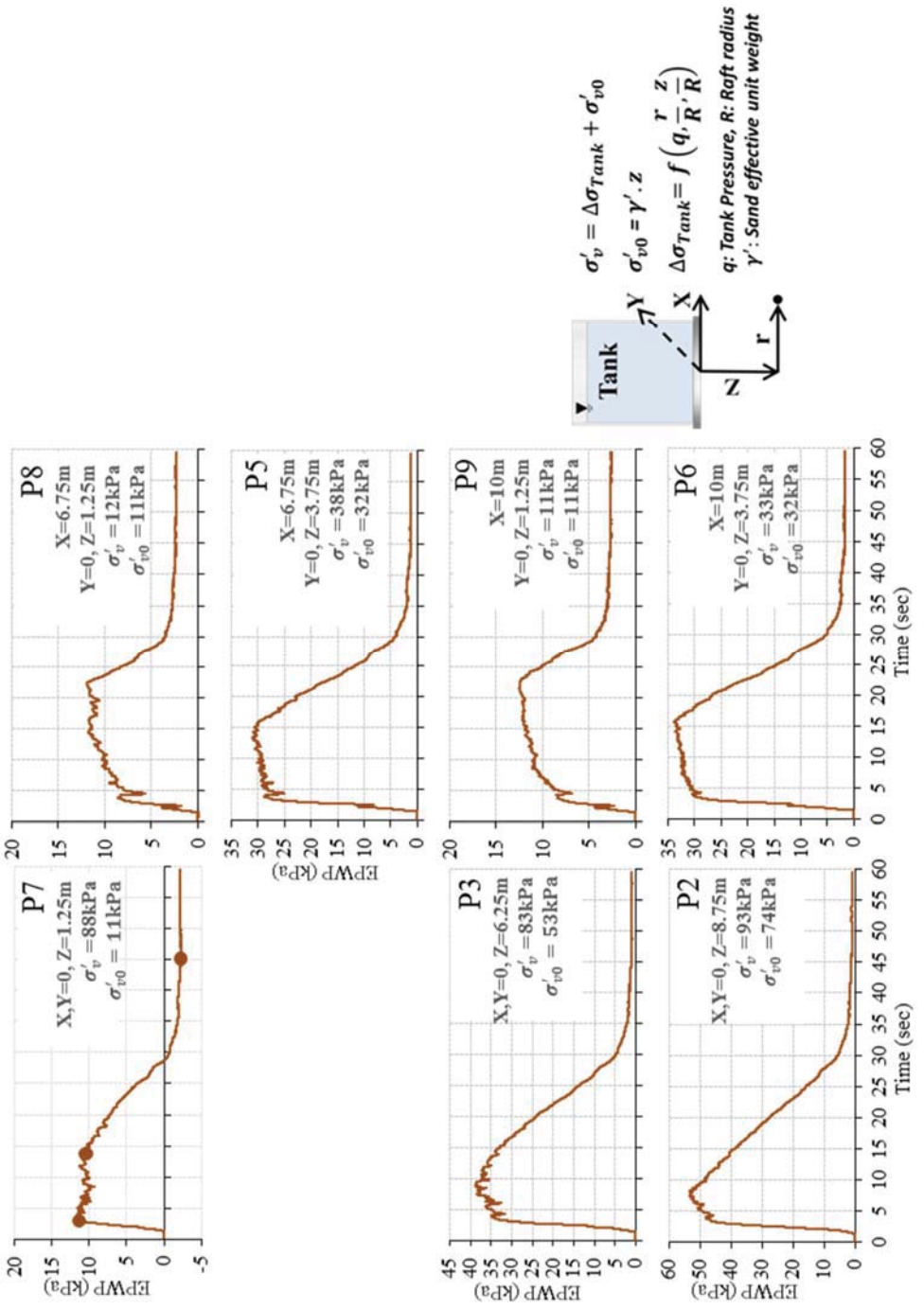

Figure A.7. Excess pore water pressures of the ground in Case 5 (Shake 1).

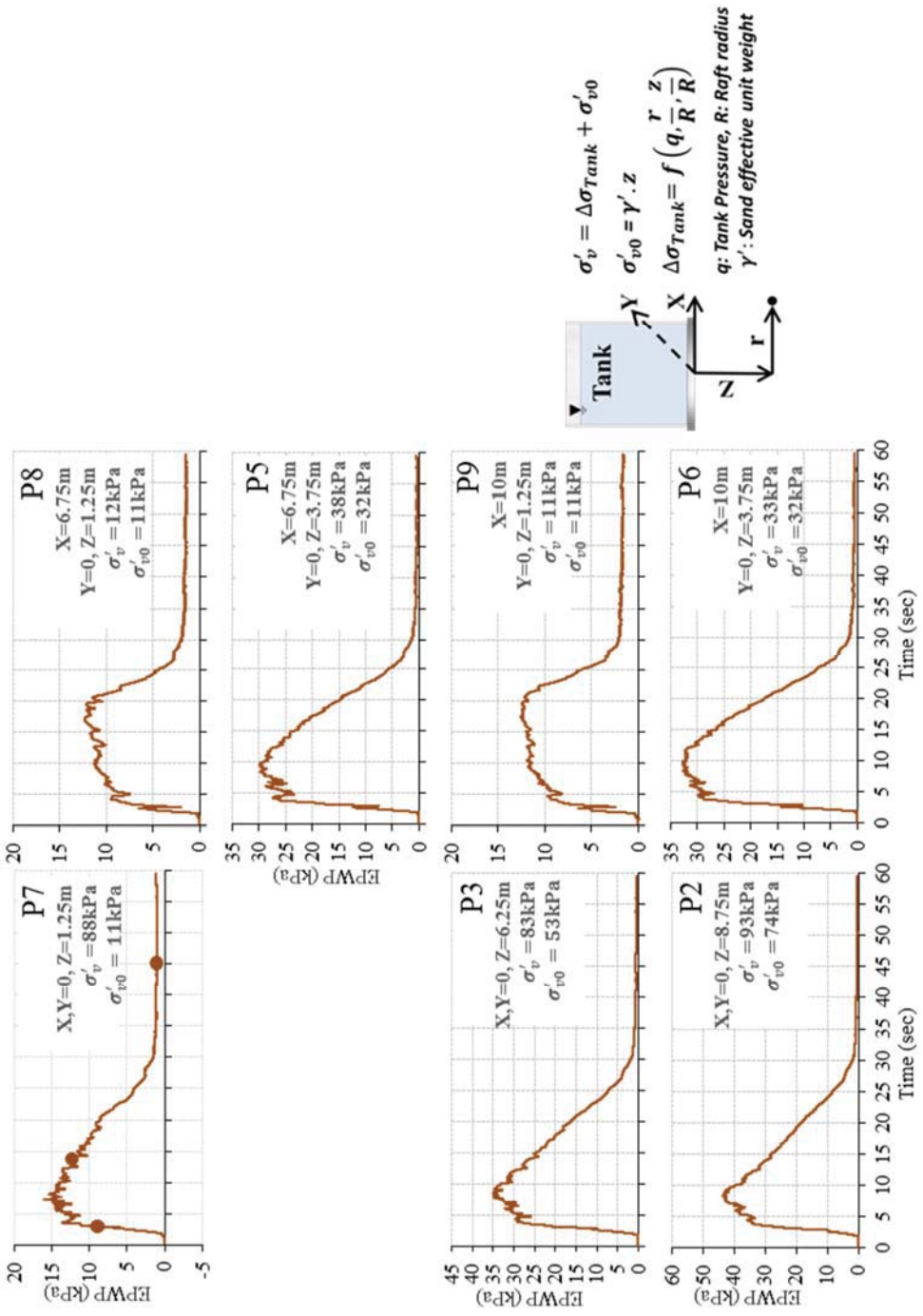

Figure A.8. Excess pore water pressures of the ground in Case 5 (Shake 2).

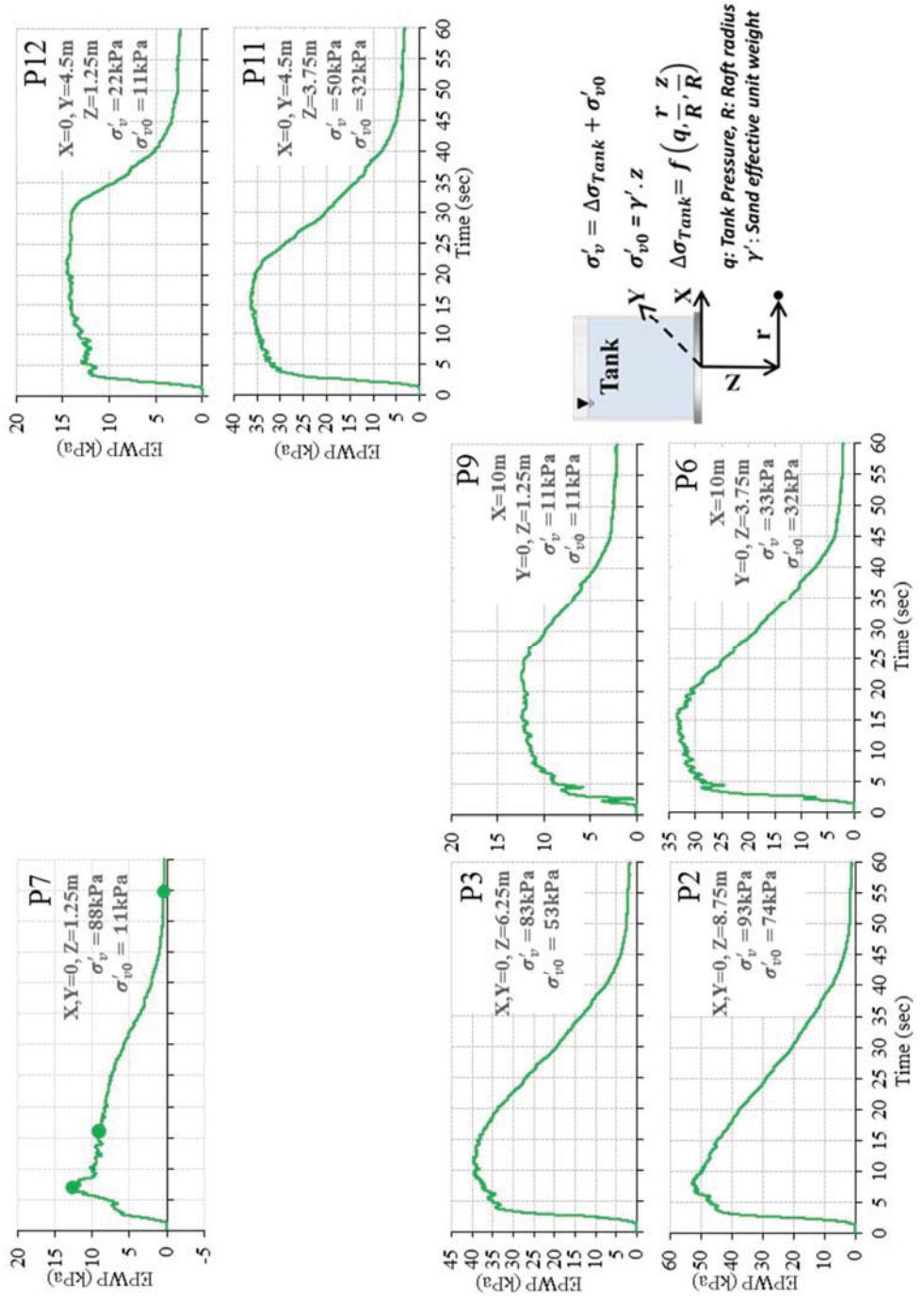

Figure A.9. Excess pore water pressures of the ground in Case 6 (Shake 1).

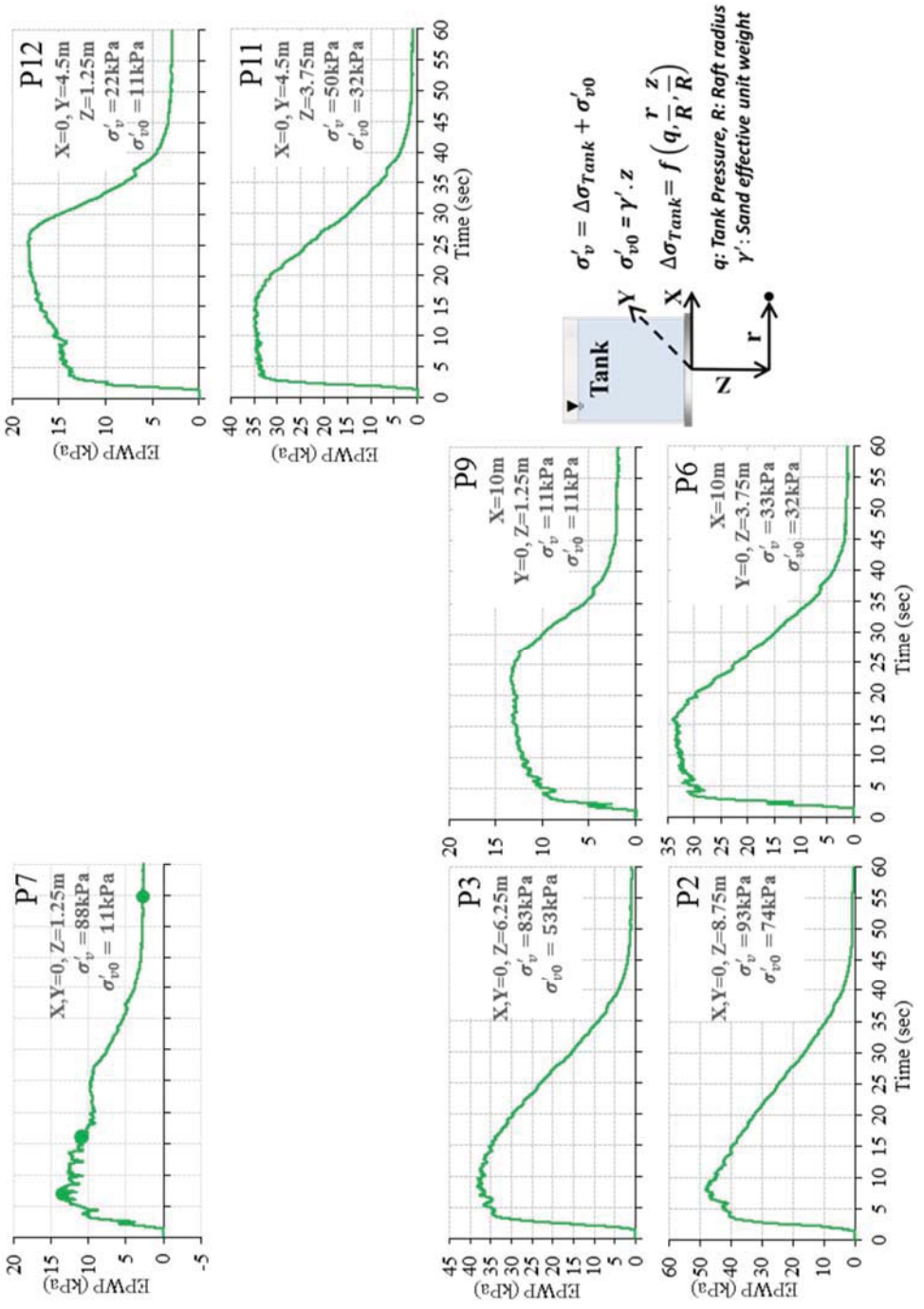

Figure A.10. Excess pore water pressures of the ground in Case 6 (Shake 2).